

University of Massachusetts Medical School

eScholarship@UMMS

---

GSBS Dissertations and Theses

Graduate School of Biomedical Sciences

---

2016-06-10

## Viruses Implicated in the Initiation of Type 1 Diabetes Affect $\beta$ Cell Function and Antiviral Innate Immune Responses: A Dissertation

Glen R. Gallagher

*University of Massachusetts Medical School*

Let us know how access to this document benefits you.

Follow this and additional works at: [https://escholarship.umassmed.edu/gsbs\\_diss](https://escholarship.umassmed.edu/gsbs_diss)



Part of the [Endocrine System Diseases Commons](#), [Immunity Commons](#), [Immunology of Infectious Disease Commons](#), and the [Virology Commons](#)

---

### Repository Citation

Gallagher GR. (2016). Viruses Implicated in the Initiation of Type 1 Diabetes Affect  $\beta$  Cell Function and Antiviral Innate Immune Responses: A Dissertation. GSBS Dissertations and Theses. <https://doi.org/10.13028/M2DW2K>. Retrieved from [https://escholarship.umassmed.edu/gsbs\\_diss/856](https://escholarship.umassmed.edu/gsbs_diss/856)

This material is brought to you by eScholarship@UMMS. It has been accepted for inclusion in GSBS Dissertations and Theses by an authorized administrator of eScholarship@UMMS. For more information, please contact [Lisa.Palmer@umassmed.edu](mailto:Lisa.Palmer@umassmed.edu).

**Viruses implicated in the initiation of type 1 diabetes affect  $\beta$  cell function  
and antiviral innate immune responses**

by

Glen R. Gallagher

Submitted to the Faculty of the

University of Massachusetts Graduate School of Biomedical Sciences, Worcester

in partial fulfillment of the requirements for the degree of

DOCTOR OF PHILOSOPHY

June 10, 2016

PhD Program in Biomedical Sciences

Immunology and Virology Program

## ACKNOWLEDGMENTS

First, I would like to express my gratitude to my co-mentors Dr. Robert Finberg and Dr. Jennifer Wang for inviting me into their lab and allowing me the freedom to pursue a variety of projects in the lab. I would like to thank Dr. Finberg for providing invaluable scientific insights into my work. In addition to scientific support, Dr. Wang also guided me through writing manuscripts, experimental design, and provided much needed cat pictures for stress relief. I know I wasn't always a model student, but thank you for all of your guidance.

The studies presented in this dissertation would have been impossible without our UMass collaborators in the Diabetes Center of Excellence. Thank you to everyone who provided advice, reagents, and  $\beta$  cell biology lessons. I would especially like to highlight the contributions of Dr. Dale Greiner, Dr. Michael Brehm, Dr. Rita Bortell and Dr. Chaoxing Yang. I would also like to thank members of the Dr. David Harlan's lab, including Dr. David Blodgett, Samba Redick, and Dr. Anthony Cura. Furthermore, thank you to Dr. Laura Alonso and Dr. Agata Jurczyk for teaching me all about the diabetes field.

The evolution of my thesis project into the work presented here would not have been possible without the guidance of my TRAC and dissertation committee members, Dr. Timothy Kowalik, Dr. Trudy Morrison, Dr. Abraham Brass, and Dr. Michael Brehm. Insights, discussion, troubleshooting advice, and difficult questions helped me grow as a scientist. An additional thank you to Dr. Bridget Wagner, my external advisor, for taking the time to review my dissertation and provide feedback during my defense.

I wish to thank many members of the Finberg lab consortium including members of the Wang and Kurt-Jones labs, including administrators and support staff. Thank you to Melvin Chan, Dr. Melanie Trombly, Debra Poliquin, Christopher MacKay, Natasha Qaisar, Michael King, Glennice Bowen, Ping Liu,

Suvana Lin, Milan Patel, Dr. Javier Ogembo, Dr. Gabriel Hendricks, and Dr. Ryan Nistler. You all make the lab a great place to conduct research.

The core facilities at UMass make it possible to conduct cutting edge research, and without their expertise, these studies would be impossible. Thank you to Ted Giehl and Susanne Pechold from the confocal and flow cytometry core. I would also like to thank the Animal Medicine staff and Pathology Core for all of their work.

Thank you to my fellow GSBS colleagues: Robin Brese, Andrew Zukauskas, Srinjoy Chakraborti, Dr. Djade Soumana, Joe Yawe, and all the others I am forgetting. I couldn't have found a better group of people to suffer through classes with.

The lunch time crew, some of the best worst people I know: Timmy Matheson, Noah Cohen, Kenny Lloyd, Brendan Hilbert, Melissa Fulham, Nick Stone, Janelle Hayes, Eric Swanson. Thanks for all the distracting, and occasionally insightful conversations.

To the late Paul D. Henion, my first research mentor, who took a chance on letting me splash around in the lab. Your kindness and encouragement gave me the confidence to give this "science" thing a shot.

For the continuing and unwavering support of my family: Mom, Dad, Megan, Erik, Kaelan. Thank you.

To my new in-laws: Sal, Rhonda, Maria, and Salvi. Thank you for feeding me and providing excuses to get out of the lab and visit.

Finally to the ones who deal with me every day: the fur-babies – Lola for making me get up from the couch occasionally for walks. Bug and Goose for snuggles and head-scratches. Belinda – your support into my crazy endeavors, even when I'm being unbearable, means the world to me. Thank you for being my partner, and I'm looking forward to our million adventures.

The work presented here was partly supported by the Innate Immunity Training Program Grant (NIH: 5T32AI095213-04) and Immunology Training Grant (NIH: A1095213-04).

## ABSTRACT

The increasing healthcare burden of type 1 diabetes (T1D) makes finding preventive or therapeutic strategies a global priority. This chronic disease is characterized by the autoimmune destruction of the insulin-producing  $\beta$  cells. This destruction leads to poorly controlled blood glucose and accompanying life threatening acute and chronic complications. The role of viral infections as initiating factors for T1D is probable, but contentious. Therefore, my goal is to better characterize the effects of viral infection on human  $\beta$  cells in their function of producing insulin and to define innate immune gene responses in  $\beta$  cells upon viral infection. These aspects were evaluated in various platforms including mice engrafted with primary human islets, cultured primary human islets,  $\beta$  cells derived from human stem cells, and a human  $\beta$  cell line. Furthermore, the contributions of cell-type specific innate immune responses are evaluated in flow cytometry-sorted primary human islet cells. Taken together, the results from these studies provide insights into the mechanisms of the loss of insulin production in  $\beta$  cells during virus infection, and characterize the antiviral innate immune responses that may contribute to the autoimmune destruction of these cells in T1D.

## TABLE OF CONTENTS

<b>ACKNOWLEDGMENTS</b>	<b>III</b>
<b>ABSTRACT</b>	<b>VI</b>
<b>TABLE OF CONTENTS</b>	<b>VII</b>
<b>LIST OF FIGURES</b>	<b>XI</b>
<b>LIST OF TABLES</b>	<b>XIII</b>
<b>LIST OF COPYRIGHTED MATERIALS</b>	<b>XIV</b>
<b>LIST OF ABBREVIATIONS USED COMMONLY IN THIS WORK</b>	<b>XV</b>
<b>CHAPTER I: INTRODUCTION</b>	<b>1</b>
1.1: THE GLOBAL IMPACT OF DIABETES MELLITUS	1
1.2: SYMPTOMS AND COMPLICATIONS OF DIABETES MELLITUS	1
1.3: DIABETES MELLITUS IS A HETEROGENEOUS DISEASE	3
1.4: AUTOIMMUNITY IN T1D	4
1.5: THE CURRENT STATE OF T1D THERAPIES	5
1.6: B CELL FUNCTIONS IN INSULIN PRODUCTION AND RELEASE	8
1.7: EVIDENCE FOR GENETIC FACTORS IN T1D	12
1.8: EVIDENCE FOR ENVIRONMENTAL FACTORS IN T1D	14
1.9: FURTHER EVIDENCE FOR ENTEROVIRUS INFECTION	17
1.10: ENTEROVIRUSES IN HUMAN DISEASE	20
1.11: ENTEROVIRUS REPLICATION	22
1.12: INNATE IMMUNE RECOGNITION OF PATHOGENS	27
1.13: ACTIVATION OF INNATE IMMUNE SIGNALING BY CVB	32
1.14: CONTRIBUTIONS OF INNATE IMMUNE SIGNALING IN THE DEVELOPMENT OF AUTOIMMUNITY	33
1.15: PREVAILING MECHANISTIC THEORIES ON THE VIRAL CONTRIBUTION TO T1D DEVELOPMENT	39
1.16: WORKING TOWARD BETTER UNDERSTANDING OF THE ROLE OF VIRUSES IN T1D	41
<b>CHAPTER II: VIRAL INFECTION OF ENGRAFTED HUMAN ISLETS LEADS TO DIABETES</b>	<b>46</b>
<b>2.1: ABSTRACT</b>	<b>47</b>
<b>2.2: INTRODUCTION</b>	<b>48</b>
<b>2.3: RESULTS</b>	<b>49</b>
2.3.1 CVB4-INFECTED MICE ENGRAFTED WITH HUMAN ISLETS DEVELOP DIABETES	49
2.3.2: GRAFTS FROM INFECTED MICE SHOW DECREASED INSULIN	56
2.3.3: CVB4 INFECTION PERSISTS IN HUMAN ISLET-ENGRAFTED MICE	59
2.3.4: PROFILING OF GENE EXPRESSION IN HUMAN ISLET GRAFTS	62
<b>2.4: DISCUSSION</b>	<b>66</b>
2.4.1: CONCLUSIONS	70
<b>2.5: MATERIALS AND METHODS</b>	<b>71</b>
2.5.1: MICE	71
2.5.2: HUMAN ISLET TRANSPLANTATION	71
2.5.3: MOUSE INFECTIONS	72

2.5.2: PCR	72
2.5.4: HISTOPATHOLOGY AND IMMUNOHISTOCHEMISTRY	73
2.5.5: IMMUNOFLUORESCENCE	73
2.5.6: GENE EXPRESSION PROFILING OF ENGRAFTED ISLETS	74
2.5.7: STATISTICAL METHODS	75

### **CHAPTER III: COMPARISON OF CVB INFECTION IN CULTURED PRIMARY HUMAN ISLETS AND IN HUMAN B CELL LINES** **76**

<b>3.1: ABSTRACT</b>	<b>77</b>
<b>3.2: INTRODUCTION</b>	<b>78</b>
3.2.1: OVERVIEW	78
3.2.2: CULTURED PRIMARY HUMAN ISLETS	79
3.2.3: ENTEROVIRUS INFECTION OF CULTURED PRIMARY HUMAN ISLETS AFFECTS B CELL FUNCTION	79
3.2.4: GENE EXPRESSION CHANGES AFTER ENTEROVIRUS INFECTION IN CULTURED PRIMARY HUMAN ISLETS	80
3.2.5: NEW MODELS OF HUMAN B CELLS	81
3.2.6: GOALS	82
<b>3.3 RESULTS</b>	<b>83</b>
3.3.1: GENE EXPRESSION PROFILING IN CULTURED HUMAN ISLETS AT 48 HPI	83
3.3.2: VIRUS TROPISM IN CULTURED PRIMARY ISLETS	86
3.3.3: KINETICS OF GENE EXPRESSION CHANGES IN PRIMARY HUMAN ISLETS AFTER INFECTION WITH CVB4	89
3.3.4: GENE EXPRESSION CHANGES IN PRIMARY HUMAN ISLETS INFECTED WITH CVB4 OR STIMULATED WITH POLY(I:C) OR POLY(DA:DT)	93
3.3.5: INFECTION AND GENE EXPRESSION IN SC-B CELLS	96
3.3.6: CVB INFECTION AND REPLICATION IN ENDOC-BH1 CELLS	100
3.3.7: GENE EXPRESSION IN CVB4-INFECTED ENDOC-BH1 CELLS	104
<b>3.4: DISCUSSION</b>	<b>106</b>
3.4.1: COMPARISON OF CVB4 INFECTION OF ENGRAFTED AND CULTURED PRIMARY HUMAN ISLETS	106
3.4.2: INSULIN STAINING OF CVB3-EGFP-INFECTED DISPERSED PRIMARY HUMAN ISLETS	109
3.4.3: GENES ASSOCIATED WITH B CELL FUNCTION ARE DECREASED AFTER CVB4 INFECTION	109
3.4.4: INNATE IMMUNE GENE EXPRESSION IN PRIMARY HUMAN ISLETS INFECTED WITH CVB4 OR TREATMENT WITH POLY(I:C) OR POLY(DA:DT)	111
3.4.5: COMPARISON OF SC-B TO PRIMARY HUMAN ISLETS	112
3.4.6: ENDOC-BH1 CELL INFECTIONS	114
3.4.7: CONCLUSIONS:	115
<b>3.5: MATERIALS AND METHODS</b>	<b>117</b>
3.5.1: VIRUS STRAINS	117
3.5.2: HUMAN ISLETS FOR EX VIVO STUDIES	117
3.5.3: SC-B CULTURE AND INFECTION	118
3.5.4: ENDOC-BH1 CULTURE AND INFECTION	118
3.5.5: GENE EXPRESSION PROFILING (FIGURE 3.1)	119
3.5.5: GENE EXPRESSION PROFILING (FIG 3.2, FIG 3-3, FIG 3.4)	119
3.5.6: ELISA	120



3.5.7: WIDEFIELD MICROSCOPY	120
3.5.8: IMMUNOFLUORESCENCE	120
3.5.9: FLOW CYTOMETRY	121
3.5.10: GENE EXPRESSION QRT-PCR	121
3.5.11: CVB GENOME QRT-PCR	122
3.5.12: STATISTICAL METHODS	122

## **CHAPTER IV: CVB4 INFECTION INDUCES CHANGES IN PDX1 LOCALIZATION IN HUMAN B CELLS** **123**

<b>4.1: ABSTRACT</b>	<b>124</b>
<b>4.2: INTRODUCTION</b>	<b>125</b>
4.2.1: OVERVIEW	125
4.2.2: PDX1 FUNCTION	125
4.2.3: CONTROL OF PDX1 TRANSCRIPTIONAL FUNCTION	126
4.2.4: PDX1 IN VIRAL INFECTION	131
4.2.5: GOALS	131
<b>4.3: RESULTS</b>	<b>132</b>
4.3.1: CHANGES IN EXPRESSION OF GENES IN THE PDX1 TRANSCRIPTIONAL NETWORK	132
4.3.2: CHANGES IN PDX1 PROTEIN LOCALIZATION UPON CVB4 INFECTION IN ENDOC-BH1 CELLS	134
4.3.3: PDX1 NUCLEAR LOCALIZATION IS ALSO DECREASED AFTER INFECTION WITH OTHER SEROTYPES OF CVB IN ENDOC-BH1 CELLS	136
4.3.4: CHANGES IN PDX1 LOCALIZATION ARE NOT A GENERALIZED VIRUS RESPONSE	138
4.3.5: CHANGES IN PDX1 LOCALIZATION IN NON-B CELLS	143
<b>4.4: DISCUSSION</b>	<b>147</b>
<b>4.5: MATERIALS AND METHODS</b>	<b>155</b>
4.5.1: CELL CULTURE AND INFECTION	155
4.5.2: VIRUS SOURCES	155
4.5.3: GENE EXPRESSION PROFILING	156
4.5.4: IMMUNOFLUORESCENCE	156
4.5.5: IMAGE QUANTIFICATION	157
4.5.6: FLOW CYTOMETRY	158
4.5.7: OVEREXPRESSION OF PDX1 IN HELA CELLS	158
4.5.8: STATISTICAL METHODS	158

## **CHAPTER V: IMMUNE STIMULATION OF ENDOCRINE CELL POPULATIONS SORTED FROM PRIMARY HUMAN ISLETS** **159**

<b>5.1: ABSTRACT</b>	<b>160</b>
<b>5.2: INTRODUCTION</b>	<b>161</b>
<b>5.3: RESULTS</b>	<b>164</b>
5.3.1: DEVELOPMENT AND ANALYSIS OF HUMAN PRIMARY ISLET CELLS SORTED BASED ON AUTOFLUORESCENCE CHARACTERISTICS.	164
5.3.2: EVALUATION OF SORTED POPULATIONS BY FLOW CYTOMETRY AND GENE EXPRESSION PROFILING	165
5.3.3: COMPARISON OF BASAL GENE EXPRESSION IN SORTED HUMAN ISLET POPULATIONS	171
5.3.4: GENE EXPRESSION PROFILING POLY (I:C) STIMULATION OF SORTED HUMAN ISLET POPULATIONS	172

<b>5.4: DISCUSSION</b>	<b>175</b>
5.4.1: PRIMARY HUMAN ISLET SORTING AND CULTURE	175
5.4.2: BASAL GENE EXPRESSION PROVIDES INSIGHTS INTO CELL-TYPE SPECIFIC VIRAL RESPONSES	176
5.4.3: GENE EXPRESSION FOR ISGs IS HIGHER IN SORTED A CELLS	178
5.4.4: FUTURE DIRECTIONS	180
5.4.5: CONCLUSIONS	180
<b>5.5: MATERIALS AND METHODS</b>	<b>181</b>
5.5.1: CULTURE AND DISSOCIATION OF HUMAN ISLETS	181
5.5.2: FLOW CYTOMETRY SORTING	181
5.5.3: CULTURE AND TREATMENT OF SORTED CELLS	181
5.5.4: FLOW CYTOMETRY ANALYSIS	182
5.5.5: NANOSTRING GENE EXPRESSION PROFILING	182
<b>CHAPTER VI: DISCUSSION</b>	<b>184</b>
6.1: OVERVIEW	184
6.2: B CELL DYSFUNCTION AND INNATE IMMUNE SIGNALING IN AN <i>IN VIVO</i> MODEL	186
6.3: COMBINING MODELS	189
6.4: POTENTIAL EXTENSIONS OF VIRAL INFECTIONS OF ENDOC-BH1 CELLS	191
6.5: CONCLUSIONS	194
<b>APPENDIX I: CHANGES IN MOUSE GENE EXPRESSION UPON CVB4 INFECTION</b>	<b>195</b>
<hr/>	
<b>APPENDIX I: MATERIALS AND METHODS</b>	<b>198</b>
CULTURE AND DISSOCIATION OF HUMAN ISLETS	198
<b>BIBLIOGRAPHY</b>	<b>200</b>
<hr/>	

## LIST OF FIGURES

Figure 1.1: Insulin release and production in response to glucose	10
Figure 1.2: Schematic of enterovirus genome	24
Figure 1.3: Overview of MDA5 signaling cascade	31
Figure 1.4: The induction of $\beta$ cell autoimmunity	38
Figure 1.5: The influence of CVB4 on $\beta$ cells	44
Figure 2.1: Overview of human islet-engrafted mouse studies.	52
Figure 2.2: Human islet-engrafted mice become hyperglycemic and have low levels of C-peptide and insulin following CVB4 infection.	53
Figure 2.3: Human islet grafts from CVB4-infected mice have diminished insulin levels compared to grafts from mock-infected control mice.	57
Figure 2.4: Viral replication is sustained following CVB4 infection of human islet-engrafted mice.	60
Figure 2.5. VP1 does not co-localize with human exocrine or ductal cells in the grafts of infected mice.	63
Figure 2.6: Graft gene expression in CVB4-infected animals by NanoString analysis.	65
Figure 3.1: Gene expression in ex vivo cultured human islets infected with CVB4 48 hpi.	84
Figure 3.2: Heatmap comparison of gene expression in CVB4 infection of primary human islets engrafted in mice or cultured ex vivo.	87
Figure 3.3: Changes in gene expression in ex vivo cultured human islets at multiple time points after CVB4 challenge.	90
Figure 3.4: Stimulation of ex vivo cultured human islets with poly(I:C) and poly(dA:dT) induces a similar IFN gene profile as CVB4, but a differential islet function genes profile.	95
Figure 3.5: SC- $\beta$ cells are permissive to CVB infection and display increased expression of antiviral response genes following infection.	97
Figure 3.6. EndoC- $\beta$ H1 cells are permissive to CVB4 infection and exhibit CPE consistent with lytic infection.	101
Figure 3.7: Assessment of gene expression in EndoC- $\beta$ H1 cells following CVB4 infection.	105
Figure 4.1: The regulatory network of the transcription factor PDX1	128
Figure 4.2: NanoString gene expression of genes in the PDX1 transcriptional network at 6 and 24 hpi in CVB4-infected primary human islets	133
Figure 4.3: EndoC- $\beta$ H1 nuclear PDX1 staining decreases upon CVB4 infection	137
Figure 4.4: EndoC- $\beta$ H1 nuclear PDX1 staining is decreased upon infection with either CVB1 or CVB5	139
Figure 4.5: EndoC- $\beta$ H1 nuclear PDX1 staining does not decrease upon	

transfection of a GFP-expressing plasmid or infections with VSV, or RSV	142
Figure 4.6: Ectopic expression of PDX1 in HeLa cells is excluded from the nucleus upon CVB4 infection.	144
Figure 5.1: Sorting strategy and evaluation of purity	166
Figure 5.2: Evaluation of basal gene expression of sorted human islet cells	170
Figure 5.3: Gene expression in sorted cell types after poly(I:C) treatment	174
Figure A1: Mouse gene expression in CVB4-infected animals by NanoString analysis	196

**LIST OF TABLES**

Table 1.1: Advantages and disadvantages of models used	45
Table 2.1: Demographic characteristics of human islet donors of engrafted islets	50
Table 6.1: Summary of $\beta$ cell function and innate immune responses	185

**LIST OF COPYRIGHTED MATERIALS**

Chapter II and portions of Chapter III are reprinted with permission.

Copyright ©2015 American Diabetes Association From Diabetes<sup>®</sup>, Vol. 64, 2015;

1358-1359 Reprinted with permission from The American Diabetes Association

Permission # CT021916-GG

**LIST OF ABBREVIATIONS USED COMMONLY IN THIS WORK**

**APC:** antigen-presenting cell

**ATF3:** Activating Transcription Factor 3 (*ATF3*)

**ATF4:** Activating Transcription Factor 4 (*ATF4*)

**AUF1:** adenosine-uridine (AU)-rich element RNA binding factor 1 (*HNRNPD*)

**c-Jun:** JUN (*JUN*)

**c/EBP $\beta$ :** CCAAT-enhancer-binding protein  $\beta$  (*CEBPB*)

**CAR:** coxsackievirus and adenovirus receptor (*CXADR*)

**CARD:** caspase activation and recruitment domain

**CHOP:** DNA-Damage-Inducible Transcript 3 (*DDIT3*)

**CPE:** cytopathic effect

**CVA:** Coxsackievirus A

**CVB:** Coxsackievirus B

**CXCL10:** Chemokine (C-X-C motif) ligand 10 (*CXCL10*)

**CXCR3:** Chemokine (C-X-C Motif) Receptor 3 (*CXCR3*)

**DAISY:** Diabetes and Autoimmunity Study in the Young (Colorado)

**DC:** dendritic cell

**DIPP:** Type 1 Diabetes Prediction and Prevention Study (Finland)

**dsRNA:** double stranded RNA

**ERK2:** Extracellular Signal-Regulated Kinase 2 (*MAPK1*)

**EV:** enterovirus

**GAD65:** glutamic acid decarboxylase-65 autoantigen

**GK:** Glucokinase

**GLUT2:** glucose transporter 2 (*SLC2A2*)

**GSK3:** Glycogen Synthase Kinase 3 Beta (*GSK3B*)

**GWAS:** genome-wide association study

**HbA1C:** glycated hemoglobin A1C

**HEV:** human enterovirus

**HLA:** human leukocyte antigen

**HN:** hormone-negative

**HNF3B:** Hepatocyte nuclear factor 3, beta (*FOXA2*)

**hTERT:** human telomerase reverse transcriptase (*TERT*)

**IA2:** tyrosine phosphatase autoantigen

**IAA:** proinsulin autoantigen

**IAPP:** islet amyloid polypeptide (*IAPP*)

**ICA:** islet cell antibodies

**IFIH1:** Interferon Induced With Helicase C Domain-containing protein 1

**IFIT2:** Interferon-Induced Protein With Tetratricopeptide Repeats 2 (*IFIT2*)

**IFN:** interferon

**IFNAR:** type I interferon receptor (*IFNAR1/2*)

**IFNGR:** Interferon gamma receptor (*IFNGR1/2*)

**IFNLR:** Interferon lambda receptor (*IFNLR1/IL10RB*)

**IIDP:** Integrated Islet Distribution Program



**IL-1 $\beta$** : interleukin 1 beta (*IL1B*)

**IL**: interleukin

**ILPR**: insulin-linked polymorphic region

**INS**: insulin (*INS*)

**IP**: intraperitoneal

**IRE1**: Inositol-Requiring Protein 1 (*ERN1*)

**IRES**: internal ribosomal entry site

**IRF3**: Interferon Regulatory Factor 3 (*IRF3*)

**ISG**: interferon stimulated genes

**ISG15**: Interferon-induced protein, 15 kDa, Ubiquitin-Like Modifier (*ISG15*)

**JAK**: Janus kinase (*JAK*)

**JNK**: c-Jun N-terminal kinase (*MAPK8*)

**LGP2**: laboratory of genetics and physiology 2 (*DHX58*)

**MAFA**: V-Maf Avian Musculoaponeurotic Fibrosarcoma Oncogene Homolog A  
(*MAFA*)

**MAVS**: Mitochondrial Antiviral Signaling Protein (*MAVS*)

**MDA5**: Melanoma Differentiation-Associated protein 5

**MHC**: major histocompatibility complex

**MX1**: Myxovirus Resistance Protein 1 (*MX1*)

**MyD88**: myeloid differentiation primary response gene 88 (*MYD88*)

**NES**: nuclear export signal

**NeuroD**: Neuronal Differentiation 1 (*NEUROD1*)

**NF- $\kappa$ B:** Nuclear Factor Of Kappa Light Polypeptide Gene Enhancer In B-Cells 1

(*NFKB1*)

**NK cells:** natural killer cells

**NLR:** NOD-like receptors

**NLS:** nuclear localization signal

**NSCS1:** NanoString CodeSet #1 (see Chapter II materials and methods for details)

**NSCS2:** NanoString CodeSet #2 (see Chapter III materials and methods for details)

**O.R.:** odds ratio

**OAS2:** 2'-5'-Oligoadenylate Synthetase 2 (*OAS2*)

**OGTT:** oral glucose tolerance test

**PABP:** poly(A)-binding protein

**PAMPS:** pathogen-associated molecular patterns

**PBMC:** peripheral blood mononuclear cells

**PC1/3 and PC2:** Proprotein convertases (*PCSK1/PCSK2*)

**PCIF1:** PDX1 C-Terminal Inhibiting Factor 1 (*PCIF1*)

**PDX1:** Pancreatic duodenal homeobox-1 (*PDX1*)

**PERK:** PRKR-Like Endoplasmic Reticulum Kinase (*EIF2AK3*)

**PKR:** protein kinase RNA-activated (*EIF2AK2*)

**Poly(I:C):** Polyinosinic:polycytidylic acid – double stranded RNA mimetic

**PRR:** pattern recognition receptors

**PTBP1:** polypyrimidine tract-binding protein 1 (*PTBP1*)

**PTPN2:** Tyrosine-protein phosphatase non-receptor type 2 (*PTPN2*)

**RdRp:** RNA-dependent RNA polymerase

**RIG-I:** retinoic acid inducible gene 1 (*DDX58*)

**RLR:** retinoic acid inducible gene 1 like receptors

**RSV:** respiratory syncytial virus

**SC- $\beta$ :**  $\beta$  cells directionally differentiated from human stem cells

**SNP:** non-synonymous single nucleotide polymorphisms

**SREBP-1c:** Sterol Regulatory Element Binding Transcription Factor 1  
(*SREBF1*)

**ssRNA:** single stranded RNA

**SST:** somatostatin (SST)

**STAT:** signal transducer and activator of transcription (STAT1)

**T1D:** type 1 diabetes mellitus

**Th1:** CD4+ T helper cells directed against intracellular pathogens

**TIR:** toll-interleukin receptor

**TLR:** Toll-like receptors

**TNF- $\alpha$ :** Tumor necrosis factor (*TNF*)

**TRIF:** TIR-domain-containing adaptor-inducing interferon- $\beta$  (*TICAM1*)

**TXNIP:** Thioredoxin Interacting Protein (*TXNIP*)

**TYK2:** Tyrosine kinase 2 (*TYK2*)

**USF1:** Upstream Transcription Factor 1 (*USF1*)

**USP18:** Ubiquitin specific peptidase 18 (*USP18*)

**UTR:** untranslated region

**VP1:** enterovirus viral protein 1

**VSV:** vesicular stomatitis virus

**WFS1:** Wolfram Syndrome 1 (Wolframin) (*WFS1*)

**ZnT8:** zinc transporter autoantigen

## CHAPTER I: INTRODUCTION

### 1.1: The global impact of diabetes mellitus

Type 1 diabetes (T1D) is a growing health issue worldwide. The incidence of T1D has increased over the past decades and is projected to continue on this trend<sup>1</sup>. The prevalence of the disease was 1.93 people per 1,000 in the United States population in 2009<sup>2</sup>. In addition to the impact of this chronic disease on the quality of life, diabetes also presents a dramatic economic burden. In the United States, the estimated cost of all diagnosed diabetes was \$176 billion in direct medical costs in 2012. As much as \$69 billion is lost due to combined reduced work productivity and inability to work<sup>3</sup>. Despite advances in diagnosis and therapies for diabetes, this disease continues to place a significant burden on patients, families, and public health.

### 1.2: Symptoms and complications of diabetes mellitus

Diabetes mellitus causes chronic hyperglycemia and includes symptoms of frequent urination, increased thirst and increased hunger, as well as non-specific symptoms of blurry vision, headache, and fatigue<sup>4</sup>. Diagnosis of diabetes mellitus is imperative to properly maintain blood glucose levels and prevent serious acute and chronic complications. A clinical diagnosis can be made with blood glucose measurements. Fasting blood glucose levels greater than 125 mg/dL and non-fasting glucose greater than 200 mg/dL both indicate a hyperglycemic state. Additionally, an oral glucose tolerance test (OGTT) can be administered to test the physiological response to a bolus of glucose. A blood

glucose measurement that is greater than 200 mg/dL 2 hours after an OGTT is indicative of diabetes. Additionally, glycated hemoglobin A1C (HbA1C), a marker of long-term glycemic control, can be utilized in diagnosis. Levels greater than 6.5% are considered in the diabetic range<sup>5</sup>. A positive test for any of these tests would require further evaluation for the therapeutic regimen to be developed.

Diabetes mellitus is associated with a variety of acute and chronic complications. The most common acute complication of diabetes mellitus is diabetic ketoacidosis. This occurs when diabetes leads to low levels of insulin, which increases breakdown of stored fatty acids in a process called lipolysis. The breakdown products of oxidative lipolysis in the liver are ketones, which can accumulate and cause metabolic acidosis. Diabetic ketoacidosis is a severe metabolic complication that can lead to coma and death<sup>6</sup>. Severe chronic complications arise from undiagnosed or poorly managed diabetes mellitus over a long period of time. Chronic diabetes mellitus is associated with atherosclerotic disease that affects the macro- and microvasculature. Perturbations in microvasculature blood flow leads to kidney damage, retinopathy, and peripheral neuropathy<sup>7</sup>. The prevention of acute and chronic complications of diabetes requires accurate diagnosis and careful management of the disease. Hypoglycemia is also a complication of diabetes and may result from skipping meals, high intensity exercise, or the improper administration of insulin or diabetes management drugs. In extreme cases a rapid drop in blood sugar causes anxiety, sweating, trembling, confusion, seizures, or even coma<sup>8</sup>.

### **1.3: Diabetes mellitus is a heterogeneous disease**

In the late 19<sup>th</sup> century, physicians began to recognize two distinct forms of diabetes mellitus that require different forms of treatment<sup>9</sup>. Prior to the purification of insulin for therapeutic use, the two forms of diabetes presented with different progression and outcomes. The first form was characterized as a rapid wasting disease where the condition of patients declined over the course of months. The second form was associated with overweight, older patients with much slower progression that could often be prolonged through alterations in diet<sup>9</sup>. The isolation of insulin from canine islets of Langerhans followed by the administration of bovine insulin extracts in diabetic patients ushered in a new era of understanding of diabetes mellitus<sup>10</sup>. The response to insulin treatment became a differentiating factor to separate patients broadly into insulin-sensitive and insulin-resistant diabetes mellitus<sup>9</sup>: insulin-sensitive patients would respond similar to healthy individuals upon administration of a bolus of glucose followed by intravenous insulin. This led to the hypothesis that insulin-sensitive diabetes is due to the deficiency of insulin production<sup>11</sup>. Eventually the insulin-sensitive form of diabetes would be referred to as type 1 diabetes mellitus<sup>9</sup>. Currently the American Diabetes Association further divides this category based on etiology. Type 1A diabetes is immune mediated and type 1B diabetes is non-immune mediated<sup>12</sup>. The remainder of this thesis will focus on type 1A diabetes mellitus, and will be referred to as simply T1D.

T1D is characterized by immune-mediated destruction of the insulin-producing  $\beta$ -cells of the pancreas. The current view of the natural progression of

this disease is as follows. Environmental triggers that may occur in utero or early in life combine with a genetic predisposition to cause immune dysregulation in the form of autoreactive B and T cells. The destruction of  $\beta$  cells by autoantibodies and cytotoxic T cells occurs over the course of months or decades before changes in glycemic control are detectable<sup>13</sup>. A considerable proportion of  $\beta$  cells are destroyed before metabolic changes in insulin production are detectable. By the time of diagnosis, most patients retain only 10-20% of  $\beta$  cell function<sup>14</sup>. Patients with T1D usually present with general diabetes mellitus symptoms, but also experience weight loss and have higher incidence of ketoacidosis. Routine testing for T1D reveals elevated fasting glucose and a positive OGTT, with only mild increases in HbA1c<sup>15</sup>.

#### **1.4: Autoimmunity in T1D**

Autoimmunity in T1D is mediated by  $\beta$  cell autoantibodies and infiltration of the islets of Langerhans with immune cells that include cytotoxic CD8<sup>+</sup> T cells. This infiltration of immune cells is referred to as insulinitis. Antibodies commonly associated with T1D are directed against proinsulin (IAA), glutamic acid decarboxylase-65 (GAD65), tyrosine phosphatase (IA2), and zinc transporter ZnT8 (Slc30A8)<sup>16</sup>. These autoantibodies are referred to collectively as islet cell antibodies (ICAs). Some of these proteins are also targets of autoreactive CD8<sup>+</sup> T cells that mediate direct killing of the targeted  $\beta$  cells<sup>17,18</sup>.

The presence of autoantibodies IAA, GAD65, and IA2 is predictive of progression to T1D<sup>19</sup>. These autoantibodies develop sequentially, with IAA antibodies often presenting first. High affinity antibodies in patients are reactive to



residues in the N-terminal region (residues 8-13) of proinsulin<sup>20</sup>. Despite autoantibodies against GAD65 often developing after IAA antibodies, GAD65 antibodies are still detectable several years before metabolic diagnosis of T1D<sup>21,22</sup>. While IAA is specific to T1D, GAD65 antibodies may be a more general marker of autoimmunity<sup>16</sup>. Detection of autoantibodies is a predictive marker for individuals who may progress to T1D and allows for early therapeutic intervention.

In addition to autoantibody production, the T cell response against proinsulin could help explain the highly efficient destruction of  $\beta$  cells in the development of T1D. The high number of CD3<sup>+</sup> T cells infiltrating the islets in T1D patients is evidence of T cells contributing to the progression of the disease<sup>23</sup>. T cells expanded from lymph nodes of T1D patients recognize a N-terminal epitope in proinsulin<sup>17</sup>. The N-terminal signal peptide and peptide cleavage site is recognized by CD8<sup>+</sup> T cells from diabetic patients<sup>24</sup>. T cell responses against GAD65 are also detected prior to the onset of clinical diabetes<sup>22</sup>. T cells cloned from patients respond and proliferate in response to presentation of GAD65 peptides<sup>18</sup>. The combination of multiple T cell reactivity against  $\beta$  cell antigens further illustrates the highly focused autoimmune reaction against  $\beta$  cells.

### **1.5: The current state of T1D therapies**

Insulin replacement therapy, first initiated in the 1920's, remains the best therapeutic option for treating T1D. Advances have occurred in the production methods and formulations of insulin, improving pharmacokinetic profiles<sup>25</sup>.

Additionally, the development of novel delivery systems of insulin pumps paired

with continuous glucose monitoring systems helps to maintain blood glucose in a more physiological range. Despite these advances, chronic complications of the disease still progress and the danger of hypoglycemic events due to improper insulin administration is real. This is especially true in younger patients where despite the use of insulin pumps, blood glucose is more variable than suggested guidelines to reduce complications<sup>26</sup>.

The development of new drugs and therapeutics focuses on modulating either the autoimmune destruction of  $\beta$  cells or methods of increasing  $\beta$  cell mass. Current approaches for modifying the immune response in T1D aim to promote immune tolerance or modulate inflammatory responses. One method that showed early promise was vaccination with GAD65 antigen. This was thought to induce immune tolerance by reducing the number of autoreactive T cells. This strategy failed to prevent the loss of C-peptide or improve clinical outcomes in a clinical trial<sup>27</sup>. Another approach was non-specific suppression of T cell function. Suppression of T cells by treatment with the anti-CD3 therapy, Teplizumab, could reduce the autoimmune attack on  $\beta$  cells. This treatment helps maintain insulin production in newly diagnosed patients<sup>28</sup>. Several other T1D immune therapies are in various stages of development, but have variable effects on the maintenance of C-peptide production and have been reviewed<sup>15</sup>. These findings are encouraging, but non-specific immune suppression can leave patients susceptible to infections.

More recently, T regulatory cells ( $T_{\text{regs}}$ ) were used to suppress the

autoimmune destruction of  $\beta$  cells. In a phase I clinical trial, autologous  $T_{\text{regs}}$  were taken from patients and expanded *in vitro*. These  $T_{\text{regs}}$  were then transferred back into patients. This led to an increase in the numbers of long-lived  $T_{\text{regs}}$ , and the maintenance of C-peptide in several patients<sup>29</sup>. This study is proof of principle that autologous  $T_{\text{regs}}$  can be used to modulate the immune responses in T1D patients without the broad depletion of T cells, which could leave patients immune compromised. While this new field of immune modulation to counteract autoimmunity is promising, the specificity and efficacy of the therapies must be improved to be considered a success.

Immunotherapy approaches may address the autoimmune cause of T1D, but  $\beta$  cell mass is usually severely diminished at the time of diagnosis. Therefore, these treatments may not be enough to reverse the course of disease<sup>30</sup>.

Regenerative and transplant approaches are being developed to replenish the  $\beta$  cell mass that is lost in T1D patients. In humans,  $\beta$  cell mass can be increased through  $\beta$  cell replication or transdifferentiation from other cells in the pancreas<sup>31</sup>. These processes may be targets for drug treatment to increase the number of  $\beta$  cells.  $\beta$  cell transplantation provides another possibility to increase  $\beta$  functional capacity. Allograft transplants of islet cells into the liver of T1D patients have some efficacy, with rates of insulin independence after transplant ranging from 10-70%. However, allograft transplantation requires immune suppression to prevent the destruction of the engrafted tissue, and many of these drugs exhibit  $\beta$  cell toxicity<sup>32</sup>. New sources of  $\beta$  cells provide alternatives to allogeneic donor

tissue.  $\beta$  cells that are directionally differentiated from stem cells can restore glycemic control in diabetic mice, and provide new therapeutic opportunities<sup>33</sup>. In the future, autologous stem cells could be differentiated into  $\beta$  cells, allowing for autologous transplantation of  $\beta$  cells to increase insulin production capacity. Such therapies may need to be combined with immune modulators to stop the underlying autoimmune reactions to allow for these cells to survive long term.

### **1.6: $\beta$ cell functions in insulin production and release**

Glucose is absorbed in the intestines and rapidly crosses into the blood stream. These sugars are delivered to all cells of the body through circulation to provide energy or for storage as glycogen. Circulating glucose levels are tightly regulated by the secretion of insulin from  $\beta$  cells. Insulin is a hormone that signals cells to increase their uptake of glucose, increase the synthesis of glycogen and triglycerides, and suppress hepatic glucose output from gluconeogenesis<sup>34</sup>. These activities act together to reduce blood glucose and increase glycogen stores. The control of insulin function incorporates gene transcription, protein processing, and control of release. In addition to signaling for the release of stored insulin, hormones from the gut trigger increased insulin biosynthesis<sup>35</sup>. In humans, insulin is encoded by a single gene<sup>36</sup>. Insulin is translated as a single polypeptide that is processed into two polypeptide chains joined by disulfide bridges<sup>37</sup>. Insulin is retained in secretory granules until the cell senses high concentrations of glucose to stimulate their release. Deficiencies in any of these steps can lead to poor control of blood glucose homeostasis, which is detrimental to the normal function of many organ systems.

$\beta$  cells respond to increased blood glucose by releasing insulin stores, and increasing insulin biosynthesis (Fig. 1.1). Sensing of increased blood glucose by  $\beta$  cells is mediated through import of glucose by the glucose transporter 2 (GLUT2) and the sensing of intracellular glucose by glucokinase (GK)<sup>38,39</sup>. GK mediates the transition of glucose to glucose-6-phosphate and is the rate-limiting step in glycolysis<sup>40</sup>. The metabolism of glucose increases mitochondrial ATP synthesis, which initiates the closure of ATP-regulated potassium channels. This causes plasma membrane depolarization and the opening of voltage-gated calcium channels<sup>41</sup>. The resulting increase in cytosolic calcium triggers the release of insulin granules that are poised for release at the cell surface<sup>42</sup>. These effects of increased glucose metabolism also trigger activation of insulin gene expression through the stimulation of the insulin promoter<sup>43</sup>.

Insulin biosynthesis begins with the regulation of insulin gene expression. Tissue specificity and control of insulin gene expression is controlled by the region 5' of the coding region. This region allows for positive and negative regulation in response to physiological stimuli through the binding of transcription factors or repressors<sup>44</sup>. The 5' flanking region of the insulin gene contains positive regulatory motifs for cis-acting elements and trans-activating factors. Several of these factors increase their activity in the presence of glucose, which could contribute to the increased insulin gene expression in response to glucose<sup>45</sup>.

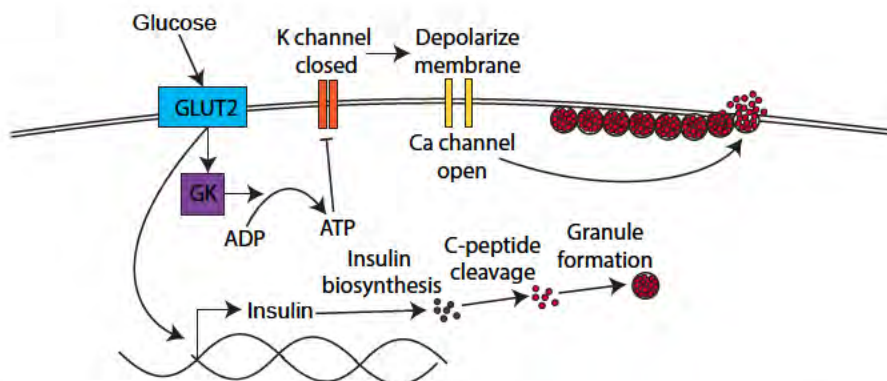


**Figure 1.1: Insulin release and production in response to glucose**

In  $\beta$  cells, glucose enters the cell through the GLUT2 receptor. Glucokinase (GK) is a key component in the metabolism of glucose and the process of producing ATP. The increase in ATP closes potassium channels, which causes the depolarization of the plasma membrane. This opens calcium channels and allows for the influx of calcium into the cell. High intracellular calcium triggers the release of insulin from granules docked at the plasma membrane. Increased glucose also triggers insulin transcription and biosynthesis. This includes processing of proinsulin in the trans-golgi network into the mature form through cleavage of the C-peptide. Matured insulin is incorporated into dense core granules and sorted for trafficking to the plasma membrane.

Insulin gene transcription is also negatively regulated through the activity of several proteins. BETA3 can inhibit E box-mediated insulin expression by inhibiting the function of E box-activating transcription factors<sup>53</sup>. The JNK-activated transcription factor c-Jun can inhibit insulin transcription through binding to E1<sup>54</sup>. This could indicate a role of reduction of insulin transcription in response to oxidative stress or the presence of pro-inflammatory cytokines. The transcription factor c/EBP $\beta$  can also reduce insulin transcription by directly binding to factors that bind to the enhancer region of the insulin gene<sup>55</sup>.

Insulin is translated as preproinsulin in the rough endoplasmic reticulum, and is co-translationally converted to proinsulin by the cleavage of the signal sequence<sup>56</sup>. To allow for the glucose-stimulated secretion, insulin must be sorted into the regulated secretory pathway of the trans-golgi network. Proinsulin is sorted and incorporated into immature dense-core granules to allow for regulated release<sup>57</sup>. The maturation of these granules includes three steps. The first is the acidification of the granules<sup>58</sup>. The second is the cleavage of proinsulin to insulin and C-peptide through proteolysis by two proprotein convertases, PC1/3 and PC2. The final step in maturation is the removal of nonspecific components of the granule including the clathrin protein coat<sup>59</sup>. These mature insulin granules exist as two populations in  $\beta$  cells. The readily releasable pool is pre-docked to the plasma membrane with a calcium-dependent fusion complex to allow for first phase insulin secretion<sup>60</sup>. The second pool allows for the prolonged second phase of insulin release<sup>61</sup>. Upon release of insulin from  $\beta$  cells, insulin enters

portal circulation and following first pass through the liver, then enters into the systemic circulation.

### **1.7: Evidence for genetic factors in T1D**

Similar to the heterogeneity of the clinical presentation of diabetes, many genetic factors can contribute to diabetes. The complexity of genetic factors is highlighted by studies in monozygotic twins. In twin cohorts under the age of 40, the concordance between siblings is around 50%. In contrast, the concordance is near 90% in cohorts older than 40 years<sup>62</sup>. The low concordance in the younger group highlights the multifactorial nature of the development of T1D.

Many factors may contribute the development of T1D, and polymorphisms at several distinct genetic loci are identified as risk factors. Many non-synonymous single nucleotide polymorphisms (SNPs) are associated with the development of the disease. While the contributions of individual SNPs to the risk for developing the disease may be small, different combinations of SNPs contribute to the overall risk for an individual. SNPs in human leukocyte antigen (HLA) genes, the insulin gene, and non-HLA immune genes are associated with the development of T1D.

Associations of HLA genes with other autoimmune diseases prompted the search for HLA genes that contribute to T1D. HLA proteins are expressed on the surface of all nucleated cells in the case of the class I major histocompatibility complex (MHC), while class II MHC HLA expression is restricted to antigen presenting cells on certain types of immune cells. HLA genotypes can account for half of the familial clustering of T1D<sup>63</sup>. Linkage analysis studies identified the



6p21 chromosomal region as a genetic susceptibility locus, which initially implicated the MHC genes<sup>64</sup>. This region confers the highest genetic risk for T1D. The class II MHC genes, HLA-DR and HLA-DQ, are the most important genetic factors and account for approximately 40% of genetic risk for T1D<sup>65</sup>. Individual HLA alleles only contribute modestly to the risk of T1D, but the combined odds ratio (O.R.) for all HLA genes together is quite high (O.R. >6.5)<sup>66</sup>. People with two predisposing haplotypes have the greatest risk. The most common risk genes are DRB1\*0301 (DR3) which often associates with DQA1\*0501-DQB1\*0201 (DQ2) and DRB1\*0401 or DRB1\*0401 (DR4) with DQA1\*0301-DQB1\*0301 (DQ8). Protection from T1D is conferred by the HLA-DR2 in association with DQB1\*0602<sup>67</sup>.

In addition to HLA genes, SNPs in other genes also contribute to T1D susceptibility. Interestingly,  $\beta$  cells themselves express mRNA of >80% of the T1D candidate genes, which highlights the role that  $\beta$  cells themselves play in the development of the autoimmune attack<sup>68</sup>. Polymorphisms in the INS gene are associated with T1D<sup>69</sup>. The rs7111341 SNP has one of the most significant associations of all the non-HLA risk SNPs<sup>70</sup>. This association could help explain the production of IAA autoantibodies produced in T1D.

Among the non-HLA SNPs are many genes that are involved in innate immune signaling in the production of antiviral interferon responses<sup>69,71</sup>. The SNPs in the innate immune double stranded RNA (dsRNA) sensor, MDA5, that decrease its function are associated with protection from T1D<sup>72</sup>. Tyrosine kinase

2 (TYK2) mediates signaling of the type I IFN receptor and SNPs that decrease its function are associated with T1D protection. The SNP rs2304256:C>A decreases the interaction with the type I interferon receptor (IFNAR1) and decreases downstream signaling<sup>73,74</sup>. TYK2 phosphorylates signal transducer and activator of transcription (STAT) to promote the production of interferon stimulated genes. SNPs that decrease the function of inhibitory genes of STAT function are associated with increased risk of T1D. PTPN2 is a phosphatase that inhibits STAT function, and the rs45450798 SNP accelerates progression to T1D after the appearance of autoantibodies<sup>75</sup>. USP18 suppresses STAT driven gene production<sup>76</sup>. The contributions of IFN-I signaling in the context of viral infection and contribution to T1D development will be discussed more below and outlined in Figure 1.3.

### **1.8: Evidence for environmental factors in T1D**

While it is clear that HLA and non-HLA genes contribute to the development of T1D, inheritance of high-risk genotypes does not completely predict the development of T1D. Therefore, it is possible that these genetic variants increase susceptibility to environmental factors that trigger the development of the disease. Seasonal incidence and spatial clustering studies provided some of the earliest evidence for the potential contribution of environment in the development of T1D. Seasonality of T1D incidence is a phenomenon first described in 1926 with an increase of cases identified during the winter months in Minnesota<sup>77</sup>. This finding is replicated in a worldwide survey of T1D incidence with peak incidence in October through January<sup>78</sup>. It is unclear

from these studies what causes the seasonal incidence. Factors of diet (cows milk proteins, vitamin D deficiency), toxins (streptozotocin and nitrites), psychological factors have been reviewed<sup>79</sup>.

In addition to seasonal variations in T1D incidence, spatial clustering of the onset of T1D occurs on both large and small scales. A number of small-scale clusters of T1D incidence have also been reported. A cluster of 27 new cases was reported in 1986 in one county in England<sup>80</sup>. Several clusters of family members being diagnosed with T1D in a short time frame, often following or coinciding with enterovirus infections have been reported (reviewed here<sup>81</sup>). In one case, simultaneous infection of monozygotic twins with enterovirus resulted in both siblings developing T1D<sup>82</sup>. These cases are rare, but they highlight the potential combinatorial nature of T1D, combining the predisposing genetic factors of family members with a simultaneous exposure to environmental triggers. Differences in T1D incidence that varies based on country cannot be entirely attributed to racial or ethnic variations between affected countries or regions<sup>83</sup>. Taken together this epidemiological evidence points to environmental factors as potential precipitating factors for T1D in genetically predisposed people.

Epidemiologists have also tried to link environmental exposures of diet, toxins, and infections with T1D through case-control studies. In a population based, case-control study of 217 T1D patients and 258 control subjects were surveyed about consumption of cow's milk, breastfeeding habits, and infections three months prior to the onset of diabetes. This study found that breast feeding

for greater than 3 months is associated with a protective effect (O.R. 0.66), while consumption of cow's milk before three months of age are associated with an increased risk (O.R. 1.52). Reports of an infection three months prior to T1D onset is a risk factor for developing T1D (O.R. 2.92)<sup>84</sup>. While these results are encouraging for a link between environmental factors, retrospective studies can introduce unintended bias in the study and are difficult to identify causality.

To mitigate the shortcomings of case-control studies, several countries have established large-scale prospective studies to identify environmental factors contributing to T1D. In the Finnish Type 1 Diabetes Prediction and Prevention Study (DIPP), newborns are screened for HLA risk alleles HLA-DQB1\*02/\*0302 or \*0302/x (where x refers to alleles other than \*02, \*0301, or \*0602).

Longitudinal samples are taken from these patients every 3-6 months in the first 2 years of life and then 6-12 months thereafter. Children are screened for the formation GAD65, IAA, and IA2 autoantibodies. Post-hoc analysis of birth cohort for enterovirus antibodies and viral RNA were both found more commonly in children that developed T1D compared to those who did not<sup>85,86</sup>. Similar results were observed in the Diabetes and Autoimmunity Study in the Young (DAISY) in children followed prospectively in Colorado. The presence of enteroviral RNA in the serum was detected more commonly in children who developed T1D<sup>83,87</sup>.

Other prospective studies found no association between enterovirus infection and the development of T1D. In the German BABYDIET study, 150 children who had genetic or familial risk for T1D were followed longitudinally with

blood and stool sample collection every 3 months for the first 3 years of life, and yearly thereafter. Infections and clinical symptoms were also logged daily for the first year. In a follow-up study, samples from 22 children who developed T1D and 82 who did not were evaluated for viral RNA. There was no difference in the detection of enterovirus RNA between these groups<sup>88</sup>. Differences in these studies could be attributed to heterogeneity in the study design, specifically the sampling frequency for viral RNA. Since viral RNA is rarely detected 3 months after infection, viremia may have gone undetected in studies with longer sampling intervals. The differences in the findings highlight the difficulty in establishing a causal link between enterovirus infection and T1D. The contrasting findings in these studies of these prospective studies make the contribution of enteroviruses to the development of T1D a contentious issue.

### **1.9: Further evidence for enterovirus infection**

Viral infections are a common environmental insult and they can have both short and long-term consequences. Infections with cytomegalovirus<sup>89</sup>, Epstein-Barr virus<sup>90</sup>, mumps virus<sup>91,92</sup>, rotavirus<sup>93</sup>, and rubella virus<sup>94</sup> have all been implicated in the development of T1D. The most evidence has accumulated for infections with enteroviruses as a precipitating factor for the development of T1D. Serology against enteroviruses, viral proteins in tissue, viral RNA, and isolation of enteroviruses from recent onset T1D patients provide compelling evidence for the etiologic role of enteroviruses in T1D. Associations are described for all six coxsackievirus B (CVB) serotypes, and several echovirus and enterovirus species (see review<sup>95</sup>).

One of the initial observations that linked virus infection with T1D was the increased incidence of T1D following seasonal enterovirus epidemics<sup>96</sup>. Furthermore, neutralizing antibodies against CVB4 in newly diagnosed T1D patients can be detected<sup>97</sup>. Other enteroviruses are also linked to the development of T1D. Following an echovirus outbreak in Cuba, autoantibodies were detected in patients that recovered from the infection<sup>98</sup>. A virus antibody survey for neutralizing antibodies against all 6 CVB serotypes indicates a link between antibodies against CVB1 and the development of T1D<sup>99</sup>. Additionally the presence of anti-CVB1 can be used to predict the development of T1D<sup>100</sup>. Neutralizing antibodies are more common against a CVB4 strain that establishes persistent infections in children with T1D and there is an association with higher antibody titers with the GAD65 autoantibodies<sup>101</sup>. Despite these trends of antibodies against enteroviruses in T1D patients, these studies are contentious due to the lack of matched HLA risk alleles in control samples<sup>102</sup>.

Enteroviral proteins are detected in pancreatic tissue specimens from individuals with T1D. Enterovirus viral protein 1 (VP1) is detected in the  $\beta$  cells of recent onset T1D patients more often than in control samples by immunohistochemical staining<sup>103</sup>. In a follow-up study, reactivity for VP1 was found in 20% of recent onset T1D patients. The presence of viral proteins also correlates with increased expression of the viral response protein, protein kinase R (PKR)<sup>104</sup>. The presence of viral protein does not necessarily indicate active replication in these samples.

Detection of viral RNA may be transient in patients and limited by the acute phase of viral replication. This complicates the association of viral infection with the development of disease. Other aspects of the progression of T1D pathogenesis that obscure the association with viral infection include variability in autoimmune development and presentation of clinical manifestations. Despite these potential difficulties in associating the presence of viral RNA with T1D progression, several studies established a correlation. Detection of enterovirus RNA sequences is associated with the presence of islet autoantibodies<sup>105</sup>. Furthermore, enteroviral RNA is detected more often in prediabetic children prior to the increase in autoantibodies against GAD65<sup>106</sup>. Enterovirus RNA is most common in the 6 months preceding the first autoantibody positive sample<sup>107</sup>. Viral RNA is also detected in peripheral blood mononuclear cells (PBMCs) in recent onset T1D patients<sup>108</sup>. A meta-analysis of 24 case-control studies found a clinically significant association between the presence of viral RNA or proteins with the development of both islet autoimmunity (O.R. 3.7) and T1D in humans (O.R. 9.8)<sup>109</sup>.

In addition to the detection of viremia prior to the development of T1D, virus has also been isolated from these patients. Mice infected with a clinical sample of CVB4 isolated from a child with diabetic ketoacidosis was able to promote the development of hyperglycemia in these mice<sup>110</sup>. CVB isolated from pancreas biopsy samples taken from six living patients with newly diagnosed T1D failed to amplify in vitro, so these viruses may replicate poorly<sup>111</sup>.

Taken together, there is substantial evidence for the presence of enteroviral infection prior to the development of T1D. However, a direct causal link between viral infection and the development of T1D is elusive. This is partly due to limitations in the detection and identification of viral infection and the poorly defined timing between the initiation and clinical onset of T1D. The first limitation is the transient nature of the production of viral RNA or proteins. The absence of viral proteins in some T1D patients highlights the difficulty of linking viral infections to the development of T1D. Even if a persistent infection is established, viral replication may be below the limit of detection or viral proteins may not be actively produced. The undefined timeframe between the putative precipitating factor and the presence of clinical T1D diagnosis further complicate establishment of a causal relationship. The intervening time may be from months to years in some cases and involve the contributions of multiple initiating factors. A better understanding of the mechanisms mediating the dysfunction of  $\beta$  cells upon viral infection and their contributions to innate immune signaling will help to develop methods to determine their role in the initiation of T1D.

#### **1.10: Enteroviruses in human disease**

The *Picornaviridae* family of viruses is a genetically diverse group of non-enveloped, positive sense, single stranded RNA viruses that cause a range of disease in humans. The genera of viruses in this family that are associated with human disease include *Enterovirus*, *Hepatovirus*, *Parechovirus*, *Cardiovirus*, and *Kobuvirus*<sup>112</sup>. Species in the *Enterovirus* genus that infect humans are HEV-A, -B, -C, -D and rhinovirus-A, -B, -C. These species include important human



pathogens polioviruses, coxsackievirus A (CVA), coxsackievirus B (CVB), echoviruses, other enteroviruses, and rhinoviruses<sup>113</sup>. While these viruses cluster together on a genetic basis, their replication and disease presentation are diverse. So historical groupings based on phenotypic manifestations in infected mice are still useful. For example, CVA and CVB can be separated based on their pathogenicity in humans and animals. CVA viruses affect skeletal and heart muscle and induce flaccid paralysis in mouse models. In contrast, CVB tropism is much broader in mouse tissue. CVB infects the central nervous system, liver, exocrine pancreas, brown fat and striated muscle and cause spastic paralysis<sup>113</sup>.

Enterovirus (EV) infection is usually transmitted fecal-orally. The virus begins replication in oropharyngeal and intestinal mucosa. After crossing the intestinal barrier, the virus travels to the lymph nodes, which allows progression to overt viremia<sup>114</sup>. Enteroviruses can be detected in stools for up to 3-4 weeks post infection, although in some cases they can be detected 2-3 months after infection. The incubation period is between 2-30 days for symptoms to develop<sup>114</sup>. Most EV infections are asymptomatic, but this varies wildly based on the type and strain of virus. EV infections are among the most common viral infections in the United States with an estimated 10-15 million symptomatic infections each year<sup>115</sup>. Incidence of reported EV infections has seasonal variation with a sharp increase in cases during late summer and autumn months. Among the EV infections reported from 1970 to 2005, CVB serotypes were often associated with fatal outcomes. Specifically, CVB4 infections have the highest

risk of death compared to other EV serotypes. Outbreaks of CVB4 are rare<sup>116</sup>. CVB infections cause a wide range of disease from asymptomatic to mild symptoms of fever, summer cold, and rash to severe outcomes like myocarditis, meningitis, and pancreatitis<sup>117</sup>. CVB frequently infects the CNS of newborns and infants and is responsible for >85% of aseptic meningitis cases<sup>118</sup>. CVB also causes fulminant pancreatitis, which leads to exocrine pancreas insufficiency<sup>119</sup>. Viruses in this family are also associated with the development of T1D as outlined above, but this association remains controversial.

While CVB infections are usually acute and self-limiting, there is some evidence that persistent viral infections do occur. CVB RNA can be found in heart tissue months after infection<sup>120</sup>. This may be associated with 5'-terminal deletions in the genome that allow for slower replication<sup>121</sup>.

### **1.11: Enterovirus replication**

Genomic RNA in the *Picornaviridae* family varies in length from 7 to 8.8kb and has stereotypical genetic organization. A 5' untranslated region (5' UTR) is followed by a protein coding region and a 3' UTR. The protein-coding region encodes for a polyprotein that is proteolytically cleaved by viral proteases during and after translation<sup>122</sup>. This processing yields four structural proteins (VP1-4) that comprise the capsid and seven nonstructural proteins (2A-C and 3A-D) that have various other functions in viral replication<sup>123</sup>. These are outlined in Figure 1.2.

The terminal UTRs provide structural motifs required for viral replication that allow transcriptional and translational regulatory factors to bind. The 5' UTR

contains structural elements that are important for translation. This includes an internal ribosomal entry site (IRES) that is required for the initiation of cap-independent translation of the viral polyprotein. The IRES recruits transactivating factors such as polypyrimidine tract-binding protein 1 (PTBP1) that recruits ribosomes to the viral RNA<sup>124</sup>. Additionally, the 5' UTR is covalently linked to The VPg (3B) protein and facilitates priming for transcription of the viral RNA dependent RNA polymerase (RdRp)<sup>125,126</sup>. Furthermore, the 3' UTR also contains important regulatory features including a pseudoknot structure and a polyA tail<sup>127,128</sup>. The mutations and deletions in the UTRs can modulate viral replication efficiency and persistence<sup>121</sup>.

Viral entry of CVB viruses into host cells is mediated primarily through binding to the coxsackievirus and adenovirus receptor (CAR)<sup>129</sup>. CAR is a transmembrane member of the tight junction protein family, so access

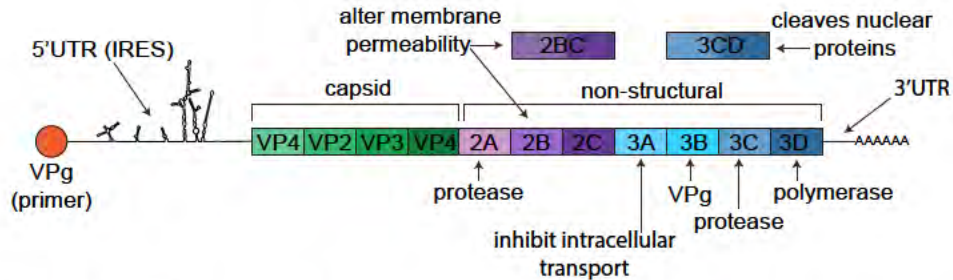


### Figure 1.2: Schematic of enterovirus genome

The enterovirus positive strand genomic RNA has a VPg (3B) protein at the 5' end that acts as a primer for replication. The 5' UTR contains an IRES for cap-independent translation. The genome is translated as a single polyprotein that is cleaved by viral proteases 2A and 3C. The resulting proteins include structural capsid proteins (VP1-4) and non-structural proteins (2A-C, 3A-D). Individual and intermediate cleavage products have a variety of functions on cell function and viral replication. Proteins 2BC and 2B alter membrane permeability, 3CD cleaves nuclear proteins, and 3D is the viral RdRp.

of the virus to CAR in polarized tissue may be limited<sup>130</sup>. Some CVB serotypes can bind to the co-receptor, decay activating factor (DAF), which delivers the virus to CAR to overcome the limited availability of the receptor in polarized cells<sup>131</sup>. Internalization of the virus bound to CAR is cell type dependent, but is sufficient for the initiation of uncoating<sup>132</sup>. Internalization is mediated through caveolin and is independent of clathrin<sup>133,134</sup>. Uncoating and viral RNA release from the virion is mediated through conformational changes that involve the loss of VP4 that allows for the formation of a pore<sup>135</sup>. While this is the main entry mechanism for CVB4, other CVB serotypes may utilize other receptors or alternate mechanisms<sup>136</sup>.

Upon entry and release of the genomic RNA, viral translation is initiated through the cap independent mechanisms described above. The polyprotein is rapidly co- and post-translationally cleaved into 11 individual proteins, and some intermediates that have independent functions. Cleavage of the polyprotein is mediated by self-activated viral proteases 2A and 3C, which are both chymotrypsin-like proteases<sup>123</sup>. Most cleavages of the polyprotein occur at defined glutamine-glycine junctions<sup>122</sup>. These proteases are also important in modulating the host cell to promote viral replication. They inhibit host mRNA translation by directly cleaving eukaryotic translation initiation factors, eIF4GI and eIF5B<sup>137,138</sup> and cleavage of polyA-binding protein (PABP)<sup>139</sup>. The precursor protein 3CD contains a nuclear localization signal (NLS) that allows for transport into the nucleus, where it can cleave TATA-box binding protein and other host

factors to further inhibit host transcription<sup>140,141</sup>. Furthermore, 2A can disrupt nucleo-cytoplasmic trafficking through cleavage of components of the nuclear pore complex<sup>142</sup>. In addition to suppression of host gene transcription, viral proteases also modulate immune activation. 3C suppresses innate immune signaling by cleavage of MAVS and TRIF proteins<sup>143</sup>. All of these protease activities modulate host proteins to optimize the intracellular environment for efficient viral replication.

Replication of the viral genome occurs through the RdRp activity of the 3D protein. 3D utilizes the VPg attached to the 5' end of the genome as a primer to initiate transcription<sup>125,126</sup>. This is a highly error prone polymerase, which incorporates 1-2 errors per genome copy<sup>144</sup>. 3D is also capable to template switching in a form of “replicative recombination.” This is thought to simultaneously ensure the stability of the genome, while also introducing additional variation.

The release of mature CVB virions from infected cells is not completely understood, but the viral protein B2 increases plasma membrane permeability, which could facilitate virion release<sup>145</sup>. Other potential mechanisms are direct lysis of infected cells or through the initiation of apoptosis<sup>146</sup>. Along with these mechanisms of virion release, viral RNA can be transferred to adjacent cells through phosphatidylserine-containing vesicles<sup>147</sup>. Viruses likely utilize a combination of these mechanisms depending on the cell-type and immune response to the viral infection.

### **1.12: Innate immune recognition of pathogens**

The innate immune system is a broad category of non-specific protective factors against pathogens. These include anatomical barriers like the skin and tightly associated epithelial tissues of the lungs and digestive tract. There are also cell intrinsic sensors that detect the presence of pathogens that are used to recruit cells of the innate immune system. These specialized immune cells include natural killer (NK) cells, monocytes, polynuclear phagocytes, and eosinophils. These cells all respond broadly to tissue injury or cytokine responses to pathogens. Some of these cells act as intermediaries between the innate and adaptive immune system by processing pathogen antigens for presentation to B and T cells in lymphatic tissues. These cells are referred to as antigen-presenting cells (APCs). The interplay between innate immune signaling and presentation of antigen can aid in efficient clearance of pathogens. But detrimental effects are possible in the case of inefficient immune response or excessive immune response. Inefficient immune response can allow for continued replication of the pathogen and pathogenesis to occur. Inefficient clearance of low virulence pathogens can also result in a persistent infection. On the other hand, excessive immune responses can cause immune pathology. Interestingly, both inefficient clearance and excessive immune response are associated with the development of autoimmunity and will be further discussed below. Here I will focus on the cell intrinsic mechanisms in the response to viral infections.

In mammals, recognition of viral infection begins with cellular pattern

recognition receptors (PRRs) that recognize stereotypical pathogen-associated molecular patterns (PAMPs). Detection of viral PAMPs is mediated through three families of PRRs, namely the Toll-like receptors (TLRs), the retinoic acid inducible gene 1 (RIG-I) like receptors (RLRs), and the NOD-like receptors (NLRs). The cell localization of these PRRs facilitates recognition of the virus at various stages of replication.

TLRs are type I transmembrane glycoproteins that are expressed in a cell type-specific manner. TLRs are expressed in immune cells including dendritic cells (DCs), macrophages, B cells, and NK cells. They are also expressed in non-immune cells including some fibroblasts, endothelial, and epithelial cells. Cell surface TLRs can recognize components of the viral envelope or capsid during virus attachment or endocytosis. TLRs 1, 2, and 4-6 are localized on the cells surface and recognize either viral proteins or lipids. Intracellular vesicle localization of TLRs in endosomes, lysosomes, and endoplasmic reticulum can detect viral components released during uncoating or through degradation of virions in endosomes. TLRs 3, 7, 8, and 9 are primarily localized in these endocytic compartments and sense nucleic acids. Upon formation of endocytic vesicles, fusion with these TLR-containing vesicles allows for recognition of endocytic cargo<sup>148</sup>.

Upon interaction of TLRs with their cognate ligands, downstream activation is mediated through adaptor proteins. The toll-interleukin receptor (TIR) domains of adaptor molecules, myeloid differentiation primary response



gene 88 (MyD88) and TIR-domain-containing adaptor-inducing interferon- $\beta$  (TRIF) interact with the TIR domains of activated TLRs. All TLRs, except for TLR3, initiate proinflammatory cytokines in macrophages and DCs through MyD88 activation of NF- $\kappa$ B. TLR3 and TLR4 recruit TRIF to activate NF- $\kappa$ B or IRF3, which induces the production of proinflammatory or IFN-I respectively<sup>149</sup>. These responses can depend on the TLRs and adaptor proteins that are expressed in different cell types.

The three members of the RLR family are expressed in the cytosol of most cells, and detect genomic nucleic acids or replication intermediates of viruses. Members of the RLR family include DExD/H helicases melanoma differentiation factor 5 (MDA5, encoded by the gene *IFIH1*), RIG-I, and laboratory of genetics and physiology 2 (LGP2)<sup>149</sup>. RIG-I and MDA5 both share similarity in their protein structure, with an RNA helicase domain, and two caspase activation and recruitment domains (CARDs). They also have a repressor domain that suppresses the activity of the CARD domains in the inactive conformation<sup>150</sup>. RIG-I recognizes the ends of both dsRNA and ssRNA in the presence of a 5'triphosphate<sup>151,152</sup>. In contrast, the dsRNA ligand for MDA5 is less well defined. MDA5 signaling occurs upon recognition of dsRNA that is 1-2kb in length<sup>153</sup>. MDA5 cooperatively binds internally to long dsRNA which results in the formation of filaments that contribute to downstream signaling<sup>154</sup>. This signaling cascade is outlined in Figure 1.3. The activation of both RIG-I and MDA5 allows the CARD domains to interact with the mitochondrial antiviral signaling (MAVS) protein.

Activated MAVS induces the transcription of type I IFN (IFN-I) genes through phosphorylation of IRF3 or the activation of proinflammatory cytokines through NF- $\kappa$ B<sup>155</sup>.

Signaling from both TLRs and RLRs converge on the production of interferons (IFNs). The IFN family includes three classes of related cytokines, type I IFN (IFN-I), type II IFN (IFN-II), and type III IFN (IFN-III). The IFN-I group includes thirteen different INF- $\alpha$  types, along with IFN- $\beta$ , IFN- $\epsilon$ , IFN- $\kappa$ , and IFN- $\omega$ . Members of this group all signal through the IFN-I receptor (IFNAR). IFN-II only contains one member, IFN- $\gamma$ . This cytokine signals through the IFN-II receptor (IFNGR)<sup>156</sup>. IFN-III is composed of three members, IFN- $\lambda$ 1 (IL-29), IFN- $\lambda$ 2 (IL-28A), and IFN- $\lambda$ 3 (IL28B). These signal through the IFN-III receptor (IFNLR) which is composed of a heterodimer of IL-28 receptor- $\alpha$  (IL-28R $\alpha$ ) and IL10R $\beta$ <sup>157</sup>. Upon the activation of the receptor by dimerization, IFNAR and IFNGR are autophosphorylated and activate their associated with members of the Janus activated kinase (JAK) family. The phosphorylated JAK proteins, including tyrosine kinase 2 (TYK2) and Janus-associated kinase 1 (JAK1), then phosphorylate signal transducer and activator

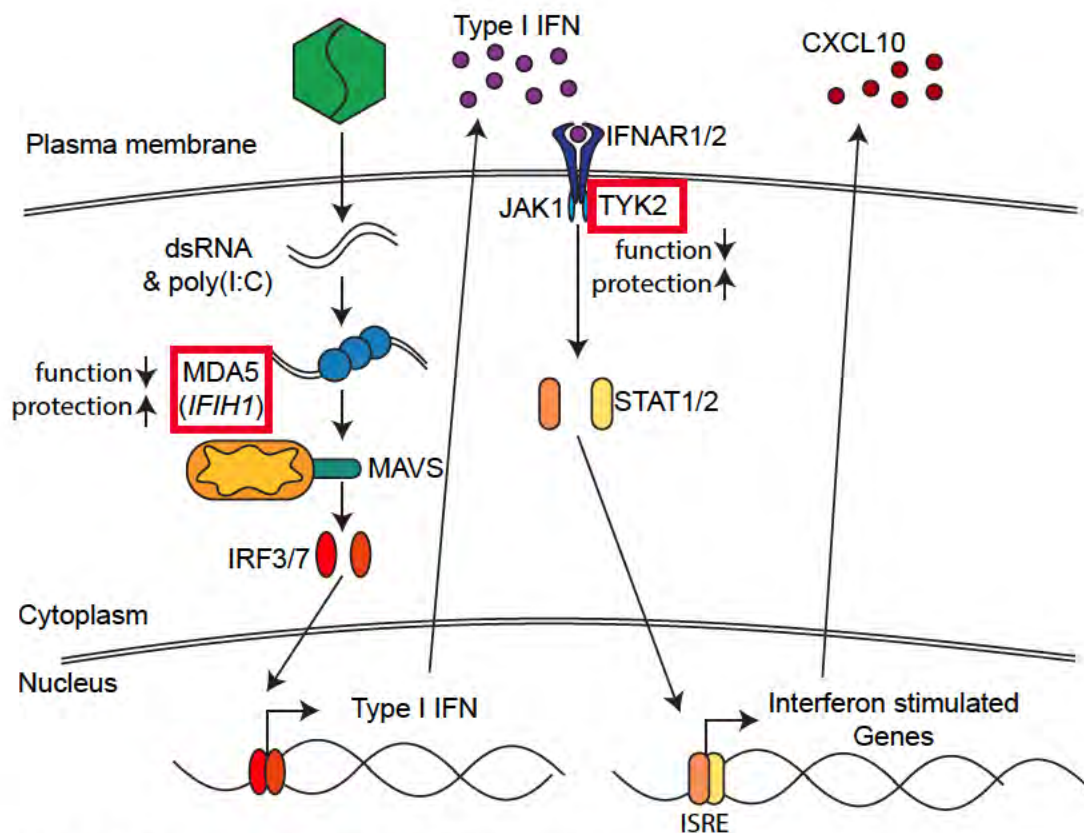


### Figure 1.3: Overview of MDA5 signaling cascade

Replication intermediates in the form of dsRNA are sensed in the cytoplasm by MDA5. MDA5 filaments signal through the mitochondrial-associated adaptor protein, MAVS, and leads to dimerization and translocation of IRF3/7 to the nucleus. This induces the production of IFN-I, which acts in an autocrine or paracrine fashion. IFN-I binds to IFNAR1/2 on the cell surface and signals through adaptor proteins, JAK1 and TYK2. This causes activation of STAT1/2 and activates the production of ISGs including CXCL10. SNPs in *IFIH1* and *TYK2* that decrease the function of these proteins are associated with protection from the progression of T1D autoimmunity (red boxes).

of transcription (STAT) proteins, which leads to their dimerization and translocation to the nucleus. STAT proteins promote the transcription of genes that can mediate various biological processes to inhibit viral replication<sup>158</sup>.

### **1.13: Activation of innate immune signaling by CVB**

Cell surface TLRs contribute to the recognition of CVB infections. TLR4 is best known for its role in sensing lipopolysaccharide during bacterial infections, but it also contributes to sensing of viral infections<sup>159</sup>. TLR4 contributes to CVB4 sensing in the pancreas and the production of cytokines. This interaction is likely to occur on the surface and does not require replication as inactivated by ultraviolet light activates TLR4 signaling. It is unclear how CVB4 directly interacts with TLR4<sup>160</sup>.

Intravesicular TLRs also mediate sensing of CVB infections. The activation of these receptors requires an acidic environment, which is usually provided by the maturation of endosomes<sup>161</sup>. TLR3 senses CVB replication intermediates in the form of dsRNA. The synthetic dsRNA mimetic, polyinosinic:polycytidylic acid (poly(I:C)), also acts as a ligand for this receptor when it is transfected into cells<sup>162</sup>. TLR3 knockout mice are highly susceptible to CVB3 infection and have more severe pathology<sup>163</sup>. TLR7 and TLR8 both recognize ssRNA<sup>164</sup>. Human cardiac inflammatory responses are largely dependent on TLR7 and TLR8 in CVB infections<sup>165</sup>. Despite the importance of TLR signaling, it is unclear if these receptors are activated during viral entry or at later stages in replication. In plasmacytoid DCs, TLR7 is only activated when CVB is bound to virus-specific antibodies<sup>166</sup>. While later RNA replication

intermediates in the cytoplasm are sequestered from the endosomal TLRs, there could be a role for autophagy in delivering viral RNA to TLRs in endosomes. CVB infection prompts the formation of autophagy-associated double-membrane structures, and blocking autophagy in CVB3 infection of HeLa cells reduces viral replication<sup>167</sup>. It is unclear if these autophagosomes contact and mature with endolysosomes to allow for the activation of TLRs.

Because of their cytoplasmic localization, the RLRs are in a prime location for sensing CVB replication. Replication intermediates include dsRNA and higher order RNA complexes due to the strand switching ability of the viral protease 3D. RIG-I does not contribute to the response to CVB, as mice lacking RIG-I are not more susceptible. This is because CVB lacks the required 5'-triphosphate on RNA due to the covalent linkage of the VPg protein on the 5' end<sup>125,151</sup>. Knockout of *Iih1* in mice renders them more susceptible to pancreatic and hepatic necrosis upon infection with CVB3. MDA5 contributes to controlling the early infection through the production of IFN-I in infected mice<sup>168</sup>.

#### **1.14: Contributions of innate immune signaling in the development of autoimmunity**

The early stages of T1D are characterized by the infiltration of immune cells into the islets of Langerhans and are called insulinitis. Insulinitis is initiated by  $\beta$  cells producing cytokines and chemokines in response to viral infection to recruit immune cells to the site of infection. Macrophages and DCs sample antigens in the area of local inflammation and present autoantigens to CD4<sup>+</sup> T helper cells. This occurs through the presentation of autoantigens through class II MHC

molecules to the T cell receptor on CD4<sup>+</sup> T cells. The resulting activated Th1 helper T cells mediate the production of cytotoxic CD8<sup>+</sup> T cells, which ultimately infiltrate the islets and specifically kill  $\beta$  cells. In line with this hypothesis, infiltrating macrophages and DCs in recent onset T1D patients produce inflammatory cytokines TNF- $\alpha$  and IL-1 $\beta$ <sup>169</sup>. This contributes to the local inflammation of the islets. Additionally, in early stages of insulinitis, the dominant infiltrating immune cells are CD8<sup>+</sup> cytotoxic T cells and CD86<sup>+</sup> macrophages<sup>23</sup>. Despite being early in the process of insulinitis, the presence of CD8<sup>+</sup> T cells in these tissues indicates this is already late in the development of cellular autoimmunity. Evidence for the early contributions of innate immune signaling that contribute to the ultimate autoimmune disease are discussed below.

Innate immune signaling is important for the development of T1D. These immune responses are likely the result of environmental triggers like CVB infection, and mediate the development of autoimmunity through their interactions with the adaptive immune system. Recently it was shown that  $\beta$  cells express >80% of the T1D candidate genes, so this means they are likely playing an active role in the development of autoimmunity<sup>68</sup>. Multiple lines of evidence implicate a signaling cascade that involves the cytosolic dsRNA sensor, MAD5 followed by the production of IFN-I and the downstream production of cytokines like CXCL10 in the progression of  $\beta$  cell dysfunction and development of T1D. This signaling cascade links the initial viral insult to the cytokine production that recruits monocytes and DCs to initiate insulinitis in the beginning stages of T1D.

SNPs in *IFIH1*, the gene encoding MDA5, are associated with T1D. A genome-wide association study (GWAS) uncovered a protective association with the minor allele of the SNP rs1990760 for T1D<sup>72</sup>. This common SNP leads to an amino acid substitution of threonine for alanine at position 946, but functional studies indicate that protein function is maintained<sup>170</sup>. The rs1990760 SNP does correlate with a reduction of *IFIH1* mRNA<sup>171</sup>. Four additional rare variant SNPs in *IFIH1* are also associated with protection against T1D. One causes a non-sense mutation resulting in a truncated mutation (rs35744605), two are at essential splice sites (rs35337543 and rs35732034), and the fourth is at a highly conserved isoleucine at position 923 (rs35667974) that decreases the function of the protein<sup>172,173</sup>. Collectively, these mutations follow the trend that lower *IFIH1* expression is protective for the development of T1D (Fig. 1.3). This would likely correlate with less IFN-I production and lower expression of downstream cytokines. In support of this hypothesis, mice with reduced levels of MDA5 induce a T<sub>reg</sub> profile as opposed to an effector T cell response<sup>174</sup>. These associations need to be explored more directly in human cells in the context of viral infections.

In contrast to these rare protective mutations, risk alleles of *IFIH1* (rs2111485) increase the 5 year progression rate to T1D 31% compared to 11% for the protective alleles have been described<sup>175</sup>. Expression of these risk alleles is associated with development of autoantibodies targeting  $\beta$  cells<sup>75</sup>. Furthermore, risk of developing T1D is associated with higher expression of

*IFIH1* in PBMCs<sup>171</sup>. MDA5 signaling in DCs stimulate CD4<sup>+</sup> T-cell proliferation, so higher expression of *IFIH1* could potentially drive autoimmune progression<sup>176</sup>.

Immunoreactive IFN- $\alpha$  is detectable in  $\beta$  cells in T1D patients<sup>177</sup>.

Additionally this expression of IFN- $\alpha$  coincides with the presence of enteroviral proteins in  $\beta$  cells in pre-diabetic or diabetic donors<sup>103,104</sup>. IFN- $\alpha$  mRNA is expressed at higher levels in islets of T1D patients compared to controls<sup>178</sup>. In patients with T1D, 70% had elevated levels of IFN $\alpha$  in their plasma<sup>179</sup>.

Furthermore, two studies highlight an IFN-I signature of associated genes that is detectable prior to the development of autoantibodies in blood of children genetically at risk<sup>180,181</sup>. The contribution of IFN- $\alpha$  expression either prior or soon after the development of diabetes is consistent with the role of IFN- $\alpha$  as important co-factor in development of Th1 immune reaction and can contribute to development of autoimmune disease<sup>182</sup>. In patients receiving recombinant IFN- $\alpha$  therapy for hepatitis C virus infection increases T1D risk by 10-18-fold<sup>183,184</sup>. Collectively, these studies point to an important role for IFN-I, which is a major response component of viral infection, in the development of T1D.

The C-X-C motif chemokine 10 (CXCL10) is an IFN-inducible cytokine that is highly expressed in CVB-infected primary human islets and contributes to the development of autoimmunity. CXCL10 interacts with CXCR3 chemokine receptors on immune cells and mediates a cytotoxic T cell response through Th1 helper T cells<sup>185</sup>. The development of cytotoxic T cells through Th1 help is important for clearance of intracellular pathogens. Serum concentrations are



higher for CXCL10 in T1D patients and those at risk for developing T1D<sup>186</sup>. CXCL10 is highly expressed in  $\beta$  cells in pancreas tissue from T1D patients and CD3<sup>+</sup> cells bearing the cognate receptor, CXCR3, are also present<sup>187</sup>. In a mouse infection model in which lymphocytic choriomeningitis virus causes diabetes, inhibition of CXCL10 signaling blocks the development of autoimmune diabetes<sup>188</sup>. In addition to its role in recruiting immune cells, CXCL10 can also induce reduce the secretion of insulin in response to glucose and induce  $\beta$  cell apoptosis through a feedback loop that involves TLR4<sup>189,190</sup>.

The data presented above support the model of  $\beta$  cell autoimmunity presented in Figure 1.4. Viral infection of  $\beta$  cells causes local cytokine production

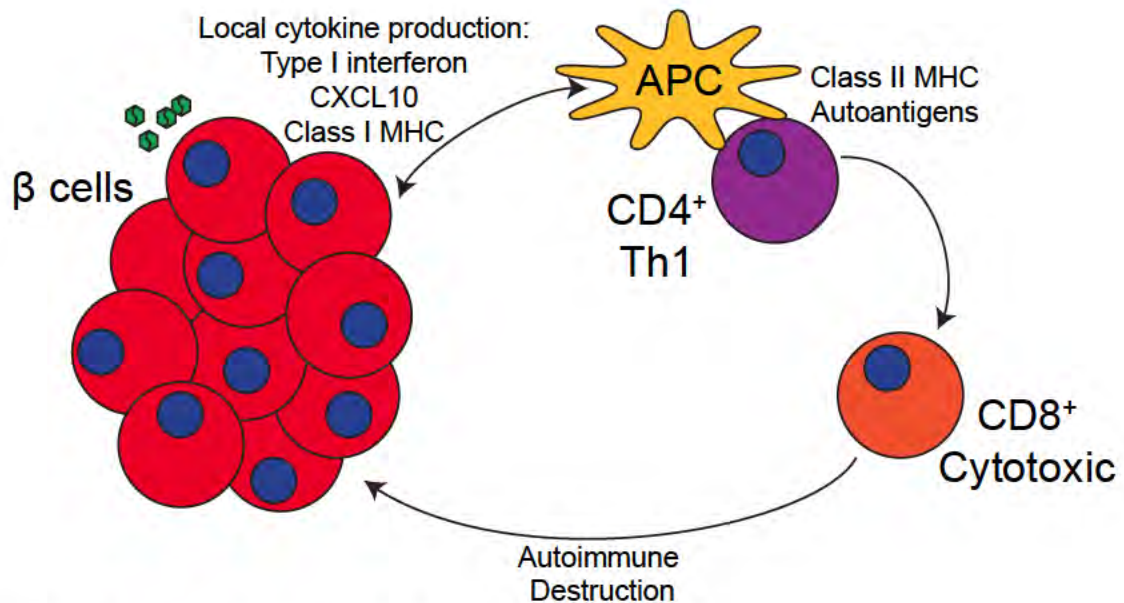


**Figure 1.4: The induction of  $\beta$  cell autoimmunity**

Environmental factors, specifically viruses, and genetics can act together to drive the autoimmune reaction against  $\beta$  cells in T1D patients. Viral infection elicits an innate immune response, and the strength of this response depends on SNPs in innate immune genes. The local cytokine production of type I IFN, CXCL10, and class I MHC hyperexpression can all be detected prior to the development of T1D in susceptible patients. This innate immune response recruits APCs to the site of infection and can further exacerbate the inflammatory response or activate Th1 responses in the thymus through interactions with class II MHC. Th1 cells then activate cytotoxic  $CD8^+$  T cells. These activated T cells somehow break through central tolerance and develop responses against  $\beta$  cell antigens. These autoreactive T cells then return to the pancreas and mediate the autoimmune destruction of  $\beta$  cells, which leads to T1D.

that includes IFN-I, CXCL10, and eventually class I MHC hyperexpression.

These signals in combination with genetic predisposition to develop autoimmunity due to class II MHC leads to the break through of central tolerance. APCs activate Th1 T cell responses through class II MHC, which then help produce autoreactive CD8<sup>+</sup> T cells. These activated, autoimmune T cells then mediate autoimmune destruction of  $\beta$  cells.

### **1.15: Prevailing mechanistic theories on the viral contribution to T1D development**

Development of autoimmunity in T1D occurs in the form of humoral and cellular immunity. Autoantibodies and autoreactive cytotoxic T cells are both present prior to the diagnosis of diabetes<sup>19</sup>. Several theories connect the putative viral trigger to the development of T1D. These include molecular mimicry, epitope spreading, bystander activation, and the “fertile field” hypothesis. While some of these mechanisms are controversial they are not mutually exclusive and may be acting in combination to potentiate the autoimmune reaction.

Molecular mimicry is the idea that an immune epitope is shared by the pathogen and the host, which results in a cross-reactive immune response. Sequence homology is shared between the viral 2C non-structural CVB protein (aa 32-47) and the T1D associated autoantigen GAD65 (aa 247-279) (PEVEKEK)<sup>191,192</sup>. Humoral and cellular responses against GAD65 are detected prior to the onset of clinical diabetes<sup>22</sup>, and autoantibodies are positive several years before diagnosis<sup>21</sup>. Despite the attractive nature of this hypothesis, the experimental evidence is lacking. In infections of mice with various strains of

CVB4, autoimmunity was only induced when a transgenic autoreactive T cell was introduced, indicating bystander activation, not molecular mimicry<sup>193</sup>. Additionally, T cells clones for GAD 247-280 generated from T1D patients failed to react with the mimicry epitope derived from 2C from CVB<sup>194</sup>.

Epitope spreading is the concept that infection releases sequestered antigens which could be presented to the adaptive immune system in draining lymph nodes, and failure of central tolerance results in autoimmunity<sup>193</sup>. In line with this hypothesis, the cytolytic infection of  $\beta$  cells by viruses leads to a cytotoxic immune response<sup>195</sup>. More pathogenic strains increase viral response and increase autoimmunity<sup>98</sup>. Also SNPs that are associated with protection of T1D temper the antiviral response<sup>75,173</sup>. The presence of viral proteins in patients shows that only 5% of endocrine cells are positive for VP1, but despite this low infection rate of endocrine cells, there is overexpression of class I MHC in all  $\beta$  cells<sup>104</sup>. This expression of class I MHC in the context of local inflammation from infected  $\beta$  cells recruits cytotoxic CD8<sup>+</sup> T cells that mediate  $\beta$  cell killing. The local cytokine profile includes IFN- $\alpha$ , IFN- $\beta$ , IFN- $\gamma$ , TNF- $\alpha$  and IL-1 $\beta$ <sup>196</sup>.

Bystander activation is the idea that autoreactive T cells could be activated independently of the T cell receptor in some scenarios. Secretion of proinflammatory cytokines by infected cells or resident macrophages and dendritic cells could initiate activation of circulating naïve islet-specific T cells. Viral infections may result in the impaired activation of self-reactive T cells through a T cell receptor independent mechanism in genetically predisposed

individuals through a distinct cytokine profile<sup>197</sup>. In support of this hypothesis, autoimmunity could be triggered through activation of transgenic autoreactive T cells by viral infection<sup>193</sup>. Targeted expression of IL-2 or IL-12 in the  $\beta$  cells of mice to promote the proliferation of T cells failed to initiate T1D<sup>198</sup>. These conflicting results indicate that factors other than just the cytokine profile are needed to activate naïve T cells. However, viral infection does not strictly meet the definition of bystander activation, where cytokines alone are activating naïve T cells. In this case, viral antigens or host proteins released during cell lysis provide antigens that may bypass peripheral tolerance in the presence of strong cytokine signaling.

The “fertile field” hypothesis combines one or more of the above mechanisms into a single paradigm. The main idea is that conditions of the intensity of infection, immune history, and mass of potentially autoreactive T cells exist at the same time and anatomical location. Molecular mimicry or bystander activation may prime the accumulation of low numbers of autoreactive T cells in initial infections. Once this field is sufficiently fertile, the right infection can overcome the thresholds of immune tolerance and develop full autoimmune destruction of cells. Complications in identifying causative agents in this paradigm are that priming events might be separated from the activating events by substantial amounts of time and may involve heterologous agents<sup>199</sup>.

#### **1.16: Working toward better understanding of the role of viruses in T1D**

Despite the increasing evidence for correlations between enterovirus infections and the development of T1D, a causal relationship is elusive. A causal

role of enterovirus infection in T1D could be strengthened by understanding how viruses suppress  $\beta$  cell function and initiate antiviral responses in these cells. Further insights into both of these processes could facilitate the development of improved therapeutic or preventive treatments to stop the development of autoimmunity against  $\beta$  cells.

Currently, the timing of sampling and lack of prognostic markers limit the early diagnosis of T1D prior to development of autoantibodies. Identification of genetic changes in  $\beta$  cell functional genes or innate immune responses could be used as earlier and more long-lasting markers for viral initiation of autoimmunity. Earlier markers provide the possibility to intervene with immunoregulatory or virus suppressing drugs to stop the development of autoimmunity. Ideally, a specific innate immune profile or a single gene marker could be identified to predict the progression to T1D. These markers may also allow for better associations between viral infection and T1D if they are more specific to viral responses that lead to the disease. In order to identify better markers for the initiation and progression of T1D, a better understanding of the basic processes of viral infections of human  $\beta$  cells is necessary. However, the inability to directly evaluate these processes in the context of human infections requires the use of specific models for infections of human  $\beta$  cells described below.

In the following chapters, I will utilize a variety models to address two overarching goals. The first determining the mechanisms involved in the loss of insulin production and secretion that occurs in CVB-infected  $\beta$  cells with a

potential role for changes in PDX1 localization after CVB infection. The second is characterizing the key innate immune signaling pathways with a focus on IFN-I and CXCL10 and identifying the cell types involved in the production of these responses (Fig. 1.5). An overview of the models presented in this thesis is described in Table 1.1. I will describe effects of CVB4 infection on both  $\beta$  cell function and innate immune signaling in immunodeficient mice engrafted with primary human islets in **Chapter II**, and in cultured primary human islets, stem cell-derived human  $\beta$  cells (SC- $\beta$ ), and a human  $\beta$  cell line, EndoC- $\beta$ H1, in **Chapter III**. In **Chapter IV** I will explore the effects of CVB4 infection on PDX1 localization and  $\beta$  cell function that may contribute to decreases in insulin production in EndoC- $\beta$ H1 cells. Finally in **Chapter V**, I will describe cell type differences in innate immune signaling in flow cytometry-sorted cells from primary human islets.

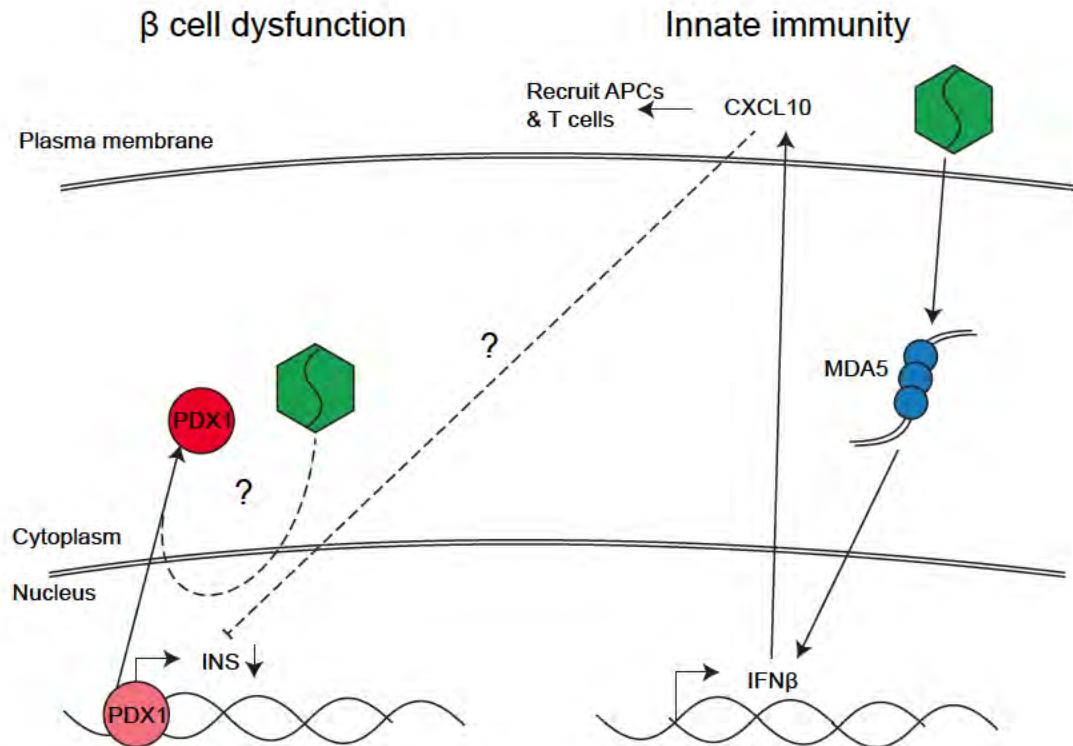


**Figure 1.5: The influence of CVB4 on β cells**

Schematic of two non-exclusive pathways that could contribute to β cell dysfunction and T1D autoimmunity. 1) CVB infection causes β cell dysfunction in the decrease of INS gene expression. One of the mechanisms involved may be the exclusion of PDX1 from the nucleus. 2) Innate immune signaling through engagement of MDA5 leads to IFN-β production, followed by the robust expression of CXCL10 upon CVB4 infection. This mediates interactions with antigen presenting cells (APC) and T cells to initiate and perpetuate autoimmune attack on β cells, leading to T1D. Overlap in these pathways may exist since CXCL10 can suppress insulin secretion<sup>190</sup>.



Model complexity	Model system	Chapter	Advantages	Disadvantages
	Engrafted primary human islets	Chapter II	<ul style="list-style-type: none"> <li>•Long-term survival of human islet cells</li> <li>•Physiologically relevant cell responses</li> <li>•No B or T cells present</li> </ul>	<ul style="list-style-type: none"> <li>•Mixed cell, organ, and species types</li> <li>•Technically complicated and expensive</li> <li>•Contributions of mouse immune system</li> </ul>
	Cultured primary human islets	Chapter III	<ul style="list-style-type: none"> <li>•Single tissue and species type</li> <li>•Technically simple</li> <li>•Need fewer islet cells</li> </ul>	<ul style="list-style-type: none"> <li>•Limited survival time</li> <li>•Mixed cell types including immune cells</li> <li>•Limited ability to knockout genes</li> </ul>
	SC- $\beta$	Chapter III	<ul style="list-style-type: none"> <li>•Enriched for <math>\beta</math> cells</li> <li>•Less genetic variability</li> <li>•Possible to knockout genes</li> <li>•No immune cells</li> </ul>	<ul style="list-style-type: none"> <li>•Cells may not be fully mature</li> <li>•Complicated differentiation protocol</li> </ul>
	EndoC- $\beta$ H1	Chapter III & IV	<ul style="list-style-type: none"> <li>•Single cell type</li> <li>•Genetically tractable</li> <li>•Can produce large numbers of cells</li> </ul>	<ul style="list-style-type: none"> <li>•Changes due to immortalization procedure</li> <li>•Limited physiological responses</li> </ul>
	Sorted primary human islet cells	Chapter V	<ul style="list-style-type: none"> <li>•Primary cells</li> <li>•Enriched for single cell types</li> </ul>	<ul style="list-style-type: none"> <li>•Cell populations are not pure</li> <li>•Limited viability</li> <li>•Low cell numbers</li> <li>•Technically complicated</li> </ul>

**Table 1.1: Advantages and disadvantages of models used**

The models utilized in this thesis are listed in order of decreasing model complexity and increasing  $\beta$  cell specificity. **Chapter II** focuses on primary human islets that are engrafted into diabetic mice. **Chapter III** compares responses of cultured primary human islets, SC- $\beta$  cells, and EndoC- $\beta$ H1 cells to CVB infection. In **Chapter IV** investigates the effects of CVB infection on localization of PDX1. Finally, flow cytometry-sorted cells from primary human islets are used to evaluate cell type specific responses to poly(I:C) in **Chapter V**.

## **CHAPTER II: VIRAL INFECTION OF ENGRAFTED HUMAN ISLETS LEADS TO DIABETES**

Glen R. Gallagher, Michael A. Brehm, Robert W. Finberg, Bruce A.  
Barton, Leonard D. Shultz, Dale L. Greiner, Rita Bortell, and Jennifer P. Wang

### **Contribution Summary:**

G.R.G. helped to design the experiments, performed the experiments, and helped to analyze the data and write the manuscript. M.A.B., R.W.F., and D.L.G.

helped to design the experiments. B.A.B. performed the statistical analysis.

L.D.S. generated the NSG-Tg(RIP-DTR) mice. R.B. helped to design the experiments and analyze the data. J.P.W. helped to design the experiments, analyze the data, and write the manuscript.

The following is reprinted from the Diabetes article of the same name.

PMID: 25392246

## 2.1: Abstract

Type 1 diabetes (T1D) is characterized by the destruction of the insulin-producing  $\beta$  cells of pancreatic islets. Genetic and environmental factors both contribute to T1D development. Viral infection with enteroviruses is a suspected trigger for T1D, but a causal role remains unproven and controversial. Studies in animals are problematic because of species-specific differences in host cell susceptibility and immune responses to candidate viral pathogens such as coxsackievirus B (CVB). In order to resolve the controversial role of viruses in human T1D, we developed a viral infection model in immunodeficient mice bearing human islet grafts. Hyperglycemia was induced in mice by specific ablation of native  $\beta$  cells. Human islets, which are naturally susceptible to CVB infection, were transplanted to restore normoglycemia. Transplanted mice were infected with CVB4 and monitored for hyperglycemia. Forty-seven percent of CVB4-infected mice developed hyperglycemia. Human islet grafts from infected mice contained viral RNA, expressed viral protein, and had reduced insulin levels compared with grafts from uninfected mice. Human-specific gene expression profiles in grafts from infected mice revealed the induction of multiple interferon-stimulated genes. Thus, human islets can become severely dysfunctional with diminished insulin production after CVB infection of  $\beta$  cells, resulting in diabetes.

## 2.2: Introduction

Animal models are helpful for understanding virus-induced diabetes but have translational limitations for human disease. For example, coxsackievirus and adenovirus receptor (CAR), the receptor for CVB, is expressed within human islets, but not mouse islets<sup>109,119,129,200</sup>, and infection of C57BL/6 mice with CVB3 or CVB4 does not result in diabetes (unpublished data). NOD mice have been used to extensively assess the parameters of viral infection on T1D, although a critical mass of autoreactive T cells rather than direct viral insult appears to accelerate progression to diabetes during CVB infection<sup>201,202</sup>.

Given these inherent limitations, we used the NOD/ Lt-*Prkdcscid* *IL2rgtm1WJL* (NSG) mouse<sup>203</sup> to study the effects of CVB infection in transplanted human islets. NOD mice express multiple alleles that alter the function of the innate and adaptive immune system<sup>204,205</sup>. The severe combined immunodeficiency (*scid*) mutation results in a complete absence of T and B lymphocytes. The addition of a targeted null mutation in the interleukin (IL)-2 receptor common  $\gamma$ -chain fully disrupts NK cell development, further reducing innate immune responses, and facilitating the engraftment of human cells and tissues<sup>206</sup>. Hyperglycemia was induced either by administering streptozotocin (STZ) or diphtheria toxin (DT) to NSG mice transgenically expressing the human DT receptor (DTR) under the control of the rat insulin II promoter (the NOD/ Lt-*Prkdcscid* *IL2rgtm1WJLTg*(Ins2-HBEGF)6832Ugfm/Sz strain [abbreviated as NSG-Tg(RIP-DTR)]). Hyperglycemic mice were engrafted with human islets to

restore normoglycemia and then were infected with CVB4. Our goal was twofold: 1) to assess viral replication and persistence in human islets in vivo; and 2) to assess for the development of hyperglycemia. Our results indicate that CVB4 directly invokes the dysfunction of human  $\beta$  cells, providing insights into the early events that precipitate T1D.

## 2.3: Results

### 2.3.1 CVB4-Infected Mice Engrafted With Human Islets Develop Diabetes

$\beta$  cells of the native pancreas were disrupted by treating NSG mice with STZ (experiment 1) or by injecting NSG-Tg (RIP-DTR) mice with DT (experiments 2 and 3). Given the extended kinetics of experiment 1, ablation of native mouse  $\beta$  cells was changed to the DTR method, mitigating the possibility of mouse  $\beta$  cells contributing to glucose homeostasis, which can occur with STZ<sup>207,208</sup>. After a hyperglycemic state was confirmed, human donor islets were transplanted into recipient mice to restore normoglycemia. Three independent transplant studies were performed with human islets from donors characterized in Table 2.1. Mice were injected with CVB4 or saline control (mock infected). The target end point of the study was the development of diabetes. At the end of the study, mice were sacrificed, and

**Table 2.1: Demographic characteristics of human islet donors of engrafted islets**

	<b>Donor 1</b>	<b>Donor 2</b>	<b>Donor 3</b>
Age, years	55	55	29
Gender (M/F)	M	F	M
Ethnicity	n.r.	White	Hispanic/Latino
Body weight, kg	85.0	109.1	87.3
BMI, kg/m <sup>2</sup>	28.4	39.9	27.5
Time in culture*	16 h	28 h	20 h
HLA	n.r.	n.r.	Class 1 – A: 2, 11 Class 1 – B: 7, 51 Class 1 – C: 7, 15 Class 2 – DR: 8, 15

**Abbreviations:** BMI, body mass index; n.r., not recorded. \*Refers to the amount of time that the human islets were cultured following isolation until shipment to our laboratory.

tissues were harvested for analysis. Figure 2.1 summarizes survival data for the three studies, and provides the numbers of animals per group plus information on animals that died prematurely and the possible causes of death. Mice that died prematurely were excluded from the final analysis.

In the first experiment, three of the six (50%) infected mice that survived greater than 21 days post-infection (dpi) developed diabetes (Fig. 2.2, A-top panel). Mice became hyperglycemic between 21 and 25 dpi, while no mock-infected control mice ( $n = 5$ ) developed diabetes over the course of the experiment (log-rank  $P = 0.08$ ). CVB4 also induced diabetes in experiments 2 and 3, although the kinetics of disease was prolonged. In experiment 2, two of four infected mice (50%) that survived greater than 35 dpi became diabetic (Fig. 2.2, A-middle panel) (log-rank  $P = 0.005$ ). In experiment 3, progression to diabetes was similar to that in experiment 2, with two of five (40%) infected mice surviving greater than 35 dpi becoming diabetic (Fig. 2.2, A-bottom panel) (log-rank  $P = 0.09$ ). Because of the small sample size and the few infected mice that developed diabetes, time to diabetes data were combined across experiments to develop a more stable estimate of the difference between the infected and control mice. Seven CVB4-infected mice developed diabetes with a mean time to diabetes of 28 days, while no control mice developed diabetes (log-rank  $P = 0.0002$ ). The percentage of mice remaining normoglycemic is plotted against time (Fig. 2.2, B).

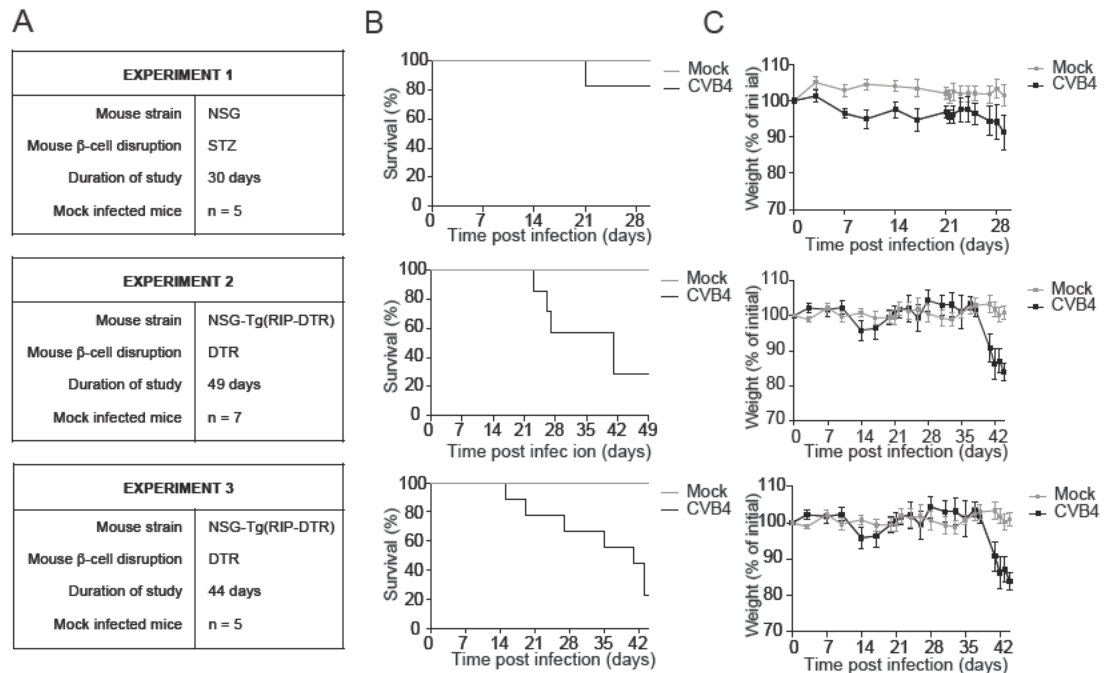


**Figure 2.1: Overview of human islet-engrafted mouse studies.**

(A) Summary of three experiments. (B) Survival of mice in each of the three experiments. Experiment 1: n = 5, mock-infected, n = 7, CVB4-infected. One infected, non-diabetic mouse required euthanasia at 21 dpi. Experiment 2: n = 7, mock-infected, n = 7, CVB4-infected. Three infected mice required euthanasia between 23 and 27 dpi due to severe fight wounds. Experiment 3: n = 5, mock-infected, n = 9, CVB4-infected. Four mice died prematurely between 15-35 dpi. (C) Average weight loss of mice in each of the three experiments. Body weight is expressed as the percent difference from the body weight of baseline. Experiment 1: n = 5, mock-infected, n = 7, CVB4-infected. Experiment 2: n = 7, mock-infected, n = 7, CVB4-infected. Experiment 3: n = 5, mock-infected, n = 9, CVB4-infected. For Experiment 1, only mice that survived beyond 21 dpi were included for further analysis. For Experiments 2 and 3, only mice that survived beyond 35 dpi were included for further analysis.



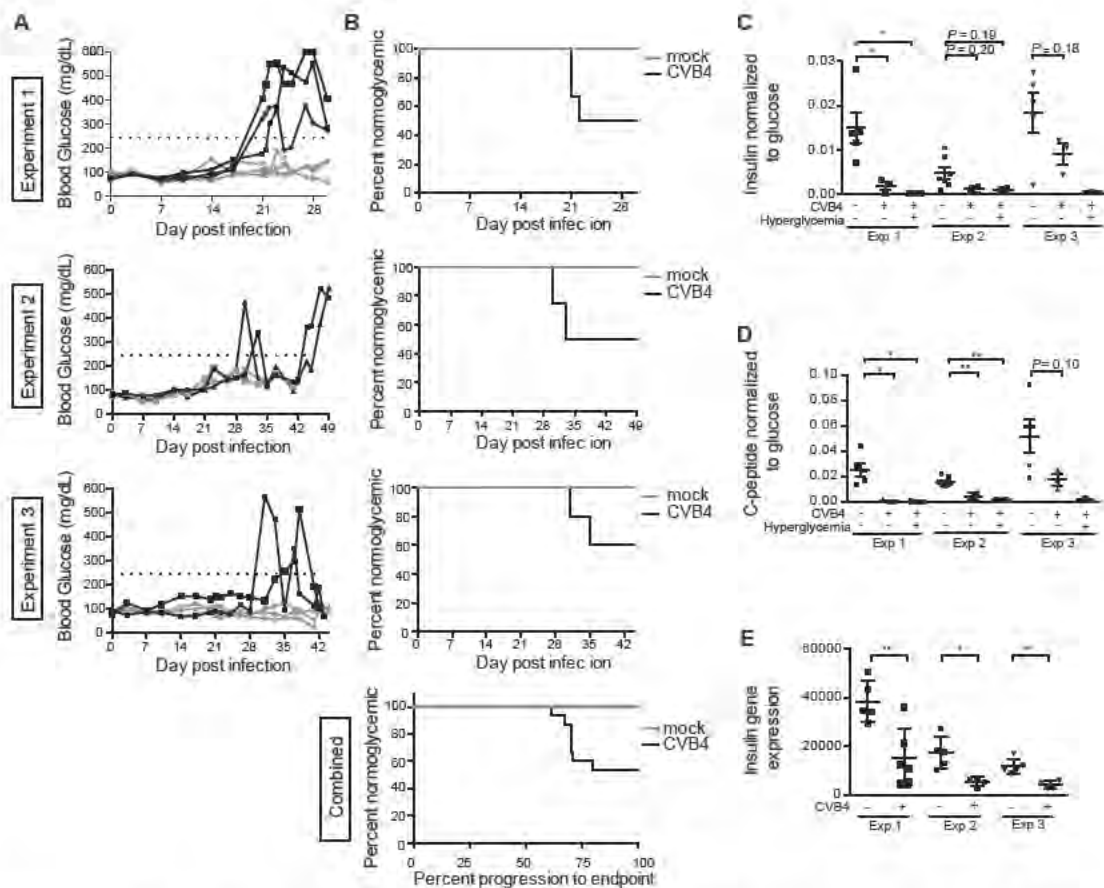


**Figure 2.2: Human islet-engrafted mice become hyperglycemic and have low levels of C-peptide and insulin following CVB4 infection.**

(A) Blood glucose values for non-fasted CVB4-infected animals. Black lines highlight animals that were diabetic. (B) The percentage of animals remaining normoglycemic is shown. Experiment 1,  $P=0.08$ . Experiment 2,  $P=0.005$ . Experiment 3,  $P=0.09$ , log-rank test. The animals remaining normoglycemic combined from all three experiments is shown (**bottom panel**) with the time to diabetes scaled by dividing the day of diabetes onset by the endpoint for the respective experiment,  $P=0.0002$ , log-rank test. Human insulin (C) and human C-peptide (D) levels as measured by ELISA in terminal serum of non-fasted animals, normalized to the serum glucose level at the time of death. Experiment 1:  $n=5$ , mock-infected normoglycemic;  $n=3$ , CVB4-infected normoglycemic;  $n=3$ , CVB4-infected hyperglycemic. Experiment 2:  $n=7$ , mock-infected normoglycemic;  $n=2$ , CVB4-infected normoglycemic;  $n=2$ , CVB4-infected hyperglycemic. Experiment 3:  $n=5$ , mock-infected normoglycemic;  $n=3$ , CVB4-infected normoglycemic;  $n=1$ , CVB4-infected hyperglycemic. (E) Human insulin gene expression in grafts measured by NanoString. Values are normalized to a panel of human housekeeping genes. Experiment 1:  $n=5$ , mock-infected;  $n=6$ , CVB4-infected. Experiment 2:  $n=5$ , mock-infected;  $n=4$ , CVB4-infected. Experiment 3:

n=5, mock-infected, n=5, CVB4-infected. Error bars in **C-E** show the S.E.M. \*,  $P<0.05$ ; \*\*,  $P<0.01$ ; Student's t-test.

The peak nonfasting blood glucose value for each mouse over the experimental observation period was assessed and was significantly higher on average for CVB4-infected mice compared with mock-infected mice. Mock-infected mice had normal mean blood glucose measurements with an average of 87.5mg/dL, and were tightly controlled (standard deviation (SD) of 14.2 mg/dL). CVB4-infected mice had a higher average non-fasting glucose of 137.3mg/dL with much more variability (SD of 113.1 mg/dL). Comparing blood glucose levels between CVB4-infected and mock-infected mice with generalized estimating equation models revealed an increase of 81.7 mg/dL in CVB4-infected mice compared with the mock-infected mice ( $P = 0.018$ ) in experiment 1, an increase of 77.5 mg/dL in the infected mice in experiment 2 ( $P = 0.0001$ ) and an increase of 32.0 mg/dL in the infected mice in experiment 3 ( $P = 0.07$ ).

Human insulin and C-peptide levels were compared in terminal serum samples from infected versus control nonfasted mice (Fig. 2.2, C & D). These values were normalized to the terminal serum glucose measurement to account for glycemic variability in nonfasted mice. Lower values were observed in infected mice compared with control mice, but no differences were noted between hyperglycemic and normoglycemic infected mice. Insulin (*INS*) gene expression in the human grafts was quantified using NanoString. In each experiment, *INS* gene expression was significantly lower in CVB4-infected mice compared with controls (Fig. 2.2, E). A threefold decrease was observed in *INS*

gene expression in grafts from CVB4-infected mice compared with controls (Fig. 2.6, A). In contrast, glucagon (*GCG*) expression ratios were not significantly impacted (Fig. 2.6, B). Thus, regardless of whether overt hyperglycemia was detected, significant decreases in both human C-peptide and insulin levels were detected in CVB4-infected animals. Across the three experiments, negative correlations were observed between peak blood glucose values and *INS* gene expression (Spearman  $\rho = 20.39$ ,  $P = 0.04$ ). Additionally, negative correlations were observed between peak blood glucose values and terminal serum human C-peptide values ( $\rho = 20.45$ ,  $P = 0.01$ ).

### **2.3.2: Grafts From Infected Mice Show Decreased Insulin**

Histopathological examination of grafts from both CVB4-infected and mock-infected mice revealed intact islets without infiltrating inflammatory cells in grafts (Fig. 2.3, A). A moderate degree of fibrosis was present. Insulin-specific immunohistochemical stains revealed a decrease in the number of insulin-positive cells in the islets from infected mice compared with those from control mice (Fig. 2.3, B). Glucagon-specific stains did not reveal glucagon depletion in the grafts of CVB4-infected mice (Fig. 2.3, C). Immunofluorescent staining for insulin and glucagon revealed similar trends (discussed below, see Fig. 2.4, D). Examples are shown from a CVB4-infected mouse that ultimately became diabetic, but the histopathological appearance of grafts from diabetic and nondiabetic CVB4-infected mice were similar overall. Histopathological changes

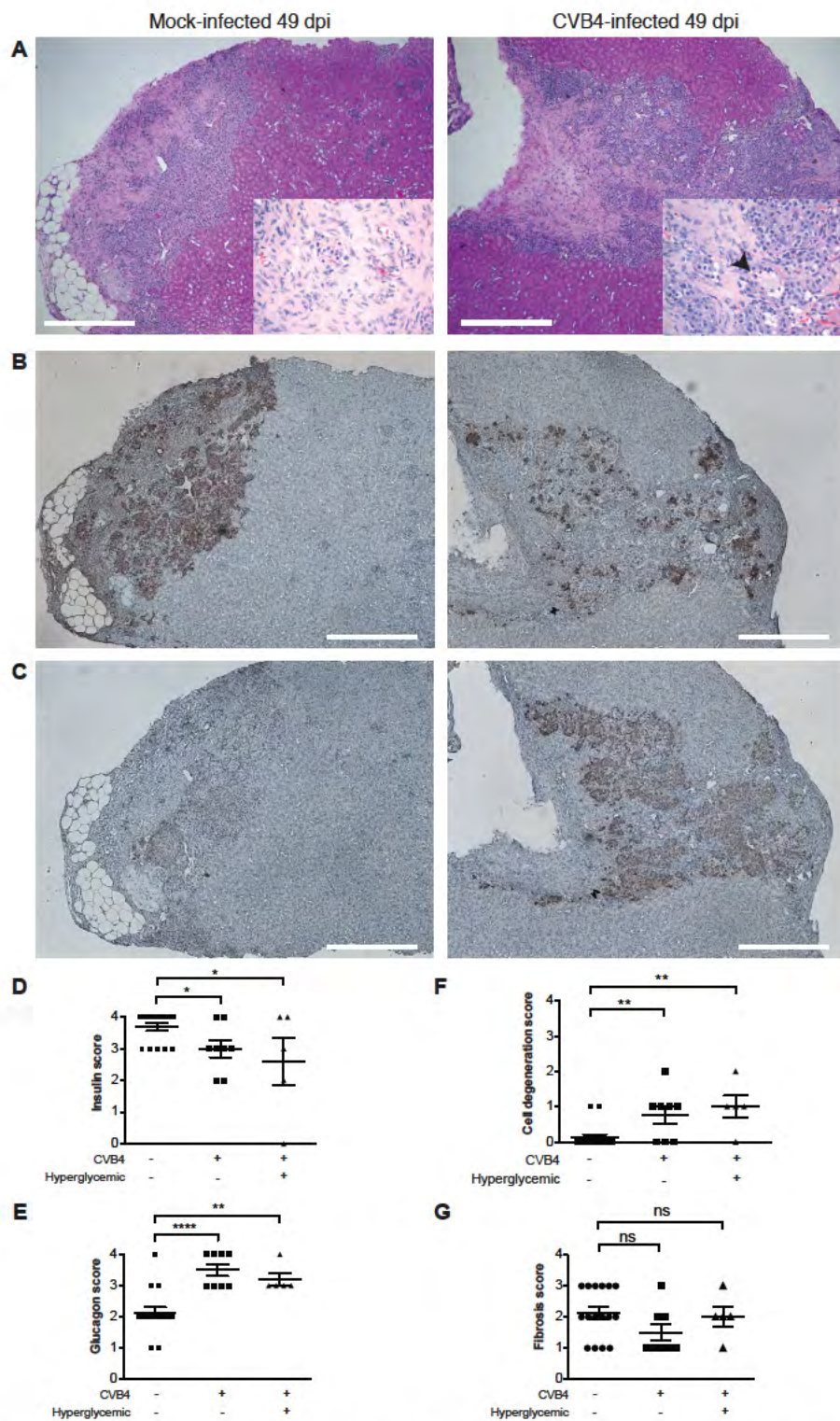


**Figure 2.3: Human islet grafts from CVB4-infected mice have diminished insulin levels compared to grafts from mock-infected control mice.**

**(A)** H & E staining on sections of human islet grafts from a representative mock-infected control (left panels) and a CVB4-infected diabetic mouse (right panels) from 49 dpi (Experiment 2). In both grafts, islets are surrounded by fibrosis and surrounding renal cells appear intact. In the CVB4-infected mouse (right panel), degenerative changes are present throughout the engrafted islets. Individual cells are shrunken with karyorrhexis and hypereosinophilic cytoplasm, and vacuolar degenerative changes are abundant (arrowhead). **(B)**

Immunohistochemical staining for insulin. ~50% of the graft is positive for insulin in the CVB4-infected mouse (right panel) compared to >75% in the control mouse (left panel). **(C)** Immunohistochemical staining for glucagon. ~75% of the graft is positive for glucagon in the CVB4-infected mouse (right panel) compared to ~50% in the control mouse (left panel). For images in A-C scale bars represent 500  $\mu$ m and final magnification is 40X (insets in A are at 400x magnification). **(D)**

Blinded histopathology scoring of human islet grafts from all available mice: n=16, Mock-infected normoglycemic; n=8, CVB4-infected normoglycemic; and n=5, CVB4-infected hyperglycemic. Insulin immunostain, percent positive cells. 0=0%, 1=25%, 2=50%, 3=75%, 4=90%. **(E)** Glucagon immunostain, percent positive cells. 0=0%, 1=25%, 2=50%, 3=75%, 4=90%. **(F)** Degeneration of implanted cells. 0=none, 1=minimal, 2=mild, 3=moderate, 4=marked. **(G)** Fibrosis of the implanted cells. 0=none, 1=minimal, 2=mild, 3=moderate, 4=marked. \*,  $P<0.05$ ; \*\*,  $P<0.01$ ; \*\*\*\*,  $P<0.0001$ ; Student's t-test. No differences were observed in scores between infected normoglycemic versus hyperglycemic mice.

were quantified for insulin, glucagon, cell degradation, and fibrosis by blinded scoring of sections from all available animals (Fig. 2.3, D–G).

### **2.3.3: CVB4 Infection Persists in Human Islet-Engrafted Mice**

Diabetes did not develop in any infected mice until at least 3 weeks post-infection. Viral RNA was present in mouse serum throughout the course of experiment 1 (Fig. 2.4, A). Plaques were recovered from terminal serum of CVB4-infected animals, indicating the presence of replication-competent virus (Fig. 2.4, B). Viral RNA was readily detected by NanoString from the terminal human graft samples (Fig. 2.4, C). Viral copy numbers were highest in the first experiment, which corresponds with the more rapid time to diabetes compared with the other two experiments. Replicating virus was also present in terminal host tissue samples; examples from experiment 2 include heart ( $1.3 \pm 0.6 \times 10^6$  pfu/g,  $n = 4$ ), pancreas ( $7.0 \pm 4.0 \times 10^6$  pfu/g,  $n = 4$ ), and the nongrafted kidney ( $4.3 \pm 2.1 \times 10^6$  pfu/g,  $n = 4$ ).

To establish that human  $\beta$  cells were infected with CVB4, coimmunofluorescence staining was performed on human islet graft sections using antibodies against insulin, glucagon, and enterovirus viral protein 1 (VP1). VP1 was readily detected in all graft samples from CVB4-infected mice at various time points; examples from 41 and 49 dpi (Fig. 2.4, D) as well as 7 dpi (Fig. 2.4, E) are shown. Notably, VP1 and insulin colocalized frequently, indicating that  $\beta$  cells were infected with CVB4. Not all VP1-positive cells were positive for insulin, however, suggesting that other cell populations within human islets can be



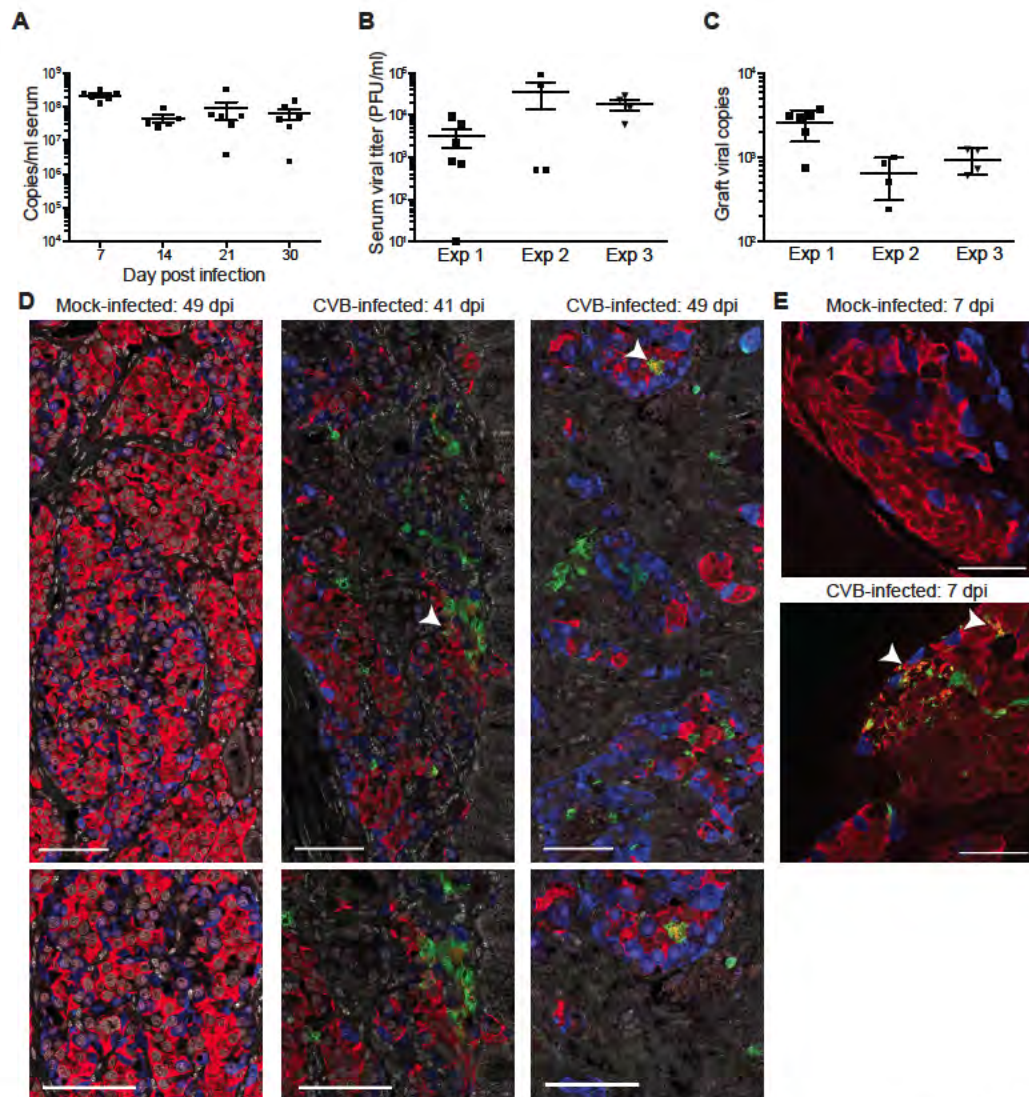


**Figure 2.4: Viral replication is sustained following CVB4 infection of human islet-engrafted mice.**

(A) Viral copies, measured by qPCR on serum from CVB4-infected mice are present throughout the duration of the study. Data from Experiment 1 are shown. Error bars show the S.E.M. (B) Replicating virus is present in serum from CVB4-infected mice at time of takedown. (C) Viral nucleic acid, quantified by NanoString, is present in the grafts of CVB4-infected animals at time of takedown. Grafts from mock-infected animals each had <10 copies by NanoString. Experiment 1: n=6. Experiment 2: n=4. Experiment 3: n=5. (D) VP1 is present within the grafts of CVB4-infected animals. Arrowheads in upper panels show examples of regions positive for both VP1 and insulin and images focused on those areas are shown in lower panels. Samples from Experiment 2 are shown, including those from a mock-infected control (49 dpi) and two CVB4-



infected mice (41 and 49 dpi). VP1 is green, glucagon blue, and insulin red. Images were acquired with a 40X objective. Scale bars represent 75  $\mu\text{m}$ . **(E)** VP1 is present in insulin-producing cells in grafts of CVB4-infected mice. Samples from an experiment in which grafts were specifically planned for harvest at 7 dpi are shown. VP1 is absent from the graft of a mock-infected control mouse (top panel). VP1 and insulin co-localize in a graft from a CVB4-infected mouse (bottom panel, arrowheads). Images were acquired with a 63x objective. Scale bars represent 50  $\mu\text{m}$ .

infected with CVB4. Since exocrine and pancreatic ductal cells can be transplanted along with human islets, we sought to determine whether these cells support viral replication.

Exocrine cells, which stain positive for amylase, were infrequently observed in the grafts, and no evidence of VP1 localization was noted (Fig. 2.5, A). Similarly, CK19-positive pancreatic ductal cells did not colocalize with VP1 (Fig. 2.5, B).

Immunofluorescent staining revealed a significant decrease in the insulin-to-glucagon signal ratio in grafts of infected mice versus control mice. In experiment 2, the insulin-to-glucagon signal ratio was  $0.74 \pm 0.16$  in grafts from CVB4-infected mice ( $n = 4$ ) compared with  $3.99 \pm 0.92$  in mock-infected controls ( $n = 6$ ,  $P = 0.02$ , Student *t* test). This result was consistent with observations for insulin and glucagon by immunohistochemical staining (Fig. 2.3, B-C).

#### **2.3.4: Profiling of Gene Expression in Human Islet Grafts**

Human graft gene expression levels after infection were assessed using a NanoString platform with species-specific probes. Combined gene expression profile results for 100 genes from graft samples are summarized in Fig. 2.6, A and B as fold change over the mock-infected animals. *INS* gene expression was significantly lower in grafts from CVB4-infected mice compared with those from the mock-infected controls (Fig. 2.2, E). Expression values of somatostatin (*SST*) and pancreatic duodenal homeobox-1 (*PDX1*), which regulates transcription of

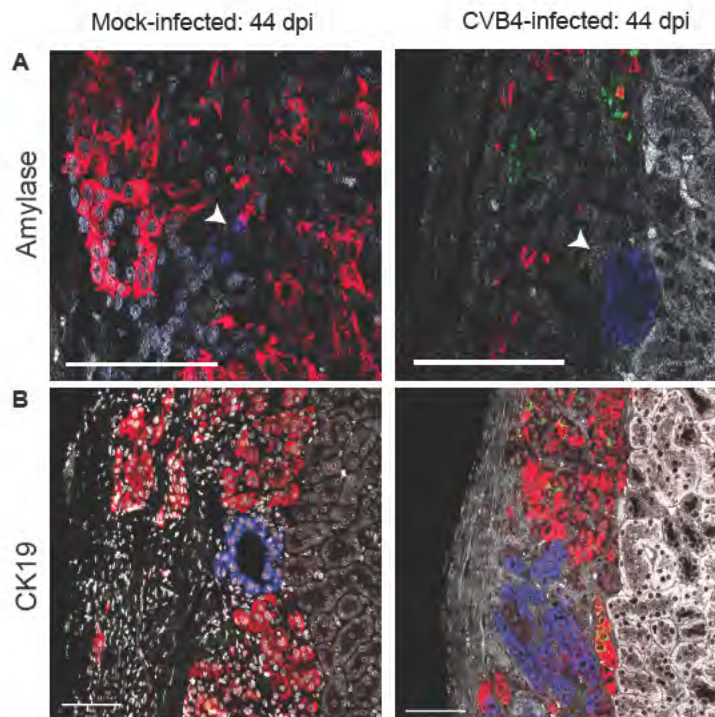


**Figure 2.5. VP1 does not co-localize with human exocrine or ductal cells in the grafts of infected mice.**

Samples from Experiment 3 at 44 dpi are shown for a mock-infected mouse (left panels) or a CVB4-infected mouse (right panels) that did not become diabetic. VP1 is not present in the graft of the mock-infected mouse but is readily detected within the human islet graft of the CVB4-infected mouse (right panels). VP1 (green) associates with insulin (red) but VP1 does not co-localize with amylase (blue) producing cells (arrowheads) (**A**) or cells expressing the ductal cell marker cytokeratin 19 (CK19, blue) (**B**); DAPI is shown in white. Images were acquired with a 40X objective. Scale bars represent 75  $\mu\text{m}$ .

*INS* and *SST*, were also significantly lower in the grafts of CVB4-infected mice relative to those of mock-infected mice.

Numerous genes in the type I IFN pathway, including *CXCL10*, *MX1*, *OAS2*, *CCL5*, *IFIH1*, and *DDX58*, were significantly induced in the grafts of infected mice (Fig. 2.6, B). A moderate but significant increase was observed for *TXNIP*, which encodes thioredoxin-interacting protein and is induced by ER stress through the protein kinase RNA-like ER kinase (PERK) and inositol-requiring enzyme 1 (IRE1) pathways. Expression for *DDIT3*, which encodes CHOP, a multifunctional transcription factor in the ER stress response, was significantly increased. *IL-1 $\beta$*  gene expression was significantly decreased, although absolute values in samples were consistently low.

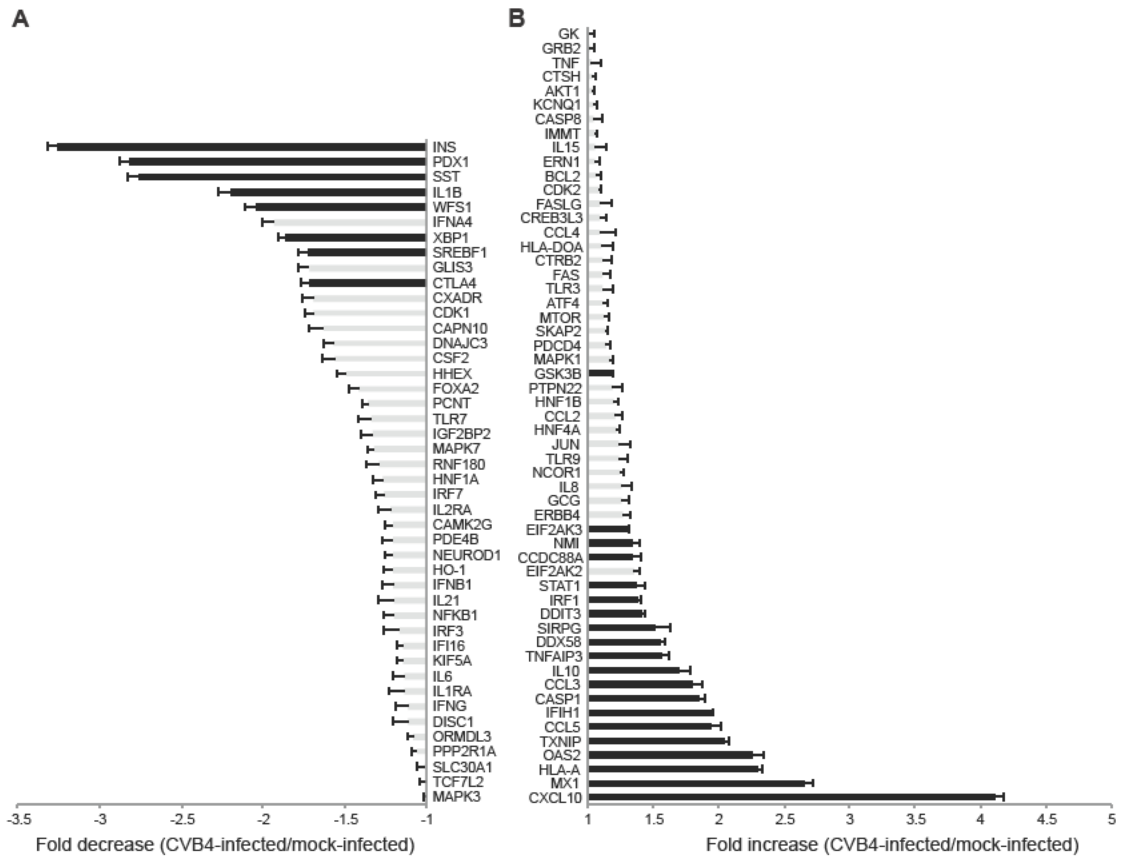


**Figure 2.6: Graft gene expression in CVB4-infected animals by NanoString analysis.**

(A) Genes that are decreased in grafts from CVB4-infected mice (n=14) versus grafts from mock-infected mice (n=15) are shown as fold decrease. (B) Genes that are increased in grafts from CVB4-infected mice (n=14) versus grafts from mock-infected mice (n=15) are shown as fold increase. Black bars indicate  $P < 0.05$ , Student's t-test. Error bars show the S.E.M. The categorical distributions for the one hundred host genes were as follows: type I IFNs=17; cytokines=16; T1D=15; apoptosis=14; endocrine=12; ER stress=9; and other=17.

## 2.4: Discussion

We describe a model in which NSG mice with induced hyperglycemia are transplanted with human islets and successfully used for studying the viral induction of diabetes. Sustained infection with a prototypical strain of CVB4 is accompanied by reversion to hyperglycemia. Interestingly, the final diabetic state appears to result from a loss of human islet insulin production rather than overt islet destruction. Despite the possibility of resident immune cells being engrafted with the human donor islets, this model provides an environment largely devoid of T cells and antibodies. The absence of an intact immune system in this model provides a new, unobscured view of how viruses can directly initiate diabetes. The diabetic state is most likely a direct consequence of viral infection of human cells that harbor CAR. To our knowledge, this aspect of human specificity has not been previously achieved in other in vivo models of viral induction of diabetes. In contrast, other models of virus-induced diabetes depend on the contributions of T cells. For example,  $\beta$  cell destruction is T cell dependent during the acceleration of diabetes in viral infection of aged NOD mice<sup>209</sup> and in the Kilham rat virus infection model in BBDR rats<sup>210</sup>.

Interexperimental variability was observed using several metrics for evaluating diabetes. Fluctuations in blood glucose measurements for some CVB4-infected mice were noted, but were not entirely unexpected given that glucose levels were randomly obtained from nonfasted animals with concurrent viral disease. Time to the development of diabetes also varied between

experiments. The human islets used for engraftment in each experiment were obtained from distinct donors, and differences in the condition of the islets upon transplantation could explain some experimental heterogeneity. Variations in the course of human T1D can be attributed to a multitude of genetic and environmental factors that have only been partially characterized. Despite the different genetic backgrounds of the primary human islets and limited sample sizes, strong patterns in gene expression were noted in islet grafts and in ex vivo cultured islets after infection (see **Chapter III**).

The prolonged course of progression of human islet engrafted mice infected with CVB4 to hyperglycemia was somewhat surprising. The lytic nature of CVB4 in other cell types and the rapid deterioration of mice infected at high doses indicate that this virus is quite pathogenic. However, these results fit well with reports that the development of T1D is prolonged over an indeterminate time period of months to years. Additionally they mesh well with the observations of seasonality of both viral infection and T1D incidence. Enterovirus incidence peaks in late summer months into autumn<sup>116</sup>. T1D incidence is the highest in the winter months<sup>78</sup>. So if viral infections in the late summer months are causing the development of T1D over the course of several months, this would fit well with the observed T1D peak in winter. However, this association is tenuous and since the time period of the development of T1D is poorly understood, this is only speculation.

Significant changes in gene expression were observed for endocrine genes, type I IFN-associated genes, and T1D susceptibility genes. The endocrine genes *INS*, *SST*, and *PDX1* had the greatest fold decreases in gene expression in both the engrafted islets and ex vivo-cultured islets. *PDX1* regulates the expression of both *INS* and *SST*; and protects against apoptosis, autophagy, and susceptibility to ER stress<sup>211-214</sup>. Interestingly, persistently infected cultures of a ductal-like cell line with CVB4 have diminished *PDX1* expression after several weeks of infection<sup>215</sup>, which provides insights for our model. The expression of type I IFN-associated genes, including *OAS2*, *MX1*, *CCL5*, and *TLR3*, was increased. The presence of a type I IFN signature in individuals genetically at risk for T1D prior to the development of autoantibodies was recently highlighted<sup>181</sup>. *CXCL10*, an IFN-stimulated gene, had the highest fold induction of expression in both in vivo and ex vivo studies. *CXCL10* recruits immune cells at inflammation sites and has been proposed to contribute to the pathogenesis of many autoimmune diseases, including T1D<sup>216,217</sup>. T1D susceptibility gene expression for *IFIH1* and *HLA-A* was significantly higher after infection. We previously reported<sup>168</sup> that *IFIH1* mediates IFN responses after CVB infection. Single nucleotide polymorphisms in *IFIH1* that could diminish the type I IFN response after viral infection are associated with protection from T1D<sup>72,172</sup>. The marked increase in the expression of *HLA-A* in grafts after infection is consistent with class I MHC hyperexpression described in patients with T1D<sup>218</sup>.



Human islet-engrafted mice developed diabetes several weeks after infection, during which time replicating virus was readily detected. CVB can cause prolonged infection in immunocompetent mice. Vella and Festenstein<sup>219</sup> reported that CVB4 infection led to persistent infection in the majority of 10 inbred mouse strains. Persistent enteroviral infections have been described in immunodeficient humans, particularly those with agammaglobulinemia (for review, see Galama<sup>220</sup>). Prolonged coxsackievirus antigen shedding was described in a patient with agammaglobulinemia, corresponding to a lack of neutralizing antibody<sup>221</sup>. Additionally, B cell-deficient mice infected with CVB3 exhibit persistent viral production up to 45 dpi<sup>222</sup>, and CVB3 persistence has been reported in SCID mice<sup>223</sup>. Mounting evidence exists that coxsackievirus can establish persistent infections in astrocytic cells and ductal cells of the pancreas<sup>215,224</sup>. In our study, we performed dual staining for VP1 and CK19 to determine whether ductal cells were acting as a viral reservoir. We did not detect any colocalization, although others have detected viral RNA from primary ductal cells, which is more sensitive than VP1 staining<sup>215</sup>. Identification of additional human cells that can be persistently infected could provide insights into relevant viral reservoirs.

The ability to investigate the long-term consequences of viral infection could provide new insights into the homeostatic balance between mechanisms of  $\beta$  cell function and death. The human islet engraftment model may reflect the earliest stages of the onset of virus-related diabetes prior to the development of

autoimmune responses. Many features are reminiscent of cases of fulminant T1D, characterized by rapid onset of hyperglycemia and ketoacidosis resulting from accelerated  $\beta$  cell failure. Tissue studies reveal the presence of enterovirus in pancreatic islet cells as well as increased expression of innate immune sensors, CXCL10, and type I IFN in  $\beta$  cells and infiltrating immune cells<sup>225,226</sup>, underscoring the importance for innate immune signaling pathways. Additionally, this model mirrored many key pathological features found in tissues of recent onset T1D patients. There is characteristic expression of IFN-I<sup>227</sup> and associated cytokines like CXCL10<sup>187</sup>, and hyperexpression of class I MHC<sup>218</sup>.

Infection models using humanized mice that include reconstitution of components of the human immune system will yield further insights into the pathogenesis of virus-induced diabetes, revealing specific contributions of both innate and adaptive immunity.

#### **2.4.1: Conclusions**

Mice with glucose homeostasis under the control of engrafted primary human islets revert to hyperglycemia after infection with CVB4. This hyperglycemia is due to the loss of insulin production of engrafted  $\beta$  cells at the level of both mRNA and protein. This loss of *INS* gene expression upon CVB4 infection is a key marker for  $\beta$  cell dysfunction. Furthermore, the infection of engrafted primary human islets initiates a robust innate immune response. The IFN-I and cytokine expression profile is characterized by the robust expression of downstream ISGs, CXCL10, MX1, CCL5, and IFIH1. The following chapters will use these findings to evaluate various models of cultured primary human islets.

## 2.5: Materials and Methods

### 2.5.1: Mice

Mice were maintained in accordance with the Institutional Animal Care and Use Committee of the University of Massachusetts Medical School. NSG male mice, 12–14 weeks old, received a single intraperitoneal injection of 160 mg/kg STZ to induce hyperglycemia (blood glucose >250 mg/dL on 2 consecutive days). B6CBA-Tg(Ins2-HBEGF)6832Ugfm mice, in which the rat insulin II promoter drives  $\beta$ -cell-specific expression of the DTR, were provided by P. Herrera (University of Geneva, Geneva, Switzerland). This transgene was backcrossed using a marker-assisted speed congenic approach to the NSG strain background (i.e., NSG-Tg[RIP-DTR])<sup>228,229</sup>. Female NSG-Tg(RIP-DTR) mice, 12–16 weeks old, were given 40 ng DT by intraperitoneal injection. Nonfasting blood glucose levels were monitored with a glucometer. To enhance survival after the induction of diabetes was confirmed, mice were given LinBit insulin pellet implants (LinShin Canada Inc.) until human islets were available for transplant.

### 2.5.2: Human Islet Transplantation

Human islets were obtained from the Integrated Islet Distribution Program under protocols approved by the Institutional Review Board of the University of Massachusetts Medical School. A total of 3,000 islet equivalent units were transplanted under the subrenal capsule of each mouse, as previously

described<sup>203</sup>. For each experiment, islets obtained from single, distinct human donors were used. Mice were allowed to recover from the surgery for 2 weeks to allow for graft revascularization and for normoglycemia to be restored.

### **2.5.3: Mouse Infections**

Mice were intraperitoneally injected with normal saline solution (control) or  $1 \times 10^4$  plaque-forming units (pfu) of the prototypical CVB4 laboratory strain JVB (catalog # VR-184; American Type Culture Collection) grown in HeLa cells<sup>230</sup>. Nonfasting blood glucose levels were measured at least twice weekly. Additional blood samples were obtained weekly for viral RNA extraction. Mice were killed if they displayed gross signs of illness (e.g., ruffling, hunching), and the native mouse pancreas and the human islet graft were harvested for RNA and histopathology. Serum, pancreas, heart, liver, spleen, and contralateral kidney were harvested for viral titers. Plaque assays were performed using previously described methods<sup>168</sup>.

### **2.5.2: PCR**

Viral RNA was extracted from serum using the QIAamp Viral RNA Mini kit (Qiagen) and cDNA generated using the High Capacity cDNA Reverse Transcriptase Kit (Applied Biosystems) followed by quantitative PCR using the Platinum Quantitative PCR SuperMix-UDG Kit (Life Technologies). Enterovirus-specific primers and probe were used for quantification of viral RNA<sup>105</sup>. A standard curve was established using the EGFP-CVB3 plasmid as a template (a gift from L. Whitton, Scripps Research Institute, La Jolla, CA)<sup>231</sup>.

#### **2.5.4: Histopathology and Immunohistochemistry**

Antigen retrieval was performed on paraffin-embedded sections with Retrieval Solution A (BD Biosciences), and endogenous biotin was blocked by Dual Endogenous Enzyme Blocking Reagent (Dako). Guinea pig antibody to insulin (Dako) or rabbit antibody to glucagon (Abcam) was added and detected with the EnVision Dual Link Kit (Dako) followed by staining with DAB Solution (Dako). Samples were counterstained with hematoxylin. A veterinary pathologist scored histopathological changes by blinded scoring of sections.

#### **2.5.5: Immunofluorescence**

Antigen retrieval was mediated at 98°C for 45 min in formalin-fixed, paraffin-embedded sections. Sections were blocked with PBS containing 1% BSA and 5% normal goat serum, then incubated with the following primary antibodies overnight: guinea pig antibody to insulin (1:150; Dako); rabbit antibody to glucagon (1:50; Dako); mouse antibody to VP1, clone 5-D8/1 (1:50; Dako); rabbit antibody to cytokeratin 19 (CK19) (1:500; Abcam); and/or rabbit antibody to amylase (1:400; Abcam). Sections were incubated with the following secondary antibodies for 1 h at 1:1,000 dilution: Alexa Fluor-594 goat antibody to guinea pig IgG; Alexa Fluor-647 donkey antibody to rabbit IgG; and Alexa Fluor-488 goat antibody to mouse IgG (catalog #A11076, #A31573, and #A11029, respectively; Life Technologies). Sections were mounted with ProLong Gold Antifade Reagent with DAPI (Life Technologies). Immunofluorescence was imaged on a Leica SP8 confocal microscope and quantified using FIJI software (version 1.48p) using automatic thresholding followed by the measure area

function<sup>232</sup>. Wide-field images were acquired using a Nikon Eclipse Ni-U microscope with a X4 plan objective using NIS-Elements imaging software (version 4.13). High-magnification wide-field images were acquired with a X40 plan objective using QCapture Pro software (version 5.1).

### **2.5.6: Gene expression profiling of engrafted islets**

A portion of the human islets that were engrafted in mice were collected at the time of sacrifice from all available animals. TRIzol reagent (Life Technologies) was used for RNA extraction from the tissue. A multiplex hybridization assay (NanoString) allowed for direct measurement of mRNA copies without the need for amplification. Probes were designed to target human genes in a species-specific manner. The NanoString CodeSet #1 (NSCS1) included type I IFN, cytokines, apoptosis, endocrine, endoplasmic reticulum (ER) stress, T1D-associated loci, and other human genes, plus seven housekeeping genes for normalization of data. A probe for a conserved CVB sequence targeting the same region as the quantitative RT-PCR primer was included<sup>105</sup>. One hundred nanograms of RNA extracted from tissue was hybridized, processed, and analyzed per the manufacturer's procedure. Data were normalized using the nSolver Analysis Software (version 1.1). Fold changes in gene expression were the ratio of normalized gene expression in CVB4-infected samples versus those in mock-infected samples. Averages of fold changes were calculated by averaging the log<sub>10</sub> of the fold change followed by a transformation of 10x. Values <1 were transformed by -1/x. For experiment 2, only five of seven

samples from mock-infected mice were analyzed because of space constraints on the NanoString assay.

#### **2.5.7: Statistical Methods**

To compare repeated blood glucose measurements between treatment groups within an experiment, generalized estimating equations were used to adjust for the inherent correlation among the measurements within each mouse. The significance of the regression coefficients was assessed using standard  $z$  tests. The relationship between the maximum glucose level and the number of insulin copies and C-peptide level was assessed using Spearman (nonparametric) correlation coefficients with Fisher transformation. The onset of diabetes within and across experiments was compared using Kaplan-Meier product-limit estimates and the log-rank statistic. To assess the significance of the fold-change of gene expression, a standard one-sample  $t$  test was used to determine the significance compared with zero. SAS (version 9.3) was used for all analyses.

**CHAPTER III: COMPARISON OF CVB INFECTION IN CULTURED PRIMARY  
HUMAN ISLETS AND IN HUMAN B CELL LINES**

Glen R. Gallagher, Robert W. Finberg, and Jennifer P. Wang

Contribution Summary:

G.R.G. designed and performed the experiments and helped to analyze the data and write the manuscript. R.W.F. helped to design the experiments. J.P.W. helped to design experiments, analyze data, and write the manuscript.

Figure 3.1 is reprinted from the *Diabetes* article PMID: 25392246



### 3.1: Abstract

Immunodeficient mice with induced hyperglycemia and engrafted with primary human islets reverted to hyperglycemia following infection with CVB4. This *in vivo* model provides important insights into  $\beta$  cell dysfunction upon CVB4 infection under physiological conditions, but the early effects of viral infection in human islets were not interrogated. Short-term culture of primary human islets, which are permissive to CVB4 infection, is possible and allows for evaluation of gene expression changes over a time course. Given that insulin gene expression decreases in primary human islets following CVB4 infection, cultured human islets can be used to define infection-specific pathways important in influencing insulin. Similarly, gene expression of innate immune genes can be interrogated. Human  $\beta$  cells derived by directed differentiation of stem cells (SC- $\beta$ ) provide a model for studying the effects of CVB4 infection of human  $\beta$  cells. Furthermore, the EndoC- $\beta$ H1 cell line provides a pure  $\beta$  cell population in which changes in gene expression after CVB4 infection can be studied. The results presented here indicate that both of these sources of  $\beta$  cells are permissive to CVB4 infection. Although inconsistencies were observed in insulin gene expression between cultured primary human islets and SC- $\beta$  and EndoC- $\beta$ H1 cells, all three sources of  $\beta$  cells had robust innate immune responses to CVB4 infection. Therefore, these other cells may provide new options for studying the nature of innate immune signaling in  $\beta$  cells.

## 3.2: Introduction

### 3.2.1: Overview

Studies with mice engrafted with human islets provide benchmarks for the viral contributions to triggering T1D. This model provides the advantage that human islet gene expression changes associated with hyperglycemia can be monitored *in vivo*. However, the dynamic processes that lead to the development of  $\beta$  cell dysfunction and hyperglycemia are difficult to study due to the technical complexity and cost of this model. Determining the underlying regulation of viral replication, how antiviral responses are initiated, which cell types contribute to the immune signaling, and how these processes contribute to  $\beta$  cell dysfunction are all challenging *in vivo*. To relieve these constraints, I turned to cultured  $\beta$  cells from either primary human islets, stem cells directionally differentiated into  $\beta$  cells, and a human  $\beta$  cell line. Identifying the pathways involved and the key mediators of  $\beta$  cell dysfunction that cause a decrease in insulin production and innate immune antiviral responses provide opportunities to develop interventions to prevent the progression to overt, autoimmune T1D.

Cultured primary human islets are a convenient replacement cell type for studying the effects of viral replication. In addition to infections of cultured primary human islets, new advances in directed differentiation of stem cells into pancreatic endocrine cells (SC- $\beta$ ), and the introduction of previously unavailable human  $\beta$ -cell lines offer new tools for studying viral infection in even more controlled conditions.

### **3.2.2: Cultured Primary Human Islets**

Cultured primary human islets are becoming more readily available and provide a platform for studying viral replication and host responses in a controlled experimental setting. Currently there are two main sources of primary human islets. The first is the not-for-profit Integrated Islet Distribution Program (IIDP), which is coordinated by the City of Hope National Medical Center and sponsored by the National Institute of Diabetes and Digestive and Kidney Diseases. The second are commercial sources that include Prodo Laboratories, Lonza, and ZenBio. These sources provide primary human islets derived from healthy donors for use in basic research. Since these cells are in a culture format, there is greater flexibility in experimental design and greater ability to control for the virus dose and timing of infection. This provides the opportunity to further dissect the interactions between enteroviruses and islet cell function. Cytopathic effects of viral infection can be directly observed by microscopy, supernatants can be sampled for insulin release or cytokine production, and islets can be harvested for RNA to measure gene expression changes. However, a major limitation of cultured primary human islets is the inability to culture the cells for long periods of time. Despite this caveat, this system provides a convenient method of evaluating early changes in  $\beta$  cell function or immune gene expression.

### **3.2.3: Enterovirus infection of cultured primary human islets affects $\beta$ cell function**

Similar to the insulin insufficiency of primary human islets engrafted in mice, infections of cultured primary human islets also exhibit signs of  $\beta$  cell dysfunction upon viral infection. Factors of viral replication efficiency, cytotoxicity,

and  $\beta$  cell tropism may all contribute to the ability of a virus to cause  $\beta$  cell dysfunction and therefore its diabetogenic potential. Cultured primary human islets are permissive to infections of various viruses in the enterovirus genus due to the presence of viral receptors. Poliovirus, Coxsackie A virus (CVA), Coxsackie B virus (CVB), echovirus and various enterovirus strains all productively replicate in primary human islets<sup>233,234</sup>. While most of these viruses exhibit lytic replication with considerable cytopathic effect (CPE), CVA serotype 9 replicates with no apparent CPE<sup>233</sup>. In addition to developing CPE after enterovirus infection of cultured primary human islets,  $\beta$  cells exhibit defects in glucose-stimulated insulin secretion<sup>234,235</sup>. However, this is not always the case. CVA serotype 9 replicates in cultured primary human islets without affecting insulin content or secretion in response to glucose<sup>234</sup>. However, the mechanisms of the suppression of insulin secretion after enterovirus infection have not been investigated. A better understanding of the kinetics of gene expression changes after enterovirus infection may elucidate the underlying mechanisms.

#### **3.2.4: Gene expression changes after enterovirus infection in cultured primary human islets**

In addition to CPE and  $\beta$  cell functional studies, cytokine production and gene expression changes in infected primary human islets could provide insights into the diabetogenic potential of strains of CVB4. CVB4-JVB infection of cultured primary human islets induces IFN- $\alpha$  production<sup>200</sup>. Infected islets similarly produced IP-10 (CXCL10) and other IFN stimulated genes (ISGs) in response to infection<sup>236</sup>. While the production of these immune responses has been identified

in cultured islets, the contributions of different cell types to the overall response are difficult to identify. If the antiviral response is different in  $\beta$  cells than other infected cell types, this could tip the balance from viral clearance to the development of autoimmunity. Therefore, understanding both the genes involved in the antiviral response and the cell types that mediate the response could provide insights into autoimmunity directed at  $\beta$  cells.

### **3.2.5: New models of human $\beta$ cells**

While the availability of cultured primary human islets enables the investigation of the interactions between human islet cells and viruses that was previously impossible, these cells still have a number of restrictions including limited availability, variability in donor genetics, limited viability in culture, and high cost. Newly available sources of human  $\beta$  cells mitigate some of these limitations.

One newly available source of human  $\beta$  cells is SC- $\beta$  cells. These cells are derived from pluripotent stem cells that are directionally differentiated to a endocrine phenotype through well-timed treatments with cocktails of small molecule agonists and growth factors<sup>33</sup>. The majority of these cells are insulin-producing  $\beta$  cells, but other hormone positive cells are also represented in the cell clusters, including glucagon-producing  $\alpha$  cells. These cells are responsive to glucose stimulation and in theory have minimal batch-to-batch genetic variability because they are differentiated from clonal progenitor cells.

Another human  $\beta$  cell platform, EndoC- $\beta$ H1 cells, provides the advantage of monotypic culture of only insulin-producing  $\beta$  cells. This cell line was produced

by the transduction of the SV40 large T-antigen into human fetal pancreas tissue. These cells were expanded by engrafting them into SCID mice followed by recovery of the cells. Recovered cells were then transduced with hTERT to further immortalize the cells, followed again by engraftment into SCID mice. The resulting cells were then used to establish the clonal, functional, human  $\beta$  cell line<sup>237</sup>. Use of this cell line eliminates the paracrine effects of other cell types during infection. Since all of the cells are phenotypically similar prior to infection, infections of these cells helps to define the cell-intrinsic effects of virus on human  $\beta$  cell gene expression and function.

### **3.2.6: Goals**

The goals of this chapter are as follows: 1) compare the gene expression changes in engrafted and cultured primary human islets following CVB4 infection to identify important  $\beta$  cell regulatory pathways and antiviral responses that contribute to the hyperglycemia observed *in vivo*, 2) evaluate the kinetics of gene expression changes in CVB4-infection of cultured primary human islets at 6, 24, 48, and 96 hpi, 3) compare gene expression in cultured primary human islets upon infection with CVB4 or stimulations with poly(I:C) or poly(dA:dT) at 24 hpi, 4) evaluate viral replication in SC- $\beta$  cells and assess expression of hallmark genes identified in human islet studies, and 5) measure CVB4 replication and CPE in EndoC- $\beta$ H1 human  $\beta$  cells and evaluate gene expression changes upon infection.

### 3.3 Results

#### 3.3.1: Gene expression profiling in cultured human islets at 48 hpi

Cultured islets from three different human donors were independently challenged with CVB4. At 48 h post-challenge, supernatants were harvested and cells were processed for RNA to assess gene expression using the same NanoString probes used for experiments in Figure 2.6 (NSCS1) (Fig. 3.1, A and B). Significant changes in gene expression were observed in CVB4-infected samples compared with those from controls. The greatest decreases were again seen with *INS*, *SST*, and *PDX1*, although statistical significance was achieved only with *INS* ( $P = 0.034$ ,  $0.071$ , and  $0.056$ , respectively, Student's *t* test). *CXCL10* had the highest increase in gene expression, however statistical significance was not reached ( $P = 0.08$ , Student *t* test). Increases in expression were observed for numerous type I IFN response genes, including *OAS2* and *MX1*, as well as *TLR3* and *IFNB1*. Interestingly, *GCG* gene expression was not significantly changed. Low levels of IFN- $\beta$  and IFN- $\alpha$  were detected in supernatants from cultured human islets 48 h post-challenge with CVB4 or the MDA5 agonist poly(I:C) (Fig. 3.1, C).

The gene expression in CVB4-infected cultured primary human islets at 48 hpi has many similarities with the gene expression observed in infections of engrafted primary human islets in mice at an average of 38 days post infection. Gene expression is similarly increased in both engrafted and cultured primary human islets for ISGs *CXCL10*, *MX1*, *OAS2*, and *IFIH1* (Fig. 3.2, A). However, there are some differences in IFN gene expression. This may be due to the

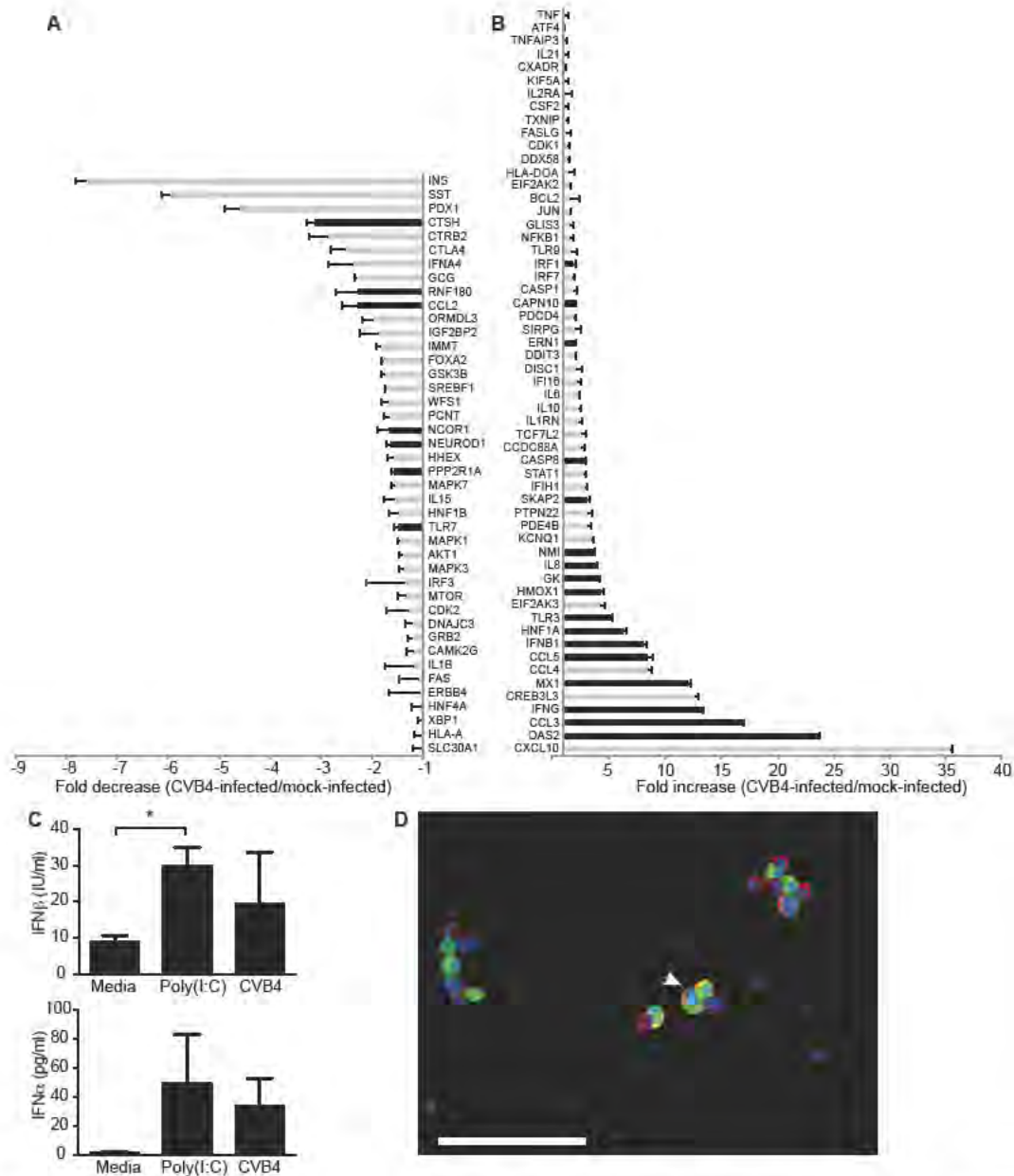


**Figure 3.1: Gene expression in ex vivo cultured human islets infected with CVB4 48 hpi.**

Islets from three independent non-diabetic human donors were challenged with CVB4. At 48 hpi, supernatants were collected and cells processed for RNA. NanoString gene expression (NSCS1) (A) Genes that are decreased in CVB4-infected ( $1 \times 10^6$  pfu/100 IEQ) islets ( $n=3$ ) versus mock-infected islets ( $n=3$ ) are shown as fold decrease. (B) Genes that are increased in CVB4-infected islets ( $n=3$ ) versus mock-infected islets ( $n=3$ ) are shown as fold increase. In A and B, black bars indicate  $P < 0.05$ , Student's t-test. Error bars indicate the S.D. (C)



Human IFN- $\beta$  and IFN- $\alpha$  were measured by ELISA from supernatants of human islets challenged with either CVB4 (1e6 pfu/100 IEQ) or poly(I:C) (100  $\mu$ g/ml) for 48 h. \*,  $P < 0.05$ , Student's t test. Error bars indicate the S.E.M. **(D)** Human islets from an independent donor were infected with eGFP-CVB3 (1e6 pfu/100 IEQ). A subset of the virus-infected cells is insulin-positive by immunofluorescent staining (arrowhead). eGFP-CVB3 is green, insulin is red, DAPI is blue. Co-localization of CVB3 and insulin is yellow. Scale bar represents 75  $\mu$ m.

differences in the kinetics of the antiviral response. In cultured primary human islets at 48 hpi, *IFNB1* and *IFNG* increase 8.15 and 13.34-fold, respectively, but their gene expression is not increased in engrafted primary human islets at the much later time points (Fig. 3.2, B). Differences in expression of other genes in the engrafted human islets during this persistent infection may highlight regulatory pathways of interferon genes in persistently infected tissues. Despite the drastic differences in the time scale of the experiments with engrafted and cultured primary human islets the three genes with the greatest decreases in gene expression are *INS*, *PDX1*, and *SST* in both cases (Fig. 3.2, B). Therefore, infections of cultured primary human islets with CVB4 provide a comparable surrogate platform for the mouse model given similarities in gene expression changes despite the large differences in time scales.

### **3.3.2: Virus tropism in cultured primary islets**

Cultured primary human islets are composed of a mixed cell-type population, so cells that are infected may be different from the cells that produce the IFN-I and inflammatory gene responses detected in Figure 3.1, A-C. It is also possible that the reduction in *INS* gene expression is mediated through a paracrine effect from viral response to cells that are infected nearby. In order to confirm the tropism of CVB for insulin-producing  $\beta$  cells in human islets, eGFP-expressing CVB3 was used to infect dispersed cultured human islets in vitro. Insulin-positive cells were detected using immunofluorescence staining and visualized by confocal microscopy (Fig. 3.1, D). eGFP and insulin frequently colocalized, providing further evidence that human  $\beta$  cells are infected with CVB. However, some cells

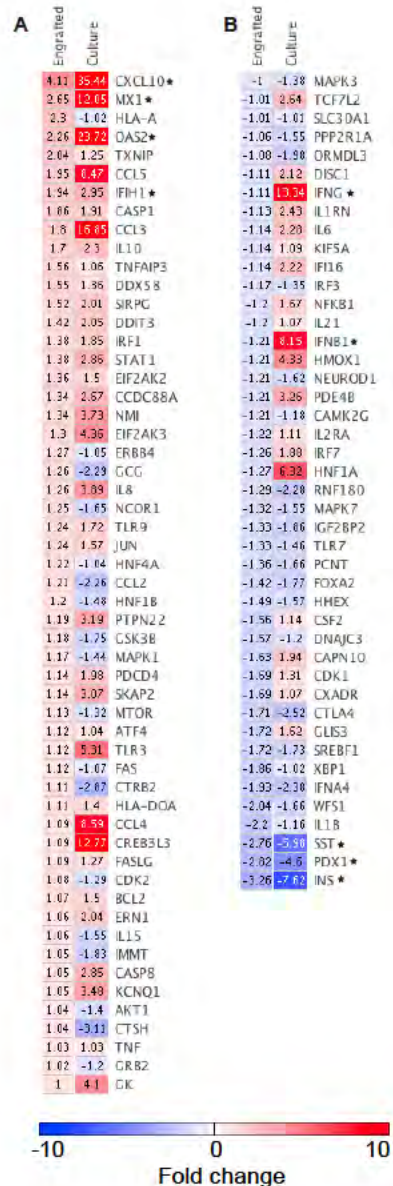


**Figure 3.2: Heatmap comparison of gene expression in CVB4 infection of primary human islets engrafted in mice or cultured *ex vivo*.**

NanoString gene expression (NSCS1) evaluation for CVB4 infection of engrafted human islets as described in Figure 2.6 at an average of 38 dpi and for CVB4 infection of primary human islets at 48 hpi as described in Figure 3.1. Each is shown for fold change relative to uninfected islets. Fold changes, displayed as a

heatmap, are sorted in decreasing order for the engrafted human islets for genes with increased expression (**A**) or decreased expression (**B**). Fold changes are indicated for each gene for each conditions. Scale from -10-fold decrease in blue to 10-fold increase in red. Genes mentioned in the text are highlighted with an asterisk.

that were infected did not stain positively for insulin production. So cells other than  $\beta$  cells are permissive to CVB4 infection and may contribute to IFN-I and cytokine response in primary human islets.

### **3.3.3: Kinetics of gene expression changes in primary human islets after infection with CVB4**

Measuring changes in gene expression at different time points after infection with CVB4 can provide insights into the pathways involved in changes in islet function genes. Early changes in gene expression can identify factors involved in mediating the later phenotypic changes in  $\beta$  cell function. To identify early changes in gene expression, I profiled changes at 6, 24, 48, and 96 hpi with CVB4 in primary human islets from a single donor using a revised panel of genes in a second NanoString CodeSet (NSCS2 - see Materials and Methods for details).

Over this time course, viral gene copies increase steadily between 6 and 48 hpi with a 0.6-log increase in viral gene copies occurring over this timeframe. This increase indicates productive viral infection in cultured primary human islet cells. Between 48 and 96 hpi a modest 0.23-log decrease in viral copies was observed (Fig. 3.3, C), which may be secondary to the innate immune response suppressing further replication. Alternatively, the replication capacity of these cells is exhausted by this time point.

At 6 hpi with CVB4, only four genes had a greater than 3 fold change compared to mock treated primary human islets (Fig 3.3, A). These genes were *CXCL10*, *IFNE1*, *CXCL11*, and *IFNA16* (in order of highest to lowest fold

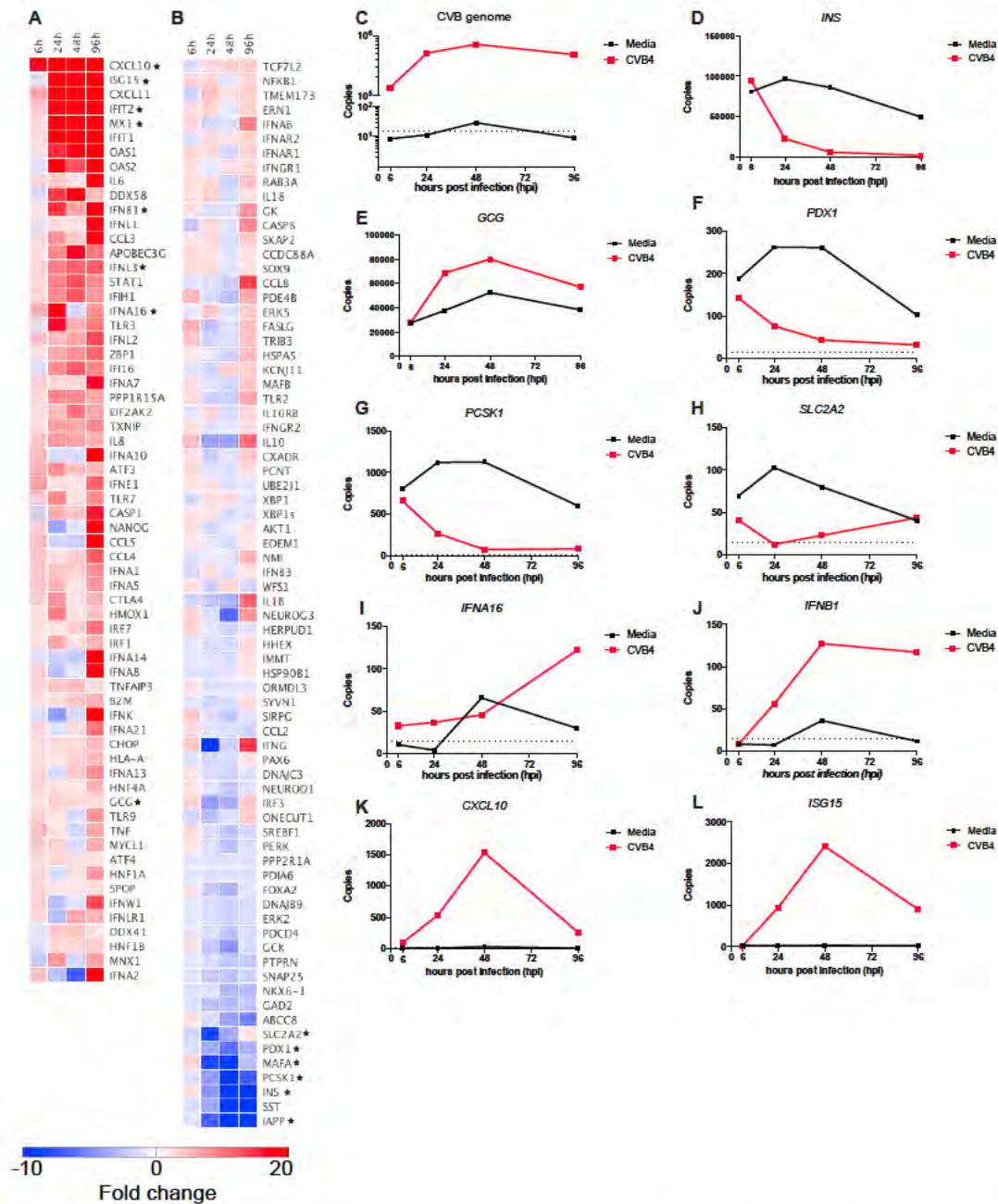


**Figure 3.3: Changes in gene expression in ex vivo cultured human islets at multiple time points after CVB4 challenge.**

Islets from a single non-diabetic human donor were challenged with CVB4 (1e6 pfu/100 IEQ) and were processed for total RNA at 6, 24, 48, and 96 hpi. Gene expression was measured by NanoString assay (NSCS2); each gene was normalized to a panel of seven housekeeping genes. Fold changes (CVB4-

challenged islets compared to uninfected islets) were sorted by the average fold change across all time points in descending order and displayed as a heatmap for genes that **(A)** increased after infection or **(B)** decreased after infection. Gene expression of selected endocrine genes, genes involved in  $\beta$  cell function, or innate immune response are plotted as relative copies with media controls in black and CVB4-challenged islets in red at 6, 24, 48, and 96 hpi for **(C)** CVB genome, **(D)** *INS*, **(E)** *GCG*, **(F)** *PDX1*, **(G)** *PCSK1*, **(H)** *SLC2A2*, **(I)** *IFNA6*, **(J)** *IFNB1*, **(K)** *CXCL10*, and **(L)** *ISG15*. Dotted line represents the limit of detection for the NanoString assay ~15 copies.

change). *IFNE1* has low total gene counts that are near the level of background, but the gene counts for the other three genes are robust at this time point. At 24 hpi, many more changes in gene expression after CVB4 infection are observed. 28 genes have a greater than 3-fold increase, and 12 genes have a greater than 3-fold decrease in expression. Genes that are among the most increased at 24 hpi include the IFN-I genes *IFNB1* and *IFNA16* and the IFN-III gene *IFNL3*. This correlates well with the expression of ISGs *CXCL10*, *IFIT2*, *ISG15*, *CXCL11*, and *MX1* that also have increased expression at this time point (Fig. 3.3, A). Most of the genes with a greater than 3-fold decrease at 24 hpi are involved in islet cell function and include genes involved in  $\beta$  cell function and insulin secretion, specifically *SLC2A2*, *MAFA*, *IAPP*, *INS*, *PCKS1* and *PDX1* (in order from highest to lowest fold change) (Fig. 3.3, B).

By 48 hpi, 23 genes with a greater than 3-fold increase, and 15 genes with a greater than 3-fold decrease are detected. The patterns are similar to results presented in Figure 3.1. By 96 hpi, the number of genes with a greater than 3-fold change are 58 genes increased and 6 genes decreased.

To better visualize the changes in gene expression over time in either mock or CVB4-infected primary human islets, I plotted the measurements for selected genes involved in islet cell function or antiviral response that for each time point. Similar to previous experiments (Fig. 3.1), *INS* expression is dramatically decreased in CVB4-infected islets. *INS* expression drops precipitously between 6 and 24 hpi and continues to decrease until 96 hpi, while



mock infected islets have only a slight reduction in *INS* expression by 96 hpi (Fig. 3.3, D). *GCG* gene expression is slightly increased in CVB4-infected islets (Fig. 3.3, E). Genes involved in insulin production and secretion, *PDX1*, *PCSK1*, and *SLC2A2* are decreased upon infection with CVB4. (Fig. 3.3, F-H). IFN genes are expressed in response to CVB4-infection (Fig. 3.3, I-J). Congruent with the expression of IFN genes, ISG expression for *CXCL10* peaks at 48 hpi (Fig. 3.3, K). Similarly *ISG15* expression reaches peak levels at 48 hpi and is among the genes with the highest difference in gene expression between CVB4-infected cells and mock at all time points (Fig. 3.3, L).

#### **3.3.4: Gene expression changes in primary human islets infected with CVB4 or stimulated with poly(I:C) or poly(dA:dT)**

Cultured primary human islets provide a relevant platform for the study of early changes in gene expression upon viral infection due to the similarities in gene profile to the infection of primary human islets engrafted in mice.

Stimulations of cultured human islets with other innate immune pathway agonists can provide insights into  $\beta$  cell responses that are specific to this viral infection and independent of general IFN responses. To identify gene expression changes that are specific to CVB4 infection of cultured primary human islets from a single islet donor, I compared gene expression after infection with CVB4 or after stimulations with synthetic agonists of IFN signaling. I transfected the dsRNA mimetic, poly(I:C), which signals through MDA5 and IRF3 to induce *IFNB* expression<sup>238</sup>. I also transfected poly(dA:dT) as a synthetic activator of the DNA sensing pathways that include ZBP1/DAI and LRRFIP1 leading to IFN-I

expression<sup>239</sup>. I evaluated gene expression using the NSCS2 gene expression panel at 24 hours after infection or treatment.

Cultured primary human islets stimulated with either poly(I:C) or poly(dA:dT) had many similar patterns of gene expression changes with those for CVB4 infection. These include robust expression of the ISGs *CXCL10*, *ISG15*, and *IFIT2* (Fig. 3.4, C). Despite these similarities, some interesting differences were noted, including those in islet function genes *INS* and *PDX1*. *INS* expression is decreased -4.3 fold at 24 hpi in CVB4 infected islets (Fig 3.4, A), which is similar to the -7.6 fold decrease observed at 48 hpi (Figure 3.1, A). No decrease in *INS* gene expression is measured in either poly(I:C) or poly(dA:dT) treated islets (Figure 3.4, A) despite the presence of a robust IFN response (Figure 3.4, B-C). *PDX1* is also decreased by CVB4 infection by -3.5 fold, while poly(I:C) and poly(dA:dT) have minimal effects on *PDX1* expression (-1.06 and 1.08 fold change respectively). These changes in gene expression after CVB4 infection may represent changes in islet function genes that are independent of the general IFN responses induced by synthetic nucleic acid analogs.

IFN production is critically important in controlling viral replication and accumulating evidence points to IFN signaling as a contributor to the development of T1D<sup>104,177,178</sup>. Since differences in expression in islet function genes are observed with nucleic acid stimulants compared to CVB4 infection, different IFN genes stimulated under these conditions could mediate the differential responses. By adding probes specific for IFN-I, IFN-II, and IFN-III

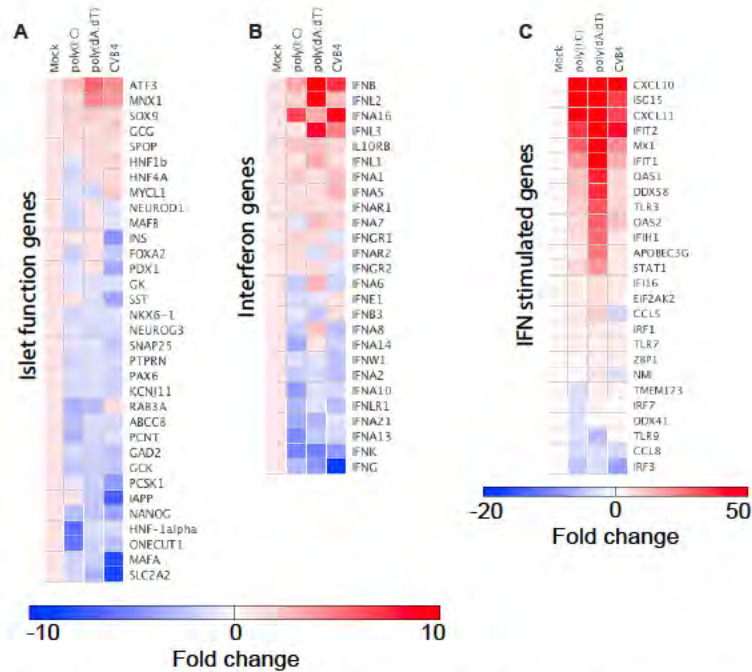


**Figure 3.4: Stimulation of *ex vivo* cultured human islets with poly(I:C) and poly(dA:dT) induces a similar IFN gene profile as CVB4, but a differential islet function genes profile.**

Islets from the same donor as Figure 3.3 were also stimulated with poly(I:C) and poly(dA:dT) and processed for RNA at 24 hpi. Normalized NanoString (NSCS2) gene copies are presented as fold change over media control in a heatmap sorted by the average change across each of these conditions as well as for CVB4. Results are displayed in three general categories: **(A)** genes associated with islet cell function, **(B)** interferon genes, or **(C)** interferon-stimulated genes. **(A-B)** scale from -10 in blue to 10 in red or **(C)** -20 in blue to 50 in red.

genes, we are able to interrogate which genes are involved in the response of cultured primary human islets. In line with the induction of *IFNB* expression at 48 hpi and secretion of IFN- $\beta$  and IFN- $\alpha$  into supernatants (Fig. 3.1, B & C), *IFNA16* and *IFNB1* are among the highest IFN-I genes induced by poly(I:C) and CVB4 infection. CVB4-infected islets also increased the IFN-III gene, *IFNL3* (IL28B) (Fig. 3.3, B). ISGs are increased at 24 hpi in all treatments.

### **3.3.5: Infection and gene expression in SC- $\beta$ cells**

To reduce the contribution of genetic variability in responses to viruses in islets from donors of primary human islets, I used cells that were directionally differentiated into pancreatic endocrine cells from human stem cells, called SC- $\beta$  cells<sup>33</sup>. Multiple endocrine cell types are present in these cell clusters, but the majority of the cells are insulin-producing  $\beta$ -cells. First, I infected these cells with a GFP-expressing strain of CVB3, CVB4 or stimulation with transfected poly(I:C) from a single batch of SC- $\beta$  cells. In mock-treated cells at 13 h, the cell clusters remained intact and had very few cells that were not associated with clusters (Fig. 3.5, A). Transfection of poly(I:C) resulted in more free-floating cells and some of the clusters appeared to be less tightly-associated, indicating some toxicity (Fig. 3.5, B). Infection with CVB4 at an MOI of 10 exhibited the highest CPE at 13 hpi, while infection with CVB3-eGFP at an MOI of 10 had slightly less CPE (Fig. 3.5, C-D). I also visualized GFP expression in these cells upon infection with CVB3-eGFP at three different MOI to evaluate the capacity of virus to replicate in SC- $\beta$  cells and gauge relative infection efficiency (Fig. 3.5, E). The

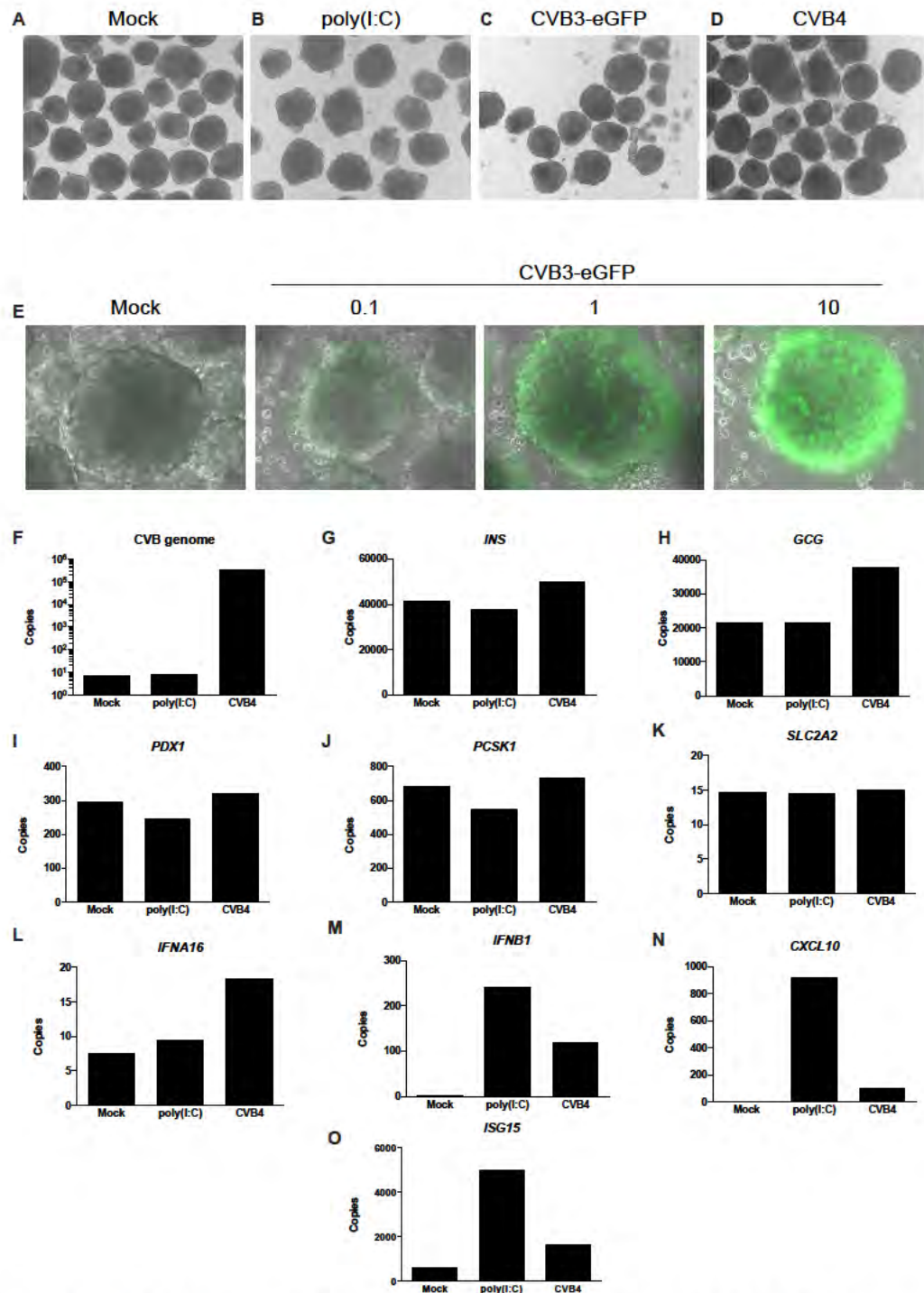


**Figure 3.5: SC- $\beta$  cells are permissive to CVB infection and display increased expression of antiviral response genes following infection.** SC- $\beta$  cells were (A) untreated, stimulated with (B) 100  $\mu$ g/ml poly(I:C), or infected with either (C) CVB3-eGFP or (D) purified CVB4-JVB and evaluated for CPE at

13 hpi by brightfield microscopy at 25x magnification. (E) GFP expression was evaluated by microscopy at 100x magnification at 13hpi for CVB3-eGFP at MOIs of 0.1, 1, and 10. Gene expression was evaluated in untreated, stimulated with 100 µg/ml poly(I:C) or infection of CVB4 at MOI of 1 at 16 hpi using the NanoString CodeSet (NSCS2) for the same genes as selected in Figure 3.3 plotted as relative copies for each of the three conditions (F) CVB genome copies, (G) *INS*, (H) *GCG*, (I) *PDX1*, (J) *PCSK1*, (K) *SLC2A2*, (L) *IFNA16*, (M) *IFNB1*, (N) *CXCL10*, and (O) *ISG15*.

mock-treated cells did not have any visible GFP expression, and a dose-dependent increase in GFP production following CVB3-eGFP infection was observed with MOIs of 0.1, 1, and 10. The CPE observed in Figure 3.4, C correlates with the viral infection evaluated by GFP expression.

In agreement with the expression of GFP in CVB3-eGFP-infected SC- $\beta$  cells and the CPE observed in CVB4-infected islets, CVB genomes are detected in RNA extracted from infected SC- $\beta$  cells by the NanoString probe. No CVB genomic RNA is present in mock or poly(I:C) treated cells (Fig. 3.5, F).

To compare gene expression changes upon treatment with poly(I:C) and CVB4 infection in SC- $\beta$  with the changes in cultured primary human islets, I measured gene expression by NanoString gene expression assay (NSCS2). While expression of many genes changed, I here focus on  $\beta$  cell function or innate immune genes that are modulated in infected cultured primary human islets. Upon treatment with poly(I:C) or CVB4 infection for 16 hpi, no changes in *INS*, *GCG*, *PDX1*, *PCSK1*, or *SLC2A2* are seen (Fig. 3.5, G-K). *IFNA16* gene expression is slightly increased with CVB4 infection, but not with poly(I:C) treatment (Fig. 3.5, L). *IFNB1* gene expression is greatly increased after treatment with poly(I:C), and a similar, although less robust increase is observed with CVB4 infection (Fig. 3.5, M). The ISGs *CXCL10* and *ISG15* both increase with each treatment. However, gene expression is higher with poly(I:C) treatment than with CVB4 infection for each gene (Fig. 3.5, N-O).

### 3.3.6: CVB infection and replication in EndoC- $\beta$ H1 cells

Infection of SC- $\beta$  cells can provide interesting insights into changes in gene expression from cells derived from a clonal stem cell population. This provides the advantage of reducing the inter-experimental variability caused by variability in donor genetics in primary human islet studies. However, these cells still are a mixed cell type population. To better define the infection, replication, and gene expression specifically in human  $\beta$  cells, I also used the recently developed EndoC- $\beta$ H1 cell line<sup>237</sup>.

EndoC- $\beta$ H1 cells grow as an adherent monolayer on ECM-coated culture dishes (Fig. 3.6, A-top row). Following CVB4-infection (MOI 1), a progressive increase in CPE is observed over time, which is characterized by cell rounding and detachment from the culture surface. At 4 hpi, minimal viral CPE is evident. By 24 hpi, approximately 40% of the cells are rounded or separated from neighboring cells. By 48 hpi, almost all of the cells become rounded and begin to detach from the culture surface (Fig. 3.6, A-bottom row). The kinetics of the development of CPE are dose-dependent based on the input MOI of CVB4. At a low MOI of 0.01, 50% CPE is not reached until after 48 hpi. Infection with an MOI of 0.1 reaches 50% CPE between 24 and 32 hpi. CVB4-infection with an MOI of 1 reaches 50% CPE before 24 hpi, and approaches 100% CPE by 48 hpi (Figure 3.6, B). To further evaluate the kinetics of viral replication, I measured the production of CVB4 viral copies in RNA extracts from EndoC- $\beta$ H1 cells at 0, 2, 4, 6, 10, and 24 hpi at an MOI of 10 by qRT-PCR. Upon adsorption with the virus for 1 h,  $3.5 \times 10^7$  copies/ $\mu$ l RNA are present, indicating that virus is either attached to



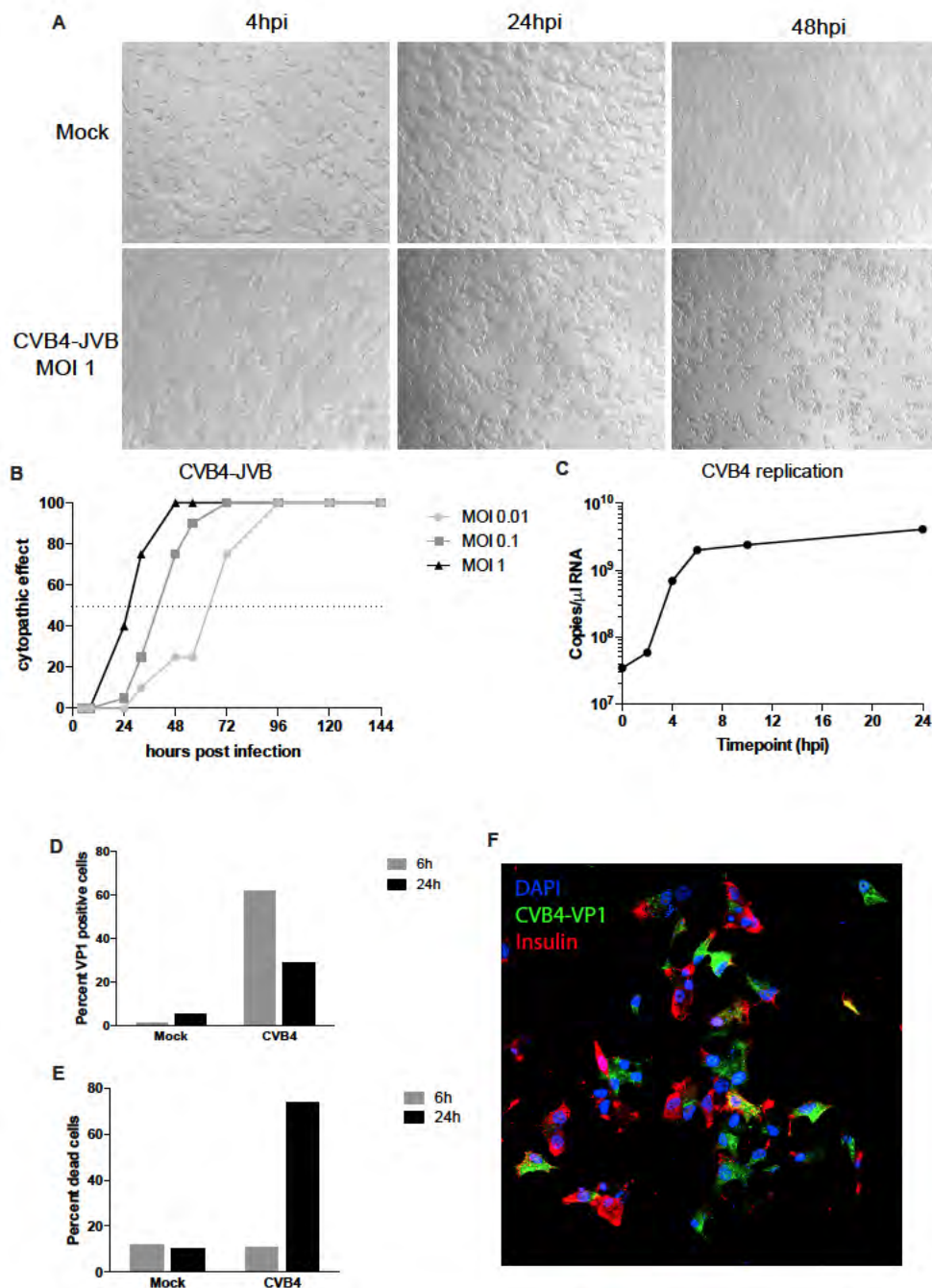


**Figure 3.6. EndoC- $\beta$ H1 cells are permissive to CVB4 infection and exhibit CPE consistent with lytic infection.**

(A) Brightfield images of EndoC- $\beta$ H1 cells that were either mock-treated (top row) or infected with CVB4 (MOI = 1) (bottom row) at 4, 24, and 48 hpi at 50x magnification. (B) Scoring of CPE for CVB4 infections of EndoC- $\beta$ H1 at three different MOIs between 4 and 144 hpi. (C) Viral copies in total RNA collected at

0, 2, 4, 6, 10, and 24 hpi evaluated by qRT-PCR. Flow cytometry of EndoC- $\beta$ H1 cells infected with CVB4 (MOI = 10) at 6 and 24 hpi for **(D)** dead cells or **(E)** VP1. **(F)** Immunofluorescence staining of EndoC- $\beta$ H1 cells infected with CVB4 (MOI = 10) at 6 hpi for DAPI (blue), VP1 (green), and insulin (red) images acquired with a 630x.

or internalized by EndoC- $\beta$ H1 cells. Between 0 and 10 hpi, the number of viral copies increased by nearly 2-logs, indicating a rapid and robust replication of CVB4 in EndoC- $\beta$ H1 (Fig. 3.6, C). The capacity of CVB to produce viral RNA and proteins demonstrates that CVB4 is able to infect and replicate specifically in these human  $\beta$  cells.

To further evaluate the replication capacity of CVB in human  $\beta$  cells, I stained infected cells for CVB capsid viral protein 1 (VP1) and cell death by flow cytometry. 62% of EndoC- $\beta$ H1 cells infected with CVB4 at an MOI of 10 are positive for VP1 staining at 6 hpi. This decreases slightly to 29% by 24 hpi (Fig. 3.6, D). CVB4-infected EndoC- $\beta$ H1 cells have a similar proportion of dead cells compared to mock treated cultures at 6 hpi. By 24 hpi, an increase to 74% dead cells after CVB4 infection is present (Fig. 3.6, E). To visualize viral protein in addition to insulin in CVB4-infected EndoC- $\beta$ H1, I stained cells infected with CVB4 at an MOI of 10 at 6 hpi with anti-VP1- (green) and anti-insulin- (red) specific antibodies. Under these conditions, VP1 was readily detected and colocalization with insulin staining is present (yellow) (Fig. 3.6, F). It is unclear from the image analysis if CVB4-infected EndoC- $\beta$ H1 cells have reduced insulin protein compared to mock-treated cells as insulin staining intensity is not significantly different between the two treatments (data not shown). Taken together, production of CPE and increases in viral RNA and protein shows that CVB4 is able to infect and replicate specifically in human  $\beta$  cells.

### 3.3.7: Gene expression in CVB4-infected EndoC- $\beta$ H1 cells

Since CVB4 productively replicates in EndoC- $\beta$ H1 cells, I measured the gene expression in these cells in response to infection. EndoC- $\beta$ H1 cells infected with CVB4 at an MOI of 10 in three independent experiments have reproducibly high numbers of viral genomic copies at both 6 and 24 hpi (Fig 3.7, A). Only a slight increase is observed between these two time points, which is expected based on the viral replication kinetics established in Figure 3.6, C.

CVB4-infection of EndoC- $\beta$ H1 cells causes a slight, but statistically significant decrease in *INS* gene expression (Fig. 3.7, B). However, no change in *PDX1* gene expression is observed at 6 hpi. At 24 hpi *PDX1* gene expression is slightly but significantly increased (Fig. 3.7, C). Both *IFNB1* and *CXCL10* gene expression are increased following infection. *IFNB1* expression is increased slightly at 6hpi and further increased by 24 hpi, however neither of these increases reached statistical significance (Fig. 3.7, D). Similarly, *CXCL10* expression is increased between 6 and 24 hpi, and again statistical significance was not reached (Fig. 3.7, E).

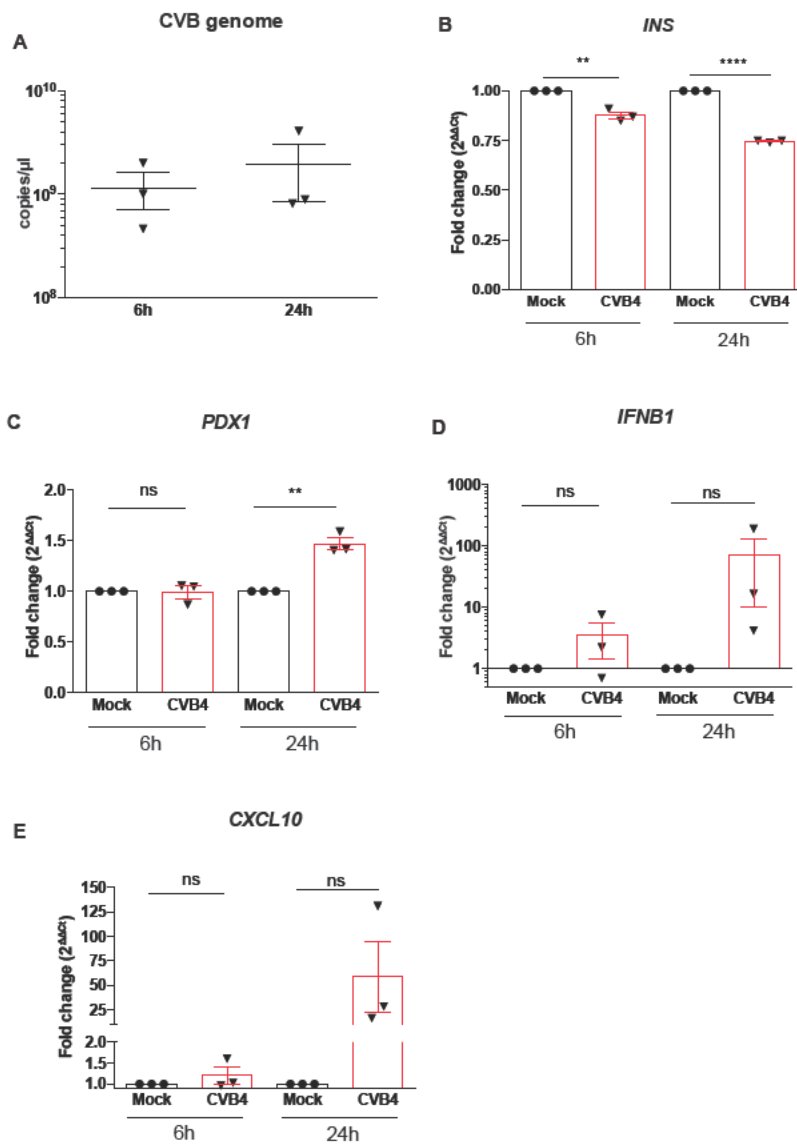


**Figure 3.7: Assessment of gene expression in EndoC- $\beta$ H1 cells following CVB4 infection.**

Gene expression studies for three independent EndoC- $\beta$ H1 infections with CVB4-JVB. (A) CVB4 copies measured in total RNA from EndoC- $\beta$ H1 cells infected for 6 or 24 hpi with CVB4-JVB at an MOI of 10. qRT-PCR gene expression in EndoC- $\beta$ H1 cells either mock treated or infected with CVB4 at MOI of 10 relative to GAPDH and normalized to the mock 6 hpi sample for (B) *INS*, (C) *PDX1*, (D) *IFNB1*, and (E) *CXCL10* plotted as  $2^{\Delta\Delta Ct}$ . Error bars represent S.E.M. ns = not significant; \*\*,  $P < 0.005$ ; \*\*\*\*,  $P < 0.0001$ , two-tailed Student's t test.

## 3.4: Discussion

### 3.4.1: Comparison of CVB4 infection of engrafted and cultured primary human islets

The first goal of this chapter is to compare the gene expression changes upon CVB4 infection in either *in vivo* or cultured cells. The gene expression in mice with engrafted primary human islets upon CVB4 infection as described in Figure 2.6 serve as the comparator for other infection platforms. The *in vivo* studies provide a physiologically relevant model for the gene expression changes in primary human islets upon viral infection that is associated with hyperglycemia in these animals. The comparison model is cultured primary human islets infected with CVB4 for 48 hours. One of the major differences in these two experimental designs is the time frame. Gene expression in the engrafted human islets is not evaluated until the endpoint of the experiment is reached, which is a mean of 38 days post infection. This scenario provides an endpoint gene expression profile for the long-term viral replication and associated hyperglycemia. The gene expression of infection in the cultured islets is measured at 48 hpi. The earlier changes in gene expression offer insights into the pathways involved in reaching the endpoint gene expression profile observed in the mouse model.

Surprisingly, there are many similarities in the genes with both the largest increases and decreases in both engrafted and cultured islets upon CVB4 infection. Expression for ISGs is similarly increased upon viral infection in both

experimental setups. *CXCL10*, *MX1*, *OAS2*, and *IFIH1* are all increased at 48 hpi in the cultured islets, and are sustained in the engrafted islets until the endpoint of the experiments (Fig. 3.2, A). Differences in IFN gene expression do indicate that there is eventually a reduction of IFN production at terminal time points in the infected islets in mice. *IFNB1* and *IFNG* expression are not increased in primary human islets engrafted in mice, but at 48 hpi in cultured primary human islets expression of these genes is robust. One possibility for this is that prolonged exposure to virus in the islets engrafted in mice eventually exhausts or destroys the cells responsible for the IFN production that is present at 48 hpi in culture. Another possibility is that there are changes in the virus that make them less recognizable to pattern recognition receptors like MDA5 and therefore less stimulatory for IFN gene expression. Persistent infection is associated with terminal deletions in the 5' UTR of virus, which may make them less stimulatory<sup>240</sup>. CVB proteins can also inhibit IFN production through the cleavage of MAVS by the protease 3C<sup>143</sup>. However, I have not investigated the changes in the virus or contributions of viral proteins in suppressing IFN signaling.

The genes with the largest decrease in both experimental designs are associated with endocrine cell function. *INS*, *PDX1*, and *SST* are similarly decreased in engrafted and cultured islets upon CVB4 infection. It is interesting that both *INS* and *PDX1* gene expression decrease by 48 hpi in cultured primary human islets, because the kinetics of the development of hyperglycemia in the mouse model of engrafted human islets indicates a slow, progressive loss in  $\beta$

cell function upon CVB4 infection. There may be a delay in the virus reaching the engrafted human islets in the systemic infection of CVB4 administered by IP injection. However, in an independent infection of mice engrafted with primary human islets, VP1 protein is present at 7 days post infection (data not shown)<sup>241</sup>. Since the cultured primary human islets are infected in a low volume for 1 h to allow the virus to adsorb to cells, the local concentration of virus may be much higher than for the systemic infection, which may accelerate the  $\beta$  cell dysfunction.

The pattern of differentially expressed genes did not completely overlap between the *ex vivo* and *in vivo* studies. The gene expression pattern of cultured human islets 48 h post-infection reflects early responses to viral infection similar to those reported by others<sup>242</sup>. In contrast, the *in vivo* gene profile in terminal graft samples reflects prolonged consequences of viral infection, and is dominated by downstream cytokines and ER stress-related unfolded protein response genes. Increases in gene expression for *DDIT3*, which encodes CHOP, and *EIF2AK3*, which encodes PERK, are observed; whereas the expression of *XBP1* is decreased. Increased CHOP levels, but not XBP-1 protein levels, are reported in islets from tissue sections of T1D patients<sup>243</sup>. *TXNIP* is also highly stimulated in grafts from infected mice. In the virus-induced BBDR rat model of diabetes, the IRE1 and PERK ER stress pathways are activated<sup>244</sup>; both of these pathways induce *TXNIP* to promote programmed cell death under unresolvable ER stress<sup>245</sup>.



### **3.4.2: Insulin staining of CVB3-eGFP-infected dispersed primary human islets**

Infection of dispersed primary human islets with a GFP-expressing strain of CVB3 indicates that these cells can be infected and they support active replication. Insulin staining of these cells reveals that viral GFP often co-localizes. GFP does not always overlap with insulin staining, so other cell types represented in human islets may also support CVB replication. However, it is also possible that these cells produced insulin prior to infection and the staining is decreased after infection.

### **3.4.3: Genes associated with $\beta$ cell function are decreased after CVB4 infection**

Early gene expression changes after CVB4 infection in cultured primary human islets indicate pathways that may be involved in the dynamic changes in antiviral response and  $\beta$  cell function. The earliest time point after viral infection that I measured was 6 hpi, and only four genes had greater than 3-fold increase in gene expression. *CXCL10* consistently has the highest increase in gene expression across all time points measured upon CVB4 infection. Interestingly, treatment of primary human islets with CXCL10 inhibits  $\beta$  cell function. Treated islets have a decrease in insulin secretion in response to glucose stimulation<sup>190</sup>. Therefore, the production of CXCL10 in response to CVB4 infection may be contributing to changes in  $\beta$  cell functions of insulin secretion. However, this suppression of insulin is not likely due to a decrease in insulin translation since stimulations of islets with innate immune agonists, poly(I:C) and poly(dA:dT) produce robust levels of *CXCL10* (Fig. 3.4, C), but they do not decrease *INS* and

*PDX1* mRNA upon stimulation (Fig3.4, A). Thus, multiple factors contribute to  $\beta$  cell dysfunction during viral infection, including host gene responses and virus-specific factors. These factors could be elucidated by expression of individual viral proteins or transfection of immune stimulatory viral RNA.

Other genes associated with proper  $\beta$  cell function are decreased in primary islets upon CVB4 infection between 6 and 24 hpi. *PCSK1*, which encodes for prohormone convertase 1, is responsible for converting proinsulin into the mature hormone<sup>246</sup>. *PCSK1* gene expression is also decreased upon CVB5 infection of primary human islets<sup>247</sup>. Additionally, *SLC2A2*, which encodes for the glucose transporter GLUT2, is decreased upon CVB4 infection of primary human islets. The import of glucose into  $\beta$  cells is a necessary step in sensing blood glucose concentrations and responding by secreting insulin<sup>246</sup>. These differences in insulin hormone processing and glucose transporter function could help to explain the reduction in insulin secretion in response to glucose stimulation upon viral infection<sup>233-235</sup>. Since these genes are involved in multiple, non-redundant pathways involved in normal  $\beta$  cell function, differential effects on individual pathways by various viruses may lead to some of the heterogeneity in their inhibition of insulin secretion.

Despite these potentially exciting findings, these experiments need to be repeated in multiple primary human islet donors. Due to the heterogeneity of genetics in human islet donors, multiple donors must be evaluated to determine if

these observed results are due to donor specific genetics or if there are more generalized responses to CVB infections.

#### **3.4.4: Innate immune gene expression in primary human islets infected with CVB4 or treatment with poly(I:C) or poly(dA:dT)**

IFN production could contribute to the development of T1D in contributing to poor  $\beta$  cell function in response to glucose or through interactions with the adaptive immune system that progress to autoimmunity. IFN and downstream cytokine production are associated with  $\beta$  cell dysfunction<sup>190,248</sup>. The presence of IFN in serum or in sections of tissue from recent onset T1D patients is also often associated with the development of T1D<sup>104,177,178</sup>. Therefore, understanding the IFN production capacity of primary human islets is important for understanding the development of T1D.

Many IFN genes increase in expression by 96 hpi in response to CVB4 infection, but IFN-I genes are among the first to increase. *IFNA16* is the first IFN gene to have a greater than 3-fold increase after CVB4 infection. This response is mediated through activation of the dsRNA sensor MDA5 through an interaction with MAVS<sup>168</sup>. Expression of *IFNA16* could be driving the antiviral response at these early time points. However, at later time points viral proteins may suppress IFN signaling through a cleavage of both MAVS and TRIF by the viral protease 3C<sup>143</sup>.

Along with IFN-I expression upon CVB4 infection, *IFNL3* gene expression is expressed 5.7-fold higher than in mock-infected islets at 48 hpi. Infections of primary human islets with other serotypes of CVB also trigger the production of

IFN-III<sup>247</sup>. Interestingly, some heterogeneity in IFN-III receptor distribution is observed on islet cells. Human  $\alpha$  cells express both receptor subunits (IFN $\lambda$ -R1 and IL-10R2), while  $\beta$  cells only express a single receptor subunit (IL-10R2)<sup>249</sup>. Cell type differences in IFN receptor expression, so response to IFN could help reconcile the specificity for  $\beta$  cells in the ultimate autoimmune manifestation of T1D. CVB-infected  $\beta$  cells could produce and respond to IFN and downstream signaling to APCs differently from other CVB-infected cells in the pancreas. This could portend the production of autoimmunity to develop only against  $\beta$  cells. These cell type differences will be further explored in **Chapter V**.

Despite subtle differences in the induction of IFN genes in CVB4 infection, and treatments with either poly(I:C) or poly(dA:dT), the ISG response is very similar increased upon treatment (Fig. 3.4, C). As in other experiments of viral infections of primary human islets *CXCL10* expression was among the genes with highest increase in gene expression. This indicates that islet cells are capable of producing robust antiviral responses, but again it is unclear if there are cell-type specific differences in the production of these responses.

#### **3.4.5: Comparison of SC- $\beta$ to primary human islets**

Treatment of SC- $\beta$  cells with poly(I:C) or infected with CVB resulted in CPE comparable to cultured primary human islets. Both SC- $\beta$  cells and primary human islets are comprised of mixed cell populations. Therefore it is difficult to determine if one cell type is more susceptible to treatment than others. Infection of SC- $\beta$  cells with CVB3-eGFP resulted in dose-dependent production of GFP by 13 hpi. The intensity and distribution of infected cells seemed similar to infections

of primary human islets. Thus SC- $\beta$  cells (*CXADR* copies = 148) appear to have virus receptor expression similar to primary human islets (*CXADR* copies = 76) to allow for virus entry.

Unexpectedly, SC- $\beta$  gene expression of islet function genes *INS*, *PDX1*, *PCSK1*, and *SLC2A2* did not decrease upon infection with CVB4. This finding is not consistent with observations in CVB4-infected cultured primary human islets. Factors of virus dose and replication kinetics in these two different cell sources could explain this discrepancy. Primary human islets have on average ~200 cells per IEQ, so primary human islets were infected with an effective MOI of 50. CVB4 MOIs of 1 and 10 in SC- $\beta$  cells were substantially lower than that for cultured primary human islets. MOI-dependent differences in the fate of cells infected with CVB could explain some of the differences observed in islet function gene expression between the two cell sources<sup>250</sup>. Despite the differences in initial dose, CVB replicated to similar levels in SC- $\beta$  and primary human islet cells. CVB4-infected SC- $\beta$  cells at express 3.1e5 genome copies at 16 hpi, which at similar to the 5e5 genome copies of CVB measured in primary human islets at 24 hpi. To better compare the outcomes of CVB4 infection on  $\beta$  cell function genes, a more comparable dose of CVB4 should be used and later time points should also be evaluated to account for possible differences in kinetics of response between the SC- $\beta$  and cultured primary human islets.

The cell composition of SC- $\beta$  cells is different from primary human islets: the majority of hormone positive cells, 35% of total cells in SC- $\beta$  clusters,

produce C-peptide, approximately 1% in these clusters also produce either glucagon or somatostatin, and another 10% produce more than one hormone<sup>33</sup>. In primary human islets, the majority of hormone-producing cells make insulin, with ~65% of total cells staining positive for insulin. In contrast to SC- $\beta$  cells, primary human islets have higher proportions of  $\alpha$  and  $\delta$  cells, with ~30% and ~5% of each, respectively<sup>251</sup>. Opposed to the cultured primary human islets, resident immune cells that contribute to the immune response should not be present in SC- $\beta$  cells. Infections of SC- $\beta$  cell clusters with CVB4 support the argument that cells other than APCs are producing IFN-I. The IFN and ISG gene response to treatment with poly(I:C) or infection with CVB4 is similar to infections of primary human islets. These cells may provide a new alternative to studying IFN signaling in human islets. Since these cells can be derived from clonal stem cells, they are more genetically tractable than primary human islet cells. The ability to modulate gene expression of innate immune sensors or IFN-I receptors may provide further insights into the innate immune responses in  $\beta$  cells upon CVB infection.

#### **3.4.6: EndoC- $\beta$ H1 cell infections**

The species-specific differences in gene expression, structure, and function of  $\beta$  cells among different species places major caveats on studies of viral infections in rodent  $\beta$  cell lines in their relevance to human disease. The development of the human  $\beta$  cell line, EndoC- $\beta$ H1, is an exciting advancement for studying viral infection in the context of species-specific interactions and responses. CVB4 productively replicates in EndoC- $\beta$ H1 cells with a dose-

dependent CPE. The kinetics of the development of CPE in these cells was somewhat surprising given the extended timeline for the development of hyperglycemia in mice engrafted with primary human islets. Engrafted islets may possibly receive growth and survival factors from other engrafted cells or mouse tissues. These could modulate the antiviral response and support the persistent infection and slow progression to hyperglycemia observed in these mice.

Gene expression in EndoC- $\beta$ H1 cells upon infection with CVB4 mirrors infection of primary human islets in some respects. In these cells there is a small but significant decrease in *INS* gene expression between 6 and 24 hpi. This is also observed in infections of cultured primary human islets, but the decrease is much more pronounced in this case. *IFNB1* and *CXCL10* production are both increased upon CVB4 infection, similar to primary human islets. In contrast to infections of cultured primary human islets, the gene expression for the transcription factor, *PDX1*, did not decrease between 6 and 24 hpi in EndoC- $\beta$ H1 cells. The reason for this discrepancy is unclear, but it is possible that the process used to immortalize these cells has made *PDX1* gene regulation more resistant to stress conditions induced by viral replication.

#### **3.4.7: Conclusions:**

Gene expression changes in engrafted primary human islets are similar to cultured primary human islets upon CVB4 infection. These similarities point to important pathways that are involved in  $\beta$  cell dysfunction during CVB4 infection. The decrease of both *INS* and *PDX1* gene expression between 6 and 24 hpi in cultured primary human islets indicates that the effects of viral replication on  $\beta$

cell function occur early. The early role of changes in PDX1 on  $\beta$  cell function will be further addressed in **Chapter IV**. Although, differences between *INS* gene expression decrease between cultured primary human islets and both SC- $\beta$  and EndoC- $\beta$ H1 cells raises questions about direct effects of this decrease caused by CVB4 infection. The strategy of sorting different cell types from primary human islets using flow cytometry methodologies discussed in **Chapter V** aimed to address these discrepancies.

Infections of cultured primary human islets are advantageous in the ability to easily evaluate the kinetics of gene expression in CVB4-infection. The time course of gene expression changes help to identify key players in the mechanistic changes in infected human islets. Specifically changes in innate immune genes after CVB4 infection further implicate a signaling pathway of detection of viral dsRNA replication intermediates by MDA5 (*IFIH1*) that leads to the production of IFN- $\beta$  and downstream cytokine CXCL10. The innate immune cytokine production directly by  $\beta$  cells could potentiate the production of autoimmunity against these cells. However, from these studies the relative contributions of different cell types to the overall antiviral response are difficult to define. Flow cytometry-sorted primary human islet cells will be explored in **Chapter V** to further evaluate these differences.

The sources of human  $\beta$  cells implicate a role for intrinsic viral interactions in  $\beta$  cells in cellular dysfunction. These cell types address experimental complications of primary human islets that include donor variability and



limitations in culture viability and cell availability. CVB4 productively replicates in SC- $\beta$  cells and produces a similar IFN profile to infections of primary human islets. EndoC- $\beta$ H1 cells also support viral replication and confirm that  $\beta$  cells are a source of IFN production upon viral infection. Either of these two sources of human  $\beta$  cells could be used in place of primary human islets in an *in vivo* model of viral induction of hyperglycemia described in **Chapter II**. The potential for developing these new models will be discussed in detail in the general discussion (**Chapter VI**).

### **3.5: Materials and methods**

#### **3.5.1: Virus strains**

The prototypical CVB4 laboratory strain JVB (#VR-184; American Type Culture Collection) was grown in HeLa cells<sup>230</sup>. Virus was purified by ultracentrifugation on a sucrose cushion as previously described<sup>252</sup>. eGFP-CVB3 plasmid was gift from L. Whitton, Scripps Research Institute, La Jolla, CA. Virus was produced by transfection of *in vitro* transcribed RNA into HeLa cells as described previously<sup>231</sup>.

#### **3.5.2: Human islets for ex vivo Studies**

Primary human islets from three independent donors (Prodo Laboratories, Inc) were cultured in supplemented CMRL-1066 media and were challenged with poly(I:C) (InvivoGen) or CVB4-JVB (1e6 pfu/100IEQ). Supernatants were collected at 48 h. TRIzol reagent (Life Technologies) was added for RNA extraction at 48h. (Figure 3.1)

Primary islets from a fourth independent donor was cultured in RPMI 1640 supplemented with 5.5mM glucose, 10% FBS, 1% L-glutamine, and antibiotics. These islets were infected with sucrose purified CVB4-JVB (1e6 pfu/100IEQ), transfected with poly(I:C) (100 µg/ml) (InvivoGen), poly(dA:dT) (100 µg/ml) (InvivoGen), or cultured in media alone. CVB4-infected and corresponding mock-infected islets were collected at 6, 24, 48, and 96 hpi for total RNA extraction by TRIzol reagent (Life Technologies). Additionally poly(I:C) and poly(dA:dT) treated islets were collected at 24 hours (Fig 3.3 & 3.4).

### **3.5.3: SC-β culture and infection**

SC-β cells were a kind gift from Doug Melton and their production has been described previously<sup>33</sup>. 500,000 cells were plated in 24 well plates and left untreated, transfected with 100µg/ml poly(I:C) (InvivoGen) using Lipofectamine 2000 reagent (ThermoFisher Scientific), or infected with CVB3-eGFP or CVB4-JVB at MOI 0.1, 1.0 or 10. Images were acquired at 13 h after treatment as described below, and total RNA was collected by TRIzol reagent (Life Technologies).

### **3.5.4: EndoC-βH1 culture and infection**

EndoC-βH1 cells were cultured as previously described<sup>237</sup>. For infection studies, cells were plated into 24well plates. Titered stocks of CVB4-JVB were added to cells at indicated MOI in a minimal volume for 1 h to allow for adsorption. Following this incubation period, cells were washed with PBS and complete culture media was replaced. At indicated time points, cells were either

fixed for immunofluorescence staining or TRIzol reagent (Life Technologies) was added for extraction of total RNA.

### **3.5.5: Gene expression profiling (Figure 3.1)**

The NSCS1 used in Figure 2.6 allowed for direct measurement of mRNA copies without the need for amplification. Probes were designed to target human genes in a species-specific manner. The CodeSet included type I IFN, cytokines, apoptosis, endocrine, endoplasmic reticulum (ER) stress, T1D-associated loci, and other human genes, plus seven housekeeping genes for normalization of data. A probe for a conserved CVB sequence targeting the same region as the quantitative RT-PCR primer was included<sup>105</sup>. 100 ng of RNA extracted from tissue was hybridized, processed, and analyzed per the manufacturer's procedure. Data were normalized using the nSolver Analysis Software (version 1.1). Fold changes in gene expression were the ratio of normalized gene expression in CVB4-infected samples versus those in mock-infected samples. Averages of fold changes were calculated by averaging the  $\log_{10}$  of the fold change followed by a transformation of  $10^x$ . Values  $<1$  were transformed by  $-1/x$ .

### **3.5.5: Gene expression profiling (Fig 3.2, Fig 3-3, Fig 3.4)**

The NanoString CodeSet #2 (NSCS2) was developed for genes associated with IFN-I (18), IFN-II (3), IFN-III (5), IFN regulated genes (20),  $\beta$  cell function (24), endocrine (9), apoptosis (8), cytokines (7), inflammation (8), ER stress (20), type 1 diabetes susceptibility genes (12), other human genes (4), the CVB-specific probe as described above, and housekeeping genes (7) for normalization of data for a total of 146 genes. Probes were designed to target

human genes in a species-specific manner. 100 ng of RNA extracted from cultured islets and was hybridized, processed, and analyzed per the manufacturer's procedure. Data were normalized using the nSolver Analysis Software (version 2.6). Fold changes in gene expression were the ratio of normalized gene expression in CVB4-infected samples versus those in mock-infected samples. Values  $<1$  were transformed by  $-1/x$ . Limit of detection was determined by the highest value from the internal negative control probes for each assay run. Heatmaps of transformed fold changes were produced with Gtools v2.2.3 (<http://gtools.org/>).

### **3.5.6: ELISA**

Human IFN- $\alpha$  and IFN- $\beta$  ELISA (PBL Assay Science) for supernatants collected from primary human islets.

### **3.5.7: Widefield microscopy**

Live cell culture images acquired on a Zeiss AxioVert 200 microscope equipped with an EXFO X-cite 120 fluorescent light source and an AxioCamMR camera running AxioVision SE64 v4.9.0.0 software. EC Plan-Neofluar objective lenses 5x/0.16 M27 or 10x/0.30 Ph1 were used where indicated. Images were adjusted with ImageJ v2.0.0-rc-39/1.50f<sup>232</sup>

### **3.5.8: Immunofluorescence**

EndoC- $\beta$ H1 cells were cultured on coverslips and infected with CVB4 at an MOI of 10 for 24 hours. Cells were fixed with 4% PFA for 30min at room temperature. Fixed cells were permeabilized and stained in PBS-AT (PBS+2% BSA +0.5% Triton X-100) with the following primary antibodies guinea pig antibody to insulin (1:1000; Dako) and mouse antibody to VP1, clone 5-D8/1

(1:500; Dako). The following fluorophore conjugated secondary antibodies at 1:1,000 dilution Alexa Fluor-594 goat antibody to guinea pig IgG and Alexa Fluor-488 goat antibody to mouse IgG (catalog #A11076 and #A11029, respectively; Life Technologies) for 1 hour. Coverslips were mounted with ProLong Gold Antifade Reagent with DAPI (Life Technologies). Immunofluorescence was imaged on a Leica SP8 confocal microscope with a 63x HC PL APO CS2 objective (1.4 oil) running Leica Advanced Fluorescence software (version 3.3.0.10134.1). Images were adjusted using FIJI software (version 1.48p) where necessary<sup>232</sup>.

### **3.5.9: Flow cytometry**

EndoC- $\beta$ H1 cells were trypsinized to obtain a single cell suspension at indicated time points. Dead cells were stained using LIVE/DEAD™ Fixable Blue Stain (1:1000) (Invitrogen) for 20 minutes. Cells were then fixed and permeabilized using BD Cytotfix/Cytoperm reagents (BD Biosciences). Cells were then stained with mouse antibody to VP1, clone 5-D8/1 (1:1000; Dako) and Alexa Fluor-488 goat antibody to mouse IgG (1:1000; Life Technologies). Staining was analyzed on an LRB LSR II A equipped with Trigon and Blue 488nm lasers running BD FACS Diva software (version 8.0.1) and analyzed using FlowJo (version 10.1r5).

### **3.5.10: Gene expression qRT-PCR**

Total RNA collected from CVB4-infected EndoC- $\beta$ H1 cells was extracted using TRIzol reagent (Life Technologies). 1  $\mu$ g of total RNA was reverse transcribed using the QuantiTect Reverse Transcription Kit (Qiagen). The 50ng

of the resulting cDNA was used as the template for QuantiFAST SYBR Green quantitative PCR kit using the following QuantiTect Primer Assay targets: GAPDH (QT00079247), INS (QT01531040), PDX1 (QT00201859), IFNB(QT00203763), and CXCL10 (QT01003065) (Qiagen). PCR was performed on a Bio-RAD CFX96 Real-Time system and cut-offs were determined automatically. Relative gene expression was calculated by calculating the  $\Delta\text{Ct}$  for target genes relative to GAPDH followed by  $\Delta\Delta\text{Ct}$  calculation for treatment relative to mock-infected cells at each time point. This was then plotted as  $2^{\Delta\Delta\text{Ct}}$  using GraphPad Prism 6.0h software.

#### **3.5.11: CVB genome qRT-PCR**

Total RNA collected from CVB4-infected EndoC- $\beta$ H1 cells was extracted using TRIzol reagent (Life Technologies). cDNA was generated using the High Capacity cDNA Reverse Transcriptase Kit (Applied Biosystems) followed by quantitative PCR using the Platinum Quantitative PCR SuperMix-UDG Kit (Life Technologies). Enterovirus-specific primers and probe were used for quantification of viral RNA<sup>105</sup>. A standard curve was established using the eGFP-CVB3 plasmid as a template to interpolate absolute copies per microliter of input RNA (a gift from L. Whitton, Scripps Research Institute, La Jolla, CA)<sup>231</sup>.

#### **3.5.12: Statistical Methods**

To assess the significance of the fold-change of NanoString gene expression, a standard one-sample *t* test was used to determine the significance compared with zero. Significance for qRT-PCR gene expression evaluated by unpaired, two-tailed *t*-test.

**CHAPTER IV: CVB4 INFECTION INDUCES CHANGES IN PDX1  
LOCALIZATION IN HUMAN B CELLS**

Glen R. Gallagher, Robert W. Finberg, and Jennifer P. Wang

**Contribution Summary:**

G.R.G. designed the experiments, performed the experiments, and analyzed the data. R.W.F. helped to design the experiments. J.P.W. helped to design the experiments and analyze the data.

## 4.1: Abstract

$\beta$  cells are the sole insulin-producing cells in the human body and the production of this hormone is critical in maintaining blood glucose levels. In the *in vivo* model in which mice engrafted with primary human islets are infected with CVB4, human *INS* gene expression is greatly decreased. Similarly, *INS* gene expression is decreased between 6 and 24 hpi in cultured primary human islets infected with CVB4. In parallel, gene expression of the transcription factor *PDX1* is also decreased in both models upon CVB4 infection. *PDX1* is a critical transcription factor in the production of insulin and the overall function of  $\beta$  cells. Yet treatment of cells with the innate immune agonists poly(I:C) and poly(dA:dT) does not induce a decrease of *INS* or *PDX1*. Therefore, I sought to determine how CVB4 infection specifically affects *PDX1* function and whether a change in *PDX1* contributes to the loss in *INS* expression. *PDX1* protein expression is sequestered to the nucleus in EndoC- $\beta$ H1 cells. However, upon infection with CVB viruses, *PDX1* staining intensity is decreased in the nuclei of infected cells. Surprisingly, this effect on *PDX1* localization is not replicated in infections with vesicular stomatitis virus or respiratory syncytial virus. The changes in *PDX1* localization upon CVB infection do not require  $\beta$  cell specific factors, as overexpression of *PDX1* in an irrelevant cell type is also excluded from the nucleus in infected cells. Taken together, these early changes in *PDX1* localization could be contributing to the decreased insulin gene expression.



## 4.2: Introduction

### 4.2.1: Overview

The gene expression for the transcription factor pancreatic duodenal homeobox 1 (PDX1) is highly decreased following CVB4-infection of either primary human islets engrafted in mice or cultured primary human islets (Fig. 2.6, 3.1). PDX1 is a critical transcription factor in  $\beta$  cell development, function, and survival. Therefore, I further investigated the role of the reduction in *PDX1* gene expression in  $\beta$  cell dysfunction upon CVB infection.

### 4.2.2: PDX1 function

PDX1 expression must be tightly regulated for the proper development of the pancreas. In people, homozygous frame-shift mutations in PDX1 are associated with pancreatic agenesis<sup>253</sup>. The levels of expression are also important in the function of differentiated  $\beta$  cells. Heterozygous mutations of PDX1 are linked to maturity-onset diabetes of the young 4 (MODY4)<sup>254</sup>. Missense mutations in PDX1 identified in clusters of patients cause late onset type 2 diabetes<sup>255</sup>. In addition to its important role in  $\beta$  cell function, PDX1 is also found in the proximal duodenum, pyloric glands of the distal stomach, occasional expression in submucosal layer of the duodenum and spleen<sup>256</sup>. However, the effects of PDX1 mutations are largely unknown in these tissues. The mutations and their associated diabetic manifestations highlight the importance of PDX1 in pancreatic development and blood glucose homeostasis in humans.

PDX1 contributes to transcriptional control of a wide range of genes involved in islet cell function (Fig 4.1). PDX1 is a transactivator of insulin

transcription through binding to the insulin promoter<sup>257</sup>. Insulin transcription by PDX1 is further modulated through co-activators, p300 and Bridge-1<sup>258</sup>. PDX1 also contributes to transcriptional regulation of other proteins that are important in  $\beta$  cell function. Genes encoding glucokinase (*GK*)<sup>259</sup>, islet amyloid polypeptide (*IAPP*)<sup>260</sup>, and glucose transporter type 2 (*SLC2A*)<sup>261</sup> all have PDX1 regulatory sites in their promoters. PDX1 is important for maintaining the  $\beta$  cell program in differentiated cells, and loss of PDX1 can cause a shift to an  $\alpha$  cell phenotype<sup>262</sup>. Additionally, ectopic expression of PDX1 during development can suppress the differentiation of  $\alpha$  cells leading to a reduction in glucagon expression<sup>263</sup>.

#### **4.2.3: Control of PDX1 transcriptional function**

Because of its diverse function in development, function and survival of  $\beta$  cells, *PDX1* is regulated through a variety of transcriptional, post-translational mechanisms. *PDX1* is transcribed as a 2573 bp mRNA (NM\_000209.3) and three transcript variants (XR\_941578.1, XR\_941579.1, XR\_941580.1) are predicted. In humans the PDX1 promoter contains a distal enhancer region along with three enhancer regions that are conserved between human and mouse, referred to as PH1-3. A conserved promoter region is also present proximal to the transcription start site<sup>264</sup>. Transcription of *PDX1* is induced by several transcription factors in addition to autoregulation by PDX1 itself (Fig. 4.1). HNF3 $\beta$  (*FOXA2*) binds to two enhancer regions in the promoter of *PDX1* (PH1&2), and PDX1 itself binds to another enhancer region (PH1)<sup>265</sup>. The transcription factor HNF1 $\alpha$  also binds to PH1 to promote *PDX1* transcription<sup>266</sup>. These transcription factors promote *PDX1* gene expression through binding to the distal enhancer

region of the PDX1 promoter at -2.7 to -1.9 kb. Furthermore, USF2 contributes to *PDX1* transcription and provides  $\beta$  cell specificity for expression through binding to a E box site proximal to the transcription start site at -107 to -102<sup>267</sup>. The expression of *PDX1* mRNA can also be negatively regulated. ATF3 is an inducible transcription factor in response to proinflammatory cytokines, nitric oxide, and ER stress<sup>268</sup>. ATF3 inhibits *PDX1* transcription by binding to the ATF/CRE responsive element in the PDX1 promoter<sup>269</sup>. The combination of positive and negative regulators of transcription underscores the importance of the dynamic PDX1 expression to maintain homeostasis in response to the needs of the organism.

In addition to transcriptional control, PDX1 function can be regulated through protein-protein interactions or post-translational modifications that can affect DNA chromatin remodeling, protein stability, and sub-cellular localization (Fig. 4.1). The PDX1 protein is translated from two exons. The N-terminal portion of the protein contains the activation domain and the C-terminal portion contains the homeodomain, which binds to DNA. Several potential protein-protein interacting domains can modulate PDX1 activity<sup>264</sup>. Since PDX1 does not contain intrinsic chromatin remodeling activity, it exerts its transcriptional activity through interactions with cofactors. These include members of the ATPase-containing Swi/Snf family of cofactors<sup>270</sup>. Interactions with these and other cofactors influence PDX1 DNA binding to modulate insulin production in response to glucose<sup>271</sup>. Interactions with other proteins can inhibit PDX1 function by

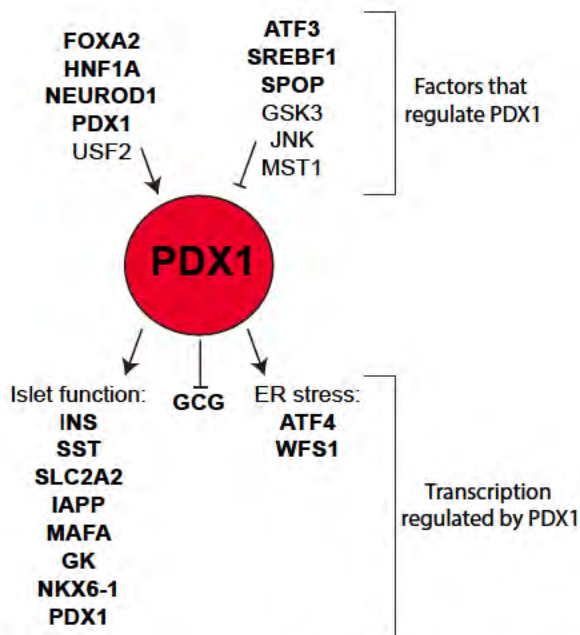


**Figure 4.1: The regulatory network of the transcription factor PDX1**

Proteins that are involved in promoting the transcription of PDX1 mRNA. Proteins involved in suppressing PDX1 activity by reducing PDX1 gene expression (**ATF3**, **SREBF1**), targeting it for degradation (**SPOP**, **GSK3**, **MST1**), or altering its nuclear localization (**JNK**). Genes that PDX1 contributes to transcriptional regulation including auto-regulation. Genes in bold are included in the NanoString analysis of gene expression presented in Figure 4.2.

increasing protein degradation, altering transcriptional activity, or changing PDX1 nuclear localization. Direct interaction of PDX1 with PCIF1 (*SPOP*) targets PDX1 for ubiquitination and proteasome degradation<sup>272</sup>. SREBP-1c (*SREBF1*) belongs to a family of transcription factors that regulate genes associated with lipid synthesis, and expression of SREBP-1c in  $\beta$  cells impairs insulin secretion<sup>273</sup>. Under lipotoxic conditions, SREBP-1c binds directly to PDX1, which disrupts the binding of PDX1 to the distal promoter site inhibiting the autoregulation of PDX1 transcription<sup>274</sup>. Changes in environmental conditions and cell stress can alter the proteins available to interact with PDX1. These modulatory proteins add an additional layer of control to allow for context-dependent PDX1 activity.

Post-translational modifications to PDX1 can also modulate its activity in response to changes in glucose or environmental stress. Glucose response is associated with several post-translational modifications. Glycosylation increases the DNA binding activity of PDX1<sup>275</sup>. Sumoylation facilitates localization of PDX1 to the nucleus and increases its stability<sup>276</sup>. Phosphorylation is also important in the glucose responsive behavior of PDX1. Glucose induces the phosphorylation of PDX1 through the activation of ERK2, which increases the transactivating activity of PDX1<sup>277</sup>. These modifications allow for rapid response to glucose to help maintain homeostasis.

Cell stress conditions caused by environmental triggers also require rapid response to mitigate damaging effects. ER stress can occur under normal conditions when  $\beta$  cells are required to increase their protein production following

high-fat or high-glucose meals. If these conditions are temporary, ER stress can be resolved without detrimental effects to the cell. For example, PDX1 contributes to  $\beta$  cell survival in mice fed a high-fat diet. This survival is mediated through the ER stress response<sup>212</sup>. To maintain cell function under temporary ER stress or proinflammatory cytokines associated with stress, PDX1 mRNA expression is maintained<sup>278</sup>. The presence of PDX1 directly promotes transcription of ER stress associated genes *Atf4* and *Wfs1*<sup>212</sup>. However, unresolved ER stress can lead to apoptotic cell death. Under apoptotic conditions, the proapoptotic factor MST1 phosphorylates Thr<sup>11</sup> of PDX1<sup>279</sup>. This leads to proteasome degradation of PDX1. Depending on the environmental stress and the protein factors present in the cell, PDX1 activity can be either maintained or inhibited.

Under oxidative stress conditions, phosphorylation inhibits PDX1 activity by decreasing its abundance in the cell through proteasome degradation. Oxidative stress induces phosphorylation of PDX1 at Ser<sup>61</sup> and Ser<sup>66</sup> through the activation of glycogen synthase kinase 3 (GSK3)<sup>280</sup>. This targets PDX1 for protein degradation through the proteasome. Oxidative stress also induces translocation of PDX1 from the nucleus to the cytoplasm through activation of JNK. The presence of JNK causes nuclear export through a nuclear export signal (NES) that overrides the nuclear localization signal (NLS) that targets PDX1 to the nucleus<sup>281</sup>. Changes in subcellular localization can quickly reduce the

transcriptional activity by sequestering PDX1 to the cytoplasm followed by degradation of the protein.

#### **4.2.4: PDX1 in viral infection**

Despite the importance of PDX1 in islet cell development, function, and survival, very little has been reported on the effects of viral infection on PDX1. Ductal cells of the pancreas express PDX1 at low levels, and are susceptible to CVB4 infection. CVB4 persists in a human ductal cell line for up to 37 weeks after infection, leading to an impaired expression of PDX1 gene expression<sup>215</sup>. However, a mechanism for inhibition of PDX1 mRNA production in these persistently infected cells is unknown. CVB infections are associated with stress responses that are associated changes in PDX1 regulation described above. In cardiomyocytes, oxidative stress is activated through cross-talk with macrophages in CVB3-infected mice<sup>282</sup>. CVB also promotes cytokine and IFN expression, and CVB-induced cell death pathways may contribute to decreases in PDX1 expression.

#### **4.2.5: Goals**

PDX1 is important in  $\beta$  cell function, and CVB directly infects  $\beta$  cells leading to  $\beta$  cell dysfunction. Since PDX1 is it is among the most highly decreased genes in both engrafted and cultured primary human islets, it is likely that CVB infection is directly mediating changes in PDX1 expression. To test the  $\beta$  cell specific effects of CVB on PDX1 expression and localization I used the EndoC- $\beta$ H1 cell line. The goals of this chapter are to 1) determine the kinetics of decrease in PDX1 mRNA and protein upon CVB infection, 2) quantify the kinetics

of gene expression changes in factors that regulate PDX1 expression and transcriptional targets of PDX1, 3) demonstrate specificity of changes in PDX1 nuclear localization in CVB-infection, and 4) determine a role for  $\beta$  cell-specific regulatory factors in the changes in PDX1 expression upon CVB infection.

### 4.3: Results

#### 4.3.1: Changes in expression of genes in the PDX1 transcriptional network

In cultured primary human islets infected with CVB4, *PDX1* gene expression decreases between 6 and 24 hpi. To further evaluate the kinetics and consequences of CVB4 infection on PDX1 transcriptional targets, I focused on expression of select genes evaluated by NanoString from the same experimental data set as presented in Figure 3.3. Upon CVB4 infection *PDX1* expression decreases by 1.3-fold at 6 hpi and 3.5-fold at 24 hpi compared to mock infected islets. In agreement with this data, genes that are at least partially controlled by PDX1 at the transcriptional level are decreased at 24 hpi: *SST*, *INS*, *IAPP*, *MAFA*, and *SLC2A2* all decrease by more than 3-fold. *GCG* gene expression, which is inhibited by PDX1, slightly increases at 24 hpi. Two ER stress-associated genes induced by PDX1, *ATF4* and *WFS1*, are minimally changed upon CVB4 infection: *ATF4* is only 1.6-fold increased over mock, and *WFS1* is decreased by 1.7-fold (Fig. 4.2). These data reinforce the hypothesis that loss of *PDX1* expression of primary human islets is a key mechanism of  $\beta$  cell dysfunction during CVB4 infection.

I also measured expression of genes that contribute to the regulation of PDX1 using the NanoString gene expression assay. While *PDX1* has an auto-



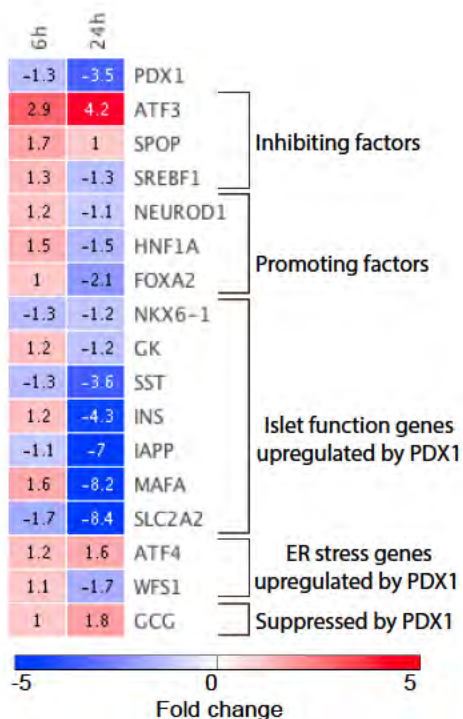


**Figure 4.2: NanoString gene expression of genes in the PDX1 transcriptional network at 6 and 24 hpi in CVB4-infected primary human islets**

Islets from a single human non-diabetic donor were infected with CVB4 (1e6pfu/100IEQ) and were processed for total RNA at 6 and 24 hpi. Gene expression of 146 genes was measured by NanoString assay (NSCS2) and normalized to a panel of seven housekeeping genes. Fold changes of gene expression of CVB4-infected islets compared to mock infected islets are displayed as a heatmap. Genes are displayed in the following categories: genes that inhibit or promote PDX1 function or expression and genes upregulated or suppressed by PDX1. Scale from -5 in blue to 5 in red.

regulatory role in promoting its own transcription, several independent transcription factors enhance its transcription. Decreases in these transcription factors would suggest their epistatic role in decreasing *PDX1* expression upon CVB4 infection. However, gene expression for the transcription factors, *FOXA2* (HNF-3 $\beta$ ), *HNF1A*, and *NEUROD1*, which have been previously described to regulate *PDX1* transcription<sup>265,266</sup>, are all maintained at levels similar to mock treated cultured islets at 6 and 24 hpi (Fig. 4.2). Several proteins, including *SPOP* and *SREBF1*, negatively regulate *PDX1* expression or function by either binding directly to *PDX1* or its promoter to inhibit transcription<sup>272,274</sup>. *SPOP* and *SREBF1* gene expression levels do not change between 6 and 24 h after CVB4 infection. *ATF3* is a transcription factor that binds to the *PDX1* promoter to inhibit transcription<sup>269</sup>. After CVB4 infection, *ATF3* gene expression is increased 2.9-fold at 6 hpi and 4.2-fold at 24 hpi compared to uninfected islets (Fig 4.2). Since this factor had the highest change in gene expression prior to the decrease in *PDX1* expression, it may be contributing to the rapid decrease in *PDX1* mRNA.

#### **4.3.2: Changes in *PDX1* protein localization upon CVB4 infection in EndoC- $\beta$ H1 cells**

The decrease in *PDX1* gene expression and its importance in  $\beta$  cell function led me to investigate the kinetics of the expression and localization of *PDX1* protein in human  $\beta$  cells after CVB4 infection. The heterogeneity of cell types and complex three-dimensional architecture of primary human islets complicate the acquisition and analysis of imaging protein expression and localization by immunofluorescence. Specifically, the heterogeneity of *PDX1*

staining makes differentiation between a cell that does not express PDX1 due to its cell-type properties and a cell that has lost PDX1 expression secondary to virus infection difficult. The availability of the EndoC- $\beta$ H1 human  $\beta$  cell line provides a convenient platform to mitigate this problem. Since these cells are homogenous in PDX1 expression preceding infection, changes in PDX1 staining can be attributed to the virus infection. Additionally, since the cells are adherent and grown on a monolayer, they are more amenable to virus infection and immunofluorescent evaluation of protein expression and localization on a single cell basis.

EndoC- $\beta$ H1 cell infection with CVB4 does not result in the decrease in PDX1 mRNA observed in cultured primary human islets (Fig. 3.3 & 3.7). However, the regulation of protein localization and function may be separate from PDX1 mRNA production. It is possible that during the transformation process of these cells, physiologic regulation of PDX1 was altered to help promote the survival of the cell line. Alternatively, the rapid cell death kinetics after CVB4 infection in EndoC- $\beta$ H1 removes cells with low PDX1 mRNA from the analysis so it seems that global decreases in mRNA are not captured. The NanoString gene expression assay was also used to profile gene expression changes in CVB4-infected EndoC- $\beta$ H1 cells, but technical issues in several of the samples made the results of this experiment uninterpretable (data not shown). Despite this discrepancy, findings of the regulation of PDX1 at the protein level may be contributing to both models and contributing to  $\beta$  cell dysfunction.

PDX1 staining is robust and mostly retained in the nucleus in uninfected EndoC- $\beta$ H1 cells (Fig 4.3, A & B). EndoC- $\beta$ H1 cells infected with CVB4 at an MOI of 1 can be identified by VP1 staining at 6 hpi (Fig. 4.3, A & C). In contrast to adjacent uninfected cells, CVB4-infected cells have less PDX1 staining in the nucleus at 6 hpi (Fig 4.3, A & C). The staining is lower than one standard deviation below the mean staining intensity of mock-treated cells in 51% of CVB4-infected cells. However, whether or not total PDX1 protein levels are decreased at this time point is unclear. PDX1 staining in an independent infection of EndoC- $\beta$ H1 cells with CVB4 at an MOI of 10 yielded similar amounts of PDX1 as at 6 hpi. Under these conditions, 51% of cells are positive for VP1 (Fig. 4.3, D). This agrees with flow cytometry quantification of VP1 in CVB4-infected EndoC- $\beta$ H1 cells under similar conditions a minimal number of cells stained with a cell death marker (Fig. 3.6, D). Quantification of nuclear PDX1 of uninfected (VP1-negative) or CVB4-infected (VP1-positive) cells confirmed a significant decrease in nuclear PDX1 staining intensity in CVB4-infected cells compared to uninfected cells. PDX1 staining intensity decreased from a mean of 3.86 in uninfected cells to 2.21 in CVB4-infected cells (Fig. 4.3, D). This reduction in nuclear PDX1 staining in CVB4-infected cells is specific to the infected cells, as uninfected cells in the same field retain PDX1 staining (Fig. 4.3, A & D).

#### **4.3.3: PDX1 nuclear localization is also decreased after infection with other serotypes of CVB in EndoC- $\beta$ H1 cells**

To identify if the changes in PDX1 protein localization in EndoC- $\beta$ H1 cells infected with CVB4 are specific to this coxsackievirus serotype, I infected cells

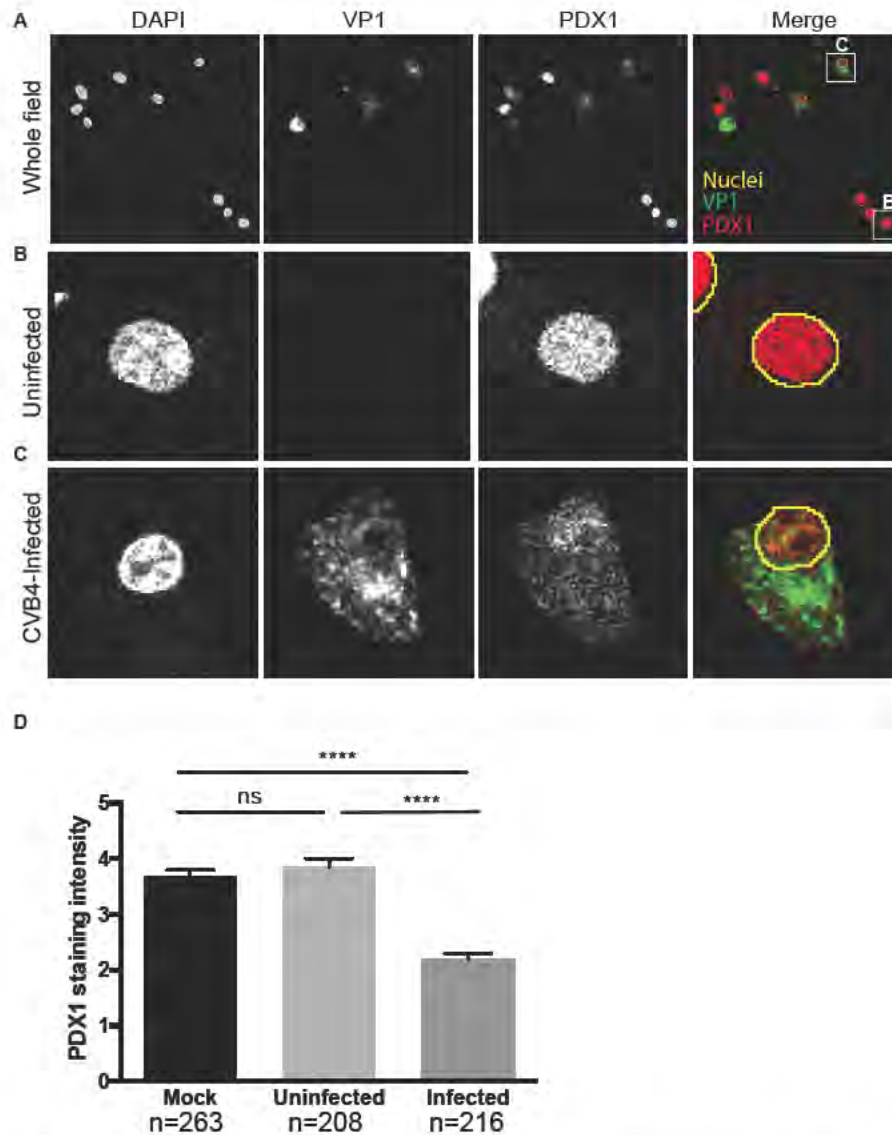


### Figure 4.3: EndoC- $\beta$ H1 nuclear PDX1 staining decreases upon CVB4 infection

Immunofluorescence of EndoC- $\beta$ H1 cells infected with CVB4, MOI 1. Staining for DAPI (outlined by ImageJ in yellow), VP1 (green), and PDX1 (red) in the merged panels. (A) Whole field of view acquired at 630x magnification with indicated cells boxed in white. Representative images of staining of (B) uninfected cells and (C) CVB4-infected cells. (D) Quantification of PDX1 nuclear staining intensity in an independent infection experiment with CVB4, MOI 10. PDX1 staining intensity in the nucleus as defined by DAPI staining from mock-infected cells (n=263 cells), or intensity from CVB4-infected cells separated into uninfected (n=208 cells) and infected (n=216 cells) groups based on VP1 staining. Error bars represent S.E.M. \*\*\*\*,  $P < 0.0001$ ; ns, not significant, two-tailed t test.

with two other serotypes to evaluate their ability to change PDX1 localization. I infected EndoC- $\beta$ H1 cells with prototypical lab strains for CVB1 (strain Conn-5) and CVB5 (strain Faulkner). At 6 hpi, 33% and 17% of EndoC- $\beta$ H1 cells are VP1-positive following infection with CVB1 or CVB5, respectively, at an MOI of 10 (Fig. 4.4, A). Nuclear staining is identified by DAPI (white rings) and PDX1 (red) appears robust in mock-infected EndoC- $\beta$ H1 (Fig. 4.4, B). In contrast, nuclear staining of PDX1 for CVB1 and CVB5 is reduced at 6 hpi. Cells infected with respective viruses stain positive for VP1 (green) (Fig. 4.4, C & D). Quantification of nuclear PDX1 staining intensity is significantly lower in both CVB1 and CVB5-infected cells compared to mock-infected cells (Fig. 4.4, E). Overall PDX1 nuclear staining is low in CVB1-infected cells, likely due to the high proportion of these cells being infected. Since cells are not separated into infected and uninfected categories in this experiment, the differences in infection efficiency between CVB1 and CVB5 likely account for the variation in PDX1 nuclear staining in these conditions. Taken together, the reduction in PDX1 nuclear localization is not a specific feature of CVB4-JVB and may be a broad effect of enterovirus infection or antiviral responses in general.

#### **4.3.4: Changes in PDX1 localization are not a generalized virus response**

The interesting finding of changed PDX1 localization in CVB4-infected cells at 6 hpi introduced the possibility that this could be a general  $\beta$  cell response to increased protein production that occurs during a viral infection or a generalized antiviral response. I transfected EndoC- $\beta$ H1 cells with a plasmid encoding GFP under the control of the CMV promoter to investigate if increased protein burden

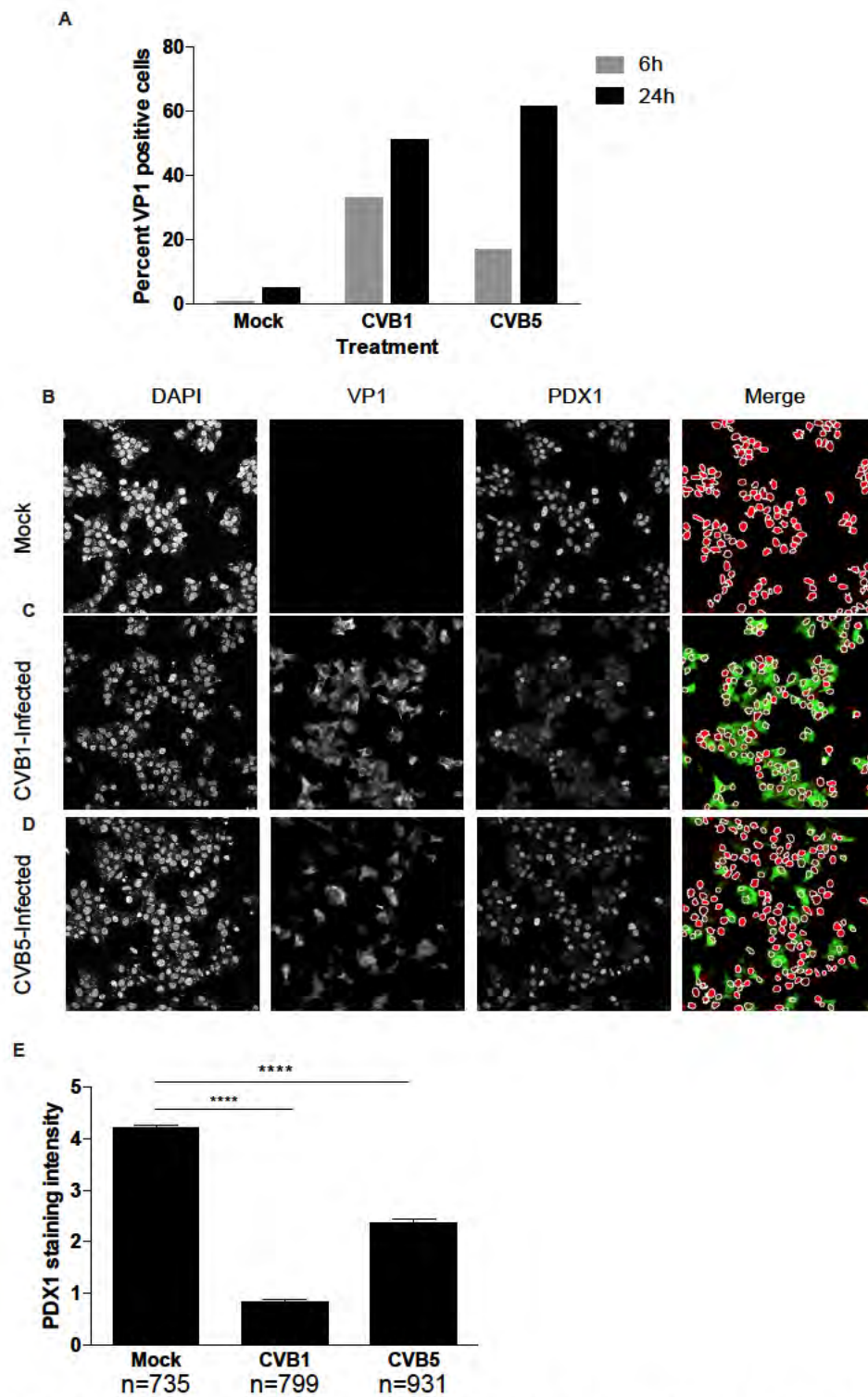


**Figure 4.4: EndoC- $\beta$ H1 nuclear PDX1 staining is decreased upon infection with either CVB1 or CVB5**

EndoC- $\beta$ H1 cells were infected with CVB1 or CVB5 at an MOI of 10. **(A)** Flow cytometry of VP1 staining to evaluate the proportion of cells infected at 6 hpi (gray bars) or 24 hpi (black bars). Immunofluorescence staining of **(B)** mock, **(C)** CVB1-infected, or **(D)** CVB5-infected EndoC- $\beta$ H1 cells at 6 hpi. Cells are stained for DAPI (white circles drawn in ImageJ), VP1 (Green), or PDX1 (red) and images are obtained at 400x magnification. **(E)** Quantification of PDX1 nuclear staining intensity as defined by DAPI staining. Nuclear PDX1 staining intensity in all cells from mock-infected (n=735 cells), CVB1-infected (n=799 cells), or CVB5-infected (n=931 cells) conditions. Error bars represent S.E.M. \*\*\*\*,  $P < 0.0001$ , two-tailed t test.



on these cells would induce a change in PDX1 localization. In this experiment, GFP was expressed in 39% (9 of 23) cells at 24 hours after transfection.

Overexpression of GFP alone did not have any effect on PDX1 nuclear localization compared to untransfected cells (Fig. 4.5, A). Quantification of nuclear PDX1 staining intensity confirmed that no significant change occurred upon overexpression of GFP (Fig. 4.5, D).

Numerous changes occur in virally-infected cells in addition to increased protein production. Viral modification of host gene expression and antiviral responses might contribute to changes in PDX1 nuclear localization. Thus, I infected EndoC- $\beta$ H1 cells with two non-CVB GFP-expressing viruses to determine if the reduction in PDX1 nuclear localization was due to a generalized antiviral response. EndoC- $\beta$ H1 cells are permissive to infection with vesicular stomatitis virus (VSV), as infection with VSV-GFP at MOI of 0.5 resulted in the 89% of the cells expressing GFP at 24 hpi (Fig. 4.5, E). Respiratory syncytial virus (RSV) also infected EndoC- $\beta$ H1 cells, albeit with much lower efficiency than VSV. At 24 hpi only 8% of cells express GFP (Fig. 4.5, F). Despite the infection of EndoC- $\beta$ H1 cells by VSV and RSV, no change in PDX1 nuclear localization was observed (Fig 4.5, B & C) and no significant change in PDX1 nuclear staining intensity was noted for either of these viruses (Fig. 4.5, E & F). Since no change in PDX1 nuclear localization upon infection with either of these single stranded, negative sense RNA viruses was seen, I concluded that the phenotype observed in CVB infection is not likely due to a generalized antiviral response.

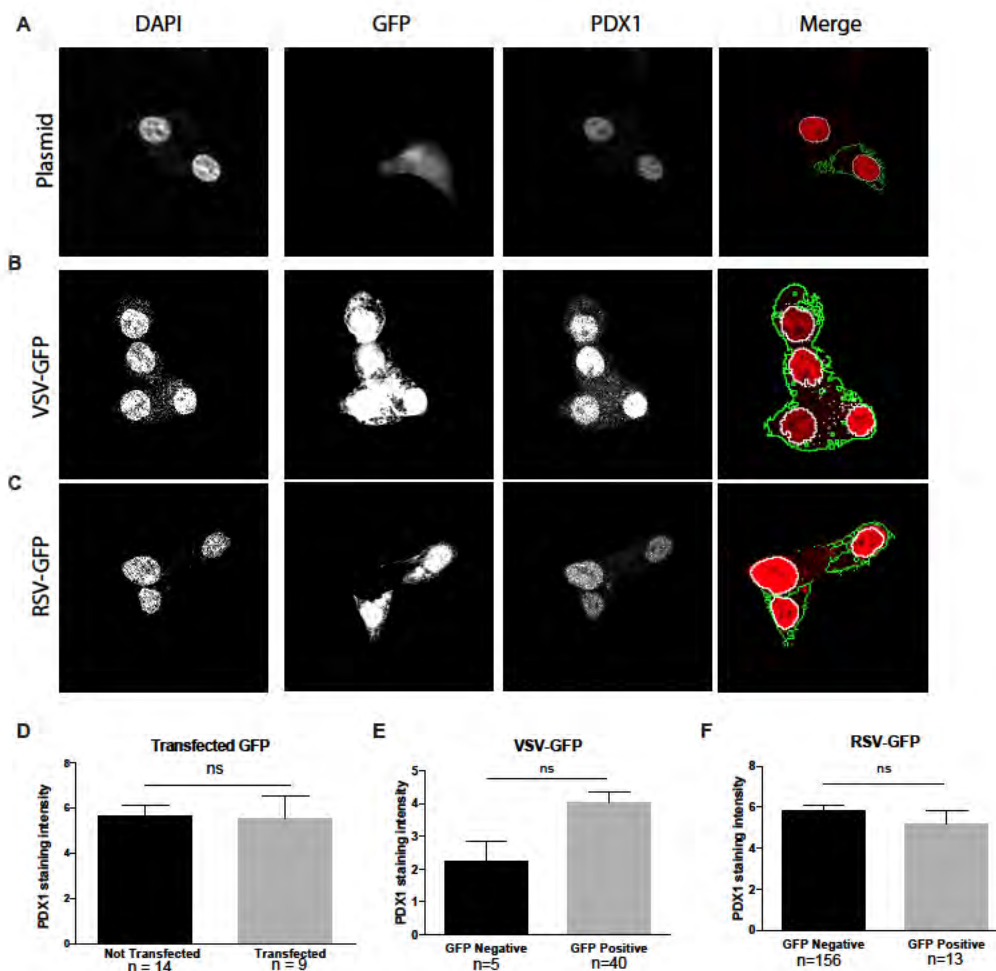


**Figure 4.5: EndoC- $\beta$ H1 nuclear PDX1 staining does not decrease upon transfection of a GFP-expressing plasmid or infections with VSV, or RSV** Immunofluorescence for DAPI (white circles), GFP expression (green outlines), or PDX1 staining (red) of EndoC- $\beta$ H1 cells (A) transfected with GFP-expressing plasmid under the control of the CMV promoter, (B) infected with VSV-GFP MOI 0.5, or (C) infected with RSV-GFP at 24 h post treatment. Images acquired at 630x magnification. Quantification of nuclear PDX1 staining intensity as defined by DAPI staining. Cells were split divided into groups based on GFP expression for (D) untransfected (n=14 cells) and transfected (n=9 cells), (E) VSV-GFP uninfected (n=5 cells) and VSV-GFP infected (n=40 cells), or (F) RSV-GFP uninfected (n=156 cells) and RSV-GFP infected (n=13 cells). Error bars represent S.E.M. ns, not significant, two-tailed t test.

#### 4.3.5: Changes in PDX1 localization in non- $\beta$ cells

The change in PDX1 nuclear localization upon CVB infection, but not negative sense viruses, prompts the possibility that CVB is directly causing this change. However, regulation of PDX1 expression in  $\beta$  cells is complicated. PDX1 expression in auto-regulated and also influenced by a variety of  $\beta$  cell transcription factors for proper physiological responses. As an alternative model for investigating the mechanisms of CVB-mediated changes in PDX1 nuclear localization, I overexpressed PDX1 in an irrelevant, more genetically tractable cell type that could be readily infected with CVB but in which many of the  $\beta$  cell specific regulatory factors may not be present. This could help me determine if the changes in expression are due to transcriptional or post-translational regulation of gene expression or stability (HeLa: GSK3b protein expression is high, PCIF1-low RNA - Human Protein Atlas).

I transduced HeLa cells with an adenoviral construct that expresses the mouse *Pdx1* gene under the control of the CMV promoter described previously (pAd-Pdx1)<sup>283</sup>. The pAd-Pdx1 construct also encodes for nuclear localized GFP (nGFP) under the control of an IRES as a marker for cells that are transduced with the virus. Cells transduced with this construct co-express nGFP and Pdx1 in 46% of cells. Overexpressed *Pdx1* is primarily nuclear as evaluated by immunofluorescence staining at 24 hours after transduction (Fig. 4.6, A & B). Upon infection of Pdx1-expressing HeLa cells with CVB4 at an MOI of 1, 27% of cells stain positive for VP1 at 6 hpi. Under these conditions, 12% of cells are both transduced with pAd-Pdx1 and infected with CVB4. Similar to observations in

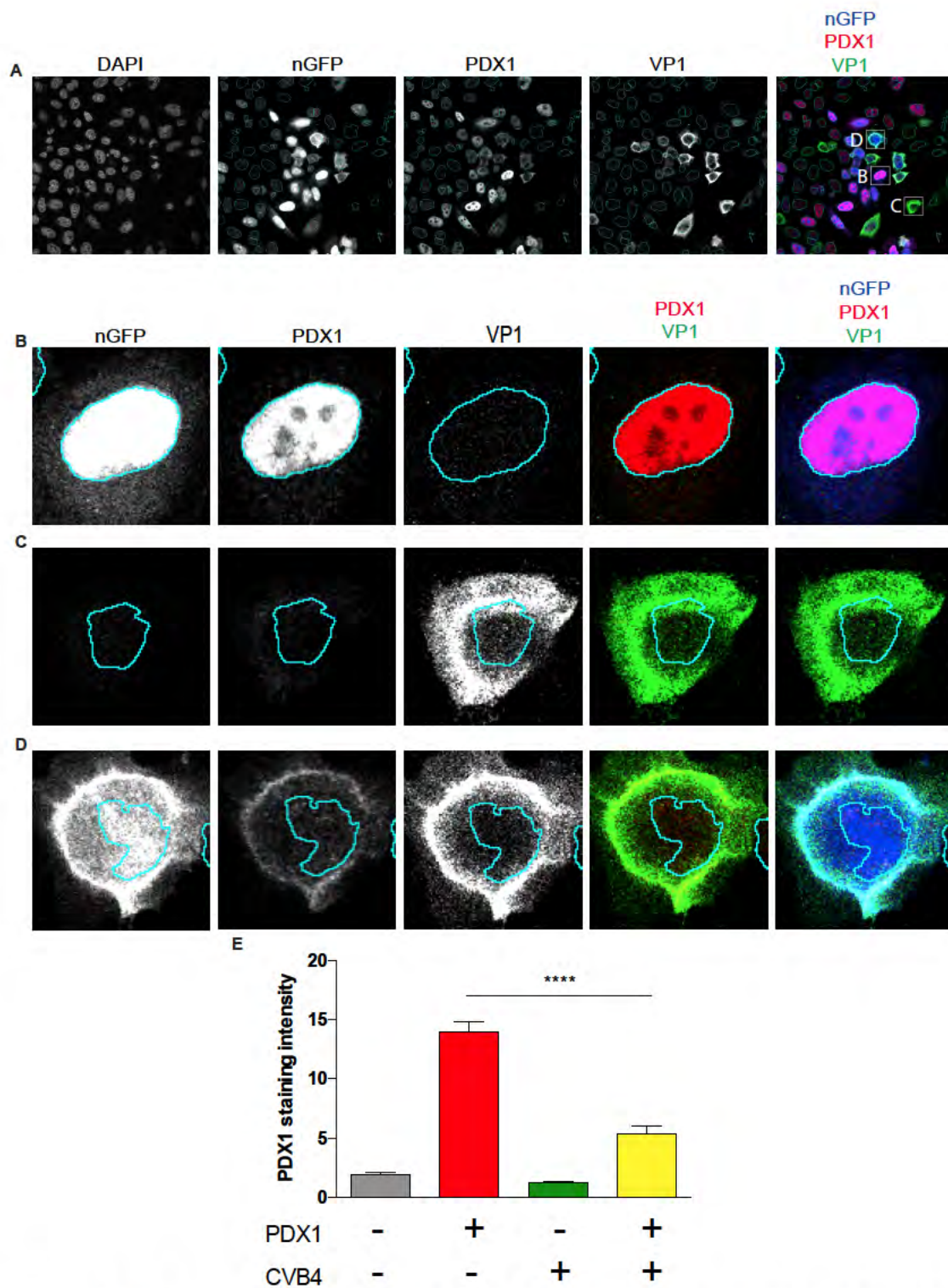


**Figure 4.6: Ectopic expression of PDX1 in HeLa cells is excluded from the nucleus upon CVB4 infection.**

Expression of PDX1 in HeLa cells by transduction of an adenovirus vector that co-expresses nGFP. Cells were cultured for 24 h after transduction followed by challenge with CVB4 virus at MOI of 1. Cells were fixed and stained 6 hpi. Immunofluorescence staining was performed for DAPI (cyan circles), nGFP (blue), VP1 (green), and PDX1 (red). **(A)** Whole field images were acquired at 400x magnification with individual examples in white boxes. **(B)** Image of a representative cell that is overexpressing the PDX1 construct alone, **(C)** a cell that infected with CVB4 only, or **(D)** a cell that is both overexpressing Pdx1 and infected with CVB4. **(E)** Quantification of nuclear PDX1 staining as defined by DAPI staining. Transduced cells were identified by the presence of nGFP, and CVB4-infected cells were identified by VP1 staining. Non-transduced and uninfected (n=279 cells); transduced and uninfected (n=245 cells); non-transduced and infected (n=108 cells); transduced and infected (n=85 cells). Error bars represent S.E.M. \*\*\*\*,  $P < 0.0001$ , two-tailed t test.

CVB4-infected EndoC- $\beta$ H1 cells, Pdx1 is excluded from the nucleus of Pdx1-expressing HeLa cells infected with CVB4 (Fig 4.6, A & D). Quantification revealed that nuclear Pdx1 staining in cells that are both transduced with pAd-Pdx1 and infected with CVB4 is significantly lower than cells that were only transduced with the pAd-Pdx1 construct (Fig. 4.6, E). In contrast to CVB4-infected EndoC- $\beta$ H1 cells, Pdx1 accumulates in the cytoplasm of CVB4-infected HeLa-Pdx1 cells. The nuclear localization of nGFP also disperses throughout the cell upon CVB4 infection (Fig. 4.6, D). Despite the differences in regulation in overexpression of Pdx1 in an irrelevant cell type, CVB4-infection still changes the nuclear localization of Pdx1. This provides further support for a viral-specific mechanism for changes in PDX1 in human  $\beta$  cell infection.

#### 4.4: Discussion

In primary human islets infected with CVB4, *PDX1* mRNA decreases. This decrease is consistent between islets engrafted in mice and in islets infected in culture. While it is difficult to determine the kinetics of *PDX1* decrease in CVB4-infected islets engrafted in mice, the expression decreases most dramatically between 6 and 24 hpi in cultured islets (Fig. 4.2). *PDX1* orchestrates many functions in  $\beta$  cell development, function, and survival. Because of its critical role in these functions, a better understanding of the mechanisms of *PDX1* decrease after CVB infection will provide insights into dysfunction in infected  $\beta$  cells. This could aid in developing therapies to maintain  $\beta$  cell function upon CVB infection, and possibly prevent the development of autoimmunity.

The idea that reduction of *PDX1* in CVB4-infected primary human islets has a profound impact on  $\beta$  cell function is supported by the changes in gene expression of downstream transcriptional targets. Gene expression for the  $\beta$  cell function genes, *INS*, *IAPP*, *MAFA*, and *SLC2A2* are all at least partly enhanced by *PDX1*. By 24 hpi all of these genes have a greater than 3-fold decrease in gene expression. *PDX1* also contributes to the expression of *SST* in  $\delta$  cells, and gene expression is similarly decreased upon CVB4 infection. Interestingly, *GCG*, which is negatively regulated by *PDX1* in  $\alpha$  cells, is slightly increased at 24 hpi (Fig. 4.2). In other models, the reduction of *PDX1* alleviates the suppression of an  $\alpha$  cell program, which leads to phenotypic and gene expression patterns that

resemble  $\alpha$  cells<sup>262</sup>. However, I have not explored the possibility of a change from  $\beta$  to  $\alpha$  cell phenotype in CVB4-infected cells.

One interesting finding in *PDX1* expression in primary human islets is that *PDX1* gene expression does not decrease upon treatments with poly(I:C) or poly(dA:dT) at 24 hours post treatment (Fig. 3.4, A). Since these synthetic IFN-I agonists did not decrease *PDX1* to the same levels as CVB4 infection, the mechanisms involved may be IFN-I independent. To confirm this, recombinant IFN could be added to EndoC- $\beta$ H1 cells followed by evaluation of nuclear PDX1 localization. While gene expression is maintained in treatments of poly(I:C) and poly(dA:dT), I have not investigated if PDX1 nuclear localization changes with these treatments.

In an effort to identify other factors that may be contributing to the changes in *PDX1* gene expression upon CVB4 infection, I measured the gene expression of factors that either promote or inhibit *PDX1* mRNA production. Transcription factors that promote *PDX1* expression were all unchanged at 6 hpi. However, the functions of these transcription factors may not be regulated at the level of gene expression. Protein-protein interactions or post-translational modifications of these transcription factors may reduce *PDX1* production and would not be detected through the NanoString gene expression assay.

Of various factors assessed that could potentially inhibit PDX1 function, only *ATF3* was highly expressed in CVB4 infected islets compared to mock (Fig. 4.2). *ATF3* represses *PDX1* expression by binding to the *PDX1* promoter<sup>269</sup>.



ATF3 expression is induced in stress conditions through NF- $\kappa$ B and JNK/SAPK pathways<sup>268</sup>. Treatment of primary human islets with either poly(I:C) or poly(dA:dT) also increased *ATF3* expression 2.5-fold and 5.6-fold, respectively, at 24 hours post treatment (Fig. 3.4, A). Since *ATF3* is expressed at comparable levels with these treatments as with CVB4-infection while *PDX1* expression is maintained, ATF3 cannot be the only factor contributing to the *PDX1* phenotype in CVB4-infected islets. The inhibitory effects of ATF3 on *PDX1* are likely compounded by changes in PDX1 nuclear localization upon CVB infection. This likely further reduces *PDX1* expression through the auto-regulatory mechanisms of PDX1 in promoting its own mRNA production<sup>265</sup>. These findings point to multiple mechanisms that could concomitantly produce the decrease in *PDX1* expression in CVB4-infected primary human islets.

While a reproducible decrease in *PDX1* gene expression in engrafted and primary human islets at 24 hpi was observed, the same decrease did not occur in SC- $\beta$  or EndoC- $\beta$ H1 (Fig. 3.5, I & 3.7, C). In SC- $\beta$  cells differences in infection efficiency or the kinetics might account for this. In infections of EndoC- $\beta$ H1 cells with CVB4 at MOI of 10, approximately 50% of cells are infected at 6 hpi. Despite, active replication in these cells, *PDX1* gene expression slightly but significantly increased at 24 hpi when compared to 6 hpi (Fig. 3.7, C). Since many environmental factors contribute to the regulation of *PDX1*, the other cells present in primary human islets could contribute to the phenotype. Cytokine production or reactive oxygen species produced in response to viral infection by

nearby cells could enhance the decrease of *PDX1* mRNA in primary human islets. Alternately, the maintenance of *PDX1* expression in EndoC- $\beta$ H1 cells could be due to mutations acquired during the passage or immortalization processes of these cells in establishing the cell line. Given that these cells are derived from human fetal islets, differences in transcriptional regulation in these cells may account for the findings distinct from those in  $\beta$  cells. Some of these differences will be further explored in studies of flow cytometry-sorted primary human islets discussed in **Chapter V**. Regardless of the differences in *PDX1* gene expression between primary human islets and EndoC- $\beta$ H1 cells, infections of EndoC- $\beta$ H1 cells provide a platform for exploring *PDX1* protein localization changes that would be difficult in primary human islets.

EndoC- $\beta$ H1 cells infected with CVB1, CVB4, or CVB5 have a decrease in nuclear *PDX1* staining at 6 hpi (Fig. 4.3 & 4.4). Changes in *PDX1* localization are one mechanism for decreasing its transcriptional activity. While some specificity in viruses leads to a change in *PDX1* localization, perhaps a mechanism shared at least within the Coxsackie B virus group. This could provide a mechanistic insight into the broad range of enteroviruses that inhibit glucose stimulated insulin secretion after infection<sup>234</sup>. It will be interesting to determine if other enteroviruses change *PDX1* localization. Specifically, CVA9 or CVB4 strain VD2921, which do not produce CPE in primary human islets, would be interesting to study<sup>234,235</sup>. The reduction of *PDX1* in CVB-infected  $\beta$  cells might also be shared with other cell types that express *PDX1*. *SST* expression

decreases in infections of primary islets, suggesting that *PDX1* might also be altered in  $\delta$  cells. Previous studies of CVB infection in ductal cells also reported a decrease in *PDX1* gene expression in persistently-infected cells<sup>215</sup>. Further identification of viruses that affect PDX1 and possible cell-type differences could provide insights into what makes some strains diabetogenic and what confers the  $\beta$  cell specificity in T1D autoimmunity.

PDX1 localization is retained in the nucleus in EndoC- $\beta$ H1 cells infected with both VSV-GFP and RSV-GFP. Both of these viruses belong to the order Mononegavirales. These single-stranded negative sense RNA viruses differ in their genomic structure to CVB viruses, which are single-stranded but positive sense. They also utilize different mechanisms for altering host gene expression and stimulated innate immune function. VSV blocks host transcription, mRNA export from the nucleus, and host translation. RSV blocks RIG-I signaling and INF-I production (reviewed here<sup>284</sup>). Despite all these affects on cell function, neither virus changes the nuclear localization of PDX1 upon infection. This could partly explain why some pancreatropic viruses are able to productively replicate in  $\beta$  cells, but do not result in hyperglycemia or the development of T1D.

Several possible regulatory mechanisms of PDX1 nucleo-cytoplasmic transition are unlikely due to the specificity of the phenotype to CVB viruses. It is unlikely that it is mediated through IFN or cytokine responses, ER stress, or apoptotic mechanisms. One possibility is oxidative stress conditions impact PDX1. CVB3 infection of cardiomyocytes is associated with the induction of

oxidative stress<sup>282</sup>. Oxidative stress in  $\beta$  cells prompts PDX1 phosphorylation and a change in localization from the nucleus to the cytoplasm<sup>280,281</sup>. Therefore, virus induction of oxidative stress may be causing the change in PDX1 localization. However, this hypothesis has not been tested yet in this model. Treatment with small molecule oxidative stress inhibitors could be tested for their efficacy in preventing PDX1 translocation upon CVB infection. Mutation of the Ser<sup>61</sup> and Ser<sup>66</sup> phosphorylation sites to make a PDX1 mutant that is resistant to oxidative stress-induced changes in PDX1 localization would be of interest, too.

The results presented here only show the change in PDX1 localization upon CVB infection by immunofluorescence in EndoC- $\beta$ H1 cells. Other methods for determining the changes in PDX1 localization include Western blot of subcellular protein fractions. These methods were used previously to show the change in PDX1 localization in response to oxidative stress conditions<sup>281</sup>. A flow cytometry approach could also be used to evaluate the presence of PDX1 in  $\beta$  cells upon CVB infection. Both of these methods would be helpful in translating the results presented here to cultured primary human islets, since microscopy is of limited utility in intact islets.

In CVB4-infected HeLa cells overexpressing *Pdx1*, the amount of cytoplasmic staining of PDX1 is higher than in EndoC- $\beta$ H1 cells. This could be due to the lack of autoregulatory activity of this construct. Since PDX1 production is under the control of the CMV promoter, PDX1 protein is continually produced even though it is being excluded from the nucleus. This also helps confirm that

the loss in nuclear staining is at least partly independent of transcriptional mechanisms.

The overexpression of *Pdx1* in HeLa cells provides further mechanistic insights into the changes in PDX1 localization upon CVB infection. First, PDX1 is excluded in an environment that is free of  $\beta$  cell-specific regulatory mechanisms of PDX1. Endogenously, HeLa cells do not express transcription factors involved in PDX1 production FOXA2 (0), HNF1A (0), NEUROD1 (0). They do express factors that inhibit PDX1 function at low levels of ATF3 (6), MST1 (2); or moderate levels of SREBF1 (37), SPOP (19), GSK3 (14), and JNK (24). Values are fragments per kilobase of exon per million reads mapped (FPKM) from RNA-Seq data available from the Human Protein Atlas cell line data ([www.proteinatlas.org](http://www.proteinatlas.org)).

Other proteins in addition to PDX1 might be similarly excluded from the nucleus of CVB infected cells. However, I have not stained for the change in localization in other transcription factors important in  $\beta$  cell function. Surprisingly, the nGFP protein co-expressed in HeLa cells transduced with the pAd-Pdx1 construct also is dispersed throughout the cell upon CVB infection. How both of these proteins change localization despite the presumptive lack of similar post-translational regulatory features in nGFP is unknown. A generalized exclusion of proteins from the nucleus in these cells may occur. In CVB-infection of other cell types, other nuclear proteins are excluded from the nucleus through cleavage of nuclear pore complexes<sup>285,286</sup>.

Another possibility is a direct cleavage of the PDX1 target protein by one of the viral proteinases. CVB viruses do directly cleave several cellular proteins during infection, including eIF4G, PABP, MAVS and TRIF, to inhibit signaling<sup>137,139,143</sup>. In poliovirus infection, the lupus antigen is excluded from the nucleus through the cleavage of the lupus antigen nuclear localization signal within 3 hpi<sup>287,288</sup>. A similar mechanism may exclude PDX1 from the nucleus in both EndoC- $\beta$ H1-infected cells and HeLa cells overexpressing Pdx1. To test if the viral protease is contributing to the change in PDX1 localization, infected cells could be treated with the small molecule inhibitor AG7088 that prevents protease 3C activity<sup>289</sup>.

Despite these interesting findings in the change in PDX1 localization, I was not able to directly link this phenomenon to the reduction in *INS* gene expression. To further evaluate this direct role, I could co-express PDX1 and a luciferase reporter under the control of the *INS* promoter. These cells could be infected and I could measure the production of *INS* as a measure of the change of PDX1 transcriptional activity under the influence of CVB infection.

### **Conclusions:**

- 1) *PDX1* mRNA expression is decreased at 24 hpi upon CVB4 infection compared to 6 hpi; this decrease is not observed upon challenge with activators of IFN-I signaling.
- 2) *PDX1* transcriptional target gene expression is reduced at 24 hpi, strengthening the association between *PDX1* decrease and  $\beta$  cell dysfunction.
- 3) *ATF3* gene expression increases prior to the decrease in *PDX1*

gene expression following CVB4 infection, which suggests a role for ATF3 in reducing PDX1 transcription. 4) Nuclear PDX1 localization decreases upon infection with three different CVB serotypes, but infections with VSV and RSV do not generate the same decrease in PDX1 nuclear localization in EndoC- $\beta$ H1 cells. 5) Ectopic expression of *Pdx1* in HeLa cells, which do not express transcriptional regulatory factors for *PDX1* expression, also have decreased nuclear Pdx1 staining upon CVB4 infection. Other nuclear proteins may be similarly excluded from the nucleus. Since PDX1 is a crucial factor in  $\beta$  cell function and CVB-infection at least somewhat specifically affects its gene expression and localization, this is a potential mechanism for the  $\beta$  cell dysfunction observed in enterovirus-infected primary human islets.

## **4.5: Materials and methods**

### **4.5.1: Cell culture and infection**

EndoC- $\beta$ H1 cells were cultured as previously described<sup>237</sup>. HeLa cells were cultured by standard protocols. For microscopy studies, cells were plated into 24 well plates with a coverslip. Titered stocks of virus were added to cells at indicated MOI in a minimal volume for 1 h to allow for adsorption. Following this incubation period, cells were washed with PBS and complete culture media was replaced. At indicated time points, cells were fixed for immunofluorescence or flow cytometry staining with 4% paraformaldehyde.

### **4.5.2: Virus sources**

The CVB4 strain JVB, CVB1 strain Conn-5, and CVB5 strain Faulkner (# VR-184, VR-28, and VR-185 respectively; American Type Culture Collection)

grown in HeLa cells<sup>230</sup>. Virus was purified by ultracentrifugation on a sucrose cushion where indicated as previously described<sup>252</sup>.

VSV-GFP, a gift from S. Whelan, was propagated as previously described<sup>290</sup>.

rgRSV224 (RSV-GFP) was a kind gift from Peter Collins and Mark Peeples. Virus was and propagated in HEp-2 cells as previously described<sup>291</sup>.

#### **4.5.3: Gene expression profiling**

The NanoString CodeSet #2 (NSCS2) was developed for genes associated with IFN-1 (18), IFN-II (3), IFN-III (5), IFN regulated genes (20),  $\beta$  cell function (24), endocrine (9), apoptosis (8), cytokines (7), inflammation (8), ER stress (20), type 1 diabetes susceptibility genes (12), other human genes (4), the CVB-specific probe as described above, and housekeeping genes (7) for normalization of data for a total of 146 genes. Probes were designed to target human genes in a species-specific manner. One hundred nanograms of RNA extracted from cultured islets and was hybridized, processed, and analyzed per the manufacturer's procedure. Data were normalized using the nSolver Analysis Software (version 2.6). Fold changes in gene expression were the ratio of normalized gene expression in CVB4-infected samples versus those in mock-infected samples. Values  $<1$  were transformed by  $-1/x$ . Heatmaps of transformed fold changes were produced with Gitools v2.2.3 (<http://gitools.org/>).

#### **4.5.4: Immunofluorescence**

Cells were cultured on coverslips and infected with CVB4 at an MOI of 10 for 24 h. Cells were fixed with 4% PFA for 30min at room temperature. Fixed



cells were permeabilized and stained in PBS-AT (PBS+2% BSA +0.5% Triton X-100) with the following primary antibodies guinea pig antibody to mouse antibody to VP1, clone 5-D8/1 (1:500; Dako) and rabbit polyclonal antibody against PDX1 (Abcam Ab47267). The following fluorophore conjugated secondary antibodies at 1:1,000 dilution; Alexa Fluor-488 or Alexa Fluor-594 goat antibody to mouse IgG (catalog #A11029 and #A11032, respectively; Life Technologies) and Alexa Fluor-594 or Alexa Fluor-647 goat antibody to rabbit IgG (Catalog #A11012 and #A31573, respectively; Life Technologies) for 1 h. Coverslips were mounted with ProLong Gold Antifade Re-agent with DAPI (Life Technologies).

Immunofluorescence was imaged on a Leica SP8 confocal microscope with a 40x (1.3 oil) or 63x (1.4 oil) HC PL APO CS2 objectives running Leica Advanced Fluorescence software (version 3.3.0.10134.1).

#### **4.5.5: Image quantification**

Brightness and contrast were adjusted and PDX1 nuclear staining intensity was quantified by FIJI software (version 1.48p)<sup>232</sup>. Briefly, automatic thresholding of DAPI staining and used to mark nuclei as regions of interest (ROI) and counted. Staining intensity of the PDX1 channel was measured as integrated density of each nuclear ROI. The resulting integrated density measurement for each measurement was scaled by dividing by 10,000 to generate single digit numbers and reported as PDX1 staining intensity. Where indicated, each cell was also scored as infected or not infected by VP1 staining.

#### **4.5.6: Flow cytometry**

EndoC-βH1 cells were trypsinized to obtain a single cell suspension at indicated time points. Cells were fixed and permeablized using BD Cytotfix/Cytoperm reagents (BD Biosciences). Cells were then stained with mouse antibody to VP1, clone 5-D8/1 (1:1000; Dako) and Alexa Fluor-488 goat antibody to mouse IgG (1:1000; Life Technologies). Staining was analyzed on an LRB LSRII A equipped with Trigon and Blue 488nm lasers running BD FACS Diva software (version 8.0.1) and analyzed using FlowJo (version 10.1r5).

#### **4.5.7: Overexpression of Pdx1 in HeLa cells**

pAd PdxI-I-nGFP was a gift from Douglas Melton (Addgene plasmid #19411) and recombinant adenovirus was produced in 293A cells as previously described<sup>283</sup>. HeLa cells were transduced with pAd PdxI-I-nGFP virus at a virus concentration that was empirically determined to maximize the number of PDX1 positive cells at 24 h post-transduction. Transduced HeLa cells were infected with CVB4-JVB at an MOI of 1 for 6 h. Cells were then fixed and stained for PDX1 and VP1 immunofluorescence as described below.

#### **4.5.8: Statistical Methods**

To assess the significance of the quantification of nuclear PDX1 staining, a standard unpaired, two-tailed *t* test was used to determine the significance.

**CHAPTER V: IMMUNE STIMULATION OF ENDOCRINE CELL POPULATIONS  
SORTED FROM PRIMARY HUMAN ISLETS**

Glen R. Gallagher, Susanne Pechhold, Robert W. Finberg, and Jennifer P. Wang

**Contribution Summary:**

G.R.G. designed and performed the experiments and analyzed the data. S.P. designed the flow cytometry-sorting strategy and analyzed the data. R.W.F. helped in the design of the experiments. J.P.W. helped in the design of the experiments and in data analysis.

## 5.1: Abstract

T1D is caused by a progressive loss in  $\beta$  cell mass due to autoimmune destruction directed at these cells. The development of this cell type-specific autoimmune reaction continues to be a poorly understood component in the pathogenesis of the disease. One area of interest is the functional differences of various endocrine cell types in response to environmental insults.  $\beta$  cells may be specifically affected in their ability to produce insulin upon CVB infection, while neighboring  $\alpha$  cells may continue to produce glucagon. Additionally, divergences in the strength or type of antiviral response in individual cell types could affect the clearance of virus, creating an environment that fosters the development of autoimmunity. To address these possibilities, I developed a flow cytometry strategy to sort live cells into enriched populations of insulin-producing, glucagon-producing, and non-hormone producing cells. Stimulation of these sorted cell types with innate immune stimuli revealed cell type-specific variations in the magnitude of responses. These findings provide insights into the initiating factors of the autoimmune targeting of  $\beta$  cells in T1D.

## 5.2: Introduction

An interesting component of the pathogenesis and development of T1D is the specificity for the autoimmune reaction against  $\beta$  cells. While the ultimate destruction mediated by T cells is characterized<sup>16</sup>, the processes that precipitate autoimmunity in a specific cell types are poorly understood. This specificity is particularly interesting in the context of viral triggers of T1D. Viruses could trigger autoimmune progression by several mechanisms.  $\beta$  cells could be particularly sensitive to viral infection leading to disproportionate presentation of  $\beta$  cell antigens to the adaptive immune system. Another possibility is that  $\beta$  cells produce or respond to innate immune signals differently than other cells. This could again shift the balance of antigen presentation from these cells to adaptive immune cells and drive autoimmunity. Understanding the differential responses of various islet cell types to viral infection could provide insights into the  $\beta$  cell specificity of T1D autoimmunity.

Viruses may have a selective  $\beta$  cell effect due to cell type-specific virus-host interactions. The expression of the viral receptor, cell-specific expression of viral restriction factors, and differences in the cell intrinsic antiviral responses all contribute to cell type virus tropism. Previous histological studies in pancreas from individuals with T1D show that CVB is detected in  $\beta$  but not  $\alpha$  cells, which suggests that CVB does not infect human  $\alpha$  cells<sup>104,292-295</sup>. One possibility for the absence viral proteins in  $\alpha$  cells is the lack of the requisite viral receptor on the cell surface. CAR protein expression is required for CVB infection and its

expression is absent in mouse  $\beta$  cells<sup>119,129</sup>. However, rat  $\beta$  and  $\alpha$  cells both express CAR protein<sup>296</sup>. This correlates with studies of sorted human islet cells, where *CXADR* (which encodes CAR) gene expression is detected in both  $\beta$  and  $\alpha$  cells<sup>297</sup>. Furthermore, pretreatment with anti-CAR antibody reduces CVB infection in both  $\beta$  and  $\alpha$  cells of cultured primary human islets<sup>200</sup>. So while some species-specific expression differences of CAR in some cell types may exist, human  $\beta$  and  $\alpha$  cells both produce the viral receptor making them susceptible to viral attachment and entry.

Intracellular restriction factors can inhibit viral replication. The adenosine-uridine (AU)-rich element RNA binding factor 1 (AUF1) can destabilize mRNAs and target them for degradation. This activity also destabilizes viral RNA in CVB infection and can inhibit viral replication if the virus is unable to cleave the protein<sup>298</sup>. Such cell type-specific restriction factors can prevent viral replication if no mechanism exists for the virus to subvert the inhibitory effect of the host factor. Other restriction factors may affect viral transcription, translation, or assembly of viral particles. Some of these factors may also contribute to cell intrinsic innate immune response signaling.

The recognition of viral RNA by cytosolic RLRs leads to an antiviral state through the production of IFN, which generates an antiviral state by regulating thousands of downstream genes. In flow cytometry-sorted rat  $\beta$  and  $\alpha$  cells, CVB5-infected  $\alpha$  cells express higher levels of the RLR gene *Ifih1* (which encodes MDA5) than  $\beta$  cells<sup>296</sup>. Therefore,  $\alpha$  cells can respond more vigorously

to CVB-infection than  $\beta$  cells, perhaps preventing efficient viral replication in  $\alpha$  cells. This response could be mediated through higher basal expression of other genes in the IFN production pathway in rat  $\alpha$  cells. Basal expression of the transcription factor downstream of IFN signaling, *Stat1*, is also higher in rat  $\alpha$  than in  $\beta$  cells<sup>296</sup>.

The findings that rat  $\alpha$  cells prevent viral replication through higher basal innate immune gene expression may not hold true to infections of human  $\alpha$  cells. Notable differences in gene expression between rodent and human  $\beta$  cells have been documented, with 1540 genes differentially expressed between mouse and human  $\beta$  cells<sup>299</sup>. Furthermore, basal gene expression in sorted human  $\beta$  cells is higher for both *IFIH1* and *STAT1* than in  $\alpha$  cells<sup>297</sup>; the immune response in these sorted human cells was not evaluated. Despite these differences in gene expression, other mechanisms of innate immune gene regulation could mediate a differential immune response in  $\beta$  compared to  $\alpha$  cells.

Gene expression studies of sorted primary human islet cells could be used to identify differentially expressed, cell-type specific immune responses. While high purification of  $\beta$  and  $\alpha$  cells is possible using sorting by cell surface staining, this method could interfere with downstream treatments and gene expression. Adding antibodies to the cells could inhibit viral infection through steric hindrance of virus-receptor interactions. Antibody binding may also induce modest activation of innate immune signaling, which would affect the basal gene expression in sorted cells. This would not be ideal for evaluating gene expression

following treatment with poly(I:C). To mitigate these potential pitfalls, I use a cell sorting strategy based on intrinsic autofluorescence and side scatter properties of human islet cells. Previous attempts to sort human cells based on autofluorescence in the FITC channel are limited due to higher accumulation of lipofuscin in human  $\beta$  cells<sup>300</sup>. Despite this technical limitation, utilizing additional excitation and emission characteristics now available on flow cytometry machines could circumvent these issues.

The goals of this chapter are to 1) develop a cell sorting strategy based on cell intrinsic autofluorescence and side scatter properties for primary human islet cells, 2) evaluate the purity of the sorted cell populations by flow cytometry and gene expression, 3) compare basal gene expression in  $\beta$  cells compared to  $\alpha$  cells, and 4) evaluate the induction of innate immune genes in sorted cells in response to treatment with poly(I:C).

## 5.3: Results

### 5.3.1: Development and analysis of human primary islet cells sorted based on autofluorescence characteristics.

Since cell sorting of human primary islets is reported to be problematic based on FITC autofluorescence characteristics alone due to the accumulation of lipofuscin in  $\beta$  cells<sup>300</sup>, I developed an alternative sorting strategy based on additional autofluorescence parameters. I dissociated primary human islets and identified live cells based on 7-Aminoactinomycin D (7-AAD) exclusion. From this population of live cells, I sorted populations based on autofluorescence and side-scatter characteristics. Cells that have high autofluorescence in the fluorescein



(FITC) spectrum (488nm excitation, 530/30 filter) and high side scatter are enriched for  $\beta$  cells. I sorted the remaining cells based on the Pacific Blue<sup>TM</sup> spectrum (405nm excitation, 450/50 filter) and FITC or side scatter. Cells that are low in Pacific Blue<sup>TM</sup> and FITC are enriched for  $\alpha$  cells, and cells that are lowest in side scatter are enriched for hormone negative cells (HN) (Fig 5.1, A).

Following the sorting procedure, I cultured the sorted cell populations for 24 h.

### **5.3.2: Evaluation of sorted populations by flow cytometry and gene expression profiling**

Following the overnight culture of the sorted populations, I evaluated the enrichment of the three major endocrine cell populations based on fluorescent antibody staining followed by flow cytometry analysis. I dissociated and stained a parallel sample from the same human islet donor that did not undergo any flow cytometry-sorting. Of these cells, referred to as “staining control sample”, 22% are  $\beta$  cells, 42% are  $\alpha$  cells, 6% are  $\delta$  cells, and 30% are hormone non-producing cells based on staining for insulin, glucagon, somatostatin, or the absence of all three respectively (Fig 5.1, B). To assess survival of cells following sorting or dispersion and overnight culture, I treated cells the same as in other sorted populations, but only collected live cells based on 7-AAD exclusion. This population is roughly equivalent to the proportions of  $\beta$  (17%),  $\alpha$  (35%),  $\delta$  (9%), or HN (39%) as the staining control sample (Fig, 5.1, B).

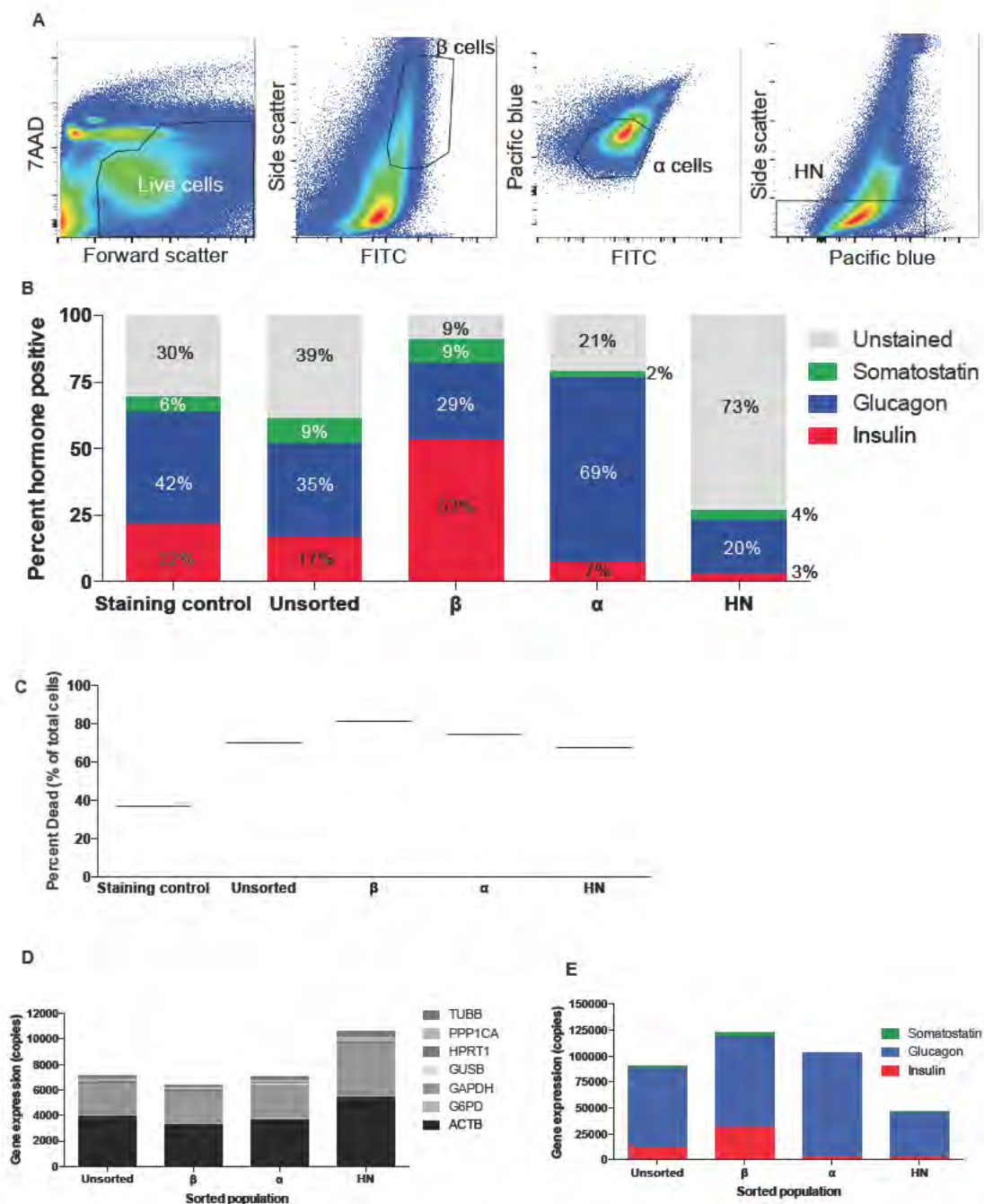


**Figure 5.1: Sorting strategy and evaluation of purity**

Cultured primary human islets were dissociated and gated for live cells based on 7AAD staining and then flow cytometry-sorted into fractions based on side scatter, FITC, and Pacific Blue™ autofluorescence. (B) Sorted cells cultured were overnight and then fixed, permeabilized and stained for intracellular insulin, glucagon, and somatostatin. Stained cells were analyzed by flow cytometry and

the percentage of hormone positive cells was calculated for each sorted population. The staining control was a sample of islets from the same donor cultured for 48 h that was dissociated just prior to staining. **(C)** Viability of sorted cell populations after overnight culture evaluated based on Zombie Violet™ staining. Percentage of dead cells was calculated based on total cells gated on forward and side scatter. Gene expression was evaluated in a parallel culture of sorted islet cells using the NanoString gene expression assay. **(D)** Raw gene counts for the seven housekeeping genes that are used for normalization. **(E)** Gene expression of hormone genes normalized to the panel of housekeeping genes.

The sorting strategy described above yielded a  $\beta$  cell population that is enriched from 17% in the unsorted sample to 53% insulin positive cells. Glucagon positive and HN cells are depleted from 35% to 29% and 39% to 9%, respectively, from the unsorted population to the sorted  $\beta$  cell population. However, somatostatin positive cells still represent 9% of the cells in this population. The sorted  $\alpha$  cell population is enriched from 35% to 69% glucagon positive cells from the unsorted to the  $\alpha$  cell population. This population is depleted for the other populations with only 7% of cells positive for insulin, 2% positive for somatostatin, and 21% HN. The sorted HN population is enriched from 39% to 73% for cells that do not stain for insulin, glucagon, or somatostatin. The hormone producing cells in the HN population are all depleted with only 3% insulin positive, 20% glucagon positive, and 4% somatostatin positive (Fig 5.1, B). While many of the cells maintained hormone staining after 24h culture as single cells, these conditions were detrimental to their survival. I evaluated cell death by identifying dead cells with Zombie Violet<sup>TM</sup> dye, which is excluded from live cells. 37% of cells are dead in the staining control sample where primary human islets were maintained in islet clusters until just prior to staining and not subjected to flow cytometry-sorting. Cell death is higher in all sorted populations cultured for 24h after sorting. 70% of cells are dead in the unsorted sample. This is comparable to the sorted  $\beta$ ,  $\alpha$ , and HN populations where 81%, 74%, and 67% of cells are dead, respectively (Fig. 5.1, C).

As a secondary means of validating enrichment in the sorted islet cell populations, I measured expression of hormone genes. I processed a portion of sorted cells that were cultured for 24 h in parallel to cells evaluated for hormone production by flow cytometry for gene expression. I used the NanoString gene CodeSet 2 (NSCS2), which includes housekeeping genes and the hormone genes, *INS*, *GCG*, and *SST*. Since there is some variation in cell survival after 24 h, I evaluated the raw gene counts for the seven housekeeping genes. The RNA counts for the unsorted population and sorted  $\beta$  or  $\alpha$  cells were similar for housekeeping genes (Fig. 5.1, D). The sorted HN population, which has the highest survival, also has the highest gene counts for the housekeeping genes. Because the survival and gene expression of housekeeping genes correlates, I can more confidently use these genes to normalize the data set. Gene expression of the hormone genes is an independent method for confirming the enrichment of the islet cell types in the sorted populations measured by flow cytometry. The normalized gene copies for the *INS*, *GCG*, and *SST* in the sorted islet populations correlates well with the staining data. The  $\beta$  cell population has more *INS* copies than the unsorted population. The  $\alpha$  cell population is enriched for *GCG* gene expression. The HN population has lower gene expression for all three hormone genes than in the unsorted population (Fig. 5.1, E & 5.2, A). Therefore, the sorted populations of human islet cells both stain and express their associated hormone genes, and thus I can evaluate the differences in these cell populations at baseline and when treated with immune-stimulatory agents.

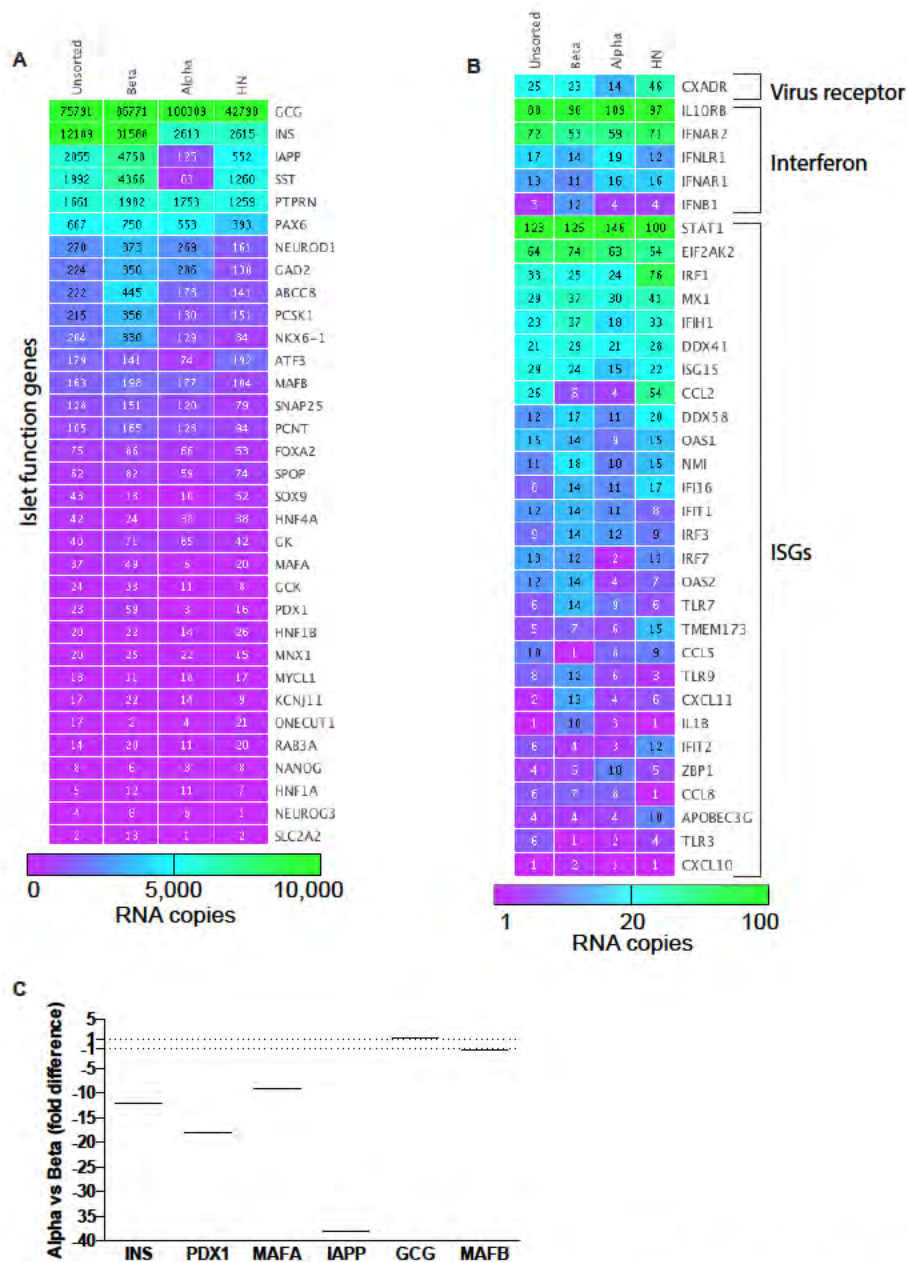


**Figure 5.2: Evaluation of basal gene expression of sorted human islet cells**  
 Evaluation of gene expression in sorted islet cells using the NanoString gene expression assay, normalized to a panel of seven housekeeping genes. **(A)** Heatmap of normalized RNA copies for genes associated with islet function. Scale from 0 (purple), 500 (cyan), and 10,000 (green). **(B)** Heatmap of normalized gene copies for genes associated with viral infection, interferon, and interferon stimulated genes (ISGs). Scale from 1 (purple), 20 (cyan), and 100 (green). **(C)** Comparison of enrichment of  $\beta$  or  $\alpha$  cell-specific genes in sorted populations. Plotted as fold-enrichment in  $\alpha$  cells compared to  $\beta$  cells.

### 5.3.3: Comparison of basal gene expression in sorted human islet populations

In addition to the hormone genes expressed in the sorted populations of primary human islets, the NanoString also measured a variety of genes associated with islet cell function and viral innate immune function. I evaluated the basal expression of these genes to assess for differential levels in each cell population. Such differences could influence  $\beta$  cell dysfunction in engrafted or cultured primary human islets upon CVB infection.

The gene expression in sorted human islet populations for other islet function genes help to confirm the enrichment of specific cell types in sorted populations. As expected, gene expression for proteins involved in  $\beta$  cell function is enriched in the sorted  $\beta$  cell population. This includes enrichment of *INS* (12-fold), *PDX1* (18-fold), *MAFA* (9-fold), *IAPP* (38-fold), and *PCSK1* (2.7-fold) in  $\beta$  cells compared the sorted  $\alpha$  cells (Fig. 5.2, A & C). These genes are also enriched in  $\beta$  cells compared to the unsorted population and the sorted HN cells. Genes associated with  $\delta$  cell function, *SST* and *HHEX*, are both enriched in the  $\beta$  cell population by 69-fold and 20.8-fold, respectively (Fig. 5.2, A & C). The sorted  $\alpha$  cell population is slightly enriched for *GCG* (1.15-fold) expression compared to the other populations (Fig. 5.2, A & C). This indicates contamination of the sorted  $\beta$  cells with  $\delta$  cells, but not  $\alpha$  cells. The HN population has lower expression for most of the islet function genes, except for a slightly higher expression of *ATF3* (Fig. 5.2, A). Taken together,  $\beta$  and  $\alpha$  cells are enriched in their respective populations while the HN population is depleted in hormone producing cells.

The normalized gene counts for genes involved in CVB infection for the unsorted,  $\beta$ ,  $\alpha$ , or HN populations under basal conditions have some cell-type variation. The basal expression of genes involved in CVB infection in different cell types may contribute to the cell-type specific nature of T1D. The viral receptor for CVB is CAR, which is encoded by the gene, *CXADR*<sup>129</sup>. *CXADR* expression is highest in the HN population and the lowest in  $\alpha$  cells. Expression of *IFIH1* is highest in  $\beta$  cells and lowest in  $\alpha$  cells. The *IFNB1* is expressed at very low levels in all populations basally, but is slightly higher in  $\beta$  cells. The genes encoding the type I (*IFNAR1*, *IFNAR2*) and type III (*IFNL1*, *IL10RB*) IFN receptors are all expressed at nearly equivalent levels in all three sorted cell populations (Fig. 5.2, B). These gene expression differences indicate the possibility of differential responses to viral infection in these cell types.

#### **5.3.4: Gene expression profiling poly (I:C) stimulation of sorted human islet populations**

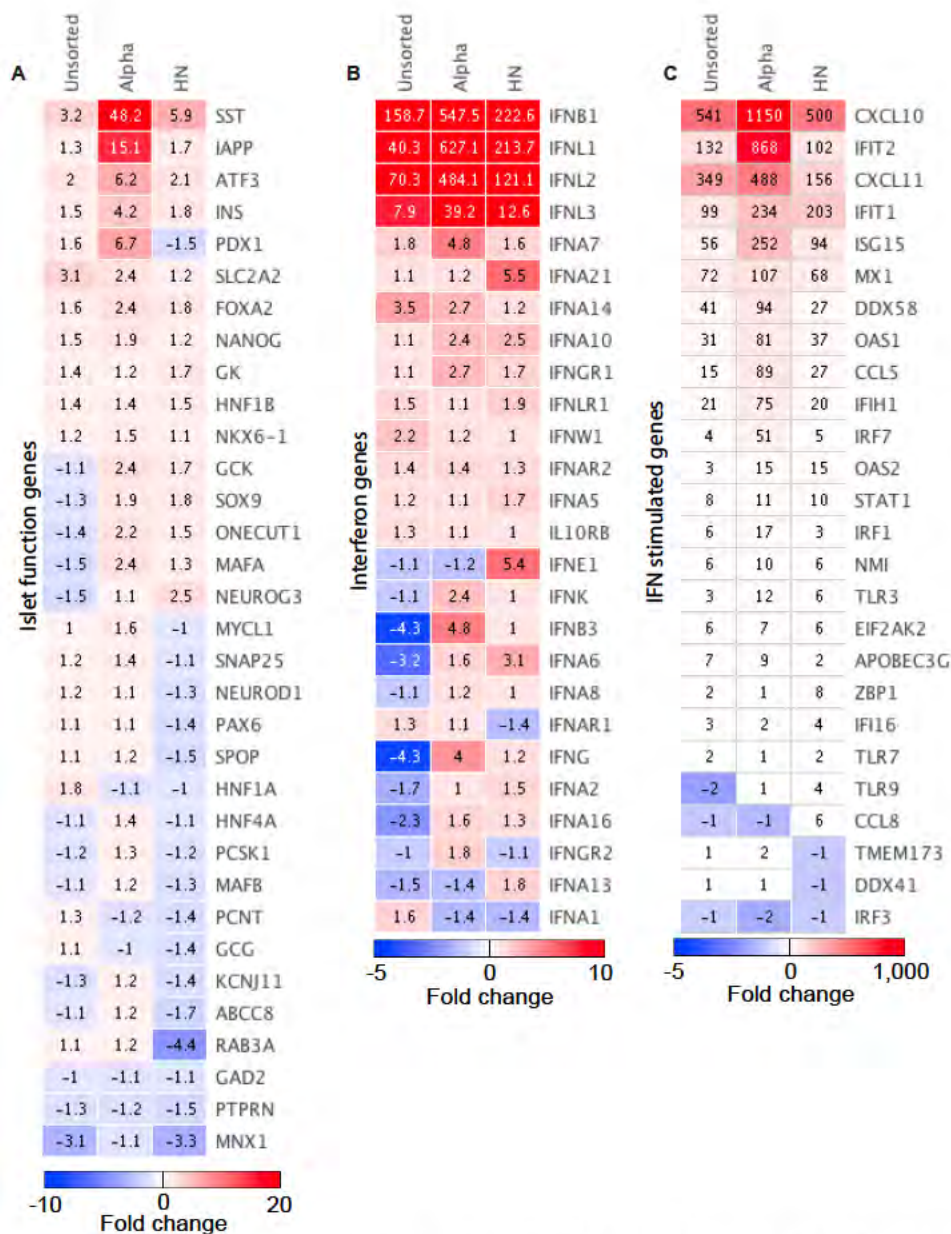
To better understand the cell-type specific differences in antiviral immune response in primary human islet cells, I quantified gene expression after stimulation with poly(I:C) in unsorted cells or populations enriched for  $\alpha$  and HN cells. While sorted  $\beta$  cells were also treated with poly(I:C), these data are not available for analysis due to the technical failure of probe hybridization during gene expression quantification. Similar to treatment of intact primary human islets with poly(I:C) (Fig. 3.4, A) only small differences in genes associated with islet function are observed in the unsorted population (Fig. 5.3, A). In the  $\alpha$  cell population after treatment with poly(I:C), a large increase in genes not normally



associated with  $\alpha$  cells is observed. *SST*, *IAPP*, *INS*, and *PDX1* are all increased greater than 5-fold. Similar to the unsorted population, islet function genes are generally unaffected in the sorted HN cells.

IFN genes are highly expressed in all cell populations upon treatment with poly(I:C). The highest expression is in the IFN-I gene *IFNB1*, and the IFN-III genes *IFNL1*, *IFNL2*, and *IFNL3*. The highest stimulation is in the sorted  $\alpha$  cells. *IFNB1* fold change is 3.4-fold higher than the unsorted cells and 2.5-fold higher than in the HN cells. Similarly, *IFNL1* fold change is 15.5-fold higher than the unsorted population, and 2.9-fold higher than the HN cells. In the HN population, the expression for *IFNA21* and *IFNE1* are higher than the other two populations. *IFNA21* is induced 5.5-fold compared to 1.1-fold and 1.2-fold in the unsorted and sorted  $\alpha$  cells respectively. *IFNE1* is upregulated 5.4-fold in HN cells compared to reductions of -1.1-fold and -1.2-fold in unsorted and  $\alpha$  cells respectively (Fig 5.3, B). While the general trend of IFN-induction by poly(I:C) may be similar in unsorted cells compared to sorted  $\alpha$  or HN cells, there are some cell-type specific responses. These could be partly due to the basal expression of immune related genes described in Figure 5.2.

In line with the findings that IFN genes are highly stimulated upon poly(I:C) treatment, ISGs are also increased. *CXCL10* is increased the most upon poly(I:C) treatment in all cell populations.



Like IFN gene expression,  $\alpha$  cells also have higher CXCL10 expression compared to the unsorted population and sorted HN cells. CXCL10 fold-increase is 2.1-fold higher than in unsorted cells and 2.3-fold higher than in sorted HN cells (Fig. 5.3, C).

## 5.4: Discussion

### 5.4.1: Primary human islet sorting and culture

$\beta$ ,  $\alpha$ , and HN cells are enriched to 53%, 69% and 73% respectively using a sorting strategy combining autofluorescence in the FITC and Pacific Blue<sup>TM</sup> channels (Fig. 5.1, B). The current sort strategy provides the highest enrichment for  $\beta$  and  $\alpha$  cells that I have tested. Despite this progress, the purity of each population does not reach that achieved in flow cytometry-sorted rat islet cells, for which  $\beta$  and  $\alpha$  cells are each >90% pure<sup>296</sup>. The major contaminating cell type in the  $\beta$  and HN populations is  $\alpha$  cells. It is possible that other sorting strategies or autofluorescence characteristics will aid in excluding these cells. Other sorting strategies are available for live human islet cells utilizing surface staining with the antibodies HPi2 and HPa2. This strategy can highly purify  $\beta$  and  $\alpha$  cells as evaluated by the gene expression of *INS* and *GCG*, although similar to my results,  $\delta$  cells are largely maintained in the  $\beta$  cell population<sup>297</sup>. Both sorting techniques have limitations in reducing the number of  $\delta$  cells in the sorted  $\beta$  cell population.

Resident immune cells of primary human islets could be major contributors to the immune responses measured here. Since I did not stain for these cells, it is unclear in which sorted population these cells reside. Adding cell

surface staining for CD45 could indicate if these cells are present in unequal proportions in the enriched populations. If CD45<sup>+</sup> cells are a potential confounding factor to measure the intrinsic responses of endocrine cells, it may be possible to deplete these cells during the cell sorting process. The exclusion of CD45<sup>+</sup> cells by the addition of an anti-CD45 antibody could be used to remove these cells prior to treatment.

Under the current culture conditions of the sorted human islet cells, viability is low even after only 24h of culture. The percentage of dead cells varies between 67% and 81% for the sorted cells (Fig. 5.1, C). Modifying the culture conditions could increase viability of dispersed, sorted cells. Culture of dispersed primary human islets on temperature-responsive polymer, poly(N-isopropylacrylamide), culture dishes coated with rat laminin-5 increases cell viability and glucose responsiveness<sup>301</sup>. This culture surface, in addition to optimizing glucose and nutrient concentrations in the media will likely allow for better cell survival.

#### **5.4.2: Basal gene expression provides insights into cell-type specific viral responses**

The evaluation of cell purity based on gene expression indicates that  $\beta$  and  $\alpha$  are enriched based on the expression of *INS* and *GCG* respectively. HN cells have a predictably lower expression of *INS*, *GCG*, and *SST* (Fig 5.1, E). These findings help validate the specificity of the autofluorescence-based sorting strategy. However, similar to the staining results, *GCG* expression remains high in the sorted  $\beta$  and HN cells. This is likely the reason for the paltry 1.15-fold

enrichment of *GCG* expression in  $\beta$  cells compared to  $\alpha$  cells (Fig. 5.2, C).

Further optimizing the sorting procedure will likely enhance this enrichment.

Despite the presence of contaminating cells in the sorted  $\beta$  cell population, *IAPP*, *PDX1*, and *MAFA* are also enriched in these sorted cells. The presence of these  $\beta$  cell specific genes in these cells further validates the sorting strategy based on autofluorescence in human islet cells.

The gene for the CVB receptor, *CXADR*, is expressed in sorted  $\beta$  and  $\alpha$  cells. Additionally HN cells also express the gene for CAR (Fig 5.2, B). *CXADR* expression in both  $\beta$  and  $\alpha$  cells therefore removes cell-type specific receptor restriction as a factor in human  $\beta$  cell specificity of CVB infections. Therefore, other restriction factors may contribute to low replication of CVB in human  $\alpha$  cells.

Marroqui *et al.* argue that the differences in CVB replication between  $\beta$  and  $\alpha$  cells is because  $\alpha$  cells produce a more robust immune response due to higher basal expression of immune genes<sup>296</sup>. In sorted primary human islet cells presented here, I also observe some cell-type specific differences in basal innate immune gene expression, albeit many of these genes are enriched in  $\beta$  cells, not  $\alpha$  cells. This finding is more in agreement with basal gene expression of human islet cells sorted based on cell surface staining<sup>297</sup>. These species-specific differences raise questions about the translatability of these mechanisms in rat islets to treatment of human disease. However, cells from additional human donors will need to be evaluated to determine the full range of the findings of sorted primary human islets.

#### 5.4.3: Gene expression for ISGs is higher in sorted $\alpha$ cells

Gene expression is generally higher for IFN and ISG gene expression upon poly(I:C) treatment in sorted  $\alpha$  cells compared to the unsorted population and sorted HN cells (Fig. 5.3) Unfortunately, due to a technical issue the gene expression in sorted  $\beta$  cells upon poly(I:C) treatment cannot be evaluated. The absence of this data set makes drawing definitive conclusions about the cell-type specific gene expression of antiviral response genes difficult. Despite this shortcoming, the presence of any differences between the sorted  $\alpha$  cells and the HN population is surprising. This is especially interesting since the HN population potentially contains resident immune cells from the primary islets. However, cell surface staining for hematopoietic surface markers needs to be evaluated to determine if these cells are actually present in this sorted population.

Consistent with findings described in **Chapter III** of the changes in islet function gene expression upon treatment with poly(I:C), most genes in this category did not change in sorted  $\alpha$  of HN cells. Interestingly the expression of *SST* and *IAPP* increased 48.2-fold and 15.1-fold respectively in sorted  $\alpha$  cells. The cause for this increase in expression of genes from cells that are depleted in this sorted population is unclear, but could be explained by a differential effect on cell survival in  $\alpha$  cells treated with poly(I:C). This could cause a relative enrichment in the other contaminating cell types in this population. Future studies of the cytotoxic effects of this treatment could help explain these findings.

Even after stimulation of the sorted cells with poly(I:C), expression of many IFN genes remained low. However, robust production of *IFNB1*, *IFNL1*,

*IFNL2*, and *IFNL3* is present. In addition to the increase in expression of these genes in the unsorted population of islet cells, the sorted  $\alpha$  and HN cells also expressed these genes upon poly(I:C) stimulation. Interestingly, the  $\alpha$  cells consistently had the highest expression of these genes.  $\alpha$  cells had a 2.5x higher fold change than HN cells for *IFNB1*, and a 2.9x higher fold change for *IFNL1* (Fig. 5.3, B). Corresponding with this higher expression of IFN-I and IFN-III expression, ISGs are also induced to higher levels in  $\alpha$  cells than HN cells. *CXCL10*, *IFIT2*, *ISG15*, and *IFIH1* expression have 2.3x, 8.5x, 2.7x, and 3.75x higher fold-changes in  $\alpha$  cells than in HN cells. While expression could not be compared with  $\beta$  cell expression of these genes after poly(I:C) treatment, these findings are consistent with findings that rat  $\alpha$  cells produce a robust antiviral cell intrinsic response<sup>296</sup>. However, cell type differences in transfection efficiency of the poly(I:C) cannot be excluded as a confounding factor in this experiment. Further characterization of the mechanisms of this robust response could help us understand the differences in response to viral infection in  $\alpha$  cells compared to neighboring  $\beta$  cells.

The robust production of an antiviral response in  $\alpha$  cells could be affecting the function and survival of nearby  $\beta$  cells. Treatment of  $\beta$  cells with cytokines inhibits insulin release<sup>190,302</sup>. Therefore, if  $\alpha$  cells in fact mount the most efficient cell-autonomous antiviral immune response, cytokine production in  $\alpha$  cells could also be signaling to  $\beta$  cells and inhibiting their function. Another possibility is that an inefficient immune response occurs in HN cells compared to  $\alpha$  cells. This

could allow for CVB infection to persist in pancreas cells. While the  $\beta$  cell response to poly(I:C) is not directly compared here, part of the  $\beta$  cell specificity in T1D could be due to protracted infection in  $\beta$  cells due to inefficient viral clearance in these cells. The low intrinsic immune response to prevent apoptosis and cell death of these important cells could lead to inefficient clearance, while  $\alpha$  cells have a more robust immune response and efficiently clear the virus. Further exploration of these mechanisms will need to be investigated to fully understand the role of differential immune responses in the development of T1D.

#### **5.4.4: Future directions**

The interpretations of the results presented here are restricted by the limited ability to purify individual endocrine cell types and the single human donor of the cells. Methods of obtaining higher cell-type purity are possible, but require the fixation of cells prior to sorting<sup>303</sup>. This would limit the experimental design of studies of viral infections to infecting intact islets followed by sorting. Efforts to evaluate the gene expression of single sorted cells by RNA-seq may provide alternatives to both my current sorting strategy and other available strategies. However, the depth of sequencing of single cells is still a limiting factor with technologies that are currently available.

#### **5.4.5: Conclusions**

Enriched populations of primary human cells can be obtained by flow cytometry-sorting cells based on intrinsic autofluorescence characteristics. Basal gene expression indicates that cell type-specific expression of innate immune genes may mediate differences in antiviral responses. Furthermore, sorted  $\alpha$



cells treated with poly(I:C) have higher expression of innate immune genes than unsorted cells or sorted HN cells. Further dissecting these cell type differences in innate immune signaling to viral infections will help to understand the development of  $\beta$  cell specific autoimmunity in T1D.

## **5.5: Materials and methods**

### **5.5.1: Culture and dissociation of human islets**

Primary human islets from a normal human donor were cultured in supplemented Primary Islet Medium (PIM(S) – Prodo Labs) overnight. Islets were dissociated into a single cell suspension using TrypLE (Invitrogen) and filtered through a 35  $\mu$ M cell strainer. Single cells were kept on ice in DMEM medium with 2.8mM glucose and 1% BSA for a minimal time until flow cytometry-sorting.

### **5.5.2: Flow cytometry sorting**

Cells were sorted on a BD FACSAria IIu Cell Sorter installed in a Baker BioProtect IV biosafety cabinet running on BD FACSDiva Software (version 8.0, firmware version 1.8). Live cells were gated on 7-AAD (488nm excitation, 695/40 filter). A sample of unsorted, live cells was collected prior to sorting as a control. Cells were then sorted three ways based on forward scatter, side scatter, FITC (488nm excitation, 530/30 filter), and Pacific Blue<sup>TM</sup> (405nm excitation, 450/50 filter) as outlined in Figure 5.1.

### **5.5.3: Culture and treatment of sorted cells**

After sorting, 15,000 cells were transferred to 96 well plates for each of the sorted populations and the unsorted, live population. These cells were either untreated or transfected with 100  $\mu$ g/ml of poly(I:C) (InvivoGen) by Lipofectamine 2000 reagent (Invitrogen). After overnight culture, a portion of untreated cells was

stained for flow cytometry analysis described below. Parallel samples of untreated or poly(I:C) treated cells were washed with PBS and lysed with RLT buffer (Qiagen). These samples were then directly analyzed by NanoString assay as described below.

#### **5.5.4: Flow cytometry analysis**

A portion of the original sample of primary human islets was not run through the flow cytometry-sorted and instead cultured for an additional day (two days total culture). Just prior to staining all samples, these cells were dissociated with TrypLE (Invitrogen). These cells served as staining controls. The staining controls and sorted cells were first stained by Zombie Violet™ to stain dead cells (BioLegend 423113). Cells were then fixed with 4% paraformaldehyde and permeabilized by 0.1% saponin. Antibodies against glucagon (Sigma, G2654) and somatostatin (Lifetech, 7G5) were conjugated with Zenon 568 or 488 kits respectively (Invitrogen). The insulin antibody is conjugated to Alexa Fluor 647 (Cell Signaling, #9008). Stained cells were then analyzed on a BD LSRII SORP running BD FACSDiva Software (version 8.0, firmware version 1.8). Proportions were calculated based on total cells identified by forward and side scatter as the denominator.

#### **5.5.5: NanoString gene expression profiling**

The NanoString CodeSet (NSCS2) used in these studies was developed to include human genes associated with IFN-I (18), IFN-II (3), IFN-III (5), IFN regulated genes (20),  $\beta$  cell function (24), endocrine (9), apoptosis (8), cytokines (7), inflammation (8), ER stress (20), T1D susceptibility genes (12), other human


genes (4), a CVB-specific probe, and housekeeping genes (7) for normalization of data for a total of 146 genes. Methods are the same as described in **Chapter III.**

## CHAPTER VI: DISCUSSION

### 6.1: Overview

The role of viruses as environmental triggers for the development of T1D is a major question in the diabetes field. Broadly, I sought to characterize two aspects of enterovirus infection of human  $\beta$  cells. The first is how CVB infection directly disrupts  $\beta$  cell function of insulin production. The second is to define how innate immune signaling in  $\beta$  cells following CVB challenge may contribute to the pathogenesis and autoimmune activation of T1D in people. A summary of the findings for changes in insulin and PDX1 expression and innate immune responses for each model system described are summarized in Table 6.1. A better understanding of these aspects of viral infection could be used to identify early markers for the progression to T1D, which could be used in clinical diagnosis and towards prevention of T1D. Biomarkers that identify patients who develop autoimmunity against  $\beta$  cells after a viral infection could aid in preventing disease. These same pathways could also be targeted for drug design to prevent the development of T1D.

In Chapter II, results from the *in vivo* infection model of mice engrafted with primary human islets indicate that a loss of insulin production causes hyperglycemia and that an islet intrinsic innate immune response to the viral infection occurs. In Chapter III, infections with various cultured human  $\beta$  cells indicate that the reduction in insulin gene expression occurs between 6 and 24 hpi. A robust IFN-I response followed by induction of downstream ISGs occurs in



Model complexity	Model system	Chapter	Insulin	PDX1	Innate immunity
	Engrafted primary human islets	Chapter II	<ul style="list-style-type: none"> <li>•Decreased in serum</li> <li>•Protein decreased in graft</li> <li>•mRNA decreased</li> </ul>	<ul style="list-style-type: none"> <li>•mRNA decreased</li> </ul>	<ul style="list-style-type: none"> <li>•Low IFN gene expression</li> <li>•High ISG expression</li> </ul>
	Cultured primary human islets	Chapter III	<ul style="list-style-type: none"> <li>•mRNA decreases between 6 and 24hpi</li> </ul>	<ul style="list-style-type: none"> <li>•mRNA slightly decreases at 6h and more at 24h</li> </ul>	<ul style="list-style-type: none"> <li>•High IFN gene expression</li> <li>•High ISG expression</li> </ul>
	SC- $\beta$	Chapter III	<ul style="list-style-type: none"> <li>•No change in mRNA</li> </ul>	<ul style="list-style-type: none"> <li>•No change in mRNA</li> </ul>	<ul style="list-style-type: none"> <li>•High IFN gene expression</li> <li>•High ISG expression</li> </ul>
	EndoC- $\beta$ H1	Chapter III & IV	<ul style="list-style-type: none"> <li>•Slight decrease in mRNA</li> </ul>	<ul style="list-style-type: none"> <li>•Slight increase in mRNA</li> <li>•Change in localization at 6hpi</li> </ul>	<ul style="list-style-type: none"> <li>•High IFN gene expression</li> <li>•High ISG expression</li> </ul>
	Sorted primary human islet cells	Chapter V	Not tested	Not tested	<ul style="list-style-type: none"> <li>•Higher IFN and ISG response in <math>\alpha</math> cells than HN cells</li> </ul>

**Table 6.1: Summary of  $\beta$  cell function and innate immune responses**

$\beta$  cell function as measured by insulin gene expression is variable after CVB infection. Insulin mRNA decreases after infection of both engrafted and cultured primary human islets. It is also slightly decreased in EndoC- $\beta$ H1 cells, but is unchanged in CVB-infected SC- $\beta$  cells. Similarly, PDX1 gene expression decreases after infection of both engrafted and cultured primary human islets. PDX1 gene expression does not change in SC- $\beta$  cells and increases slightly in EndoC- $\beta$ H1 cells after CVB infection. However, PDX1 nuclear staining decreases after CVB infection in EndoC- $\beta$ H1 cells. All models exhibit an increase in IFN and ISG production upon CVB infection. Primary islet cells enriched for  $\alpha$  cells have a higher IFN and ISG response than HN cells.

these cells in response to poly(I:C) treatment or infection with CVB4. In Chapter IV, I identified a shift in nuclear PDX1 localization in CVB-infected EndoC- $\beta$ H1 cells at 6 hpi. Infection with viruses other than CVB did not result the same shift in localization. These results indicate a potential early mechanism in  $\beta$  cell dysfunction upon CVB infection. Finally, in Chapter V, immune responses in populations of flow cytometry-sorted cells are evaluated upon poly(I:C) stimulation. These results indicate that IFN and ISG responses are different in  $\alpha$  cells compared to hormone-negative cells. Cell type differences in innate immune responses could identify factors that are important in the cell type specificity of the autoimmune reaction against  $\beta$  cells in T1D. As a whole, many changes in gene expression are observed in CVB4-infected  $\beta$  cells compared to uninfected control, and it is likely that some or all of these changes act in concert to initiate a cascade that contributes to the autoimmune destruction of  $\beta$  cells and the development of T1D.

## **6.2: $\beta$ cell dysfunction and innate immune signaling in an *in vivo* model**

In Chapter II, I utilized an *in vivo* model of primary human islets engrafted into immunodeficient mice with induced hyperglycemia to define effects of CVB4 infection on  $\beta$  cell function and innate immune signaling. At a mean time of 28 days post infection with CVB4, mice developed hyperglycemia due to reduced insulin production (Fig. 2.2). This finding was the impetus for further exploring  $\beta$  cell dysfunction after CVB4 infection. CVB4 infection of engrafted primary human islets also produces a strong innate immune gene response that is indicative of the induction of IFN-I. The dsRNA sensor *IFIH1*, which initiates IFN-I responses

and is itself an ISG, and the IFN-inducible cytokine *CXCL10* are both significantly increased following infections.

This *in vivo* model could be modified in several ways to further understand  $\beta$  cell dysfunction and innate immune responses after virus infection. Drugs could be used to modulate viral replication or immune responses, other virus strains could be evaluated, and human immune cells could be added to the system. Each is discussed below in further detail.

The above-described *in vivo* model could be extended through drug modification of viral replication or cellular responses. The antiviral drug, pleconaril, suppresses CVB4 replication by binding to VP1 and interfering with the uncoating of the virus in cultured primary human islets<sup>304</sup>. So treatment of infected mice with this drug may also reduce viral replication, increase viral clearance, and prevent hyperglycemia. Administration of drug after the development of hyperglycemia could help determine if the hyperglycemia is reversible. However, this recovery may be limited due to the poor proliferation of human  $\beta$  cells. It may also be possible to reduce  $\beta$  cell stress in infected mice to determine if hyperglycemia can be delayed or prevented. Modulations in viral replication or the ability of  $\beta$  cells to tolerate viral replication may extend the time until hyperglycemia develops.

Viral pathogens besides CVB could be used for infection to determine if they can cause hyperglycemia in the relative absence of immune cells. While other viruses can infect and replicate in  $\beta$  cells, including VSV and RSV, they

may not be able to promote hyperglycemia similar to CVB4. Because VSV and RSV do not impact PDX1 localization in the same manner as CVB4 in EndoC- $\beta$ H1 cells (see Chapter IV), these viruses might not affect insulin or induce hyperglycemia in these mice. If they do promote the development of hyperglycemia, they may do so more rapidly or through different mechanisms. Another potentially interesting virus to try is CVA9, which reportedly infects and replicates in cultured primary human islets, but does not affect insulin secretion<sup>233,234</sup>. This could provide the opportunity to compare gene expression through unbiased RNA-seq techniques to identify similarities and differences in these responses.

Another means for expanding the *in vivo* model is to add back components of the human immune system to provide insight on the interaction of the innate immune signaling from infected islet cells to the adaptive immune system. Engraftment human fetal liver and thymus tissue to provide macrophages, T, and B cells could be transplanted along with autologous human fetal islets. Challenging these mice with virus would provide for a better understanding of the mechanisms behind development of beta cell dysfunction in human tissue in the context of adaptive immune responses. The infiltration of these cells into engrafted islets could further enhance the local inflammatory niche in the infected islets, potentially leading to a cytotoxic T cells response against  $\beta$  cells. This may accelerate the progression to hyperglycemia in this model. However, a major challenge is the significant dual morbidity of graft



versus host disease and virus infection in the model.

### **6.3: Combining models**

Engraftment of either SC- $\beta$  or EndoC- $\beta$ H1 in mice can rescue hyperglycemia in mice<sup>33,237</sup>, i.e., these sources of human  $\beta$  cells can be used in place of primary human islets in the *in vivo* model with viral challenge to induce diabetes. These alternative cells provide less genetic variability between experiments, greater availability of cells, and the possibility for genetic manipulation of the engrafted cells. Studying engraftment of these cells in mice provides advantages over culture given more physiologically relevant conditions and vascularization that maintains long-term viability.

Two potential outcomes from these experiments are considered; each can be leveraged to reveal new insights on  $\beta$  cell biology and innate immune responses that precipitate autoimmunity. These mice become hyperglycemic after CVB challenge just as in the experiments with engrafted primary human islets. If this is the case, *in vivo* models of these engrafted cells could provide a more reproducible model with more genetic stability between experiments to test other strains of CVB4 or other viruses implicated in T1D. This also provides for a genetically tractable system for testing components of the type I IFN pathway in the development of hyperglycemia after viral infection, given that candidate genes can be targeted using CRISPR-Cas9 approach. Knockouts for *IFIH1* or type I interferon receptor (IFNAR) would be candidates for suppressing IFN-I signaling following CVB4 challenge and could help to dissect the relative contributions of direct viral effects and innate immune responses on the

production or secretion of insulin.

A second potential outcome is that mice engrafted with either SC- $\beta$  or EndoC- $\beta$ H1 cells do not revert to hyperglycemia following CVB4 infection. Differences in insulin gene expression of these cells compared to cultured primary human islets following in vitro challenge with virus have been observed. Since insulin mRNA production is maintained in SC- $\beta$  and EndoC- $\beta$ H1 cells, it is possible that these cells may be resistant to the mechanisms that suppress insulin expression in cultured primary human islets. These artificial  $\beta$  cell sources lack some of the cellular diversity in cultured primary human islets. Cultured and engrafted islets include resident immune cells, endothelial cells, ductal cells, and low levels of exocrine cells, which may be contributing to the decrease in insulin gene expression via an undefined mechanism during infection. If hyperglycemia were induced by CVB4 in SC- $\beta$  or EndoC- $\beta$ H1 cell-engrafted mice, this would suggest that the non-endocrine cells are non-essential in the mechanism. RNA-seq of infected cultured primary human islets could be compared with that of SC- $\beta$  or EndoC- $\beta$ H1 to identify genetic factors that may be absent in the latter two cell types. The differential gene expression could identify pathways involved in the loss of *INS* and *PDX1* gene expression and islet dysfunction in CVB4 infection.

Altogether, these alternative sources of  $\beta$  cells in the mouse model could provide new insights into virus-host interactions between CVB and human  $\beta$  cells. Results could be leveraged to gain insights into  $\beta$  cell dysfunction after viral

infection and the innate immune responses induced in response to viral infection.

#### **6.4: Potential extensions of viral infections of EndoC- $\beta$ H1 cells**

Because a  $\beta$  cell line derived from human cells has only recently become available, most of the information about  $\beta$  cell changes after virus infection is from experiments carried out in rodent  $\beta$  cell lines. Because of limitations in translating the findings in rodent models into therapies for human disease, these species-specific differences are critical. The availability of EndoC- $\beta$ H1 cells and their permissiveness to CVB infection allow for investigation of other aspects of the virus-host relationship. The effects on aspects of insulin secretion and changes in viral genome in adaptation to  $\beta$  cells should be evaluated. This platform also provides a system for identifying and characterizing early biomarkers of viral infection and  $\beta$  cell function that could be translated into diagnostic assays.

In addition to decreases in *INS* gene expression after CVB infection, other aspects of the insulin response may be disrupted including insulin translation, maturation in secretory granules, or secretion. In the mouse  $\beta$  cell line, MIN6, CVB5 infection directly impairs glucose-stimulated insulin secretion by reducing the amount of insulin in secretory granules<sup>305</sup>. This may also contribute to the  $\beta$  cell dysfunction observed in engrafted primary human islets after infection that results in hyperglycemia (Chapter II). In addition to reduction in insulin production or packaging, CVB infection may interfere with aspects of insulin secretion. The increase in intracellular calcium upon glucose sensing is required for release of insulin granules docked at the plasma membrane for immediate release. The

CVB viral proteins 2B and 2BC integrate into ER and golgi membranes and increase calcium efflux<sup>145</sup>. This could interfere with the normal calcium control in  $\beta$  cells and reduce their ability to release insulin in response to glucose. The combination of these factors in disruption of insulin responses might explain the loss of glycemic control in the *in vivo* model. These possibilities for additional mechanisms of  $\beta$  cell dysfunction may help explain why infections with CVB are often associated with the development of T1D.

The persistence of viral infection in our *in vivo* engrafted primary human islet model was surprising and raises questions about possible changes in the viral genome over the course of the infection. Conditions of CVB3 persistent infection are associated with deletions in the 5' UTR<sup>121</sup>. These viruses are poorly replicative and less cytopathic. Evaluating virus present in the engrafted primary human islets of infected mice for mutations and deletions acquired over the course of persistent infection would be of interest. RNA-seq on samples from the engrafted primary human islets could reveal if 5' UTR deletions are present; viral genome populations from the input inoculum virus could be compared to the viruses that remain during persistent infection. These data may provide insights into viruses that are slowly replicating and well adapted to the  $\beta$  cells, and are consistent with the hypothesis that persistent enteroviruses may precipitate T1D development by promoting persistent inflammatory conditions in the islets<sup>306</sup>.

Another method to explore the changes in virus genome after adaptation to human  $\beta$  cells is to serially passage CVB4 in EndoC- $\beta$ H1 cells to see if this

reduces the virulence and CPE induced by these viruses and to determine if these viruses become more  $\beta$  cell tropic. This may lead to increased the penetrance of virus infection in the *in vivo* model, which is currently ~50% (Chapter II). Adaptation of CVB5 to MIN6 cells allowed for a more  $\beta$  cell tropic virus in infections of mice<sup>307</sup>. A similar approach could be applied to CVB in human  $\beta$  cells. In addition to passaging CVB in human  $\beta$  cells, selective pressures could be added to learn more why viruses selected under different conditions may or may not induce hyperglycemia *in vivo*. For example, CVB could be passaged in the presence of recombinant IFN-I. This IFN-I resistant strain could upset the balance of viral replication and innate immune control in the engrafted primary human islets, and would be predicted to be more likely to precipitate hyperglycemia in mice.

Infections of EndoC- $\beta$ H1 cells provide an attractive platform for discovery of biomarkers that could be used clinically to identify enterovirus infections affecting  $\beta$  cells that could lead to the induction of T1D. These cells have the advantage of being a monoculture, so the changes measured will be  $\beta$  cell-specific. Infections of non- $\beta$  cell types could help identify markers for the production of secreted or cell-intrinsic factors induced upon CVB infection. Proteomics of supernatants from CVB-infected EndoC- $\beta$ H1 cells would identify factors secreted or released from infected cells. Furthermore, samples at different time points could identify factors that identify early or late markers for  $\beta$  cell infection.

## **6.5: Conclusions**

Overall, I hypothesized that CVB4 infection of human  $\beta$  cells results in  $\beta$  cell dysfunction characterized by reduced insulin production and innate immune responses, including induction of *IFNB* and *CXCL10* gene expression. Further insights into these responses will help to better identify, diagnose, treat, and prevent the development of T1D in genetically predisposed people.

## APPENDIX I: CHANGES IN MOUSE GENE EXPRESSION UPON CVB4 INFECTION

In **Chapter II**, I describe the response of primary human islets engrafted into diabetic, immunodeficient mice. To differentiate the gene expression changes after CVB4 infection, I utilized the NanoString gene expression assay. This allowed for the design of species-specific probes to determine if the changes in gene expression were because of viral responses in the engrafted human tissue or the surrounding mouse kidney tissue.

The species-specificity of the probes can be evaluated based on the expression of endocrine genes that should not be expressed in mouse kidney tissue. The human-specific NanoString detected robust expression of endocrine genes including *INS*, *SST*, and *GCG*. In contrast, the gene expression from these same samples using the mouse-specific NanoString had RNA copies below the level of detection for *Ins2* and *Sst*. Some cross-reactivity may occur between some of the probes because the probe that was designed to be specific for mouse *Gcg* detects at high levels.

The human-specific NanoString showed many genes that are decreased after CVB4 infection in the engrafted islets (Fig. 2.6, A). In the same samples from Experiment 1 where diabetes was induced by STZ treatment, there are very few mouse genes that decrease after CVB4 infection, and none of these changes reach statistical significance (Fig. A1, A). Comparison of human genes increased after CVB4 infection (Fig. 2.6, B) with increased mouse-specific genes shows

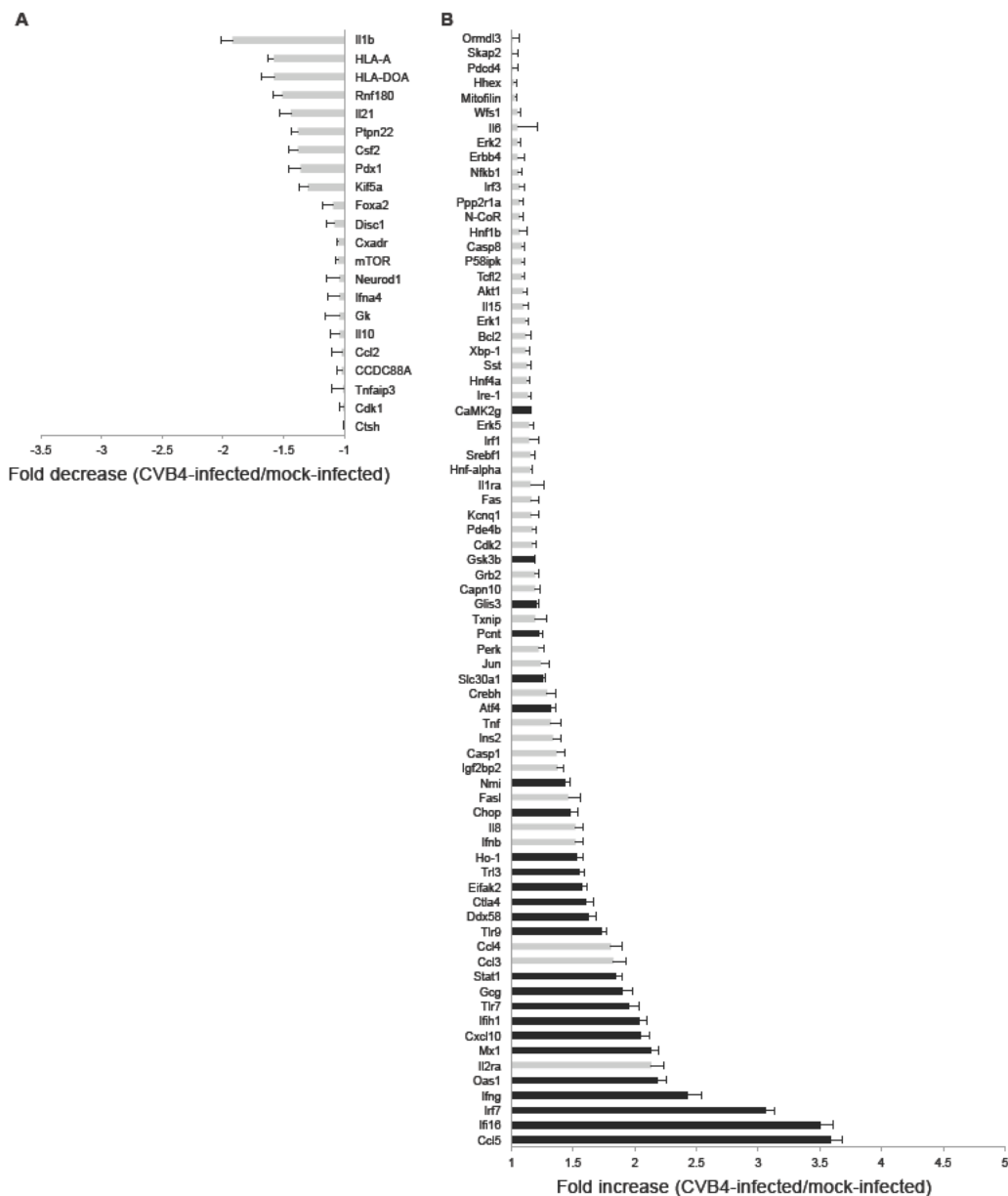


**Figure A1: Mouse gene expression in CVB4-infected animals by NanoString analysis**

Gene expression in kidney tissue surrounding engrafted primary human islets from CVB4-infected mice (n=7) and mock-infected mice (n=5) from Experiment 1 (STZ-induced diabetes). **(A)** Genes with decreases in gene expression plotted as the fold change of the CVB4-infected mice over the mock-infected mice. **(B)** Genes with increased fold change in CVB4-infected mice over mock-infected mice. Black bars indicate  $P < 0.05$ , Student's t-test. Error bars show the S.E.M.



that several of the genes with the highest increases are the same. *Ccl5*, *Oas*, *Mx1*, *Cxcl10*, *Ifih1*, and *Stat1* are all significantly increased in both human-specific and mouse-specific probe sets (Fig. A1, B). However, in general the fold increases are lower with the mouse-specific probes. Several genes are significantly increased with the mouse-specific probes that are not significantly changed with the human-specific probes, including *Ifi16*, *Irf7*, *Ifng*, *Tlr7*, and *Tlr9* (Fig. A1, B). These genes may represent species-specific differences or tissue-type specificity. These differences could help to understand the innate immune responses to CVB infection between different cell types, and why infection of  $\beta$  cells could trigger autoimmunity.

While some response to the CVB-infection in the mouse tissue is observed, the gene signature is unique from that of the engrafted primary human islets. The response in mouse tissue also seems to be weaker than the human gene response. However, it is unclear how much the expression of these genes from mouse tissue influences the function and response of the engrafted primary human islets.

When these experiments were conducted, it was not possible to specifically recover the engrafted primary human islet cells from the mouse tissue. Recently, methods have been developed that will allow the separation of the human cells from the mouse tissue. This will further mitigate the complications of cross-reactive probes. However, these techniques will not account for the potential for cross-species signaling that may occur during the

viral infection. The response of the mouse dendritic cells, macrophages, and granulocytes, which are still present in NSG mice, could be mediating some of the changes in gene expression in human cells in this model. It is encouraging that in cultured islets, which are devoid of any mouse tissue or cells, the gene expression patterns are similar to the islets engrafted in mice. Therefore, it is likely that the gene expression changes in this model of viral infection of primary human islets are due to cell-intrinsic responses to the virus and not due to responses to mouse immune cells.

## **Appendix I: Materials and methods**

### **Culture and dissociation of human islets**

A portion of the human islets that were engrafted in mice was collected at the time of sacrifice from Experiment 1 (STZ-treatment) from CVB4-infected mice (n=7) and mock-infected mice (n=5). TRIzol reagent (Life Technologies) was used for RNA extraction from the tissue. Probes were designed to target mouse genes in a species-specific manner against the same genes as described for NanoString CodeSet #1 (NSCS1), which included type I IFN, cytokines, apoptosis, endocrine, endoplasmic reticulum (ER) stress, T1D-associated loci, and other human genes, plus seven housekeeping genes for normalization of data. One hundred nanograms of RNA extracted from tissue was hybridized, processed, and analyzed per the manufacturer's procedure. Data were normalized using the nSolver Analysis Software (version 1.1). Fold changes in gene expression were the ratio of normalized gene expression in CVB4-infected samples versus those in mock-infected samples. Averages of fold changes were

calculated by averaging the  $\log_{10}$  of the fold change followed by a transformation of  $10x$ . Values  $<1$  were transformed by  $-1/x$ . Statistical significance was determined by Student's t-test.

## BIBLIOGRAPHY

1. Dabelea, D. The accelerating epidemic of childhood diabetes. *Lancet* **373**, 1999–2000 (2009).
2. Dabelea, D. *et al.* Prevalence of Type 1 and Type 2 Diabetes Among Children and Adolescents From 2001 to 2009. *JAMA* **311**, 1778–1786 (2014).
3. American Diabetes Association. Economic costs of diabetes in the U.S. in 2012. *Dia Care* **36**, 1033–1046 (2013).
4. American Diabetes Association. Diagnosis and classification of diabetes mellitus. *Diabetes Care* **27 Suppl 1**, S5–S10 (2004).
5. Chiang, J. L., Kirkman, M. S., Laffel, L. M. B., Peters, A. L. Type 1 Diabetes Sourcebook Authors. Type 1 diabetes through the life span: a position statement of the American Diabetes Association. *Dia Care* **37**, 2034–2054 (2014).
6. Kitabchi, A. E., Umpierrez, G. E., Miles, J. M. & Fisher, J. N. Hyperglycemic crises in adult patients with diabetes. *Dia Care* **32**, 1335–1343 (2009).
7. Nathan, D. M. Long-term complications of diabetes mellitus. *N Engl J Med* (1993).
8. Kenny, C. When hypoglycemia is not obvious: Diagnosing and treating under-recognized and undisclosed hypoglycemia. *Primary Care Diabetes* **8**, 3–11 (2014).
9. Gale, E. A. M. The Discovery of Type 1 Diabetes. *Diabetes* **50**, 217–226 (2001).
10. Banting, F. G., Best, C. H., Collip, J. B., Campbell, W. R. & Fletcher, A. A. Pancreatic Extracts in the Treatment of Diabetes Mellitus. *Canadian Medical Association Journal* **12**, 141–146 (1922).
11. Himsworth, H. P. *Diabetes mellitus: its differentiation into insulin-sensitive and insulin-insensitive types. 1936. International journal of epidemiology* **42**, 1594–1598 (Oxford University Press, 2013).
12. American Diabetes Association. Diagnosis and classification of diabetes mellitus. *Diabetes Care* **33 Suppl 1**, S62–9 (2010).
13. Bonifacio, E. & Ziegler, A.-G. Advances in the Prediction and Natural History of Type 1 Diabetes. *Endocrinology and Metabolism Clinics of North America* **39**, 513–525 (2010).
14. Gepts, W. Pathologic anatomy of the pancreas in juvenile diabetes mellitus. *Diabetes* **14**, 619–633 (1965).
15. Atkinson, M. A., Eisenbarth, G. S. & Michels, A. W. Type 1 diabetes. (2014). doi:10.1016/S0140-6736(13)60591-7
16. Kahaly, G. J. & Hansen, M. P. Type 1 diabetes associated autoimmunity. *Autoimmunity Reviews* (2016). doi:10.1016/j.autrev.2016.02.017

17. Kent, S. C. *et al.* Expanded T cells from pancreatic lymph nodes of type 1 diabetic subjects recognize an insulin epitope. *Nature* **435**, 224–228 (2005).
18. Hou, J., Said, C., Franchi, D., Dockstader, P. & Chatterjee, N. K. Antibodies to Glutamic Acid Decarboxylase and P2-C Peptides in Sera From Coxsackie Virus B4-Infected Mice and IDDM Patients. *Diabetes* **43**, 1260–1266 (1994).
19. Verge, C. F. *et al.* Prediction of Type I Diabetes in First-Degree Relatives Using a Combination of Insulin, GAD, and ICA512bdc/IA-2 Autoantibodies. *Diabetes* **45**, 926–933 (1996).
20. Achenbach, P. *et al.* Mature high-affinity immune responses to (pro)insulin anticipate the autoimmune cascade that leads to type 1 diabetes. *J. Clin. Invest.* **114**, 589–597 (2004).
21. Baekkeskov, S. *et al.* Identification of the 64K autoantigen in insulin-dependent diabetes as the GABA-synthesizing enzyme glutamic acid decarboxylase. , *Published online: 13 September 1990; | doi:10.1038/347151a0* **347**, 151–156 (1990).
22. Kaufman, D. L. *et al.* Autoimmunity to two forms of glutamate decarboxylase in insulin-dependent diabetes mellitus. *J. Clin. Invest.* **89**, 283–292 (1992).
23. Willcox, A., Richardson, S. J., Bone, A. J., Foulis, A. K. & Morgan, N. G. Analysis of islet inflammation in human type 1 diabetes. *Clin. Exp. Immunol.* **155**, 173–181 (2009).
24. Kronenberg, D. *et al.* Circulating preproinsulin signal peptide-specific CD8 T cells restricted by the susceptibility molecule HLA-A24 are expanded at onset of type 1 diabetes and kill  $\beta$ -cells. *Diabetes* **61**, 1752–1759 (2012).
25. Brange, J. & Vølund, A. Insulin analogs with improved pharmacokinetic profiles. *Adv. Drug Deliv. Rev.* **35**, 307–335 (1999).
26. Miller, K. M. *et al.* Current state of type 1 diabetes treatment in the U.S.: updated data from the T1D Exchange clinic registry. *Dia Care* **38**, 971–978 (2015).
27. Ludvigsson, J. *et al.* GAD65 antigen therapy in recently diagnosed type 1 diabetes mellitus. *N Engl J Med* **366**, 433–442 (2012).
28. Herold, K. C. *et al.* Teplizumab (anti-CD3 mAb) treatment preserves C-peptide responses in patients with new-onset type 1 diabetes in a randomized controlled trial: metabolic and immunologic features at baseline identify a subgroup of responders. *Diabetes* **62**, 3766–3774 (2013).
29. Bluestone, J. A. *et al.* Type 1 diabetes immunotherapy using polyclonal regulatory T cells. *Science Translational Medicine* **7**, 315ra189–315ra189 (2015).
30. Burn, P. Type 1 diabetes. *Nat Rev Drug Discov* **9**, 187–188 (2010).
31. Pittenger, G. L., Taylor-Fishwick, D. & Vinik, A. I. A role for islet neogenesis in curing diabetes. *Diabetologia* **52**, 735–738 (2009).

32. Robertson, R. P. Islet transplantation for type 1 diabetes, 2015: what have we learned from alloislet and autoislet successes? *Dia Care* **38**, 1030–1035 (2015).
33. Pagliuca, F. W. *et al.* Generation of Functional Human Pancreatic  $\beta$  Cells In Vitro. *Cell* **159**, 428–439 (2014).
34. Sonksen, P. & Sonksen, J. Insulin: understanding its action in health and disease. *Br. J. Anaesth.* **85**, 69–79 (2000).
35. Holst, J. J. The Physiology of Glucagon-like Peptide 1. *Physiol. Rev.* **87**, 1409–1439 (2007).
36. Harper, M. E., Ullrich, A. & Saunders, G. F. Localization of the human insulin gene to the distal end of the short arm of chromosome 11. *PNAS* **78**, 4458–4460 (1981).
37. Chan, S. J., Keim, P. & Steiner, D. F. Cell-free synthesis of rat preproinsulins: characterization and partial amino acid sequence determination. *PNAS* **73**, 1964–1968 (1976).
38. Thorens, B., Sarkar, H. K., Kaback, H. R. & Lodish, H. F. Cloning and functional expression in bacteria of a novel glucose transporter present in liver, intestine, kidney, and beta-pancreatic islet cells. *Cell* **55**, 281–290 (1988).
39. Matschinsky, F. M. Glucokinase as Glucose Sensor and Metabolic Signal Generator in Pancreatic  $\beta$ -Cells and Hepatocytes. *Diabetes* **39**, 647–652 (1990).
40. Magnuson, M. A. & Matschinsky, F. M. *Glucokinase as a Glucose Sensor: Past, Present and Future. Glucokinase and Glycemic Disease: From Basics to Novel Therapeutics* **16**, 1–17 (Karger Publishers, 2004).
41. Ligon, B., Boyd, A. E. & Dunlap, K. Class A calcium channel variants in pancreatic islets and their role in insulin secretion. *Journal of Biological Chemistry* **273**, 13905–13911 (1998).
42. Giugliano, D. *et al.* Impairment of insulin secretion in man by nifedipine. *Eur J Clin Pharmacol* **18**, 395–398 (1980).
43. Goodison, S., Kenna, S. & Ashcroft, S. J. H. Control of insulin gene expression by glucose. *Biochemical Journal* **285**, 563–568 (1992).
44. Melloul, D., Marshak, S. & Cerasi, E. Regulation of insulin gene transcription. **45**, 309–326 (2002).
45. German, M. S. & Wang, J. The insulin gene contains multiple transcriptional elements that respond to glucose. *Molecular and Cellular Biology* **14**, 4067–4075 (1994).
46. Naya, F. J., Stellrecht, C. M. & Tsai, M. J. Tissue-specific regulation of the insulin gene by a novel basic helix-loop-helix transcription factor. *Genes Dev.* **9**, 1009–1019 (1995).
47. German, M. *et al.* The insulin gene promoter. A simplified nomenclature. *Diabetes* **44**, 1002–1004 (1995).
48. Petersen, H. V., Serup, P., Leonard, J., Michelsen, B. K. & Madsen, O. D. Transcriptional regulation of the human insulin gene is dependent on the

- homeodomain protein STF1/IPF1 acting through the CT boxes. *PNAS* **91**, 10465–10469 (1994).
49. Rafiq, I., da Silva Xavier, G., Hooper, S. & Rutter, G. A. Glucose-stimulated preproinsulin gene expression and nuclear trans-location of pancreatic duodenum homeobox-1 require activation of phosphatidylinositol 3-kinase but not p38 MAPK/SAPK2. *Journal of Biological Chemistry* **275**, 15977–15984 (2000).
  50. Kennedy, G. C. & Rutter, W. J. Pur-1, a zinc-finger protein that binds to purine-rich sequences, transactivates an insulin promoter in heterologous cells. *PNAS* **89**, 11498–11502 (1992).
  51. Bennett, S. T., and & Todd, J. A. HUMAN TYPE 1 DIABETES AND THE INSULIN GENE: Principles of Mapping Polygenes. <http://dx.doi.org/10.1146/annurev.genet.30.1.343> **30**, 343–370 (2003).
  52. Kennedy, G. C., German, M. S. & Rutter, W. J. The minisatellite in the diabetes susceptibility locus IDDM2 regulates insulin transcription. *Nature Genetics* **9**, 293–298 (1995).
  53. Peyton, M. *et al.* BETA3, a novel helix-loop-helix protein, can act as a negative regulator of BETA2 and MyoD-responsive genes. *Molecular and Cellular Biology* **16**, 626–633 (1996).
  54. Robinson, G. L., Henderson, E., Massari, M. E., Murre, C. & Stein, R. c-jun inhibits insulin control element-mediated transcription by affecting the transactivation potential of the E2A gene products. *Molecular and Cellular Biology* **15**, 1398–1404 (1995).
  55. Lu, M., Seufert, J. & Habener, J. F. Pancreatic beta-cell-specific repression of insulin gene transcription by CCAAT/enhancer-binding protein beta. Inhibitory interactions with basic helix-loop-helix transcription factor E47. *Journal of Biological Chemistry* **272**, 28349–28359 (1997).
  56. Dodson, G. & Steiner, D. The role of assembly in insulin's biosynthesis. *Current Opinion in Structural Biology* **8**, 189–194 (1998).
  57. Rhodes, C. J. & Halban, P. A. Newly synthesized proinsulin/insulin and stored insulin are released from pancreatic B cells predominantly via a regulated, rather than a constitutive, pathway. *The Journal of Cell Biology* **105**, 145–153 (1987).
  58. Orci, L. *et al.* Conversion of proinsulin to insulin occurs coordinately with acidification of maturing secretory vesicles. *The Journal of Cell Biology* **103**, 2273–2281 (1986).
  59. Orci, L. *et al.* Proteolytic maturation of insulin is a post-Golgi event which occurs in acidifying clathrin-coated secretory vesicles. *Cell* **49**, 865–868 (1987).
  60. Daniel, S., Noda, M., Straub, S. G. & Sharp, G. W. Identification of the docked granule pool responsible for the first phase of glucose-stimulated insulin secretion. *Diabetes* **48**, 1686–1690 (1999).
  61. Straub, S. G. & Sharp, G. W. G. Glucose-stimulated signaling pathways in biphasic insulin secretion. *Diabetes/Metabolism Research and Reviews*

- 18**, 451–463 (2002).
62. Barnett, A. H., Eff, C., Leslie, R. D. & Pyke, D. A. Diabetes in identical twins. A study of 200 pairs. *Diabetologia* **20**, 87–93 (1981).
  63. Aly, T. A. *et al.* Genetic prediction of autoimmunity: Initial oligogenic prediction of anti-islet autoimmunity amongst DR3/DR4–DQ8 relatives of patients with type 1A diabetes. *Journal of Autoimmunity* **25**, 40–45 (2005).
  64. Davies, J. L. *et al.* A genome-wide search for human type 1 diabetes susceptibility genes. *Nature* **371**, 130–136 (1994).
  65. Jones, E. Y., Fugger, L., Strominger, J. L. & Siebold, C. MHC class II proteins and disease: a structural perspective. *Nature Reviews Immunology* **6**, 271–282 (2006).
  66. Pociot, F. & McDermott, M. F. Genetics of type 1 diabetes mellitus. *Genes and Immunity* **3**, 235–249 (2002).
  67. Kantarova, D. & Buc, M. Genetic susceptibility to type 1 diabetes mellitus in humans. *Physiological research* (2007).
  68. de beeck, A. O. & Eizirik, D. L. Viral infections in type 1 diabetes mellitus - why the  $\beta$  cells? *Nat Rev Endocrinol* (2016). doi:10.1038/nrendo.2016.30
  69. Bell, G. I., Horita, S. & Karam, J. H. A Polymorphic Locus Near the Human Insulin Gene Is Associated with Insulin-dependent Diabetes Mellitus. *Diabetes* **33**, 176–183 (1984).
  70. Barrett, J. C. *et al.* Genome-wide association study and meta-analysis find that over 40 loci affect risk of type 1 diabetes. *Nature Genetics* **41**, 703–707 (2009).
  71. Barratt, B. J. *et al.* Remapping the insulin gene/IDDM2 locus in type 1 diabetes. *Diabetes* **53**, 1884–1889 (2004).
  72. Smyth, D. J. *et al.* A genome-wide association study of nonsynonymous SNPs identifies a type 1 diabetes locus in the interferon-induced helicase (IFIH1) region. *Nature Genetics* **38**, 617–619 (2006).
  73. Richter, M. F., Duménil, G., Uzé, G., Fellous, M. & Pellegrini, S. Specific Contribution of Tyk2 JH Regions to the Binding and the Expression of the Interferon  $\alpha/\beta$  Receptor Component IFNAR1. *Journal of Biological Chemistry* **273**, 24723–24729 (1998).
  74. Marroqui, L. *et al.* TYK2, a Candidate Gene for Type 1 Diabetes, Modulates Apoptosis and the Innate Immune Response in Human Pancreatic  $\beta$ -Cells. *Diabetes* **64**, 3808–3817 (2015).
  75. Lempainen, J. *et al.* Non-HLA gene effects on the disease process of type 1 diabetes: From HLA susceptibility to overt disease. *Journal of Autoimmunity* **61**, 45–53 (2015).
  76. Santin, I. *et al.* USP18 is a key regulator of the interferon-driven gene network modulating pancreatic beta cell inflammation and apoptosis. *Cell Death & Disease* **3**, e419 (2012).
  77. ADAMS, S. F. THE SEASONAL VARIATION IN THE ONSET OF ACUTE DIABETES: THE AGE AND SEX FACTORS IN 1,000 DIABETIC



- PATIENTS. *Arch Intern Med (Chic)* **37**, 861–864 (1926).
78. Moltchanova, E. V., Schreier, N., Lammi, N. & Karvonen, M. Seasonal variation of diagnosis of Type 1 diabetes mellitus in children worldwide. *Diabet. Med.* **26**, 673–678 (2009).
  79. Carla Sanchez Bergamin, S. A. D. Enterovirus and type 1 diabetes: What is the matter? *World Journal of Diabetes* **6**, 828–839 (2015).
  80. Bodington, M. J., Muzulu, S. I. & Burden, A. C. Spatial Clustering in Childhood Diabetes: Evidence of an Environmental Cause. *Diabet. Med.* **12**, 865–867 (1995).
  81. Taylor, K. W. in *Diabetes and viruses* 101–107 (Springer New York, 2012). doi:10.1007/978-1-4614-4051-2\_11
  82. Smith, C. P. *et al.* Simultaneous onset of Type 1 diabetes mellitus in identical infant twins with enterovirus infection. *Diabet. Med.* **15**, 515–517 (1998).
  83. Karvonen, M. *et al.* Incidence of childhood type 1 diabetes worldwide. Diabetes Mondiale (DiaMond) Project Group. *Dia Care* **23**, 1516–1526 (2000).
  84. Verge, C. F. *et al.* Environmental factors in childhood IDDM. A population-based, case-control study. *Dia Care* **17**, 1381–1389 (1994).
  85. Lönnrot, M. *et al.* Enterovirus infection as a risk factor for beta-cell autoimmunity in a prospectively observed birth cohort: the Finnish Diabetes Prediction and Prevention Study. *Diabetes* **49**, 1314–1318 (2000).
  86. Salminen, K. *et al.* Enterovirus infections are associated with the induction of  $\beta$ -cell autoimmunity in a prospective birth cohort study. *J. Med. Virol.* **69**, 91–98 (2003).
  87. Graves, P. M. *et al.* Prospective study of enteroviral infections and development of beta-cell autoimmunity. *Diabetes Research and Clinical Practice* **59**, 51–61 (2003).
  88. Simonen-Tikka, M. L. *et al.* Human enterovirus infections in children at increased risk for type 1 diabetes: the Babydiet study. *Diabetologia* **54**, 2995–3002 (2011).
  89. Pak, C., McArthur, R., Eun, H.-M. & Yoon, J.-W. ASSOCIATION OF CYTOMEGALOVIRUS INFECTION WITH AUTOIMMUNE TYPE 1 DIABETES. *Lancet* **332**, 1–4 (1988).
  90. Chikazawa, K. *et al.* [Acute onset of insulin-dependent diabetes mellitus caused by Epstein-Barr virus infection]. *Nihon Sanka Fujinka Gakkai Zasshi* **37**, 453–456 (1985).
  91. Khakpour, M. & Nik-Akhtar, B. Diabetes mellitus following a mumps epidemic. *Journal of Tropical Medicine and Hygiene* **78**, 262–263 (1975).
  92. Helmke, K., Otten, A. & Willems, W. *Islet cell antibodies in children with mumps infection.* (The Lancet, 1980).
  93. Honeyman, M. C. *et al.* Association between rotavirus infection and pancreatic islet autoimmunity in children at risk of developing type 1

- diabetes. *Diabetes* **49**, 1319–1324 (2000).
94. Forrest, J., Menser, M. & Burgess, J. A. HIGH FREQUENCY OF DIABETES MELLITUS IN YOUNG ADULTS WITH CONGENITAL RUBELLA. *Lancet* **298**, 332–334 (1971).
  95. Craig, M. E., Nair, S., Stein, H. & Rawlinson, W. D. Viruses and type 1 diabetes: a new look at an old story. *Pediatr Diabetes* n/a–n/a (2013). doi:10.1111/pedi.12033
  96. Gamble, D. R. & Taylor, K. W. Seasonal Incidence of Diabetes Mellitus. *BMJ* **3**, 631–633 (1969).
  97. Gamble, D. R., Taylor, K. W. & Cumming, H. Coxsackie Viruses and Diabetes Mellitus. *Br Med J* **4**, 260–262 (1973).
  98. Sarmiento, L., Cubas-Dueñas, I. & Cabrera-Rode, E. Evidence of association between type 1 diabetes and exposure to enterovirus in Cuban children and adolescents. *MEDICC Review* **15**, 29–32 (2013).
  99. Oikarinen, S. *et al.* Virus antibody survey in different European populations indicates risk association between coxsackievirus B1 and type 1 diabetes. *Diabetes* **63**, 655–662 (2014).
  100. Laitinen, O. H. *et al.* Coxsackievirus B1 is associated with induction of  $\beta$ -cell autoimmunity that portends type 1 diabetes. *Diabetes* **63**, 446–455 (2014).
  101. Frisk, G. & Tuvemo, T. Enterovirus infections with  $\beta$ -cell tropic strains are frequent in siblings of children diagnosed with type 1 diabetes children and in association with elevated levels of GAD65 antibodies. *J. Med. Virol.* **73**, 450–459 (2004).
  102. Green, J., Casabonne, D. & Newton, R. Coxsackie B virus serology and Type 1 diabetes mellitus: a systematic review of published case-control studies. *Diabet. Med.* **21**, 507–514 (2004).
  103. Dotta, F. *et al.* Coxsackie B4 virus infection of beta cells and natural killer cell insulinitis in recent-onset type 1 diabetic patients. *PNAS* **104**, 5115–5120 (2007).
  104. Richardson, S. J., Leete, P., Bone, A. J., Foulis, A. K. & Morgan, N. G. Expression of the enteroviral capsid protein VP1 in the islet cells of patients with type 1 diabetes is associated with induction of protein kinase R and downregulation of Mcl-1. **56**, 185–193 (2013).
  105. Moya-Suri, V. *et al.* Enterovirus RNA sequences in sera of schoolchildren in the general population and their association with type 1-diabetes-associated autoantibodies. *J. Med. Microbiol.* **54**, 879–883 (2005).
  106. Lönnrot, M. *et al.* Enterovirus RNA in serum is a risk factor for beta-cell autoimmunity and clinical type 1 diabetes: A prospective study. *J. Med. Virol.* **61**, 214–220 (2000).
  107. Oikarinen, S. *et al.* Enterovirus RNA in blood is linked to the development of type 1 diabetes. *Diabetes* **60**, 276–279 (2011).
  108. Schulte, B. M. *et al.* Detection of enterovirus RNA in peripheral blood mononuclear cells of type 1 diabetic patients beyond the stage of acute

- infection. *Viral Immunol.* **23**, 99–104 (2010).
109. Yeung, W. C. G., Rawlinson, W. D. & Craig, M. E. Enterovirus infection and type 1 diabetes mellitus: systematic review and meta-analysis of observational molecular studies. *BMJ* **342**, d35–d35 (2011).
  110. Yoon, J. W., Austin, M. & Onodera, T. Virus-induced diabetes mellitus: isolation of a virus from the pancreas of a child with diabetic ketoacidosis. *New England Journal of ...* (1979).
  111. Krogvold, L. *et al.* Detection of a low-grade enteroviral infection in the islets of Langerhans of living patients newly diagnosed with type 1 diabetes. *Diabetes* **64**, DB\_141370–1687 (2014).
  112. Santti, J., Vainionpää, R. & Hyypiä, T. Molecular detection and typing of human picornaviruses. *Virus Research* (1999).
  113. Tapparel, C., Siegrist, F., Petty, T. J. & Kaiser, L. Picornavirus and enterovirus diversity with associated human diseases. *Infection, Genetics and Evolution* **14**, 282–293 (2013).
  114. Knipe, D. M. *Fields Virology*. (LWW, 2013).
  115. Strikas, R. A., Anderson, L. J. & Parker, R. A. Temporal and Geographic Patterns of Isolates of Nonpolio Enterovirus in the United States, 1970–1983. *J. Infect. Dis.* **153**, 346–351 (1986).
  116. Khetsuriani, N., LaMonte-Fowlkes, A. & Oberst, S. Enterovirus surveillance—United States, 1970–2005. *MMWR Surveill ...* (2006).
  117. Petzold, A., Solimena, M. & Knoch, K.-P. Mechanisms of Beta Cell Dysfunction Associated With Viral Infection. *Curr. Diab. Rep.* **15**, 654–10 (2015).
  118. Norris, C. M., Danis, P. G. & Gardner, T. D. Aseptic meningitis in the newborn and young infant. *Am Fam Physician* **59**, 2761–2770 (1999).
  119. Mena, I. *et al.* Coxsackievirus Infection of the Pancreas: Evaluation of Receptor Expression, Pathogenesis, and Immunopathology. *Virology* **271**, 276–288 (2000).
  120. Tam, P. E., Schmidt, A. M., Ytterberg, S. R. & Messner, R. P. Viral persistence during the developmental phase of Coxsackievirus B1-induced murine polymyositis. *Journal of Virology* **65**, 6654–6660 (1991).
  121. Kim, K.-S. *et al.* 5'-Terminal deletions occur in coxsackievirus B3 during replication in murine hearts and cardiac myocyte cultures and correlate with encapsidation of negative-strand viral RNA. *Journal of Virology* **79**, 7024–7041 (2005).
  122. Kitamura, N. *et al.* Primary structure, gene organization and polypeptide expression of poliovirus RNA. *Nature* **291**, 547–553 (1981).
  123. Whitton, J. L., Cornell, C. T. & Feuer, R. Host and virus determinants of picornavirus pathogenesis and tropism. *Nature Reviews Microbiology* **3**, 765–776 (2005).
  124. Hellen, C. U. *et al.* A cytoplasmic 57-kDa protein that is required for translation of picornavirus RNA by internal ribosomal entry is identical to the nuclear pyrimidine tract-binding protein. *PNAS* **90**, 7642–7646 (1993).

125. Flanegan, J. B., Petterson, R. F., Ambros, V., Hewlett, N. J. & Baltimore, D. Covalent linkage of a protein to a defined nucleotide sequence at the 5'-terminus of virion and replicative intermediate RNAs of poliovirus. *PNAS* **74**, 961–965 (1977).
126. Flanegan, J. B. & Van Dyke, T. A. Isolation of a soluble and template-dependent poliovirus RNA polymerase that copies virion RNA in vitro. *Journal of Virology* **32**, 155–161 (1979).
127. Jacobson, S. J., Konings, D. A. & Sarnow, P. Biochemical and genetic evidence for a pseudoknot structure at the 3' terminus of the poliovirus RNA genome and its role in viral RNA amplification. *Journal of Virology* **67**, 2961–2971 (1993).
128. Yogo, Y. & Wimmer, E. Polyadenylic acid at the 3'-terminus of poliovirus RNA. *PNAS* **69**, 1877–1882 (1972).
129. Bergelson, J. M. *et al.* Isolation of a common receptor for Coxsackie B viruses and adenoviruses 2 and 5. *Science* **275**, 1320–1323 (1997).
130. Cohen, C. J. *et al.* The coxsackievirus and adenovirus receptor is a transmembrane component of the tight junction. *PNAS* **98**, 15191–15196 (2001).
131. Shafren, D. R. *et al.* Coxsackieviruses B1, B3, and B5 use decay accelerating factor as a receptor for cell attachment. *Journal of Virology* **69**, 3873–3877 (1995).
132. Marjomäki, V., Turkki, P. & Huttunen, M. Infectious Entry Pathway of Enterovirus B Species. *Viruses* **7**, 6387–6399 (2015).
133. Karjalainen, M. *et al.* A Raft-derived, Pak1-regulated entry participates in alpha2beta1 integrin-dependent sorting to caveosomes. *Mol. Biol. Cell* **19**, 2857–2869 (2008).
134. Coyne, C. B. & Bergelson, J. M. Virus-Induced Abl and Fyn Kinase Signals Permit Coxsackievirus Entry through Epithelial Tight Junctions. *Cell* **124**, 119–131 (2006).
135. Danthi, P., Tosteson, M., Li, Q.-H. & Chow, M. Genome delivery and ion channel properties are altered in VP4 mutants of poliovirus. *Journal of Virology* **77**, 5266–5274 (2003).
136. Bergelson, J. M. *et al.* Coxsackievirus B3 adapted to growth in RD cells binds to decay-accelerating factor (CD55). *Journal of Virology* **69**, 1903–1906 (1995).
137. Lamphear, B. J. *et al.* Mapping the cleavage site in protein synthesis initiation factor eIF-4 gamma of the 2A proteases from human Coxsackievirus and rhinovirus. *Journal of Biological Chemistry* **268**, 19200–19203 (1993).
138. de Breyne, S., Bonderoff, J. M., Chumakov, K. M., Lloyd, R. E. & Hellen, C. U. T. Cleavage of eukaryotic initiation factor eIF5B by enterovirus 3C proteases. *Virology* **378**, 118–122 (2008).
139. Joachims, M., Van Breugel, P. C. & Lloyd, R. E. Cleavage of poly(A)-binding protein by enterovirus proteases concurrent with inhibition of

- translation in vitro. *Journal of Virology* **73**, 718–727 (1999).
140. Sharma, R., Raychaudhuri, S. & Dasgupta, A. Nuclear entry of poliovirus protease-polymerase precursor 3CD: implications for host cell transcription shut-off. *Virology* **320**, 195–205 (2004).
  141. Clark, M. E., Lieberman, P. M., Berk, A. J. & Dasgupta, A. Direct cleavage of human TATA-binding protein by poliovirus protease 3C in vivo and in vitro. *Molecular and Cellular Biology* **13**, 1232–1237 (1993).
  142. Gustin, K. E. & Sarnow, P. Effects of poliovirus infection on nucleocytoplasmic trafficking and nuclear pore complex composition. *The EMBO Journal* **20**, 240–249 (2001).
  143. Mukherjee, A. *et al.* The Coxsackievirus B 3C pro Protease Cleaves MAVS and TRIF to Attenuate Host Type I Interferon and Apoptotic Signaling. *PLoS Pathog* **7**, e1001311 (2011).
  144. Ward, C. D., Stokes, M. A. & Flanagan, J. B. Direct measurement of the poliovirus RNA polymerase error frequency in vitro. *Journal of Virology* **62**, 558–562 (1988).
  145. van Kuppeveld, F. J. M. *et al.* Coxsackievirus protein 2B modifies endoplasmic reticulum membrane and plasma membrane permeability and facilitates virus release. *The EMBO Journal* **16**, 3519–3532 (1997).
  146. Xin, L. *et al.* Coxsackievirus B3 induces crosstalk between autophagy and apoptosis to benefit its release after replicating in autophagosomes through a mechanism involving caspase cleavage of autophagy-related proteins. *Infection, Genetics and Evolution* **26**, 95–102 (2014).
  147. Altan-Bonnet, N. & Chen, Y.-H. Intercellular Transmission of Viral Populations with Vesicles. *Journal of Virology* **89**, 12242–12244 (2015).
  148. Beutler, B. Microbe sensing, positive feedback loops, and the pathogenesis of inflammatory diseases. *Immunological Reviews* **227**, 248–263 (2009).
  149. Kumar, H., Kawai, T. & Akira, S. Pathogen Recognition by the Innate Immune System. *International Reviews of Immunology* **30**, 16–34 (2011).
  150. Kato, H. *et al.* Differential roles of MDA5 and RIG-I helicases in the recognition of RNA viruses. *Nature* **441**, 101–105 (2006).
  151. Hornung, V. *et al.* 5'-Triphosphate RNA Is the Ligand for RIG-I. *Science* **314**, 994–997 (2006).
  152. Pichlmair, A. *et al.* RIG-I-Mediated Antiviral Responses to Single-Stranded RNA Bearing 5'-Phosphates. *Science* **314**, 997–1001 (2006).
  153. Kato, H. *et al.* Length-dependent recognition of double-stranded ribonucleic acids by retinoic acid-inducible gene-I and melanoma differentiation-associated gene 5. *J. Exp. Med.* **205**, 1601–1610 (2008).
  154. Wu, B. *et al.* Structural Basis for dsRNA Recognition, Filament Formation, and Antiviral Signal Activation by MDA5. *Cell* **152**, 276–289 (2013).
  155. Seth, R. B., Sun, L., Ea, C.-K. & Chen, Z. J. Identification and Characterization of MAVS, a Mitochondrial Antiviral Signaling Protein that Activates NF- $\kappa$ B and IRF3. *Cell* **122**, 669–682 (2005).

156. Platanias, L. C. Mechanisms of type-I- and type-II-interferon-mediated signalling. *Nature Reviews Immunology* **5**, 375–386 (2005).
157. Kottenko, S. V. *et al.* IFN- $\lambda$ s mediate antiviral protection through a distinct class II cytokine receptor complex. *Nature Immunology* **4**, 69–77 (2003).
158. Darnell, J. E., Kerr, I. M. & Stark, G. R. Jak-STAT pathways and transcriptional activation in response to IFNs and other extracellular signaling proteins. *Science* **264**, 1415–1421 (1994).
159. Kurt-Jones, E. A. *et al.* Pattern recognition receptors TLR4 and CD14 mediate response to respiratory syncytial virus. *Nature Immunology* **1**, 398–401 (2000).
160. Triantafyllou, K. & Triantafyllou, M. Coxsackievirus B4-induced cytokine production in pancreatic cells is mediated through toll-like receptor 4. *Journal of Virology* **78**, 11313–11320 (2004).
161. Kemball, C. C., Alirezai, M. & Whitton, J. L. Type B coxsackieviruses and their interactions with the innate and adaptive immune systems. *Future Microbiol* **5**, 1329–1347 (2010).
162. Alexopoulou, L., Holt, A. C., Medzhitov, R. & Flavell, R. A. Recognition of double-stranded RNA and activation of NF- $\kappa$ B by Toll-like receptor 3. *Nature* **413**, 732–738 (2001).
163. Negishi, H. *et al.* A critical link between Toll-like receptor 3 and type II interferon signaling pathways in antiviral innate immunity. *Proc. Natl. Acad. Sci. U.S.A.* **105**, 20446–20451 (2008).
164. Heil, F. *et al.* Species-Specific Recognition of Single-Stranded RNA via Toll-like Receptor 7 and 8. *Science* **303**, 1526–1529 (2004).
165. Triantafyllou, K. *et al.* Human cardiac inflammatory responses triggered by Coxsackie B viruses are mainly Toll-like receptor (TLR) 8-dependent. *Cellular Microbiology* **7**, 1117–1126 (2005).
166. Wang, J. P., Asher, D. R., Chan, M., Kurt-Jones, E. A. & Finberg, R. W. Cutting Edge: Antibody-mediated TLR7-dependent recognition of viral RNA. *J Immunol* **178**, 3363–3367 (2007).
167. Wong, J. *et al.* Autophagosome supports coxsackievirus B3 replication in host cells. *Journal of Virology* **82**, 9143–9153 (2008).
168. Wang, J. P. *et al.* MDA5 and MAVS mediate type I interferon responses to coxsackie B virus. *Journal of Virology* **84**, 254–260 (2010).
169. Uno, S. *et al.* Macrophages and dendritic cells infiltrating islets with or without beta cells produce tumour necrosis factor- $\alpha$  in patients with recent-onset type 1 diabetes. *Diabetologia* **50**, 596–601 (2007).
170. Shigemoto, T. *et al.* Identification of loss of function mutations in human genes encoding RIG-I and MDA5: implications for resistance to type I diabetes. *Journal of Biological Chemistry* **284**, 13348–13354 (2009).
171. Liu, S. *et al.* IFIH1 polymorphisms are significantly associated with type 1 diabetes and IFIH1 gene expression in peripheral blood mononuclear cells. *Hum. Mol. Genet.* **18**, 358–365 (2009).

172. Nejentsev, S., Walker, N., Riches, D., Egholm, M. & Todd, J. A. Rare Variants of IFIH1, a Gene Implicated in Antiviral Responses, Protect Against Type 1 Diabetes. *Science* **324**, 387–389 (2009).
173. Downes, K. *et al.* Reduced expression of IFIH1 is protective for type 1 diabetes. *PLoS ONE* **5**, (2010).
174. Lincez, P. J., Shanina, I. & Horwitz, M. S. Reduced expression of the MDA5 gene IFIH1 prevents autoimmune diabetes. *Diabetes* db141223 (2015). doi:10.2337/db14-1223
175. Winkler, C. *et al.* An interferon-induced helicase (IFIH1) gene polymorphism associates with different rates of progression from autoimmunity to type 1 diabetes. *Diabetes* **60**, 685–690 (2011).
176. Longhi, M. P. *et al.* Dendritic cells require a systemic type I interferon response to mature and induce CD4+ Th1 immunity with poly IC as adjuvant. *J. Exp. Med.* **206**, 1589–1602 (2009).
177. Foulis, A., Farquharson, M. & Meager, A. IMMUNOREACTIVE  $\alpha$ -INTERFERON IN INSULIN-SECRETING  $\beta$  CELLS IN TYPE 1 DIABETES MELLITUS. *The Lancet* **330**, 1423–1427 (1987).
178. Huang, X. *et al.* Interferon Expression in the Pancreases of Patients With Type I Diabetes. *Diabetes* **44**, 658–664 (1995).
179. Chehadeh, W. *et al.* Increased level of interferon-alpha in blood of patients with insulin-dependent diabetes mellitus: relationship with coxsackievirus B infection. *J. Infect. Dis.* **181**, 1929–1939 (2000).
180. Reynier, F. *et al.* Specific gene expression signature associated with development of autoimmune type-I diabetes using whole-blood microarray analysis. *Genes and Immunity* **11**, 269–278 (2010).
181. Ferreira, R. C. *et al.* A type I interferon transcriptional signature precedes autoimmunity in children genetically at-risk of type 1 diabetes. *Diabetes* **63**, DB\_131777–2550 (2014).
182. Conlon, K. C., Urba, W. J., Smith, J. W., Steis, R. G. & Longo, D. L. Exacerbation of Symptoms of Autoimmune Disease in Patients Receiving Alpha-Interferon Therapy. *Cancer* (1990).
183. Nakamura, K. *et al.* Type 1 diabetes and interferon therapy: a nationwide survey in Japan. *Dia Care* **34**, 2084–2089 (2011).
184. Zornitzki, T. Interferon therapy in hepatitis C leading to chronic type 1 diabetes. *WJG* **21**, 233 (2015).
185. Sallusto, F., Lenig, D., Mackay, C. R. & Lanzavecchia, A. Flexible programs of chemokine receptor expression on human polarized T helper 1 and 2 lymphocytes. *J. Exp. Med.* **187**, 875–883 (1998).
186. Nicoletti, F. *et al.* Serum concentrations of the interferon- $\gamma$ -inducible chemokine IP-10/CXCL10 are augmented in both newly diagnosed Type I diabetes mellitus patients and subjects at risk of developing the disease. *Diabetologia* **45**, 1107–1110 (2002).
187. Uno, S. *et al.* Expression of chemokines, CXC chemokine ligand 10 (CXCL10) and CXCR3 in the inflamed islets of patients with recent-onset

- autoimmune type 1 diabetes. *Endocr. J.* **57**, 991–996 (2010).
188. Christen, U., McGavern, D. B., Luster, A. D., Herrath, von, M. G. & Oldstone, M. B. A. Among CXCR3 Chemokines, IFN- $\gamma$ -Inducible Protein of 10 kDa (CXC Chemokine Ligand (CXCL) 10) but Not Monokine Induced by IFN- $\gamma$  (CXCL9) Imprints a Pattern for the Subsequent Development of Autoimmune Disease. *J Immunol* **171**, 6838–6845 (2003).
  189. Paroni, F., Domsgen, E. & Maedler, K. CXCL10- a path to  $\beta$ -cell death. *Islets* **1**, 256–259 (2009).
  190. Schulthess, F. T. *et al.* CXCL10 Impairs  $\beta$  Cell Function and Viability in Diabetes through TLR4 Signaling. *Cell Metab.* **9**, 125–139 (2009).
  191. Atkinson, M. A. *et al.* Cellular immunity to a determinant common to glutamate decarboxylase and coxsackie virus in insulin-dependent diabetes. *J. Clin. Invest.* **94**, 2125–2129 (1994).
  192. Tian, J., Lehmann, P. V. & Kaufman, D. L. T cell cross-reactivity between coxsackievirus and glutamate decarboxylase is associated with a murine diabetes susceptibility allele. *J. Exp. Med.* **180**, 1979–1984 (1994).
  193. Horwitz, M. S. *et al.* Diabetes induced by Coxsackie virus: Initiation by bystander damage and not molecular mimicry. *Nature Medicine* **4**, 781–785 (1998).
  194. Schloot, N. C. *et al.* Molecular mimicry in type 1 diabetes mellitus revisited: T-cell clones to GAD65 peptides with sequence homology to Coxsackie or proinsulin peptides do not crossreact with homologous counterpart. *Human Immunology* **62**, 299–309 (2001).
  195. Drescher, K. M., Kono, K., Bopegamage, S., Carson, S. D. & Tracy, S. Coxsackievirus B3 infection and type 1 diabetes development in NOD mice: insulinitis determines susceptibility of pancreatic islets to virus infection. *Virology* **329**, 381–394 (2004).
  196. Slifka, M. K., Rodriguez, F. & Whitton, J. L. Rapid on/off cycling of cytokine production by virus-specific CD8<sup>+</sup> T cells. *Nature* **401**, 76–79 (1999).
  197. Yeung, W.-C. G. *et al.* Children with islet autoimmunity and enterovirus infection demonstrate a distinct cytokine profile. *Diabetes* **61**, 1500–1508 (2012).
  198. Holz, A., Brett, K. & Oldstone, M. B. A. Constitutive  $\beta$  cell expression of IL-12 does not perturb self-tolerance but intensifies established autoimmune diabetes. *J. Clin. Invest.* **108**, 1749–1758 (2001).
  199. Herrath, von, M. G., Fujinami, R. S. & Whitton, J. L. Microorganisms and autoimmunity: making the barren field fertile? *Nature Reviews Microbiology* **1**, 151–157 (2003).
  200. Chehadeh, W. *et al.* Persistent infection of human pancreatic islets by coxsackievirus B is associated with alpha interferon synthesis in beta cells. *Journal of Virology* **74**, 10153–10164 (2000).
  201. Tracy, S. *et al.* Toward testing the hypothesis that group B



- coxsackieviruses (CVB) trigger insulin-dependent diabetes: inoculating nonobese diabetic mice with CVB markedly lowers diabetes incidence. *Journal of Virology* **76**, 12097–12111 (2002).
202. Pearson, T. *et al.* NOD congenic mice genetically protected from autoimmune diabetes remain resistant to transplantation tolerance induction. *Diabetes* **52**, 321–326 (2003).
203. Jurczyk, A., Diiorio, P., Brostowin, D., Leehy, L. & Yang, C. Improved function and proliferation of adult human beta cells engrafted in diabetic immunodeficient NOD-scid IL2 $\gamma$  (null) mice treated with alogliptin. (2013).
204. Shultz, L. D. *et al.* Multiple defects in innate and adaptive immunologic function in NOD/LtSz-scid mice. *J Immunol* **154**, 180–191 (1995).
205. D'Alise, A. M. *et al.* The defect in T-cell regulation in NOD mice is an effect on the T-cell effectors. *Proc. Natl. Acad. Sci. U.S.A.* **105**, 19857–19862 (2008).
206. Shultz, L. D., Ishikawa, F. & Greiner, D. L. Humanized mice in translational biomedical research. *Nature Reviews Immunology* **7**, 118–130 (2007).
207. Brehm, M. A. *et al.* Human immune system development and rejection of human islet allografts in spontaneously diabetic NOD-Rag1null IL2rgammanull Ins2Akita mice. *Diabetes* **59**, 2265–2270 (2010).
208. Guz, Y., Nasir, I. & Teitelman, G. Regeneration of Pancreatic  $\beta$  Cells from Intra-Islet Precursor Cells in an Experimental Model of Diabetes. <http://dx.doi.org/10.1210/endo.142.11.8501> **142**, 4956–4968 (2013).
209. Serreze, D. V., Ottendorfer, E. W., Ellis, T. M., Gauntt, C. J. & Atkinson, M. A. Acceleration of type 1 diabetes by a coxsackievirus infection requires a preexisting critical mass of autoreactive T-cells in pancreatic islets. *Diabetes* **49**, 708–711 (2000).
210. Guberski, D. L. *et al.* Induction of type I diabetes by Kilham's rat virus in diabetes-resistant BB/Wor rats. *Science* **254**, 1010–1013 (1991).
211. Fujimoto, K. *et al.* Autophagy Regulates Pancreatic Beta Cell Death in Response to Pdx1 Deficiency and Nutrient Deprivation. *Journal of Biological Chemistry* **284**, 27664–27673 (2009).
212. Sachdeva, M. M. *et al.* Pdx1 (MODY4) regulates pancreatic beta cell susceptibility to ER stress. *Proc. Natl. Acad. Sci. U.S.A.* **106**, 19090–19095 (2009).
213. Johnson, J. D. *et al.* Increased islet apoptosis in Pdx1 $\pm$  mice. *J. Clin. Invest.* **111**, 1147–1160 (2003).
214. Hayes, H. L. *et al.* Pdx-1 Activates Islet  $\alpha$ - and  $\beta$ -Cell Proliferation via a Mechanism Regulated by Transient Receptor Potential Cation Channels 3 and 6 and Extracellular Signal-Regulated Kinases 1 and 2. *Molecular and Cellular Biology* **33**, 4017–4029 (2013).
215. Sane, F. *et al.* Coxsackievirus B4 can infect human pancreas ductal cells and persist in ductal-like cell cultures which results in inhibition of Pdx1

- expression and disturbed formation of islet-like cell aggregates. *Cell. Mol. Life Sci.* (2013). doi:10.1007/s00018-013-1383-4
216. Antonelli, A., Ferrari, S. M., Corrado, A., Ferrannini, E. & Fallahi, P. CXCR3, CXCL10 and type 1 diabetes. *Cytokine Growth Factor Rev.* **25**, 57–65 (2014).
  217. Lacotte, S., Brun, S., Muller, S. & Dumortier, H. CXCR3, Inflammation, and Autoimmune Diseases. *Ann. N. Y. Acad. Sci.* **1173**, 310–317 (2009).
  218. Coppieters, K. T. *et al.* Demonstration of islet-autoreactive CD8 T cells in insulinitic lesions from recent onset and long-term type 1 diabetes patients. *J. Exp. Med.* **209**, 51–60 (2012).
  219. Vella, C., Brown, C. L. & McCarthy, D. A. Coxsackievirus B4 infection of the mouse pancreas: acute and persistent infection. *J. Gen. Virol.* **73 ( Pt 6)**, 1387–1394 (1992).
  220. Galama, J. M. D. Enteroviral infections in the immunocompromised host. *Reviews in Medical Microbiology* **8**, 33 (1997).
  221. Johnson, J. P., Yolken, R. H., Goodman, D., Winkelstein, J. A. & Nagel, J. E. Prolonged Excretion of Group A Coxsackievirus in an Infant with Agammaglobulinemia. *J. Infect. Dis.* **146**, 712–712 (1982).
  222. Mena, I. *et al.* The Role of B Lymphocytes in Coxsackievirus B3 Infection. *The American Journal of Pathology* **155**, 1205–1215 (1999).
  223. Chow, L. H., Beisel, K. W. & McManus, B. M. Enteroviral infection of mice with severe combined immunodeficiency. Evidence for direct viral pathogenesis of myocardial injury. *Lab. Invest.* **66**, 24–31 (1992).
  224. Zhang, X. *et al.* Human astrocytic cells support persistent coxsackievirus B3 infection. *Journal of Virology* **87**, 12407–12421 (2013).
  225. Aida, K. *et al.* RIG-I- and MDA5-initiated innate immunity linked with adaptive immunity accelerates beta-cell death in fulminant type 1 diabetes. *Diabetes* **60**, 884–889 (2011).
  226. Tanaka, S. *et al.* Enterovirus Infection, CXC Chemokine Ligand 10 (CXCL10), and CXCR3 Circuit: A Mechanism of Accelerated  $\beta$ -Cell Failure in Fulminant Type 1 Diabetes. *Diabetes* **58**, 2285–2291 (2009).
  227. Dotta, F., Galleri, L., Sebastiani, G. & Vendrame, F. Virus Infections: Lessons from Pancreas Histology. *Curr. Diab. Rep.* **10**, 357–361 (2010).
  228. Greiner, D. L. *et al.* Humanized mice for the study of type 1 and type 2 diabetes. *Ann. N. Y. Acad. Sci.* **1245**, 55–58 (2011).
  229. Brehm, M. A., Powers, A. C., Shultz, L. D. & Greiner, D. L. Advancing animal models of human type 1 diabetes by engraftment of functional human tissues in immunodeficient mice. *Cold Spring Harbor Perspectives in Medicine* **2**, a007757–a007757 (2012).
  230. Sickles, G. M., Feorino, P. & PLAGER, H. Isolation and type determination of Coxsackie virus, group B, in tissue culture. *Proceedings of the Society for Experimental Biology and Medicine* **88**, 22–24 (1955).
  231. Feuer, R., Mena, I., Pagarigan, R., Slifka, M. K. & Whitton, J. L. Cell Cycle Status Affects Coxsackievirus Replication, Persistence, and

- Reactivation In Vitro. *Journal of Virology* **76**, 4430–4440 (2002).
232. Schindelin, J. *et al.* Fiji: an open-source platform for biological-image analysis. *Nature Methods* **9**, 676–682 (2012).
233. Roivainen, M. *et al.* Mechanisms of coxsackievirus-induced damage to human pancreatic beta-cells. *J. Clin. Endocrinol. Metab.* **85**, 432–440 (2000).
234. Roivainen, M. *et al.* Functional impairment and killing of human beta cells by enteroviruses: the capacity is shared by a wide range of serotypes, but the extent is a characteristic of individual virus strains. *Diabetologia* **45**, 693–702 (2002).
235. Frisk, G. & Diderholm, H. Tissue Culture of Isolated Human Pancreatic Islets Infected With Different Strains of Coxsackievirus B4: Assessment of Virus Replication and Effects on Islet Morphology and Insulin Release. *Journal of Diabetes Research* **1**, 165–175 (2000).
236. Schulte, B. M. *et al.* Cytokine and Chemokine Production by Human Pancreatic Islets Upon Enterovirus Infection. *Diabetes* **61**, 2030–2036 (2012).
237. Ravassard, P. *et al.* A genetically engineered human pancreatic  $\beta$  cell line exhibiting glucose-inducible insulin secretion. *J. Clin. Invest.* **121**, 3589–3597 (2011).
238. Palchetti, S. *et al.* Transfected poly(I:C) activates different dsRNA receptors, leading to apoptosis or immunoadjuvant response in androgen-independent prostate cancer cells. *J. Biol. Chem.* **290**, 5470–5483 (2015).
239. Jones, J. W. *et al.* Absent in melanoma 2 is required for innate immune recognition of Francisella tularensis. *Proc. Natl. Acad. Sci. U.S.A.* **107**, 9771–9776 (2010).
240. Tracy, S., Smithee, S. & Alhazmi, A. Coxsackievirus can persist in murine pancreas by deletion of 5' terminal genomic sequences. *Journal of medical ...* (2015). doi:10.1002/jmv.24039
241. Gallagher, G. R. *et al.* Viral infection of engrafted human islets leads to diabetes. *Diabetes* **64**, 1358–1369 (2015).
242. Ylipaasto, P. *et al.* Global profiling of coxsackievirus- and cytokine-induced gene expression in human pancreatic islets. **48**, 1510–1522 (2005).
243. Marhfour, I. *et al.* Expression of endoplasmic reticulum stress markers in the islets of patients with type 1 diabetes. *Diabetologia* **55**, 2417–2420 (2012).
244. Yang, C. *et al.* Pathological endoplasmic reticulum stress mediated by the IRE1 pathway contributes to pre-insulinitic beta cell apoptosis in a virus-induced rat model of type 1 diabetes. **56**, 2638–2646 (2013).
245. Osowski, C. M. *et al.* Thioredoxin-interacting protein mediates ER stress-induced  $\beta$  cell death through initiation of the inflammasome. *Cell Metab.* **16**, 265–273 (2012).

246. Rutter, G. A., Pullen, T. J., Hodson, D. J. & Martinez-Sanchez, A. Pancreatic  $\beta$ -cell identity, glucose sensing and the control of insulin secretion. *Biochem. J.* **466**, 203–218 (2015).
247. Ylipaasto, P. *et al.* Enterovirus-induced gene expression profile is critical for human pancreatic islet destruction. **55**, 3273–3283 (2012).
248. Yeung, T. Y. *et al.* Human mesenchymal stem cells protect human islets from pro-inflammatory cytokines. *PLoS ONE* **7**, e38189 (2012).
249. Lind, K., Hühn, M. H. & Flodström-Tullberg, M. Immunology in the clinic review series; focus on type 1 diabetes and viruses: the innate immune response to enteroviruses and its possible role in regulating type 1 diabetes. *Clin. Exp. Immunol.* **168**, 30–38 (2012).
250. Rasilainen, S. *et al.* Mechanisms of coxsackievirus B5 mediated  $\beta$ -cell death depend on the multiplicity of infection. *J. Med. Virol.* **72**, 586–596 (2004).
251. Arrojo e Drigo, R. *et al.* New insights into the architecture of the islet of Langerhans: a focused cross-species assessment. *Diabetologia* **58**, 2218–2228 (2015).
252. Huber, M. *et al.* Cleavage of RasGAP and phosphorylation of mitogen-activated protein kinase in the course of coxsackievirus B3 replication. *Journal of Virology* **73**, 3587–3594 (1999).
253. DA, S., NT, Z., Stanojevic, V., WL, C. & JF, H. Pancreatic agenesis attributable to a single nucleotide deletion in the human IPF1 gene coding sequence. *Nature Genetics* **15**, 106–110 (1997).
254. Stoffers, D. A., Ferrer, J., Clarke, W. L. & Habener, J. F. Early-onset type-II diabetes mellitus (MODY4) linked to IPF1. *Nature Genetics* **17**, 138–139 (1997).
255. Gragnoli, C. *et al.* IPF-1/MODY4 gene missense mutation in an Italian family with type 2 and gestational diabetes. *Metab. Clin. Exp.* **54**, 983–988 (2005).
256. Stoffers, D. A., Heller, R. S., Miller, C. P. & Habener, J. F. Developmental Expression of the Homeodomain Protein IDX-1 in Mice Transgenic for an IDX-1 Promoter/lacZ Transcriptional Reporter1. *Endocrinology* **140**, 5374–5381 (2013).
257. Ohlsson, H., Karlsson, K. & Edlund, T. IPF1, a homeodomain-containing transactivator of the insulin gene. *The EMBO Journal* **12**, 4251–4259 (1993).
258. Stanojevic, V., Habener, J. F. & Thomas, M. K. Pancreas Duodenum Homeobox-1 Transcriptional Activation Requires Interactions with p300. *Endocrinology* **145**, 2918–2928 (2013).
259. Watada, H. *et al.* The Human Glucokinase Gene  $\beta$ -Cell-Type Promoter: An Essential Role of Insulin Promoter Factor 1/PDX-1 in Its Activation in HIT-T15 Cells. *Diabetes* **45**, 1478–1488 (1996).
260. BRETHERTON-WATT, D., GORE, N. & BOAM, D. S. W. Insulin upstream factor 1 and a novel ubiquitous factor bind to the human islet

- amyloid polypeptide/amylin gene promoter. *Biochemical Journal* **313**, 495–502 (1996).
261. Cerf, M. E. Transcription factors regulating beta-cell function. *Eur. J. Endocrinol.* **155**, 671–679 (2006).
  262. Gao, T. *et al.* Pdx1 maintains  $\beta$  cell identity and function by repressing an  $\alpha$  cell program. *Cell Metab.* **19**, 259–271 (2014).
  263. Yang, Y.-P., Thorel, F., Boyer, D. F., Herrera, P. L. & Wright, C. V. E. Context-specific  $\alpha$ - to- $\beta$ -cell reprogramming by forced Pdx1 expression. *Genes Dev.* **25**, 1680–1685 (2011).
  264. Melloul, D., Marshak, S. & Cerasi, E. Regulation of pdx-1 gene expression. *Diabetes* **51 Suppl 3**, S320–5 (2002).
  265. Marshak, S. *et al.* Functional conservation of regulatory elements in the pdx-1 gene: PDX-1 and hepatocyte nuclear factor 3beta transcription factors mediate beta-cell-specific expression. *Molecular and Cellular Biology* **20**, 7583–7590 (2000).
  266. Gerrish, K., Cissell, M. A. & Stein, R. The Role of Hepatic Nuclear Factor 1 $\alpha$  and PDX-1 in Transcriptional Regulation of the pdx-1 Gene. *Journal of Biological Chemistry* **276**, 47775–47784 (2001).
  267. QIAN, J., KAYTOR, E. N., TOWLE, H. C. & OLSON, L. K. Upstream stimulatory factor regulates Pdx-1 gene expression in differentiated pancreatic  $\beta$ -cells. *Biochemical Journal* **341**, 315–322 (1999).
  268. Hartman, M. G. *et al.* Role for activating transcription factor 3 in stress-induced beta-cell apoptosis. *Molecular and Cellular Biology* **24**, 5721–5732 (2004).
  269. Jang, M. K., Park, H. J. & Jung, M. H. ATF3 represses PDX-1 expression in pancreatic  $\beta$ -cells. *Biochemical and Biophysical Research Communications* **412**, 385–390 (2011).
  270. McKenna, B., Guo, M., Reynolds, A., Hara, M. & Stein, R. Dynamic recruitment of functionally distinct Swi/Snf chromatin remodeling complexes modulates Pdx1 activity in islet  $\beta$  cells. *Cell Rep* **10**, 2032–2042 (2015).
  271. Petersen, H. V. *et al.* Glucose stimulates the activation domain potential of the PDX-1 homeodomain transcription factor. *FEBS Letters* **431**, 362–366 (1998).
  272. Claiborn, K. C. *et al.* Pcif1 modulates Pdx1 protein stability and pancreatic  $\beta$  cell function and survival in mice. *J. Clin. Invest.* **120**, 3713–3721 (2010).
  273. Shimano, H. *et al.* Sterol regulatory element-binding protein-1c and pancreatic  $\beta$ -cell dysfunction. *Diabetes Obes Metab* **9**, 133–139 (2007).
  274. Amemiya-Kudo, M. *et al.* Suppression of the pancreatic duodenal homeodomain transcription factor-1 (Pdx-1) promoter by sterol regulatory element-binding protein-1c (SREBP-1c). *J. Biol. Chem.* **286**, 27902–27914 (2011).
  275. Gao, Y., Miyazaki, J.-I. & Hart, G. W. The transcription factor PDX-1 is

- post-translationally modified by O-linked N-acetylglucosamine and this modification is correlated with its DNA binding activity and insulin secretion in min6  $\beta$ -cells. *Archives of Biochemistry and Biophysics* **415**, 155–163 (2003).
276. Kishi, A., Nakamura, T., Nishio, Y., Maegawa, H. & Kashiwagi, A. Sumoylation of Pdx1 is associated with its nuclear localization and insulin gene activation. *American Journal of Physiology - Endocrinology and Metabolism* **284**, E830–E840 (2003).
277. Khoo, S. *et al.* Regulation of insulin gene transcription by ERK1 and ERK2 in pancreatic beta cells. *Journal of Biological Chemistry* **278**, 32969–32977 (2003).
278. Templin, A. T., Maier, B., Tersey, S. A., Hatanaka, M. & Mirmira, R. G. Maintenance of Pdx1 mRNA Translation in Islet  $\beta$ -Cells During the Unfolded Protein Response. *Mol. Endocrinol.* **28**, 1820–1830 (2014).
279. Ardestani, A. *et al.* MST1 is a key regulator of beta cell apoptosis and dysfunction in diabetes. *Nature Medicine* **20**, 385–397 (2014).
280. Boucher, M. J., Selander, L. & Carlsson, L. Phosphorylation marks IPF1/PDX1 protein for degradation by glycogen synthase kinase 3-dependent mechanisms. *Journal of Biological ...* (2006).  
doi:10.1074/jbc.M511597200
281. Kawamori, D. *et al.* Oxidative stress induces nucleo-cytoplasmic translocation of pancreatic transcription factor PDX-1 through activation of c-Jun NH(2)-terminal kinase. *Diabetes* **52**, 2896–2904 (2003).
282. Ursu, O. N., Sauter, M., Ettischer, N., Kandolf, R. & Klingel, K. Heme oxygenase-1 mediates oxidative stress and apoptosis in coxsackievirus b3-induced myocarditis. *Cell. Physiol. Biochem.* **33**, 52–66 (2014).
283. Zhou, Q., Brown, J., Kanarek, A., Rajagopal, J. & Melton, D. A. In vivo reprogramming of adult pancreatic exocrine cells to  $\beta$ -cells. *Nature* **455**, 627–632 (2008).
284. Gerlier, D. & Lyles, D. S. Interplay between innate immunity and negative-strand RNA viruses: towards a rational model. *Microbiol. Mol. Biol. Rev.* **75**, 468–90– second page of table of contents (2011).
285. Fitzgerald, K. D., Chase, A. J., Cathcart, A. L., Tran, G. P. & Semler, B. L. Viral proteinase requirements for the nucleocytoplasmic relocation of cellular splicing factor SRp20 during picornavirus infections. *Journal of Virology* **87**, 2390–2400 (2013).
286. Yarbrough, M. L., Mata, M. A., Sakthivel, R. & Fontoura, B. M. A. Viral subversion of nucleocytoplasmic trafficking. *Traffic* **15**, 127–140 (2014).
287. Shiroki, K. *et al.* Intracellular redistribution of truncated La protein produced by poliovirus 3Cpro-mediated cleavage. *Journal of Virology* **73**, 2193–2200 (1999).
288. Meerovitch, K. *et al.* La autoantigen enhances and corrects aberrant translation of poliovirus RNA in reticulocyte lysate. *Journal of Virology* **67**, 3798–3807 (1993).

289. Yun, S.-H. *et al.* Antiviral activity of coxsackievirus B3 3C protease inhibitor in experimental murine myocarditis. *J. Infect. Dis.* **205**, 491–497 (2012).
290. Iannacone, M. *et al.* Subcapsular sinus macrophages prevent CNS invasion on peripheral infection with a neurotropic virus. *Nature* **465**, 1079–1083 (2010).
291. Hallak, L. K., Spillmann, D., Collins, P. L. & Peeples, M. E. Glycosaminoglycan sulfation requirements for respiratory syncytial virus infection. *Journal of Virology* **74**, 10508–10513 (2000).
292. Ylipaasto, P. *et al.* Enterovirus infection in human pancreatic islet cells, islet tropism in vivo and receptor involvement in cultured islet beta cells. **47**, 225–239 (2004).
293. Richardson, S. J., Willcox, A., Bone, A. J., Foulis, A. K. & Morgan, N. G. The prevalence of enteroviral capsid protein vp1 immunostaining in pancreatic islets in human type 1 diabetes. **52**, 1143–1151 (2009).
294. Anagandula, M. *et al.* Infection of human islets of langerhans with two strains of Coxsackie B virus serotype 1: assessment of virus replication, degree of cell death and induction of genes involved in the innate immunity pathway. *J. Med. Virol.* **86**, 1402–1411 (2014).
295. Morgan, N. G. & Richardson, S. J. Enteroviruses as causative agents in type 1 diabetes: loose ends or lost cause? *Trends Endocrinol. Metab.* (2014). doi:10.1016/j.tem.2014.08.002
296. Marroqui, L. *et al.* Differential cell autonomous responses determine the outcome of coxsackievirus infections in murine pancreatic  $\alpha$  and  $\beta$  cells. *Elife* **4**, e06990 (2015).
297. Dorrell, C. *et al.* Transcriptomes of the major human pancreatic cell types. *Diabetologia* **54**, 2832–2844 (2011).
298. Wong, J. *et al.* Cytoplasmic redistribution and cleavage of AUF1 during coxsackievirus infection enhance the stability of its viral genome. *FASEB J.* **27**, 2777–2787 (2013).
299. Benner, C. *et al.* The transcriptional landscape of mouse beta cells compared to human beta cells reveals notable species differences in long non-coding RNA and protein-coding gene expression. *BMC Genomics* **2014 15:1** **15**, 1 (2014).
300. Cnop, M. *et al.* The long lifespan and low turnover of human islet beta cells estimated by mathematical modelling of lipofuscin accumulation. *Diabetologia* **53**, 321–330 (2010).
301. Yamashita, S. *et al.* Quality of Air-Transported Human Islets for Single Islet Cell Preparations. *Cell Med* **6**, 33–38 (2013).
302. Wu, J. J., Chen, X., Cao, X.-C., Baker, M. S. & Kaufman, D. B. Cytokine-Induced Metabolic Dysfunction of MIN6  $\beta$  Cells Is Nitric Oxide Independent. *Journal of Surgical Research* **101**, 190–195 (2001).
303. Blodgett, D. M. *et al.* Novel Observations from Next Generation RNA Sequencing of Highly Purified Human Adult and Fetal Islet Cell Subsets.

- Diabetes* db150039 (2015). doi:10.2337/db15-0039
304. Berg, A.-K., Olsson, A., Korsgren, O. & Frisk, G. Antiviral treatment of Coxsackie B virus infection in human pancreatic islets. *Antiviral Res.* **74**, 65–71 (2007).
  305. Knoch, K.-P. *et al.* PTBP1 is required for glucose-stimulated cap-independent translation of insulin granule proteins and Coxsackieviruses in beta cells. *Mol Metab* **3**, 518–530 (2014).
  306. Alidjinou, E. K., Sane, F., Engelmann, I., Geenen, V. & Hober, D. Enterovirus persistence as a mechanism in the pathogenesis of type 1 diabetes. *Discov Med* **18**, 273–282 (2014).
  307. Hello, A., H. *et al.* Amino acids of Coxsackie B5 virus are critical for infection of the murine insulinoma cell line, MIN-6. *J. Med. Virol.* **81**, 296–304 (2009).